

Yttrium and Lanthanum Bis(phosphine-oxide)methanides: Structurally Diverse, Dynamic, and Reactive

Kerry C. Casey,^a Alexander M. Brown,^a Jerome R. Robinson*^a

^a 324 Brook St., Department of Chemistry, Brown University, Providence, RI 02912, United States
Phone: (+1)-401-863-3249; e-mail: jerome_robinson@brown.edu

Supporting Information

1. General Methods	S03-S05
2. Synthetic Details and Characterization	S05-S11
Figure S1. ^1H and $^{13}\text{C}\{\text{H}\}$, $^{31}\text{P}\{\text{H}\}$ NMR and IR of H_2MeL	S11-S13
Figure S2. ^1H and $^{13}\text{C}\{\text{H}\}$, $^{31}\text{P}\{\text{H}\}$ NMR and IR of $\text{Y}_2(\text{H}^{\text{Me}}\text{L})_6$	S13-S16
Figure S3. ^1H and $^{13}\text{C}\{\text{H}\}$, $^{31}\text{P}\{\text{H}\}$ NMR and IR of $\text{La}_2(\text{H}^{\text{Me}}\text{L})_6$	S17-S18
Figure S4. Overlay of IR spectra (Nujol Mull) of $\text{RE}_2(\text{H}^{\text{Me}}\text{L})_6$ and H_2MeL	S19
Figure S5. ^1H and $^{13}\text{C}\{\text{H}\}$, $^{31}\text{P}\{\text{H}\}$ NMR and IR of $\text{Y}(\text{H}^{\text{Ph}}\text{L})_3$	S20-S21
Figure S6. ^1H and $^{13}\text{C}\{\text{H}\}$, $^{31}\text{P}\{\text{H}\}$ NMR and IR of $\text{La}(\text{H}^{\text{Ph}}\text{L})_3$	S22-S24
Figure S7. Overlay of IR spectra (Nujol Mull) of $\text{RE}(\text{H}^{\text{Ph}}\text{L})_3$ and H_2PhL	S25
Figure S8. ^1H , $^{13}\text{C}\{\text{H}\}$, and $^{31}\text{P}\{\text{H}\}$ NMR of (<i>E</i>)-dimethyl(styryl)phosphine oxide	S26-S28
Figure S9. IR spectra of $\text{Y}(\text{O}_2\text{PMe}_2)_3$	S29
Figure S10. ^1H and $^{13}\text{C}\{\text{H}\}$ NMR of (<i>E</i>)-diphenyl(styryl)phosphine	S29-S30
Figure S11. IR spectra of $\text{Y}(\text{O}_2\text{PPh}_2)_3$	S30
Figure S12. ^1H , $^{13}\text{C}\{\text{H}\}$, and $^{31}\text{P}\{\text{H}\}$ NMR of (<i>E</i>)-dimethyl(styryl)phosphine oxide	S31-S32
Figure S13. IR spectra of $\text{La}(\text{O}_2\text{PMe}_2)_3$	S32
Figure S14. ^1H and $^{13}\text{C}\{\text{H}\}$ NMR of (<i>E</i>)-diphenyl(styryl)phosphine	S33
Figure S15. IR spectra of $\text{La}(\text{O}_2\text{PPh}_2)_3$	S34
Figure S16. Variable temperature ^1H and $^{31}\text{P}\{\text{H}\}$ -NMR experiment of $\text{Y}_2(\text{H}^{\text{Me}}\text{L})_6$	S35-S37
Figure S17. Variable temperature ^1H and $^{31}\text{P}\{\text{H}\}$ -NMR experiment of $\text{Y}(\text{H}^{\text{Ph}}\text{L})_3$	S38-S39
Figure S18. ^1H , ^2H , and $^{31}\text{P}\{\text{H}\}$ NMR of reaction of $\text{Y}_2(\text{H}^{\text{Me}}\text{L})_6$ with MeOD	S40-S42
Figure S19. ^1H , ^2H , and $^{31}\text{P}\{\text{H}\}$ NMR of reaction of $\text{Y}(\text{H}^{\text{Ph}}\text{L})_3$, with MeOD	S43-S45
Table S1. Diffusion coefficients and estimated hydrodynamic radii of $\text{Y}_2(\text{H}^{\text{Me}}\text{L})_6$ and $\text{Y}(\text{H}^{\text{Ph}}\text{L})_3$	S46
Figure S20. DOSY of a mixture of $\text{Y}_2(\text{H}^{\text{Me}}\text{L})_6$ and decamethylferrocene	S47
Figure S21. DOSY of a mixture of $\text{La}_2(\text{H}^{\text{Me}}\text{L})_6$ and decamethylferrocene	S47
Figure S22. DOSY of a mixture of $\text{Y}(\text{H}^{\text{Ph}}\text{L})_3$ and decamethylferrocene	S48
Figure S23. DOSY of a mixture of $\text{La}(\text{H}^{\text{Ph}}\text{L})_3$ and decamethylferrocene	S48
Figure S24. Points used for determination of r_{H} (theo) from the crystal structure of Fc^*	S49
Figure S25. Points used for determination of r_{H} (theo) from the crystal structure of $\text{Y}_2(\text{H}^{\text{Me}}\text{L})_6$	S49
Figure S26. Points used for determination of r_{H} (theo) from the DFT optimized structure of $\text{Y}(\text{H}^{\text{Me}}\text{L})_3$	S50
Figure S27. Points used for determination of r_{H} (theo) from the crystal structure of $\text{La}_2(\text{H}^{\text{Me}}\text{L})_6$	S50
Figure S28. Points used for determination of r_{H} (theo) from the DFT optimized structure of $\text{La}(\text{H}^{\text{Me}}\text{L})_3$	S51
Figure S29. Points used for determination of r_{H} (theo) from the crystal structure of $\text{Y}(\text{H}^{\text{Ph}}\text{L})_3$	S51
Figure S30. Points used for determination of r_{H} (theo) from the crystal structure of $\text{La}(\text{H}^{\text{Ph}}\text{L})_3$	S52
Figure S31. Thermal ellipsoid plot (50% probability) for $\text{La}(\text{H}^{\text{Ph}}\text{L})_3$	S53
Table S2. Crystallographic parameters for $\text{RE}_2(\text{H}^{\text{Me}}\text{L})_6$ and $\text{RE}(\text{H}^{\text{Ph}}\text{L})_3$	S54-S55
Table S3. Distances and angles for $\text{Y}_2(\text{H}^{\text{Me}}\text{L})_6$	S56-S57
Table S4. Distances and angles for $\text{La}_2(\text{H}^{\text{Me}}\text{L})_6$	S57-S60
Table S5. Distances and angles for $\text{Y}(\text{H}^{\text{Ph}}\text{L})_3$	S60-S65
Table S6. Distances and angles for $\text{La}(\text{H}^{\text{Ph}}\text{L})_3$	S65-S79
3. Computational Studies	S80

Figure S32. Labelled image of $\mathbf{Y}(\mathbf{H}^{\text{Ph}}\mathbf{L})_3$.	S80
Table S7. DFT predicted bond distances and angles for $\mathbf{Y}(\mathbf{H}^{\text{Ph}}\mathbf{L})_3$.	S80-S81
Table S8. Hybridization, hyperconjugation, and $E(2)$ stabilization energy for $\mathbf{Y}(\mathbf{H}^{\text{Ph}}\mathbf{L})_3$.	S82
Table S9. Cartesian coordinates of $\mathbf{Y}(\mathbf{H}^{\text{Ph}}\mathbf{L})_3$.	S82-S85
Figure S33. Labelled image of $\mathbf{La}(\mathbf{H}^{\text{Ph}}\mathbf{L})_3$.	S86
Table S10. DFT predicted bond distances and angles for $\mathbf{La}(\mathbf{H}^{\text{Ph}}\mathbf{L})_3$.	S86-S87
Table S11. Hybridization, hyperconjugation, and $E(2)$ stabilization energy for $\mathbf{La}(\mathbf{H}^{\text{Ph}}\mathbf{L})_3$.	S88
Table S12. Cartesian coordinates of $\mathbf{La}(\mathbf{H}^{\text{Ph}}\mathbf{L})_3$	S88-S91
Figure S34. Labelled image of $\mathbf{Y}(\mathbf{H}^{\text{Me}}\mathbf{L})_3$.	S92
Table S13. DFT predicted bond distances and angles for $\mathbf{Y}(\mathbf{H}^{\text{Me}}\mathbf{L})_3$.	S92-S93
Table S14. Hybridization, hyperconjugation, and $E(2)$ stabilization energy for $\mathbf{Y}(\mathbf{H}^{\text{Me}}\mathbf{L})_3$.	S94
Table S15. Cartesian coordinates of $\mathbf{Y}(\mathbf{H}^{\text{Me}}\mathbf{L})_3$.	S94-S96
Figure S35. Labelled image of $\mathbf{La}(\mathbf{H}^{\text{Me}}\mathbf{L})_3$.	S99
Table S16. DFT predicted bond distances and angles for $\mathbf{La}(\mathbf{H}^{\text{Me}}\mathbf{L})_3$.	S96-S97
Table S17. Hybridization, hyperconjugation, and $E(2)$ stabilization energy for $\mathbf{La}(\mathbf{H}^{\text{Me}}\mathbf{L})_3$.	S98
Table S18. Cartesian coordinates of $\mathbf{La}(\mathbf{H}^{\text{Me}}\mathbf{L})_3$.	S98-S100
Figure S36. Labelled image of $\mathbf{Y}_2(\mathbf{H}^{\text{Me}}\mathbf{L})_6\text{-A}$.	S100
Table S19. DFT predicted bond distances and angles for $\mathbf{Y}_2(\mathbf{H}^{\text{Me}}\mathbf{L})_6\text{-A}$.	S100-S101
Table S20. Hybridization, hyperconjugation, and $E(2)$ stabilization energy for $\mathbf{Y}_2(\mathbf{H}^{\text{Me}}\mathbf{L})_6\text{-A}$.	S102
Table S21. Cartesian coordinates of $\mathbf{Y}_2(\mathbf{H}^{\text{Me}}\mathbf{L})_6\text{-A}$.	S102-S105
Figure S37. Labelled image of $\mathbf{La}_2(\mathbf{H}^{\text{Me}}\mathbf{L})_6\text{-A}$.	S106
Table S22. DFT predicted bond distances and angles for $\mathbf{La}_2(\mathbf{H}^{\text{Me}}\mathbf{L})_6\text{-A}$.	S106-S107
Table S23. Hybridization, hyperconjugation, and $E(2)$ stabilization energy for $\mathbf{La}_2(\mathbf{H}^{\text{Me}}\mathbf{L})_6\text{-A}$.	S107-S108
Table S24. Cartesian coordinates of $\mathbf{La}_2(\mathbf{H}^{\text{Me}}\mathbf{L})_6\text{-A}$.	S108-S11
Figure S38. Labelled image of $\mathbf{Y}_2(\mathbf{H}^{\text{Me}}\mathbf{L})_6\text{-B}$.	S123
Table S25. DFT predicted bond distances and angles for $\mathbf{Y}_2(\mathbf{H}^{\text{Me}}\mathbf{L})_6\text{-B}$.	S112-S115
Table S26. Hybridization, hyperconjugation, and $E(2)$ stabilization energy for $\mathbf{Y}_2(\mathbf{H}^{\text{Me}}\mathbf{L})_6\text{-B}$.	S115
Table S27. Cartesian coordinates of $\mathbf{Y}_2(\mathbf{H}^{\text{Me}}\mathbf{L})_6\text{-B}$.	S116-S119
Figure S39. Labelled image of $\mathbf{La}_2(\mathbf{H}^{\text{Me}}\mathbf{L})_6\text{-B}$.	S119
Table S28. DFT predicted bond distances and angles for $\mathbf{La}_2(\mathbf{H}^{\text{Me}}\mathbf{L})_6\text{-B}$.	S119-S122
Table S29. Hybridization, hyperconjugation, and $E(2)$ stabilization energy for $\mathbf{La}_2(\mathbf{H}^{\text{Me}}\mathbf{L})_6\text{-B}$.	S122
Table S30. Cartesian coordinates of $\mathbf{La}_2(\mathbf{H}^{\text{Me}}\mathbf{L})_6\text{-B}$.	S123-S126
4. References	S127-S128

1. General Methods.

Instruments and measurements: Unless specified, all reactions were performed under inert conditions (N_2) using standard Schlenk techniques or in a MBraun drybox equipped with a standard catalyst purifier and solvent trap. Glassware was oven-dried for at least 2 h at 150 °C prior to use. Celite and 3 Å molecular sieves were heated under reduced pressure at 300 °C for at least 24 h and then cooled under vacuum prior to use. The following spectrometers were used for NMR characterization: Bruker Avance III HD Ascend (1H : 600 MHz, ^{13}C : 152 MHz, ^{31}P : 243 MHz) and a Bruker DRX (1H : 400 MHz, ^{13}C : 101 MHz, ^{31}P : 162 MHz.). 1H - and ^{13}C -NMR shifts are referenced relative to the solvent signal ($CDCl_3$: 1H : 7.26 ppm, ^{13}C : 77.16 ppm; C_6D_6 : 1H : 7.16 ppm, ^{13}C : 128.06 ppm), while ^{31}P -NMR shifts are referenced relative to external solution standards (H_3PO_4 , 0 ppm). Both instruments were equipped with Z-gradient BBFO probes. Probe temperatures were calibrated using ethylene glycol and methanol as previously described.¹

IR spectra were recorded on Jasco 4100 FTIR spectrometers using Nujol mulls sandwiched between KBr plates. Elemental analyses were performed by Robertson Microlit Laboratories (Ledgewood, NJ; $Y(H^{Ph}L)_3$) Midwest Microlab, LLC (Indianapolis, IN $La,(H^{Ph}L)_3$), and the University of Rochester ($RE(H^{OiPr}L)_3$ and $RE_2(H^{Me}L)_6$). Elemental analyses performed by the University of Rochester used a PerkinElmer 2400 Series II Analyzer. Samples were shipped in vacuum sealed plastic bags within a sealed 2 mL vial placed in a sealed 20 mL scintillation vial.

Materials: Tetrahydrofuran (inhibitor-free), diethyl ether (inhibitor-free), toluene, hexanes, and pentane were purchased from Fisher Scientific. Solvents were sparged for 20 min with dry Ar and dried using a commercial two-column solvent purification system (LC Technologies). Solvents were further dried by storing them over 3 Å molecular sieves for at least 48 h prior to use. Benzene (DriSolv®) was purchased from Sigma-Aldrich, degassed with 3 freeze-pump-thaw cycles, and stored over 3 Å molecular sieves for at least 48 h prior to use. Deuterated solvents were purchased from Cambridge Isotope Laboratories, Inc. C_6D_6 and CD_2Cl_2 were degassed with 3 freeze-pump-thaw cycles and stored over 3 Å molecular sieves for at least 48 h prior to use. Qualitative assessment of moisture-content was performed by adding 1 drop of a concentrated solution of a sodium benzophenone radical anion (purple) to 10 mL of solvent where maintenance of a dark blue color for at least 5 minutes was sufficient for use.

Potassium hexamethyldisilazide (Sigma-Aldrich; 95%), 1,1,3,3-Tetramethyldisilazane (TCI, 97%), $RECl_3$ (Strem; RE = La, Y; 99.9%), methylene bis(dimethylphosphine) (Sigma-Aldrich; 97%), methylene bis(diphenylphosphine) (Alfa Aesar; 97%) were purchased and used as received. Methylenebis(diphenylphosphine oxide),¹ $RE[N(SiMe_3)_2]_3$ (RE = La and Y),² and $RE[N(SiHMe_2)_2]_3(THF)_2$ (RE = La and Y),³ were prepared according to reported procedures.

X-ray Crystallography: Samples were collected in Paraton™ oil on a petri dish in a glovebox and then quickly evaluated and mounted with the assistance of an optical microscope. X-ray reflection intensity data were collected on a Bruker D8 Quest with a Photon 100 CMOS detector or Photon II CPAD detector employing graphite-monochromated Mo-K α radiation ($\lambda = 0.71073 \text{ \AA}$) at a temperature of 173(1) K. Rotation frames were integrated using SAINT,⁴ producing a listing of unaveraged F^2 and $\sigma(F^2)$ values which were then passed to the SHELXT⁵ program

package for further processing and structure solution. The intensity data were corrected for Lorentz and polarization effects and for absorption using SADABS.⁶ The structures were solved by direct methods (SHELXT).⁵ Refinement was by full-matrix least squares based on F² using SHELXL.⁷ All reflections were used during refinements. Non-hydrogen atoms were refined anisotropically and hydrogen atoms were refined using a riding model. One methanide position, C(6)–H(6), was found to be disordered over two positions in **La**₂(**H^MeL**)₆ and were refined with the help of similarity restraints using standard/default values on 1,2 and 1,3 distances. Two toluene molecules were refined with the help of a rigid group constraint in the case of **La(H^PhL)**₃. In the case of **Y(H^PhL)**₃, there was an area of disordered solvent (toluene, 1 molecule in the asymmetric unit) for which reliable disorder models could not be devised; the X-ray data were corrected for the presence of disordered solvent using the solvent mask function (BYPASS) in Olex2. Crystallographic parameters are summarized in Tables S2a and S2b and distances and angles are summarized in Tables S3-S6.

¹H DOSY NMR. The NMR experiments for the determination of the self-diffusion coefficients and hydrodynamic radii were performed at 298 K. In Bipolar-LED experiments, diffusion time (D20, Δ) was 150 ms for all samples, and the duration (P30, δ) of the sine shaped gradients was set to 1.0 ms. Data were systematically accumulated by linearly varying the diffusion gradients from 95% to 5% for 16 gradient increment values. Data processing was accomplished with Bruker TOPSPIN 3.6.1 DOSY software and Bruker TOPSPIN 3.6.1 T1/T2 software. Diffusion coefficients (D_o) were obtained after fitting area data to the Stejskal-Tanner expression with the Bruker TOPSPIN 3.6.1 T1/T2 software and the reported D_o is an average value calculated from the different NMR responses within the same compound. Similarly, standard deviations associated with values of D_o were calculated from differences in D_o in the same sample using different NMR responses. The hydrodynamic radii (r_H (sample)) were determined following Eqn S1:

$$r_H(\text{sample}) = \left(\frac{D_o(\text{reference})}{D_o(\text{sample})} \right) \times r_H(\text{reference}) \quad (\text{Eqn S1})$$

where $D_o(\text{reference})$ was the diffusion coefficient for the corresponding internal standard, $D_o(\text{sample})$ was the diffusion coefficient of the sample, and $r_H(\text{reference})$ was the hydrodynamic radii of the internal reference (Fc*). (Fc*) was selected as an ideal internal standard for ¹H DOSY NMR as it (i) is unreactive with **RE(H^RL)**₃ and **RE**₂(**H^MeL**)₆, (ii) is highly soluble in common organic solvents, (iii) chemical shift that is open, and (iv) is roughly spherical in shape. Equation S1 was used to minimize errors between samples due to variations in viscosity and temperature, and is derived from the Stokes-Einstein equation:^{8,9}

$$D_o = \frac{kT}{6r_H\pi\eta} \quad (\text{Eqn S2})$$

where D_o is the diffusion coefficient, k is the Boltzmann constant, T is temperature, r_H is the hydrodynamic radius, and η is the viscosity of the solution. The theoretical hydrodynamic radii ($r_{H(\text{theo})}$) were determined from their reported crystal structures, taking the centroid of the molecule and measuring the distance to the furthest point in the molecule.

Estimated hydrodynamic radii are taken from crystal structures or DFT optimized structures by measuring the furthest point from the centroid of the molecules. This method was found to be satisfactory for sphere-like molecules. In the case of non-spherical molecules an estimated r_H was

found by taking the average of half lengths of the principal axes of the homogeneous ellipsoid with the same principal moments of inertia of the molecule.

The modified Stokes-Einstein equation¹⁰ utilizing Perrin's frictional ratios¹¹ was employed in the case of oblate or prolate ellipsoids to correct experimental r_H when necessary.

$$D_o = \frac{kT}{C(rsolv,rH)f_s(a,b)r_H\pi\eta} \quad \text{Eq. S3}$$

Where C is the ratio of the solvent r_H to the r_H of the molecule and f_s is Perrin's frictional coefficient for oblate (Eq. S4) or prolate (Eq. S5) ellipsoids.

$$f_s = \frac{\frac{2\sqrt{1-\frac{b^2}{a}}}{b/a^{\frac{2}{3}} \ln \frac{\sqrt{1-\frac{b^2}{a}}}{b/a}}}{\frac{2\sqrt{\frac{b^2}{a}-1}}{b/a^{\frac{2}{3}} \arctan + \sqrt[4]{b/a^2-1}}} \quad \text{Eq. S4}$$

$$f_s = \frac{\frac{2\sqrt{\frac{b^2}{a}-1}}{b/a^{\frac{2}{3}} \arctan + \sqrt[4]{b/a^2-1}}}{\frac{2\sqrt{1-\frac{b^2}{a}}}{b/a^{\frac{2}{3}} \ln \frac{\sqrt{1-\frac{b^2}{a}}}{b/a}}} \quad \text{Eq. S5}$$

The modified derived Stokes-Einstein equation can now be written as

$$r_H(\text{sample}) = \frac{\frac{D_o(\text{reference})}{D_o(\text{standard})} r_H(\text{reference})}{f_s(a,b)} \quad \text{Eq. S6}$$

2. Synthetic Details and Characterization

Synthesis of methylenebis(dimethylphosphine oxide), H₂^{Me}L

In an N₂-filled glovebox a 50 mL Schlenk flask was charged with bis(dimethylphosphino)methane (500 mg, 3.67 mmol, 1 equiv, MW: 136.11 g·mol⁻¹), toluene (3 mL), and a Teflon coated stir bar. The flask was sealed, taken out of the glovebox, and an inert atmosphere was established on the Schlenk line. The Schlenk flask was cooled to 0 °C, and hydrogen peroxide (37% w/w, 1.68 mL, ρ = 1.10 g/mL; 1.85 g, 14.70 mmol, 4 equiv, MW: 34.01 g·mol⁻¹) was added dropwise (2 min) to the vigorously stirring colorless solution. The clear biphasic solution was allowed to warm to RT over 16 h, after which the solvent was removed under reduced pressure. Toluene (8 mL) was added to the clear, colorless oil and the flask was fitted with a dean stark trap. The biphasic solution was heated to reflux for 16 h to remove residual water. Upon completion of the azeotropic distillation, the solution was cooled to RT under N₂ flow to yield clear, colorless crystals upon standing (2 h). The solvent was removed under reduced pressure (16 h, 50 mTorr), and the white solid was then transferred to a sublimator in an N₂-filled glovebox. The sublimator was brought back outside the glovebox and the hygroscopic white solid was then sublimed (110 °C, 50 mTorr) to yield anhydrous bis(dimethylphosphine-oxide)methane, H₂^{Me}L, as a white solid. Yield: 385.5 mg (2.29 mmol, 62%; MW: 168.11 g·mol⁻¹). NMR spectra matched the previous literature report.¹²

¹H-NMR (400 MHz, (CD₃)₂CO, 298 K): δ = 1.74 (d, ²J_{P-H} = 13.1 Hz, 12H, P(CH₃)₂), 2.63 (t, ²J_{P-H} = 13.18 hz, 2H, PC_{H2}P).

¹H-NMR (400 MHz, CD₂Cl₂, 298 K): δ = 1.62 (d, ²J_{P-H} = 12.4 Hz, 12H, P(CH₃)₂), 2.23 (t, ²J_{P-H} = 13.1 hz, 2H, PC_{H2}P). ¹³C{¹H}-NMR (100 MHz, CD₂Cl₂, 298 K): δ = 19.2 (d, ¹J_{P-C} = 73.6 Hz, P(CH₃)₃), 35.2 (t, ¹J_{P-C} = 123.5 Hz, PC_{H2}P). ³¹P{¹H}-NMR (100 MHz, CD₂Cl₂, 298 K): δ = 36.3.

IR (Nujol): cm⁻¹; 1297(s), 1156(s, P=O), 1071(s), 939(s), 869(s), 849(s), 787(s), 747(s), 680(w), 644(w)

Synthesis of Y₂(H^{Me}L)₆

A 20 mL scintillation vial was charged with bis(dimethylphosphine-oxide)methane, H₂^{Me}L, (102.7 mg, 0.61 mmol, 3 equiv, MW: 168.11 g·mol⁻¹), Y[N(SiHMe₂)₂]₃(THF)₂ (128.3 mg, 0.20 mmol, 1 equiv, MW: 630.12 g·mol⁻¹), tetrahydrofuran (3 mL), and a Teflon-coated stir bar. The light-yellow mixture solution was stirred for 1h at 65 °C, and solvents were removed under reduced pressure. The crude yellow solid was triturated with pentane (3 x 1 mL) to help remove residual amine. The yellow was dissolved in diethyl ether (5 mL) and filtered through a glass pipet padded with Celite® to remove insoluble materials. Volatiles were removed under reduced pressure and the yellow oily solid was dissolved in diethyl ether (2 mL). Clear crystals formed after sitting undisturbed at -35 °C for 2 h. The solvent was decanted, the solid was washed with RT pentane (1 mL), and the sample was dried under reduced pressure to yield Y₂(H^{Me}L)₆ as a white solid. Yield: 72.4 mg (0.126 mmol, 60%; MW: 590.22 g·mol⁻¹).

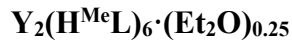
¹H-NMR (400 MHz, C₆D₆, 298 K): δ = 0.90 (t, ²J_{P-H} = 7.4 Hz, 3H, PC_{H2}P), 1.34 (d, ²J_{P-H} = 12.16 Hz, 36 H, P(CH₃)₂). ¹³C{¹H}-NMR (100 MHz, C₆D₆, 298 K): δ = 20.4 (t, ¹J_{P-C} = 123.5 Hz, PC_{H2}P), 22.7 (d, ¹J_{P-C} = 77.1 Hz, P(CH₃)₃). ³¹P{¹H}-NMR (100 MHz, C₆D₆, 298 K): δ = 45.4 (d, ²J_{P-Y} = 6.1 Hz).

¹H-NMR (400 MHz, CD₂Cl₂, 298 K): δ = 0.91 (t, ²J_{P-H} = 6.31 Hz, 3H, PC_{H2}P), 1.39 (d, ²J_{P-H} = 12.01 hz, 36 H, P(CH₃)₂). ¹³C{¹H}-NMR (100 MHz, CD₂Cl₂, 298 K): δ = 21.1 (t, ¹J_{P-C} = 117.1 Hz, PC_{H2}P), 22.2 (d, ¹J_{P-C} = 77.0 Hz, P(CH₃)₃). ³¹P{¹H}-NMR (100 MHz, CD₂Cl₂, 298 K): δ = 46.4 (d, ²J_{P-Y} = 6.1 Hz,)

IR (Nujol): cm⁻¹; 1283(m, CH₃), 1211(m, C–H), 1180(m, C–H), 1178(m, C–H), 1085(s, P=O), 1060 (s, P=O), 979 (m), 951 (s), 921 (m), 887 (w), 861(m), 772(m), 668 (m), 433(w)

Elemental Analysis calcd. (%) for C₁₆H_{41.5}O_{6.25}P₆Y : C 31.57; H 6.87. Found: C 31.63; H 6.91.

Note: 0.25 equiv. of interstitial diethyl ether were found even after extended drying under high vacuum. (¹H-NMR and combustion analysis). The MW and yield are given for



Synthesis of La₂(H^{Me}L)₆

A 20 mL scintillation vial was charged with H₂^{Me}L (117.0 mg, 0.70 mmol, 3 equiv, MW: 168.11 g·mol⁻¹), La[N(SiHMe₂)₂]₃(THF)₂ (157.8 mg, 0.23 mmol, 1 equiv, MW: 680.12 g·mol⁻¹), tetrahydrofuran (3 mL), and a Teflon-coated stir bar. The light-yellow mixture solution was

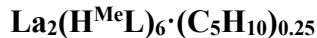
stirred for 1 h at 65 °C, and solvents were removed under reduced pressure. The crude yellow solid was triturated with pentane (3 x 1 mL) to help remove residual amine. The yellow was dissolved in diethyl ether (5 mL) and filtered through a glass pipet padded with Celite® to remove insoluble materials. Volatiles were removed under reduced pressure and the resulting yellow oily solid was dissolved in pentane (2 mL). Clear, colorless crystals formed after sitting undisturbed at –35 °C for 2 h. The solvent was decanted, the solid was washed with cold pentane (1 mL, –35 °C), and the sample was dried under reduced pressure to yield **La₂(H^{Me}L)₆** as a white solid. Yield: 53.0 mg (0.08 mmol, 36%; MW: 640.22 g·mol⁻¹). X-ray quality crystals were acquired by slow diffusion of pentane into a concentrated diethyl ether solution.

¹H-NMR (400 MHz, C₆D₆, 298 K): δ = 1.20 (t, ²J_{P-H} = 6.61 Hz, 3H, PCH₂P), 1.59 (d, ²J_{P-H} = 12.16 Hz, 36 H, P(CH₃)₂). ¹³C{¹H}-NMR (100 MHz, C₆D₆, 298 K): δ = 23.1 (t, ¹J_{P-C} = 117.3 Hz, PCH₂P), 33.5 (d, ¹J_{P-C} = 77.2 Hz, P(CH₃)₃). ³¹P{¹H}-NMR (100 MHz, C₆D₆, 298 K): δ = 40.7.

IR (Nujol): cm⁻¹; 1288(s, CH₃), 1179(m, C–H), 1155 (m, C–H), 1114(s, P=O), 1,080(s, P=O), 1,054(m, P=O), 1,041(m, P=O), 1,031 (sh, P=O), 979(m), 956(s), 875, 850, 772, 680, 422

Elemental Analysis calcd. (%) for C_{16.25}H₄₂LaO₆P₆: C 29.65; H 6.43. Found: C 29.98; H 6.14.

Note: ~0.25 equiv. of interstitial pentane were found even after extended drying under high vacuum (¹H-NMR and combustion analysis). The MW and yield are given for



Synthesis of Y(H^{Ph}L)₃

A 20 mL scintillation vial was charged with bis(diphenylphosphine-oxide)methane, **H₂PhL**, (627.3 mg, 1.51 mmol, 3 equiv, MW: 416.40 g·mol⁻¹), **Y[N(SiHMe₂)₂]₃(THF)₂** (316.4 mg, 0.50 mmol, 1 equiv, MW: 630.12 g·mol⁻¹), benzene (3 mL), tetrahydrofuran (3 mL), and a Teflon-coated stir bar. The light-yellow mixture was stirred for 1 h at 70 °C, and solvents were removed under reduced pressure. The crude light-yellow solid was triturated with pentane (3 x 1 mL) to help remove residual amine. The yellow was dissolved in toluene (4 mL), and tetrahydrofuran (1 mL), and filtered through a glass pipet padded with Celite® to remove insoluble materials. The clear light-yellow solution was layered with pentane (4 mL). Clear, colorless crystals formed after sitting undisturbed at RT for 24 h. The solvent was decanted, the solid was washed with pentane (3 mL), and the sample was dried under reduced pressure to yield **Y(H^{Ph}L)₃** as a white solid. Yield: 454.9 mg (0.34 mmol, 68%; MW: 1335.1 g·mol⁻¹).

¹H-NMR (400 MHz, CD₂Cl₂, 298 K): δ = 2.26 (t, ²J_{P-H} = 2.03 Hz, 3H, PCH₂P), 7.18 (dt, ³J = 8.05 Hz, ⁴J = 2.41 Hz, 24 H, *m*-CH_{Ar}), 7.33 (m, 12 H, *p*-CH_{Ar}), 7.83 (m, 24, *o*-CH_{Ar}). ¹³C{¹H}-NMR (100 MHz, CD₂Cl₂, 298 K): δ = 21.52 (t, ²J_{P-C} = 111.8 Hz, PCH₂P), 128.0 (virtual quintet, J_{P-C} = 6.04, *m*-C_{Ar}), 131.2 (*p*-C_{Ar}), 131.6 (virtual quintet, J_{P-C} = 5.47, *o*-C_{Ar}), 138.4 (dd, J_{P-C} = 111.8, J_{Y-C} = 2.29, *i*-C_{Ar}). ³¹P{¹H}-NMR (100 MHz, CD₂Cl₂, 298 K): δ = 37.8 (d, ²J_{P-Y} = 5.8 Hz,).

IR (Nujol): cm⁻¹; 1148(s, P=O), 1118 (m), 1078 (m), 1060 (s), 938 (m, C–H), 814 (m), 740(m), 691 (m), 584 (w), 541 (m), 522 (m).

Elemental Analysis calcd. (%) for C₇₅H₆₃O₆P₆Y: C 67.47; H 4.76. Found: C 67.62; H 4.43.

Synthesis of $\text{La}(\text{H}^{\text{Ph}}\text{L})_3$

A 20 mL scintillation vial was charged with $\text{H}_2^{\text{Ph}}\text{L}$ (367.5 mg, 0.88 mmol, 3 equiv, MW: 416.40 g·mol⁻¹), $\text{La}[\text{N}(\text{SiHMe}_2)_2]_3(\text{THF})_2$ (316.4 mg, 0.29 mmol, 1 equiv, MW: 680.12 g·mol⁻¹), benzene (3 mL), tetrahydrofuran (3 mL), and a Teflon-coated stir bar. The light-yellow mixture was stirred for 1 h at 70 °C, and solvents were removed under reduced pressure. The crude light-yellow solid was triturated with pentane (3 x 1 mL) to help remove residual amine. The yellow was dissolved in toluene (4 mL), and tetrahydrofuran (1 mL), and filtered through a glass pipet padded with Celite® to remove insoluble materials. The clear light-yellow solution was layered with pentane (4 mL). Clear colorless crystals formed after sitting undisturbed at room temperature for 24 h. The solvent was decanted, the solid was washed with pentane (3 mL), and the sample was dried under reduced pressure to yield $\text{La}(\text{H}^{\text{Ph}}\text{L})_3$ as a white solid. Yield: 302.2 mg (0.34 mmol, 74%; MW: 1385.1 g·mol⁻¹).

¹H-NMR (400 MHz, CD_2Cl_2 , 298 K): δ = 2.28 (br s, 3H, PCH_2P), 7.13 (dt, ³J = 7.91 Hz, ⁴J = 2.41 Hz, 24 H, *m*-CH_{Ar}), 7.27 (m, 12 H, *p*-CH_{Ar}), 7.77 (m, 24, *o*-CH_{Ar}). ¹³C{¹H}-NMR (100 MHz, C_6D_6 , 298 K): δ = 22.9 (t, ²J_{P-C} = 111.2 Hz, PCH_3 , 128.1 (virtual quintet, ³J_{P-C} = 6.04, *m*-C_{Ar}), 130.2 (*p*-C_{Ar}), 131.6 (virtual quintet, ³J_{P-C} = 5.47, *o*-C_{Ar}), 138.2 (dd, ³J_{P-C} = 111.8, *i*-C_{Ar}). ³¹P{¹H}-NMR (100 MHz, CD_2Cl_2 , 298 K): δ = 35.4.

IR (Nujol): cm⁻¹; 1303 (w), 1147(m, C–H), 1118(m), 1076(m, P=O), 1050(m, P=O), 940(s, C–H), 813(w), 740(s), 691(s), 583(w), 539 (s), 511(s).

Elemental Analysis calcd. (%) for $\text{C}_{75}\text{H}_{63}\text{O}_6\text{P}_6\text{Y}$: C 65.04; H 4.58. Found: C 64.57; H 4.70.

Reaction of $\text{Y}_2(\text{H}^{\text{Me}}\text{L})_6$ with Benzaldehyde

A 20 mL scintillation vial was charged with $\text{Y}_2(\text{H}^{\text{Me}}\text{L})_6$ (31.0 mg, 0.05 mmol, 1 equiv, MW: 590.22 g·mol⁻¹), toluene (2 mL), and a Teflon-coated stir bar. Benzaldehyde (16.7 mg, 0.15 mmol, 3 equiv, MW: 106.12) was added to the stirring colorless solution and stirred for 1.5 h at RT. During this time, formation of a white fluffy solid was observed.. The solvents were removed under reduced pressure and the crude white solid was extracted with toluene (3 x 2 mL). The slurry was filtered through a medium porosity glass frit, and both the clear colorless filtrate and the collected white insoluble solid were dried under reduced pressure. The dried filtrate contained (*E*)-dimethyl(styryl)phosphine oxide as a white solid. Yield: 26.6 mg (0.15 mmol, 94%; MW: 180.19 g·mol⁻¹).

(E)-dimethyl(styryl)phosphine oxide. ¹H-NMR (600 MHz, CDCl_3 , 298 K): δ = 1.58 (d, ²J_{P-H} = 13.02 Hz, 6 H, $\text{P}(\text{CH}_3)_2$), 6.40 (dd, ²J_{P-H} = 24.63 Hz, ³J_{H-H} = 17.43 Hz, 1 H, $\text{PCH}=\text{CH}$), 7.30-7.36 (m, 3 H, CH_{Ar}), 7.41 (dd, ³J_{P-H} = 19.80 Hz, ³J_{H-H} = 17.43 Hz, $\text{PCH}=\text{CH}$), 7.46 (m, 2 H, CH_{Ar}). ¹³C{¹H}-NMR (151 MHz, C_6D_6 , 298 K): δ = 17.81 (d, ²J_{P-C} = 73.21 Hz, PCH_3) 121.2 (d, ²J_{P-C} = 6.04, $\text{PCH}=\text{CH}$), 24.1 ($\text{CH}_3)_2$), 127.5 (C_{Ar}), 128.9 (C_{Ar}), 129.9 (C_{Ar}), 135.0 (d, ²J_{P-C} = 17.4 Hz, *i*-C_{Ar}), 145.8 (d, ²J_{P-C} = 3.07 $\text{PCH}=\text{CH}$). ³¹P{¹H}-NMR (162 MHz, C_6D_6 , 298 K): δ = 31.6.

HRMS (ESI-MS) m/z: (M + Na)⁺ Calcd for $\text{C}_{10}\text{H}_{13}\text{OP}$ 203.06; Found 203.0598

In accordance with mass-balance and characteristic IR spectra, the white insoluble powder solid should be **Y(O₂PMe₂)₃**. The solid is insoluble in organic and aqueous media, which prevented solution characterization. Yield: 17.5 mg (0.48 mmol, 91%; MW: 368.03 g·mol⁻¹). **Y(O₂PMe₂)₃**. IR (Nujol): cm⁻¹; 1301(m), 1151(m, P=O) 1061(m, P=O), 864 (m), 728 (m), 435 (w)

Reaction of La₂(H^{Me}L)₆ with Benzaldehyde

A 20 mL scintillation vial was charged with **La₂(H^{Me}L)₆** (30.5 mg, 0.048mmol, 1 equiv, MW: 640.22 g·mol⁻¹), THF (2 mL), and a Teflon-coated stir bar. Benzaldehyde (15.3 mg, 0.146 mmol, 3 equiv, MW: 106.12) was added to the stirring colorless solution and stirred for 1.5 h at RT. During this time, formation of a white fluffy solid was observed. The solvents were removed under reduced pressure and the crude white solid was extracted with toluene (3 x 2 mL). The slurry was filtered through a medium porosity glass frit, and both the clear colorless filtrate and the collected white insoluble solid were dried under reduced pressure. The dried filtrate contained **(E)-dimethyl(styryl)phosphine oxide** as a white solid. Yield: 22.2 mg (0.12 mmol, 86%; MW: 180.19 g·mol⁻¹).

(E)-dimethyl(styryl)phosphine oxide. ¹H-NMR (600 MHz, CDCl₃, 298 K): δ = 1.58 (d, ²J_{P-H} = 13.02 Hz, 6 H, P(CH₃)₂), 6.40 (dd, ²J_{P-H} = 24.63 Hz, ³J_{H-H} = 17.43 Hz, 1 H, PC_H=CH), 7.30-7.36 (m, 3 H, CH_{Ar}), 7.41 (dd, ³J_{P-H} = 19.80 Hz, ³J_{H-H} = 17.43 Hz, PCH=CH), 7.46 (m, 2 H, CH_{Ar}). ¹³C{¹H}-NMR (151 MHz, C₆D₆, 298 K): δ = 17.81 (d, ²J_{P-C} = 73.21 Hz, PCH₃) 121.2 (d, ²J_{P-C} = 6.04, PC_H=CH), 24.1 (CH₃)₂), 127.5 (C_{Ar}), 128.9 (C_{Ar}), 129.9 (C_{Ar}), 135.0 (d, ²J_{P-C} = 17.4 Hz, i-C_{Ar}), 145.8 (d, ²J_{P-C} = 3.07 PCH=CH). ³¹P{¹H}-NMR (162 MHz, C₆D₆, 298 K): δ = 31.6.

In accordance with mass-balance and characteristic IR spectra, the white insoluble powder solid should be **La(O₂PMe₂)₃**. The solid is insoluble in organic and aqueous media, which prevented solution characterization. Yield: 17.5 mg (0.48 mmol, 88%; MW: 418.03 g·mol⁻¹).

La(O₂PMe₂)₃. IR (Nujol): cm⁻¹; 1297(s), 1139(s, P=O), 1110(s,P=O), 1049(m, P=O), 865 (s), 507 (m), 464 (w), 432(w)

Reaction of Y(H^{Ph}L)₃ with Benzaldehyde

A 20 mL scintillation vial was charged with **Y(H^{Ph}L)₃** (60.0 mg, 0.045mmol, 1 equiv, MW: 1335.07 g·mol⁻¹), tetrahydrofuran (3 mL), and a Teflon-coated stir bar. Benzaldehyde (14.31 mg, 0.135mmol, 3 equiv, MW: 106.12) was added to the stirring colorless solution and stirred for 1.5 h at RT forming a fluffy white solid. The solvents were removed under reduced pressure and the crude white solid was extracted with toluene (3 x 2 mL). The slurry was filtered through a medium porosity glass frit, and both the clear colorless filtrate and the collected white insoluble solid were dried under reduced pressure. The crude organic product was purified by dissolving in DCM (2mL) and running the solution through a plug of silica gel. The DCM fraction was discarded and a solution of DCM:MeOH (90:10, 3 mL) was used to recover the desired **(E)-diphenyl(styryl)phosphine oxide** from the silica gel. The clear colorless solution was dried under reduced pressure to yield **(E)-diphenyl(styryl)phosphine oxide** as a white solid. Yield: 38.5 mg (0.26 mmol, 94%; MW: 304.33 g·mol⁻¹).

(E)-diphenyl(styryl)phosphine oxide ^1H -NMR (600 MHz, CDCl_3 , 298 K): δ = 6.84 (dd, $^2J_{P-H}$ = 22.3 Hz, $^3J_{H-H}$ = 17.43 Hz, 1 H, $\underline{\text{PCH=CH}}$), 7.40-7.36 (m, 3 H, CH_{Ar}), 7.56-7.45 (m, 9H), 7.78-7.73 (m, 4H). $^{13}\text{C}\{\text{H}\}$ -NMR (151 MHz, C_6D_6 , 298 K): δ = 119.4 (d, $^2J_{P-C}$ = 104.47 Hz, $\underline{\text{PCH=CH}}$), 127.8 (C_{Ar}), 128.7 (d, J_{P-C} = 12.1 Hz, C_{Ar}), 128.9 (C_{Ar}), 130.2 (C_{Ar}), 131.4 (d, J_{C-P} = 10.0 Hz), 131.9 (d, J_{C-P} = 2.0 Hz), 133.1 (d, J_{C-P} = 105.6 Hz), 135.2 (d, J_{C-P} = 17.8 Hz), 147.6 (d, J_{C-P} = 3.6 Hz) (d, $^2J_{P-C}$ = 3.07 $\text{PCH}=\underline{\text{CH}}$). $^{31}\text{P}\{\text{H}\}$ -NMR (243 MHz, C_6D_6 , 298 K): δ = 24.43

In accordance with mass-balance and characteristic IR spectra, the white insoluble powder solid should be $\text{Y(O}_2\text{PPh}_2)_3$. The solid is insoluble in organic and aqueous media, which prevented solution characterization. Yield: 28.7 mg (0.42 mmol, 92%; MW: 695.33 g \cdot mol $^{-1}$). $\text{Y(O}_2\text{PPh}_2)_3$. IR (Nujol): cm^{-1} ; 1202(s), 1141(s, P=O), 1109 (m), 1080 (s), 1003 (s), 897 (m), 787 (m), 592(w), 521(m), 429 (s).

Reaction of $\text{La(H}^{\text{Ph}}\text{L})_3$ with Benzaldehyde

A 20 mL scintillation vial was charged with $\text{La(H}^{\text{Ph}}\text{L})_3$ (71.7 mg, 0.052 mmol, 1 equiv, MW: 1385.07 g \cdot mol $^{-1}$), tetrahydrofuran (3 mL), and a Teflon-coated stir bar. Benzaldehyde (16.48 mg, 0.155 mmol, 3 equiv, MW: 106.12) was added to the stirring colorless solution and stirred for 1.5 h at RT forming a fluffy white solid. The solvents were removed under reduced pressure and the crude white solid was extracted with toluene (3 x 2 mL). The slurry was filtered through a medium porosity glass frit, and both the clear colorless filtrate and the collected white insoluble solid were dried under reduced pressure. The crude organic product was purified by dissolving in DCM (2mL) and running the solution through a plug of silica gel. The DCM fraction was discarded and a solution of DCM:MeOH (90:10, 3 mL) was used to recover the desired **(E)-diphenyl(styryl)phosphine oxide** from the silica gel. The clear colorless solution was dried under reduced pressure to yield **(E)-diphenyl(styryl)phosphine oxide** as a white solid. Yield: 36.2 mg (0.12 mmol, 77%; MW: 304.33 g \cdot mol $^{-1}$).

(E)-diphenyl(styryl)phosphine oxide ^1H -NMR (600 MHz, CDCl_3 , 298 K): δ = 6.84 (dd, $^2J_{P-H}$ = 22.3 Hz, $^3J_{H-H}$ = 17.43 Hz, 1 H, $\underline{\text{PCH=CH}}$), 7.40-7.36 (m, 3 H, CH_{Ar}), 7.56-7.45 (m, 9H), 7.78-7.73 (m, 4H). $^{13}\text{C}\{\text{H}\}$ -NMR (151 MHz, C_6D_6 , 298 K): δ = 119.4 (d, $^2J_{P-C}$ = 104.47 Hz, $\underline{\text{PCH=CH}}$), 127.8 (C_{Ar}), 128.7 (d, J_{P-C} = 12.1 Hz, C_{Ar}), 128.9 (C_{Ar}), 130.2 (C_{Ar}), 131.4 (d, J_{C-P} = 10.0 Hz), 131.9 (d, J_{C-P} = 2.0 Hz), 133.1 (d, J_{C-P} = 105.6 Hz), 135.2 (d, J_{C-P} = 17.8 Hz), 147.6 (d, J_{C-P} = 3.6 Hz) (d, $^2J_{P-C}$ = 3.07 $\text{PCH}=\underline{\text{CH}}$). $^{31}\text{P}\{\text{H}\}$ -NMR (243 MHz, C_6D_6 , 298 K): δ = 24.43

In accordance with mass-balance and characteristic IR spectra, the white insoluble powder solid should be $\text{La(O}_2\text{PPh}_2)_3$. The solid is insoluble in organic and aqueous media, which prevented solution characterization. Yield: 28.7 mg (0.42 mmol, 92%; MW: 695.33 g \cdot mol $^{-1}$).

$\text{La(O}_2\text{PPh}_2)_3$. IR (Nujol): cm^{-1} ; 1304(w), 1132(s, P=O), 1045 (s), 1021 (m), 997 (s), 694 (m), 558 (s), 535(m)

General procedure for reactions of $\text{Y(H}^{\text{R}}\text{L})_3$ or $\text{Y}_2(\text{H}^{\text{Me}}\text{L}$ with MeOD ($\text{Y}_2(\text{H}^{\text{Me}}\text{L})_6$).

In an N_2 -filled glovebox, a screw-cap NMR tube was charged with $\text{Y}_2(\text{H}^{\text{Me}}\text{L})_6$ (18.0 mg, 0.0305 mmol, 1.0 equiv; MW: 590.22 g \cdot mol $^{-1}$) and CD_2Cl_2 (0.5 mL). ^1H -, ^2H -, and $^{31}\text{P}\{\text{H}\}$ -NMR spectra were taken prior to and after the addition of further reagents. A CH_2Cl_2 solution of

MeOD (1% w/w, 0.227 mL, $\rho = 1.33 \text{ g/mL}$; 3.02 mg, 0.0915 mmol, 3.0 equiv; MW: 33.05 g·mol⁻¹) was then added to the light-pink solution. A small amount of colorless precipitate was formed at this time. After 10 min, a CH₂Cl₂ solution of benzoic acid (2% w/w, 0.421 mL, $\rho = 1.33 \text{ g/mL}$; 11.17 mg, 0.0915 mmol, 3.0 equiv; MW: 122.12 g·mol⁻¹) was added to the light-pink mixture to yield a light-pink clear solution. All volatiles were removed under reduced pressure resulting in a colorless solid, which was redissolved in CD₂Cl₂ and NMR spectra were collected.

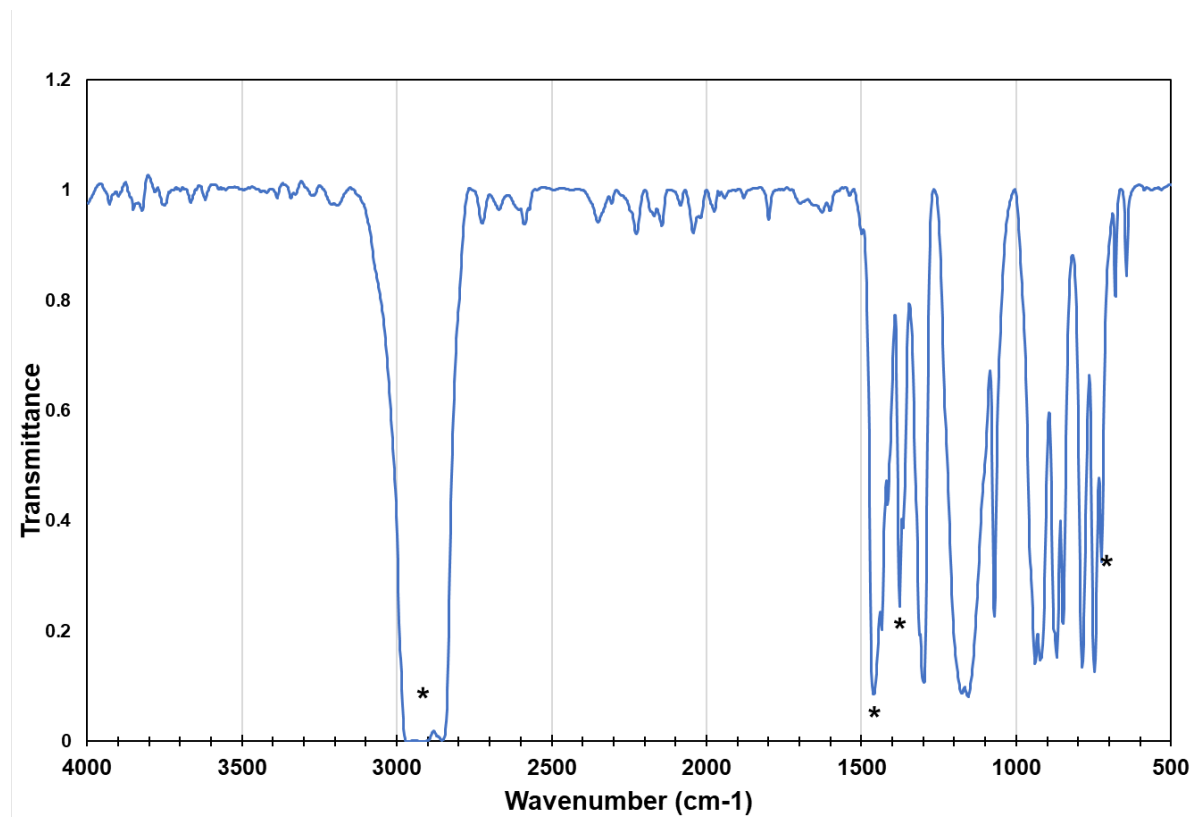


Figure S1a. IR (Nujol) spectrum of H₂^{Me}L (*: Nujol)

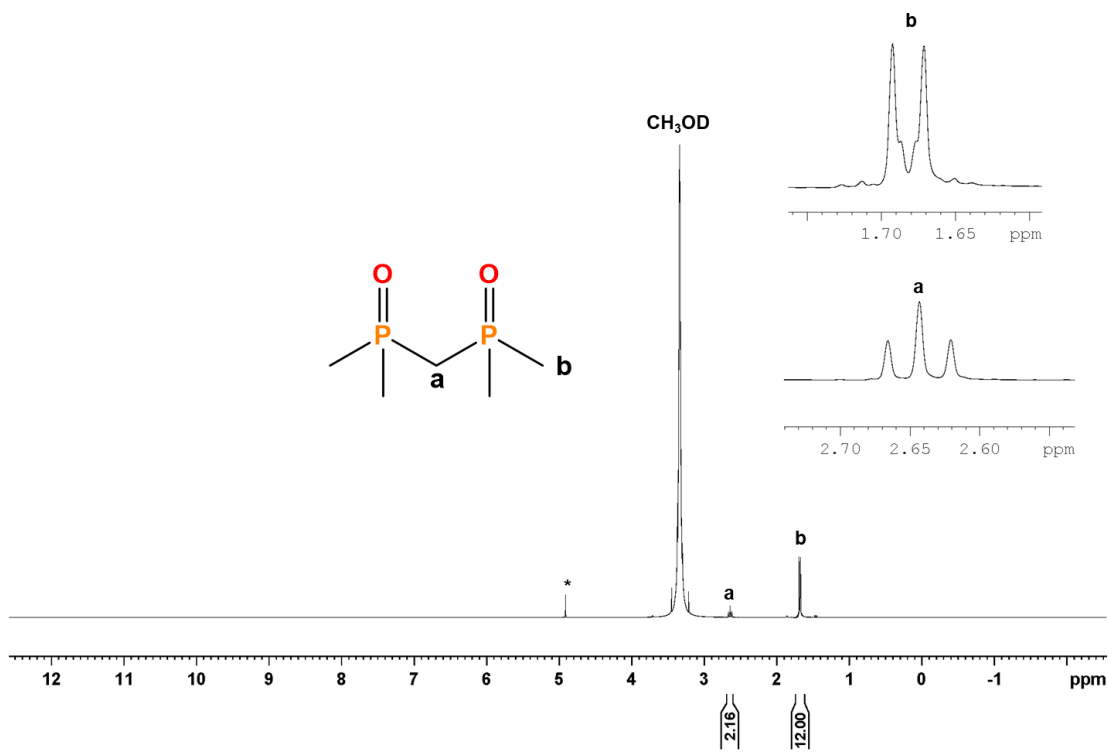


Figure S1b. ^1H -NMR (CH_3OD , 600 MHz) spectrum of $\text{H}_2^{\text{Me}}\text{L}$. * = H_2O (present in NMR solvent).

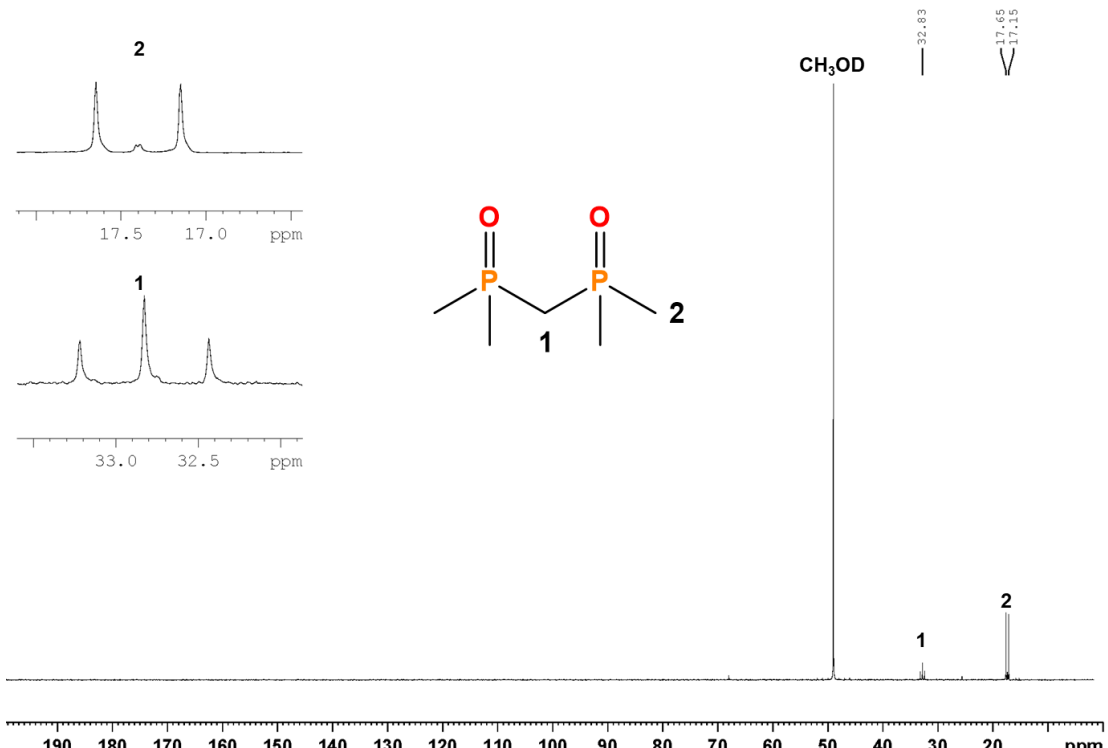


Figure S1c. $^{13}\text{C}\{^1\text{H}\}$ -NMR (CH_3OD , 152 MHz) spectrum of $\text{H}_2^{\text{Me}}\text{L}$

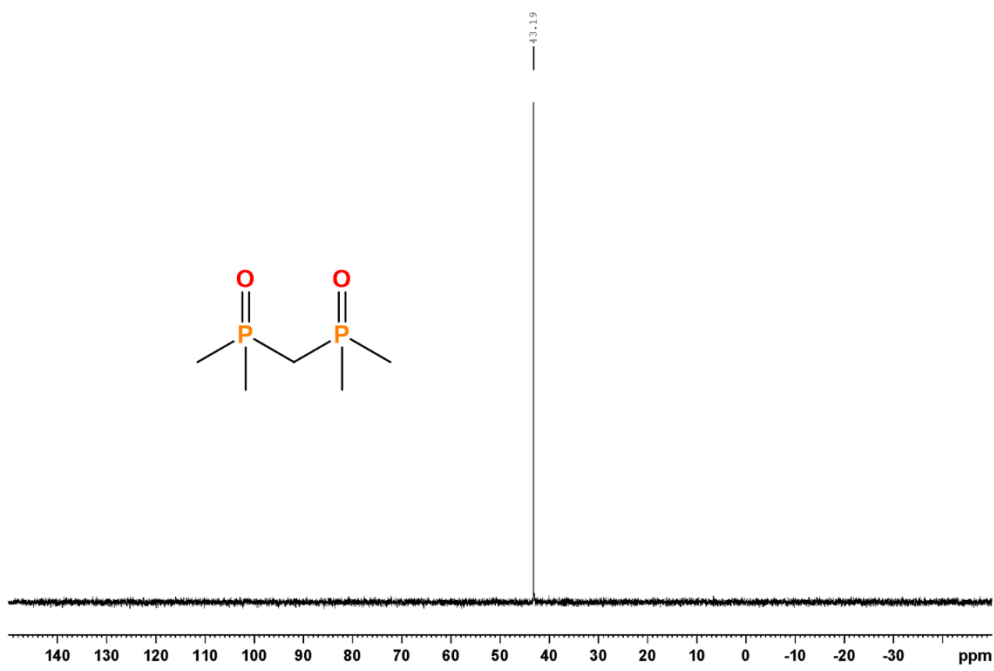


Figure S1d. $^{31}\text{P}\{\text{H}\}$ -NMR (CH_3OD , 242 MHz) of **1**.

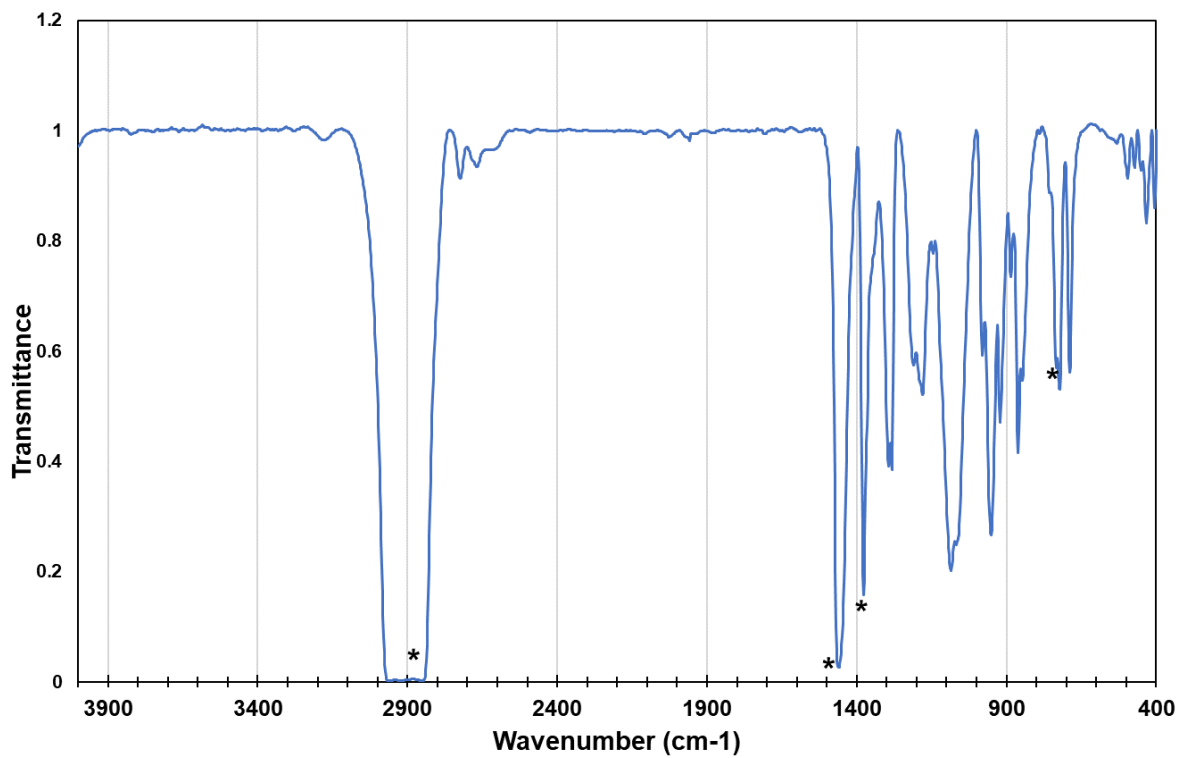


Figure S2a. IR (Nujol) spectrum of $\text{Y}_2(\text{H}^{\text{Me}}\text{L})_6$ (*: Nujol)

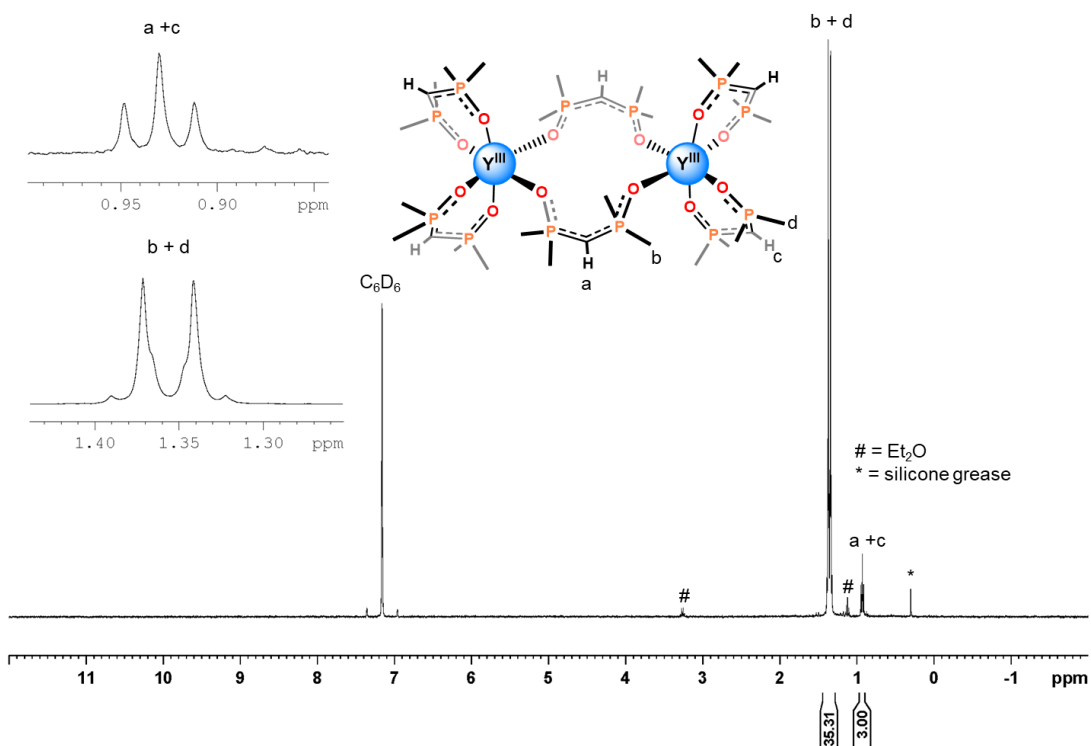


Figure S2b. ^1H -NMR (C_6D_6 , 400 MHz) spectrum of $\text{Y}_2(\text{H}^{\text{Me}}\text{L})_6$.

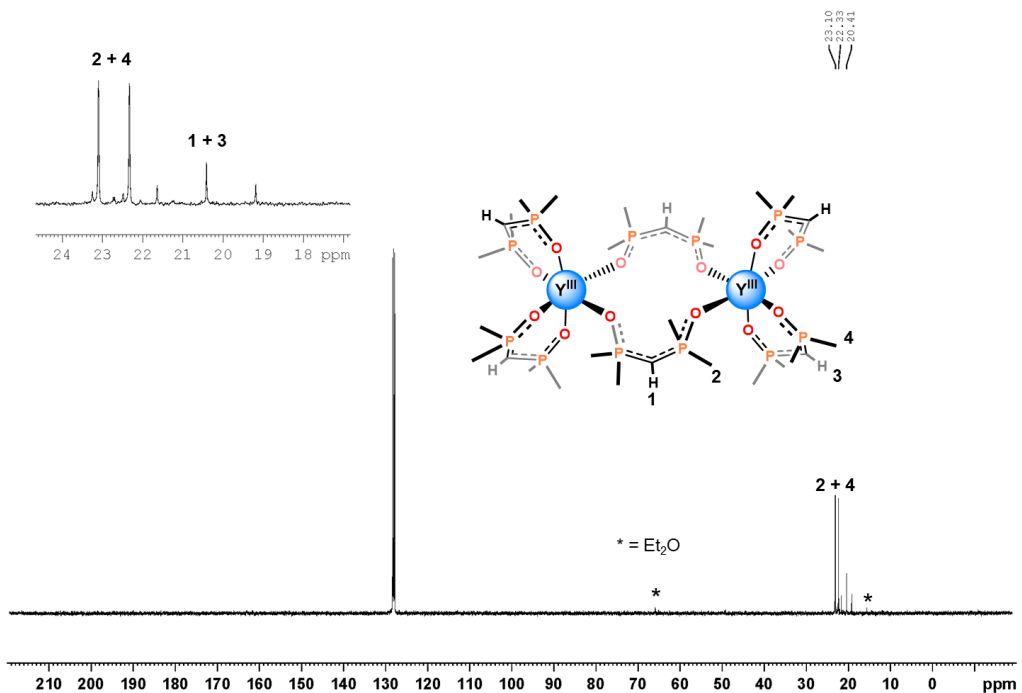


Figure S2c. $^{13}\text{C}\{^1\text{H}\}$ -NMR (C_6D_6 , 100 MHz) spectrum of $\text{Y}_2(\text{H}^{\text{Me}}\text{L})_6$.

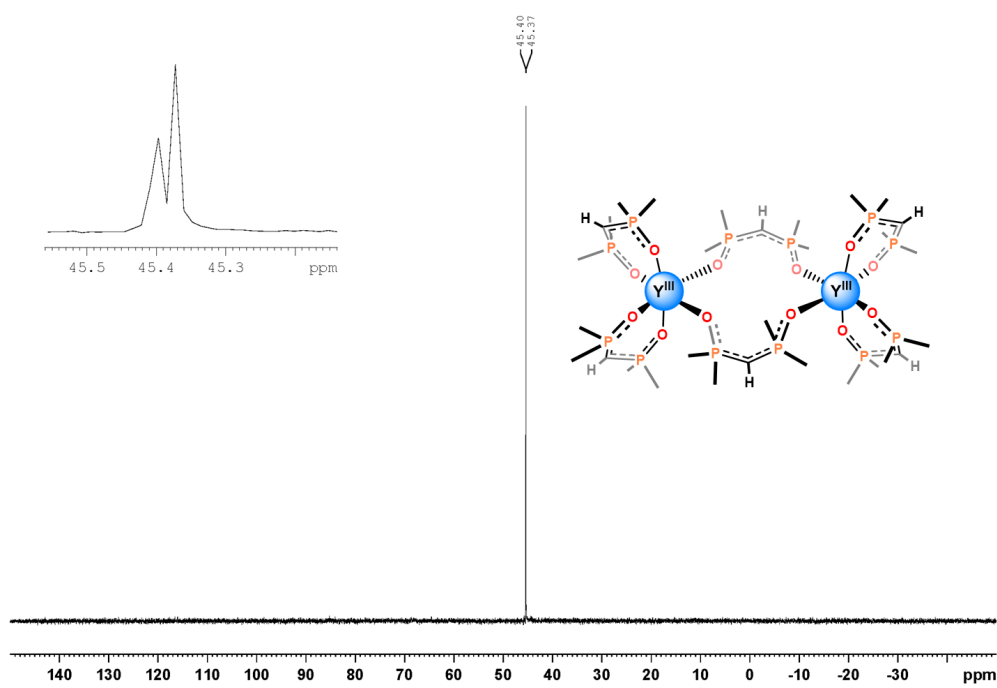


Figure S2d. $^{31}\text{P}\{\text{H}\}$ -NMR (C_6D_6 , 242 MHz) spectrum of $\text{Y}_2(\text{H}^{\text{Me}}\text{L})_6$.

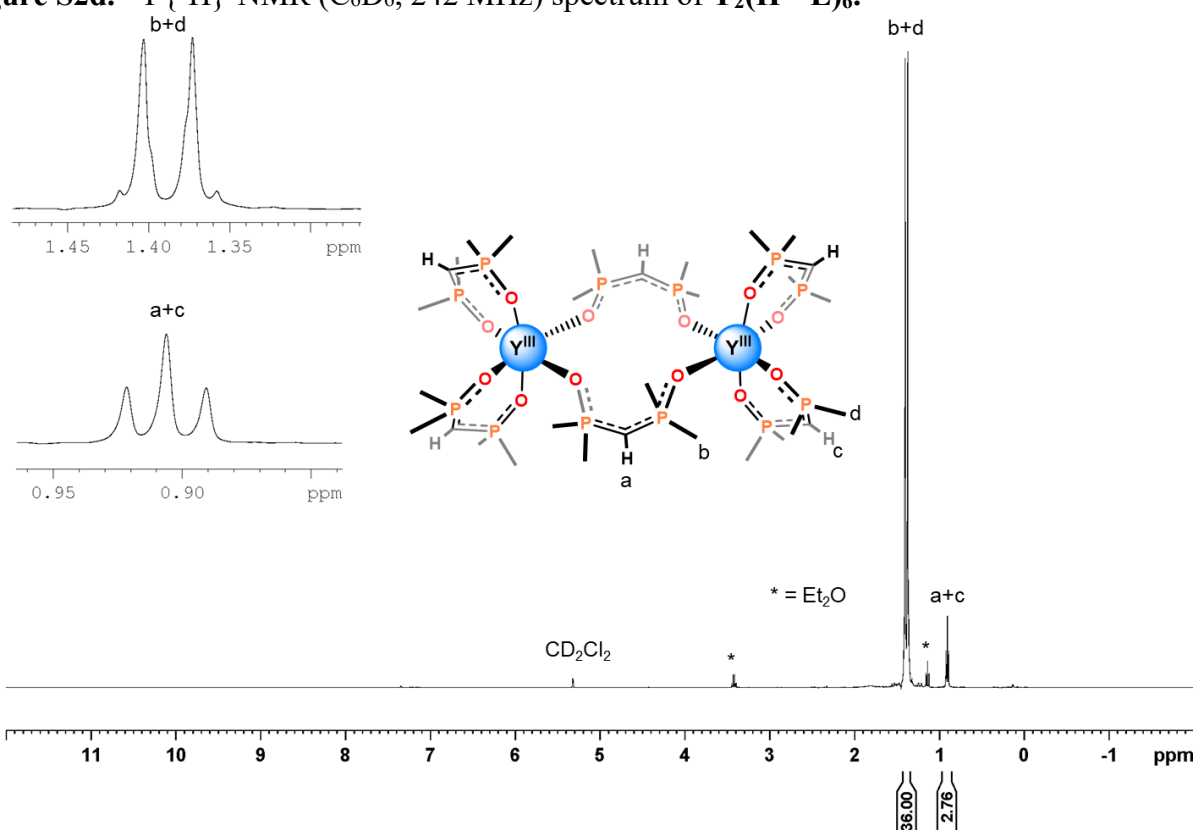


Figure S2e. ^1H -NMR (CD_2Cl_2 , 400 MHz) spectrum of $\text{Y}_2(\text{H}^{\text{Me}}\text{L})_6$.

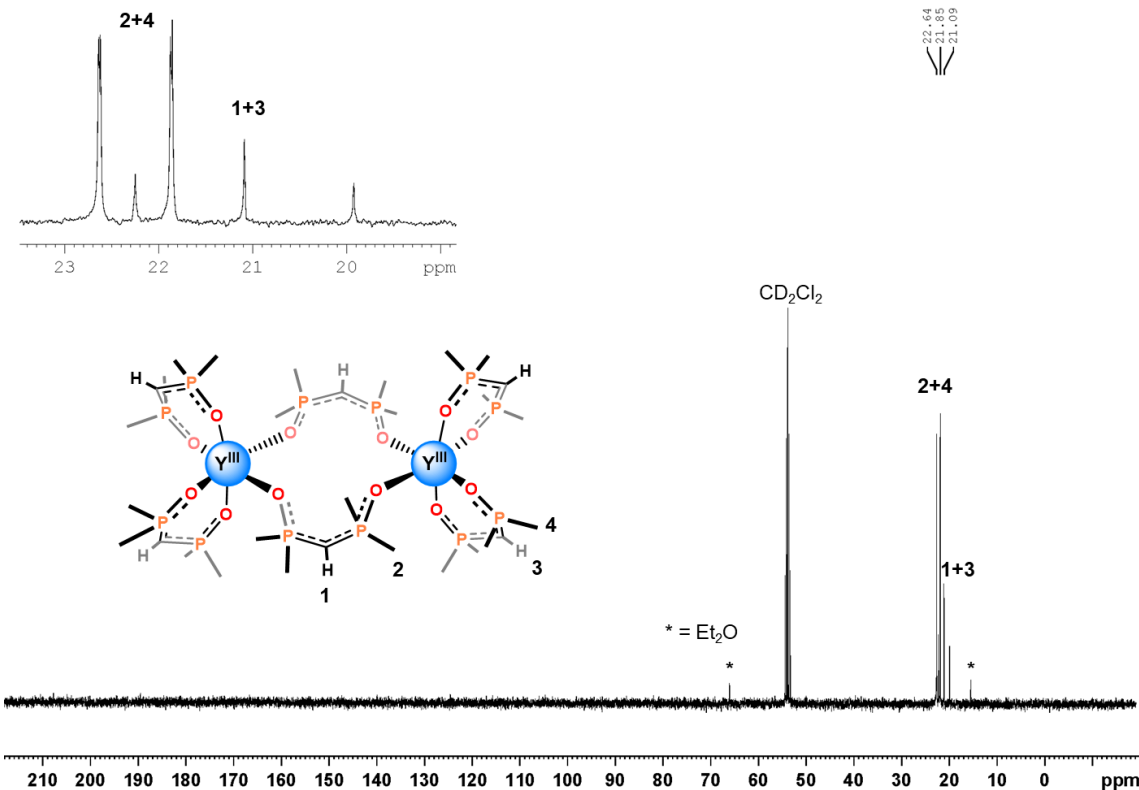


Figure S2f. $^{13}\text{C}\{^1\text{H}\}$ -NMR (CD₂Cl₂, 100 MHz) spectrum of $\text{Y}_2(\text{H}^{\text{Me}}\text{L})_6$.

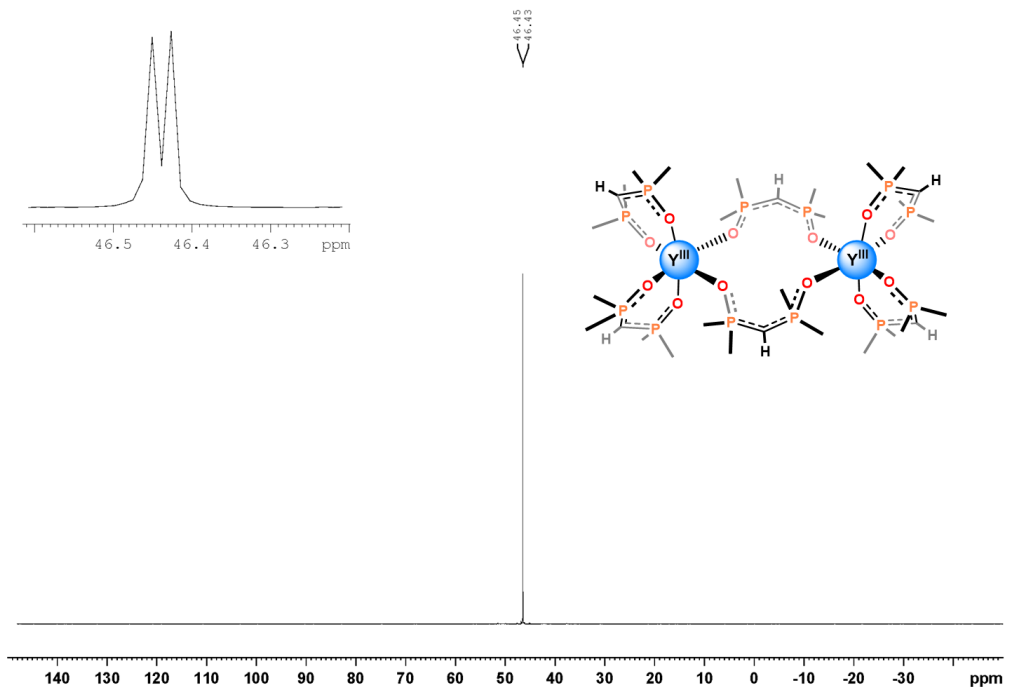


Figure S2g. $^{31}\text{P}\{^1\text{H}\}$ -NMR (CD₂Cl₂, 242 MHz) spectrum of $\text{Y}_2(\text{H}^{\text{Me}}\text{L})_6$.

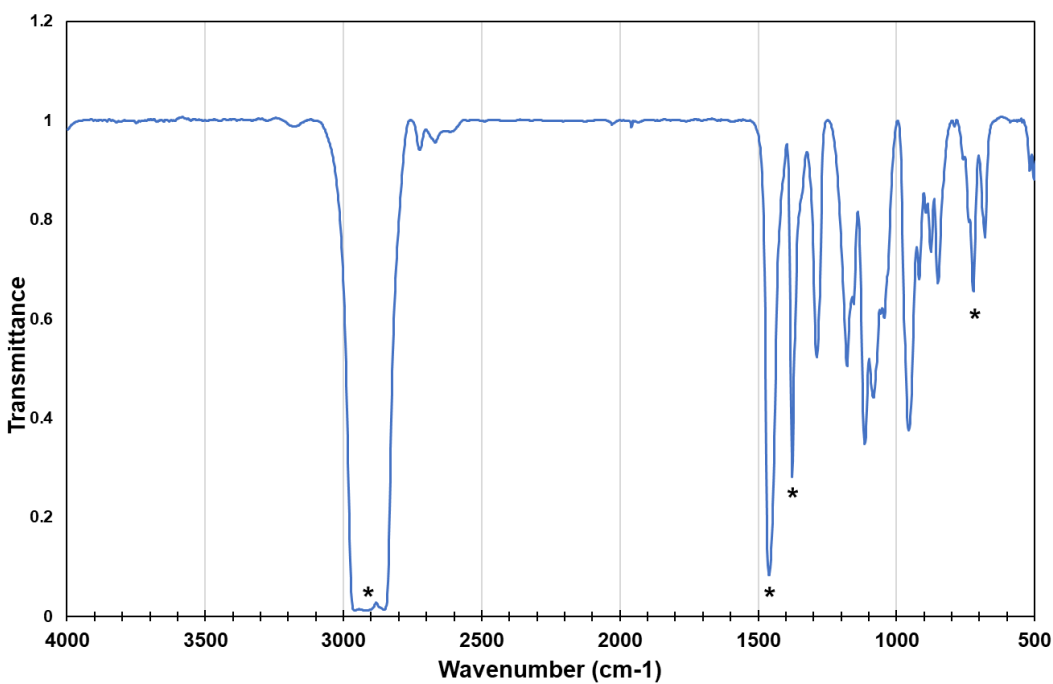


Figure S3a. IR (Nujol) spectrum of $\text{La}_2(\text{H}^{\text{Me}}\text{L})_6$ (*: Nujol)

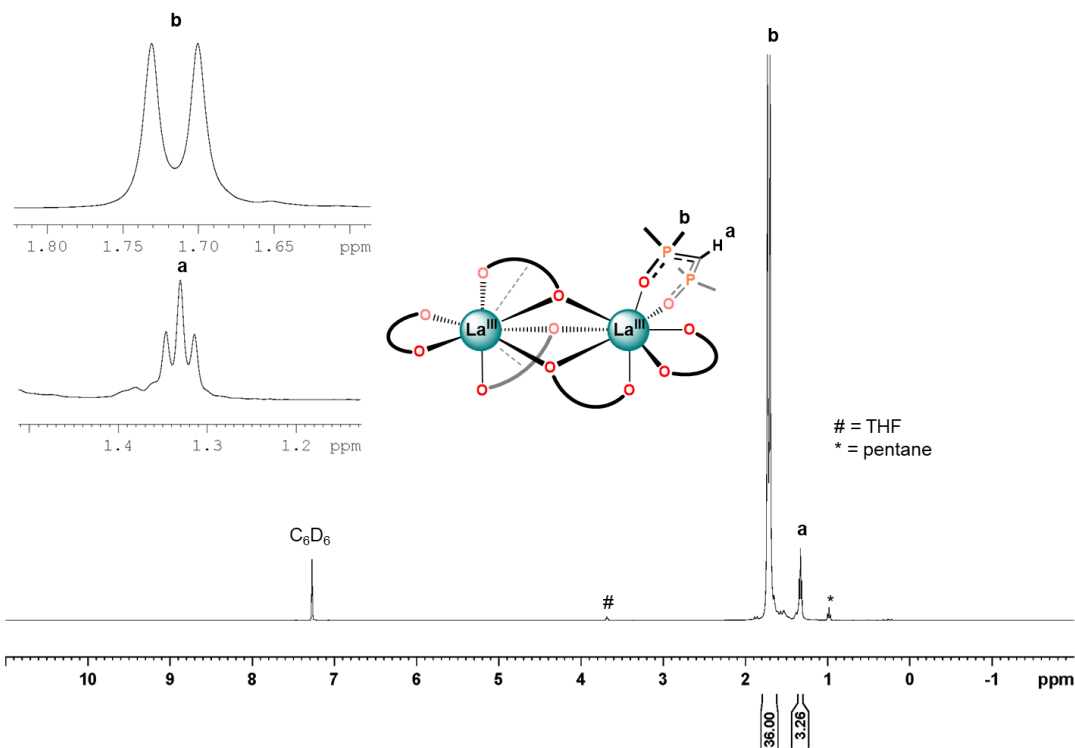


Figure S3a. ^1H -NMR (C_6D_6 , 400 MHz) spectrum of $\text{La}_2(\text{H}^{\text{Me}}\text{L})_6$.

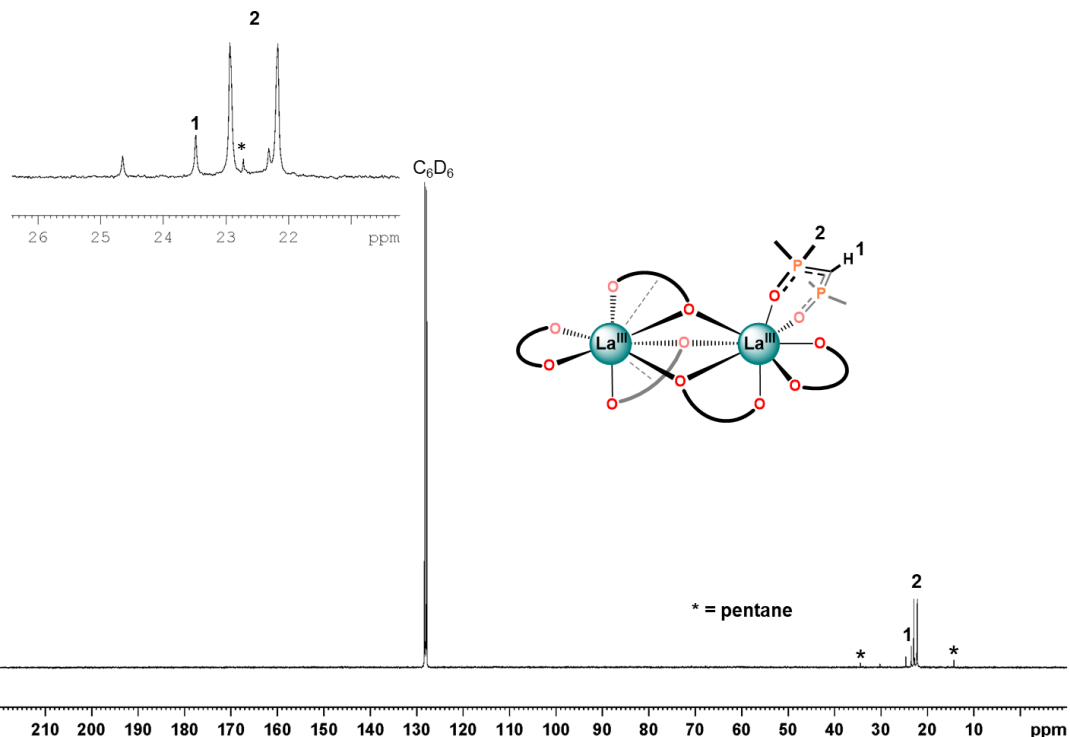


Figure S3b. $^{13}\text{C}\{^1\text{H}\}$ -NMR (C_6D_6 , 100 MHz) spectrum of $\text{La}_2(\text{H}^{\text{Me}}\text{L})_6$.

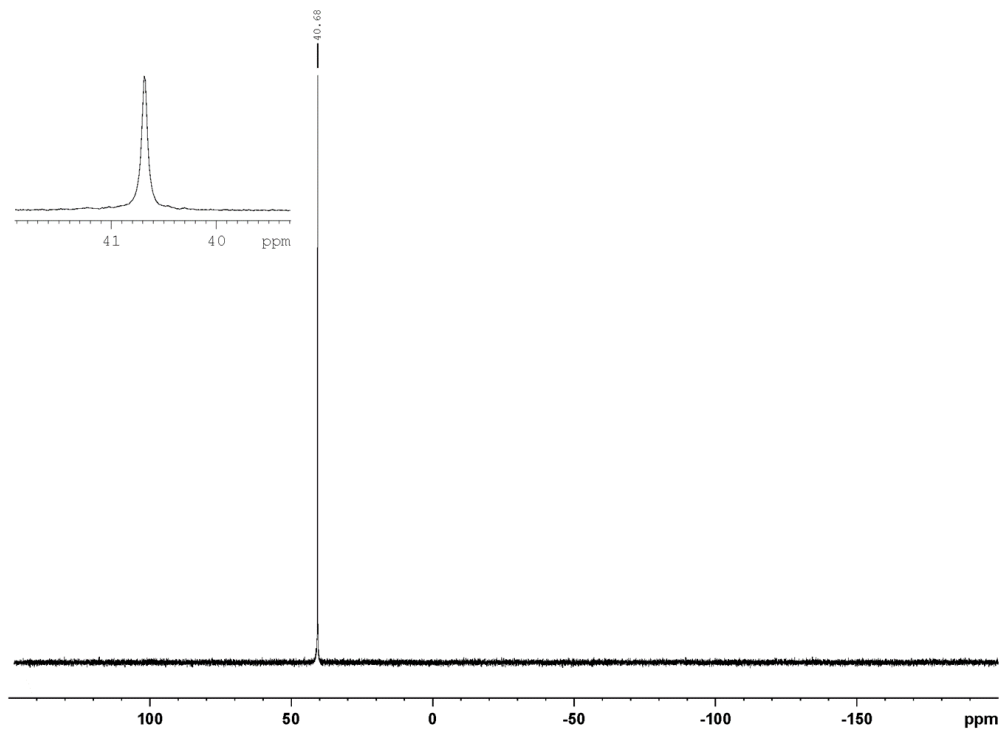


Figure S3c. $^{31}\text{P}\{^1\text{H}\}$ -NMR (C_6D_6 , 242 MHz,) spectrum of $\text{La}_2(\text{H}^{\text{Me}}\text{L})_6$.

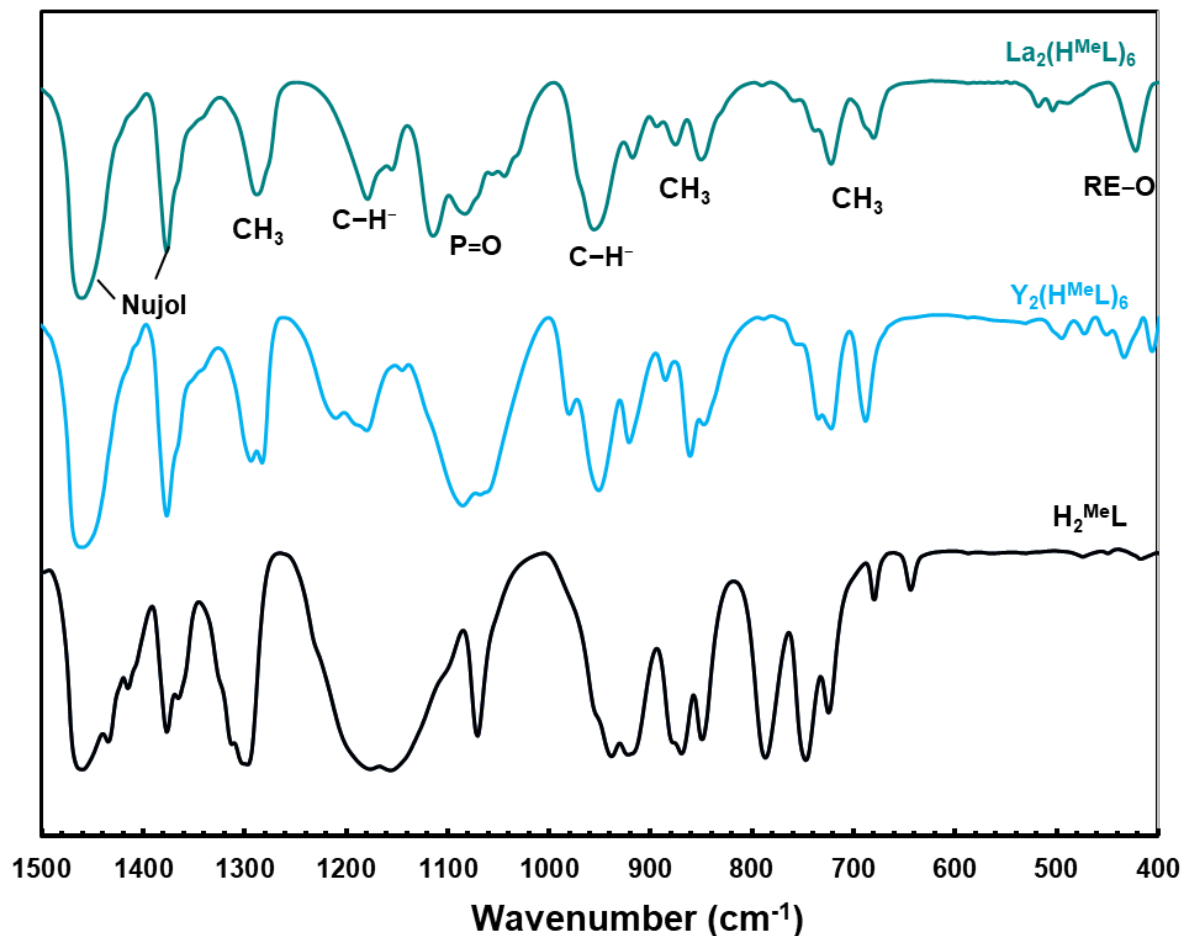


Figure S4. Overlay of IR spectrum (Nujol Mull) of $\text{RE}_2(\text{H}^{\text{Me}}\text{L})_6$ and $\text{H}_2^{\text{Me}}\text{L}$ from $1500 - 400 \text{ cm}^{-1}$.

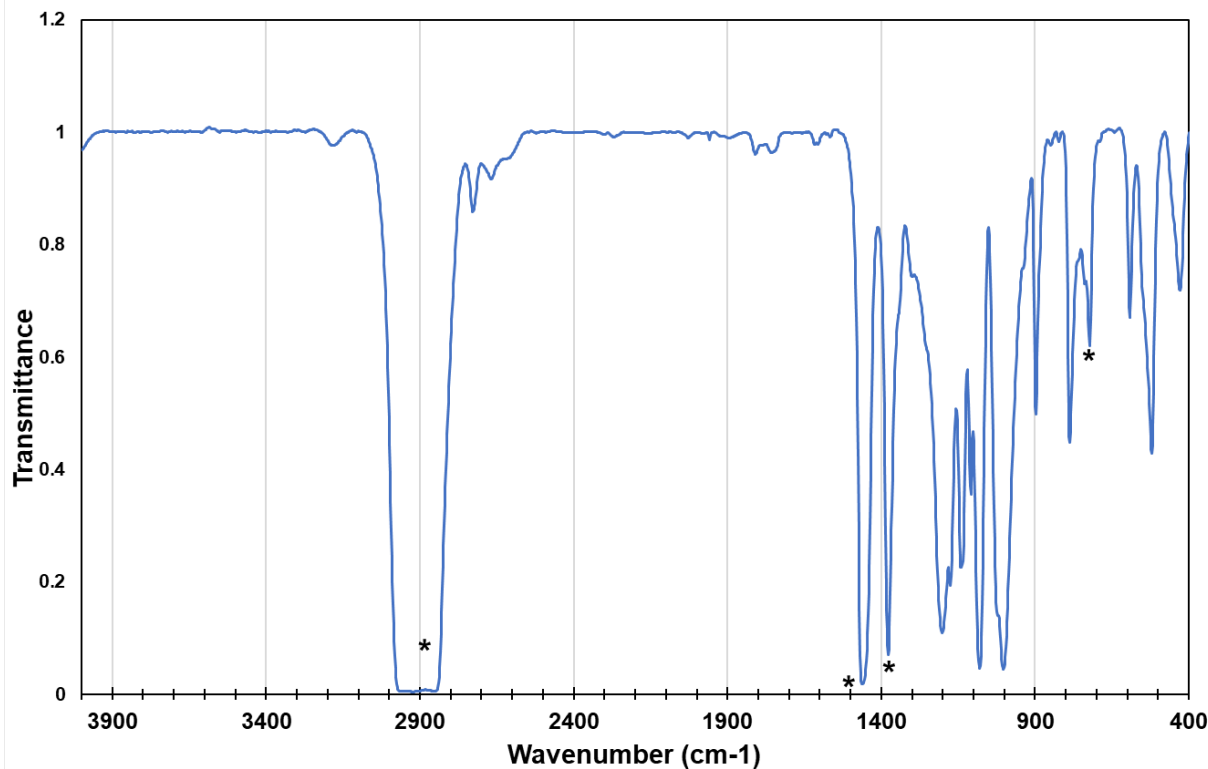


Figure S5a. IR (Nujol) spectrum of $\text{Y}(\text{H}^{\text{Ph}}\text{L})_3$ (*: Nujol)

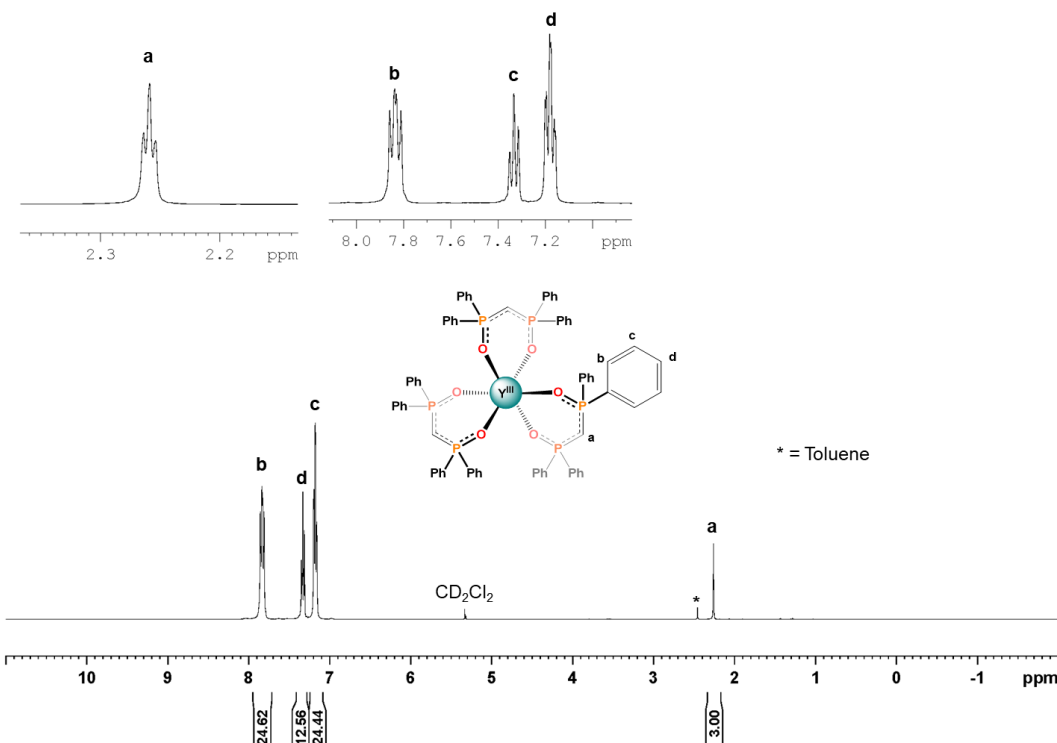


Figure S5b. ¹H-NMR (CD_2Cl_2 , 400 MHz) spectrum of $\text{Y}(\text{H}^{\text{Ph}}\text{L})_3$.

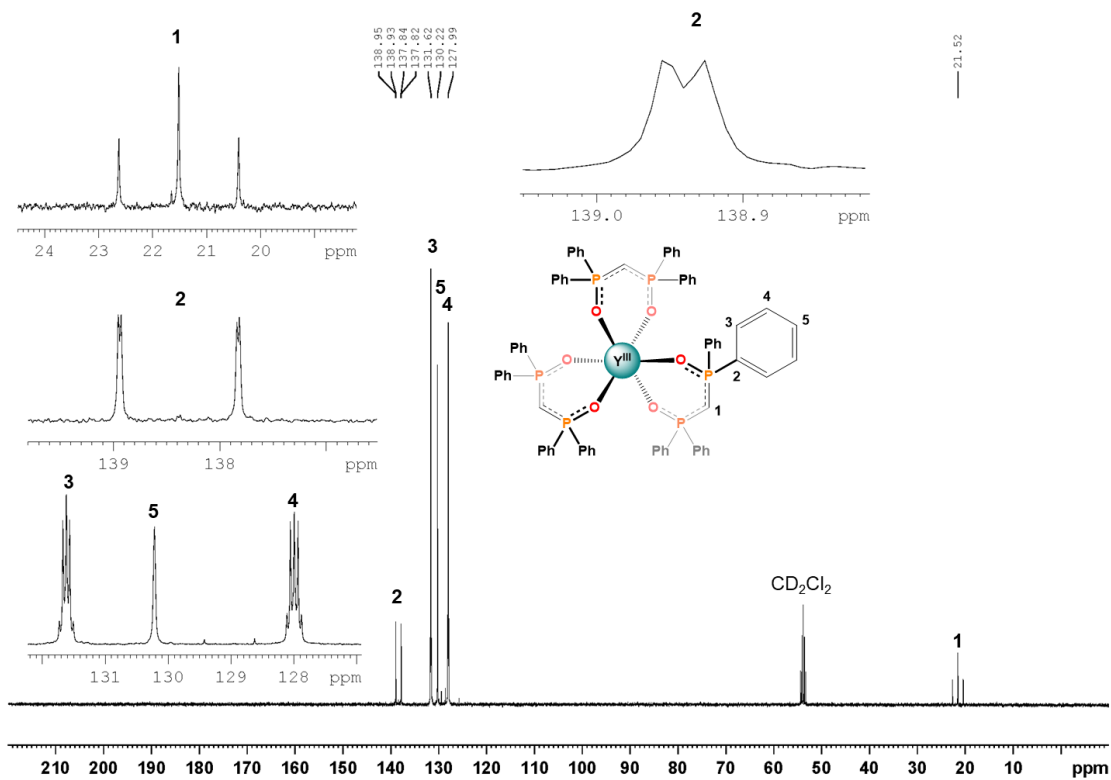


Figure S5c. $^{13}\text{C}\{^1\text{H}\}$ -NMR (CD_2Cl_2 , 100 MHz) spectrum of $\text{Y}(\text{H}^{\text{Ph}}\text{L})_3$.

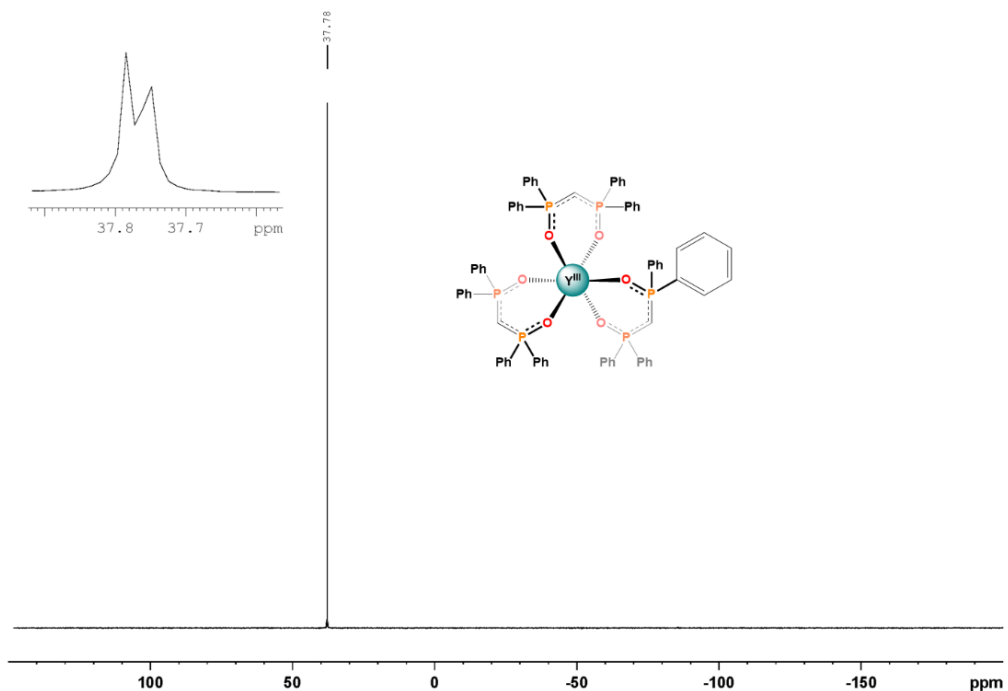


Figure S5d. $^{31}\text{P}\{^1\text{H}\}$ -NMR (CD_2Cl_2 , 162 MHz) spectrum of $\text{Y}(\text{H}^{\text{Ph}}\text{L})_3$.

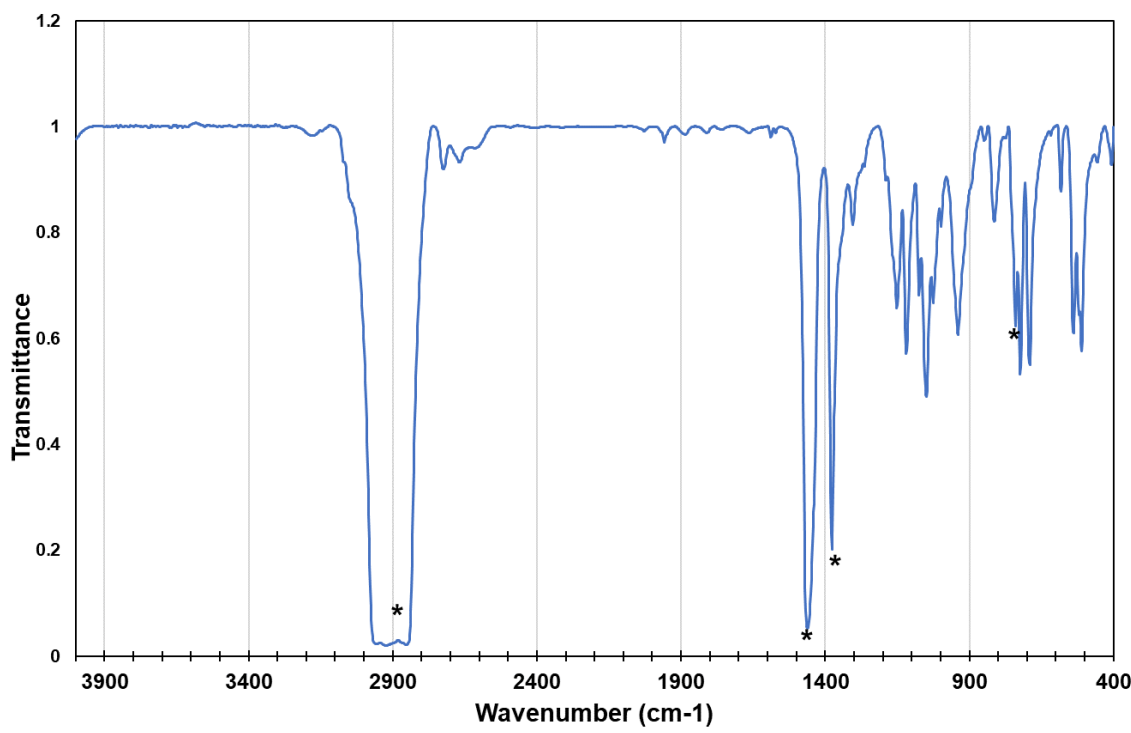


Figure S6a. IR (Nujol) spectrum of $\text{La}(\text{H}^{\text{Ph}}\text{L})_3$. (*: Nujol)

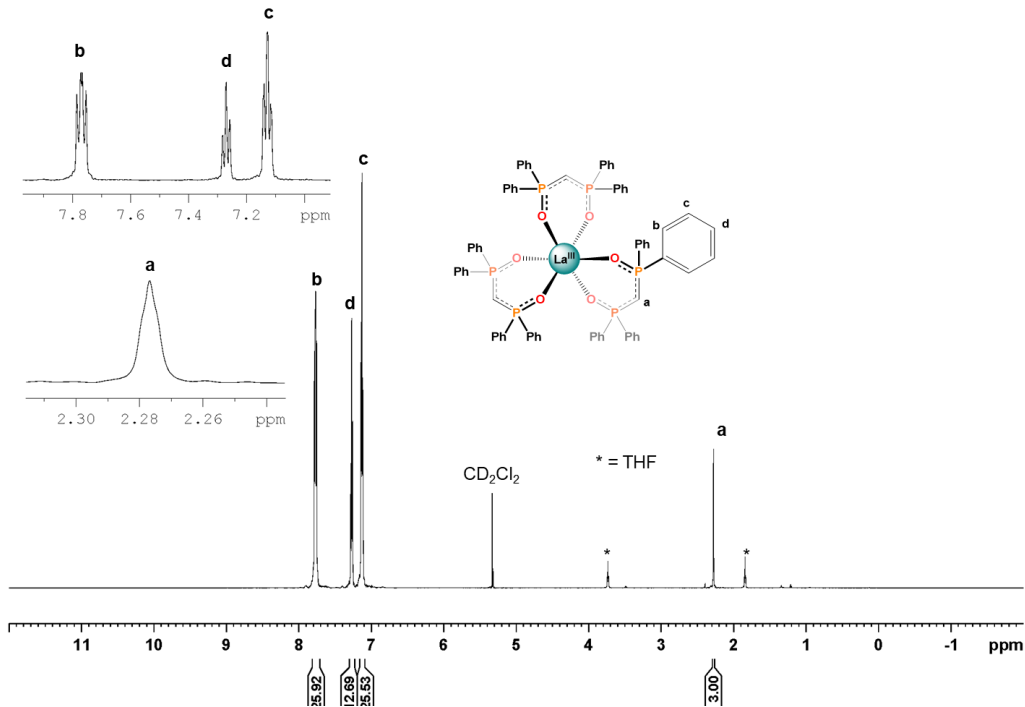


Figure S6b. ^1H -NMR (CD_2Cl_2 , 400 MHz) spectrum of $\text{La}(\text{H}^{\text{Ph}}\text{L})_3$.

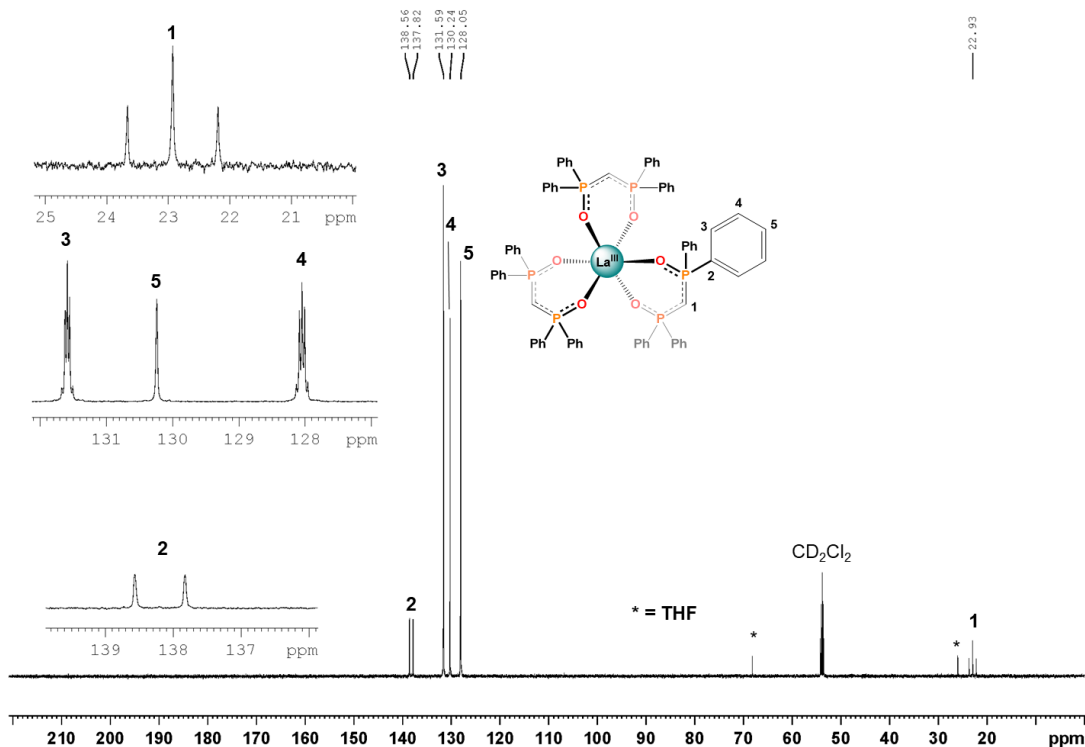


Figure S6c. $^{13}\text{C}\{^1\text{H}\}$ -NMR (CD_2Cl_2 , 100 MHz) spectrum of $\text{La}(\text{H}^{\text{Ph}}\text{L})_3$.

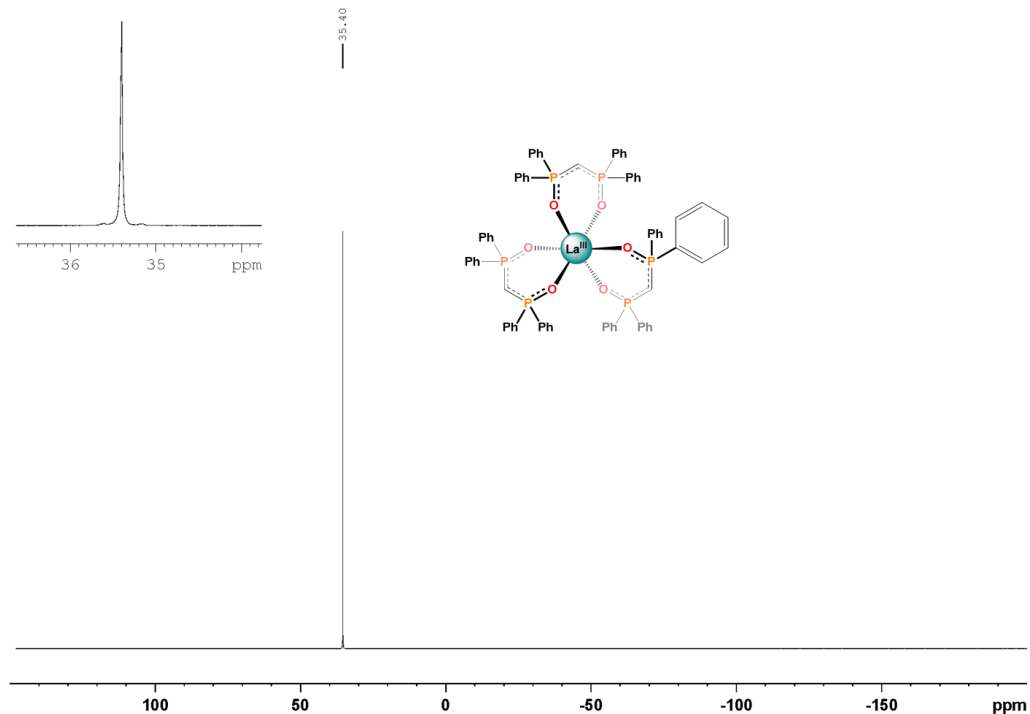


Figure S6d. $^{31}\text{P}\{^1\text{H}\}$ -NMR (CD_2Cl_2 , 162 MHz) spectrum of $\text{La}(\text{H}^{\text{Ph}}\text{L})_3$.

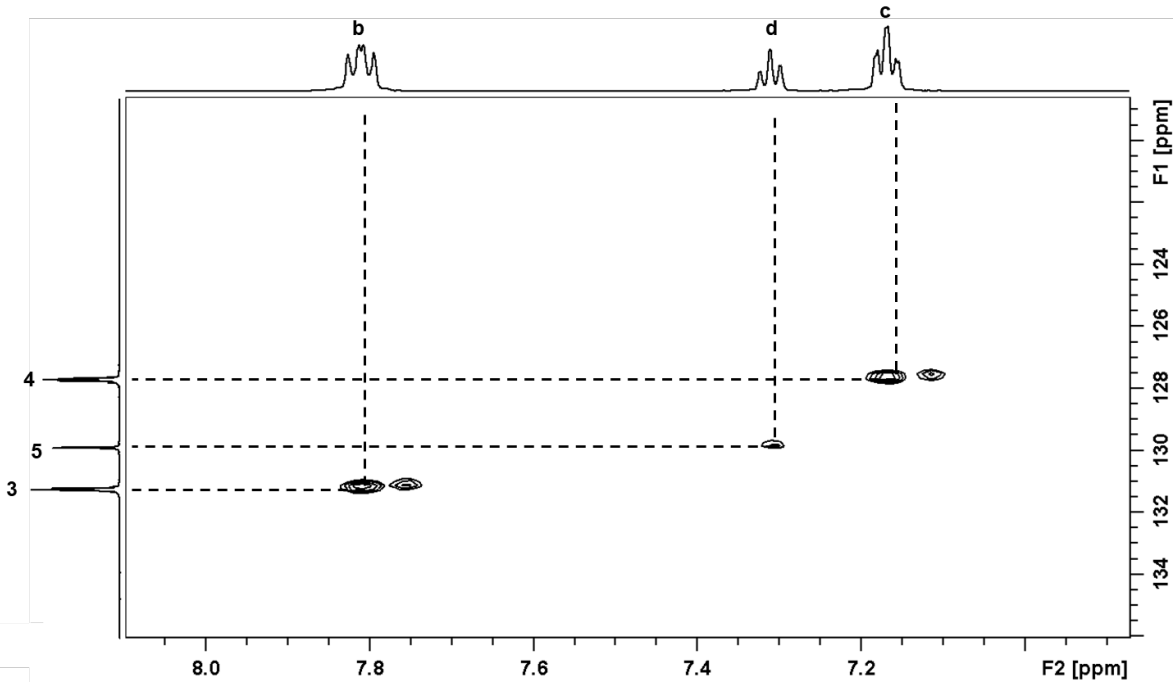


Figure S6e. Selected region of ^1H - $^{13}\text{C}\{^1\text{H}\}$ HSQC (CD_2Cl_2) of $\text{La}(\text{H}^{\text{Ph}}\text{L})_3$. Note: $^1\text{H} = 400$ MHz

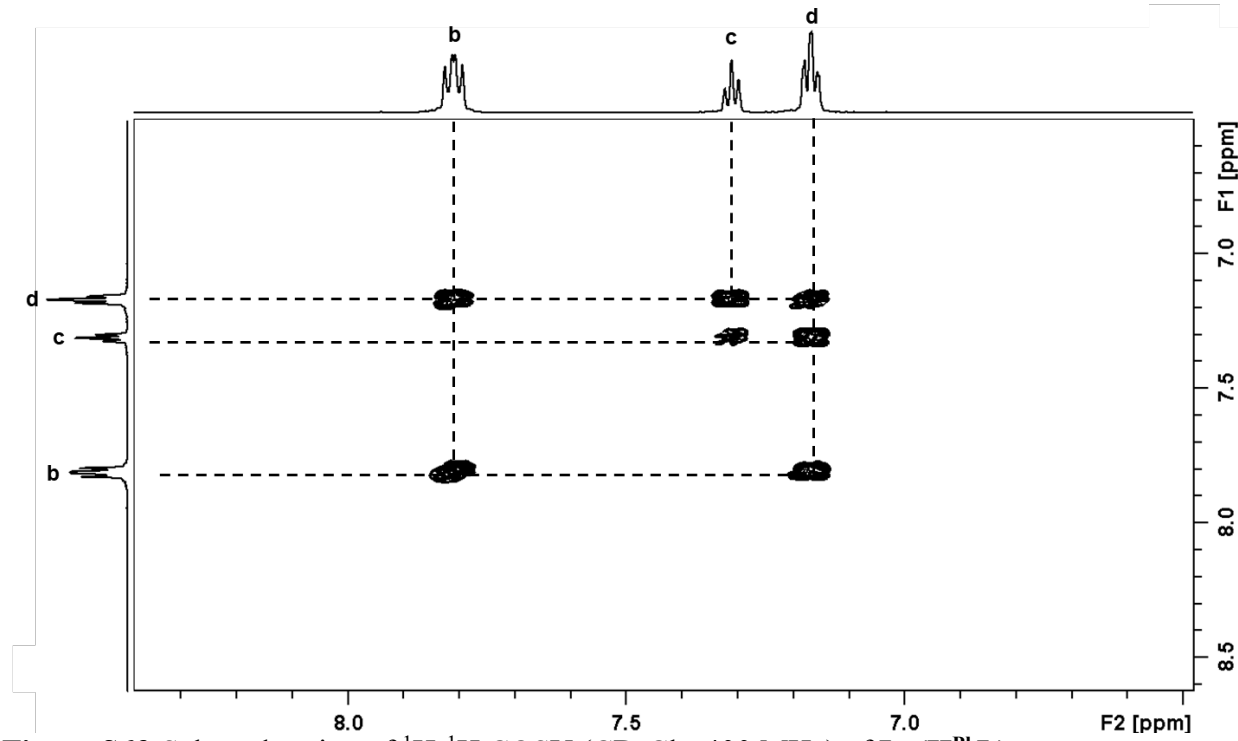


Figure S6f. Selected region of ^1H - ^1H COSY (CD_2Cl_2 , 400 MHz) of $\text{La}(\text{H}^{\text{Ph}}\text{L})_3$.

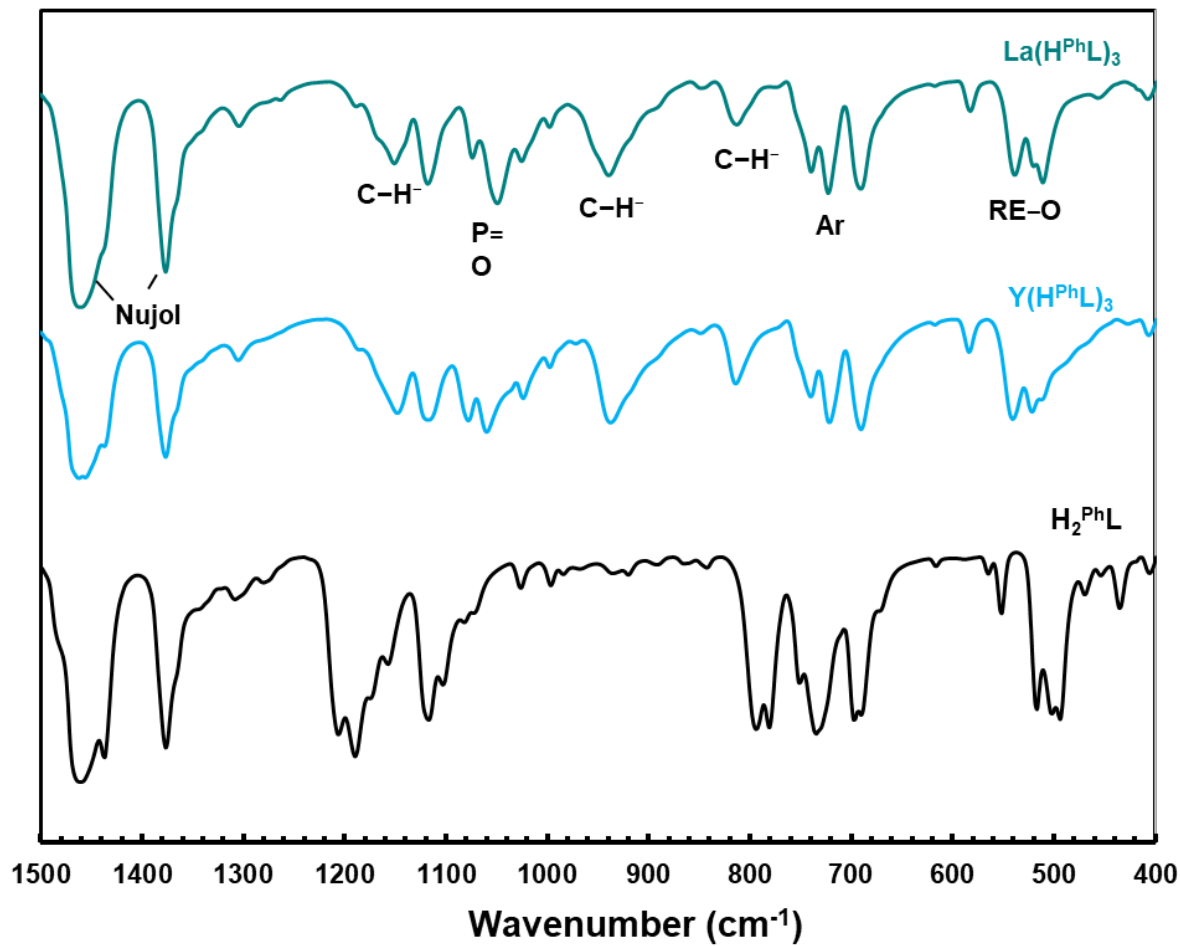


Figure S7. Overlay of IR spectrum (Nujol Mull) of $\text{RE}(\text{H}^{\text{Ph}}\text{L})_3$ and $\text{H}_2^{\text{Ph}}\text{L}$ from 1500 – 400 cm⁻¹.

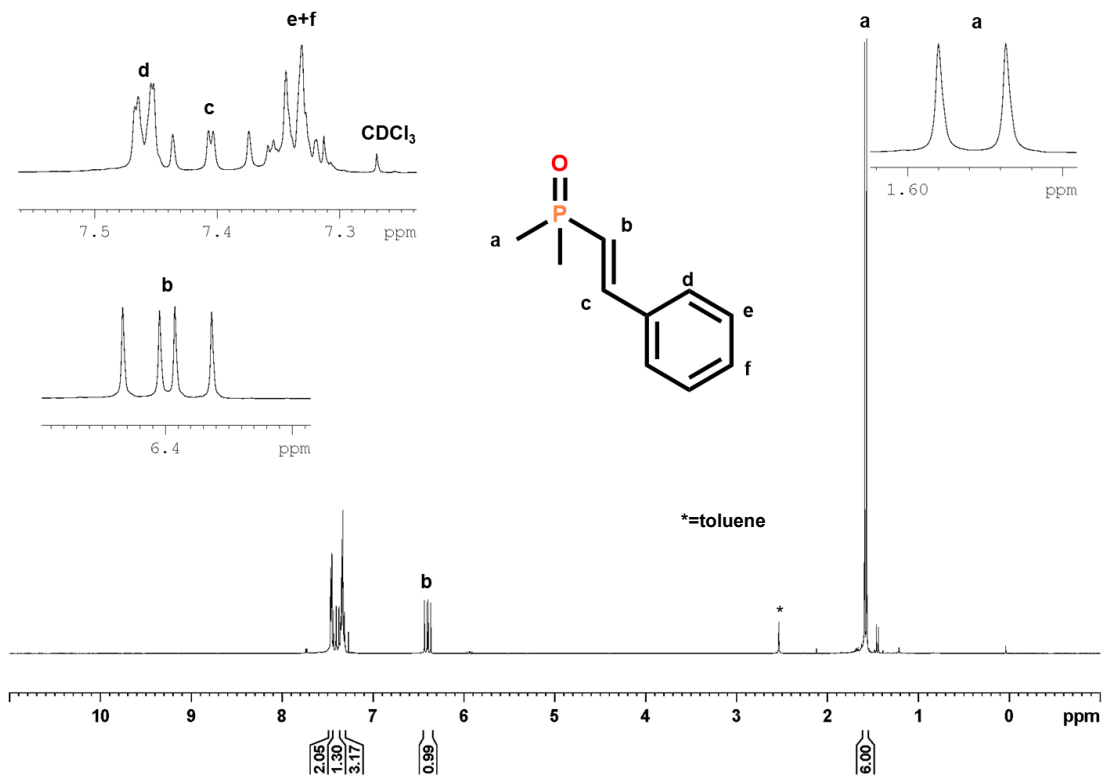


Figure S8a. ^1H -NMR (CDCl_3 , 600 MHz) spectrum of **(E)-dimethyl(styryl)phosphine oxide** from reaction of **Y₂(H^{Me}L)₆** with benzaldehyde.

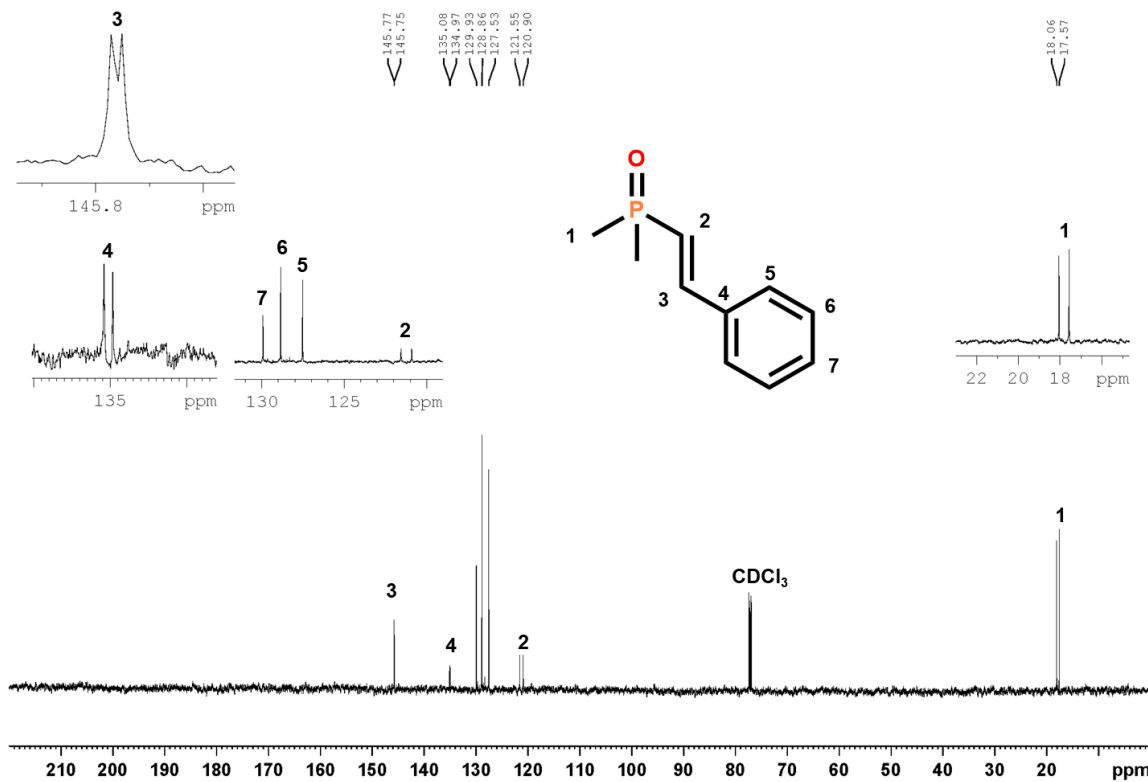


Figure S8b. $^{13}\text{C}\{^1\text{H}\}$ -NMR (CDCl_3 , 152 MHz) spectrum of **(E)-dimethyl(styryl)phosphine oxide** from reaction of $\text{Y}_2(\text{H}^{\text{Me}}\text{L})_6$ with benzaldehyde.

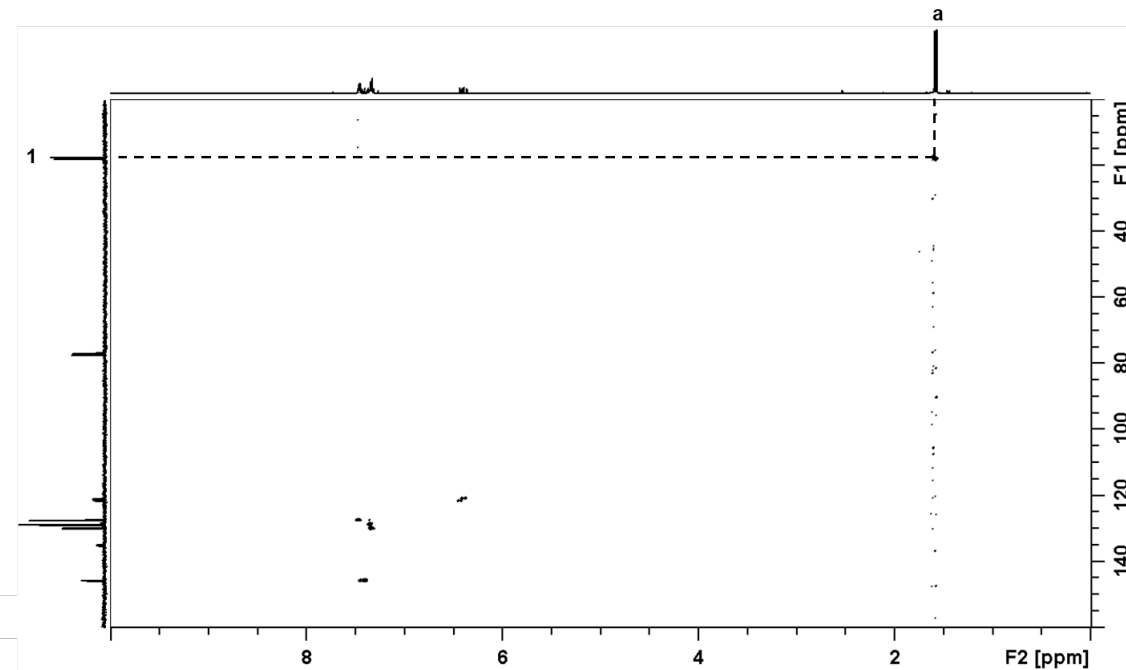


Figure S8c. ^1H - $^{13}\text{C}\{^1\text{H}\}$ HSQC (CDCl_3) of **(E)-dimethyl(styryl)phosphine oxide**. Note: ^1H = 600 MHz

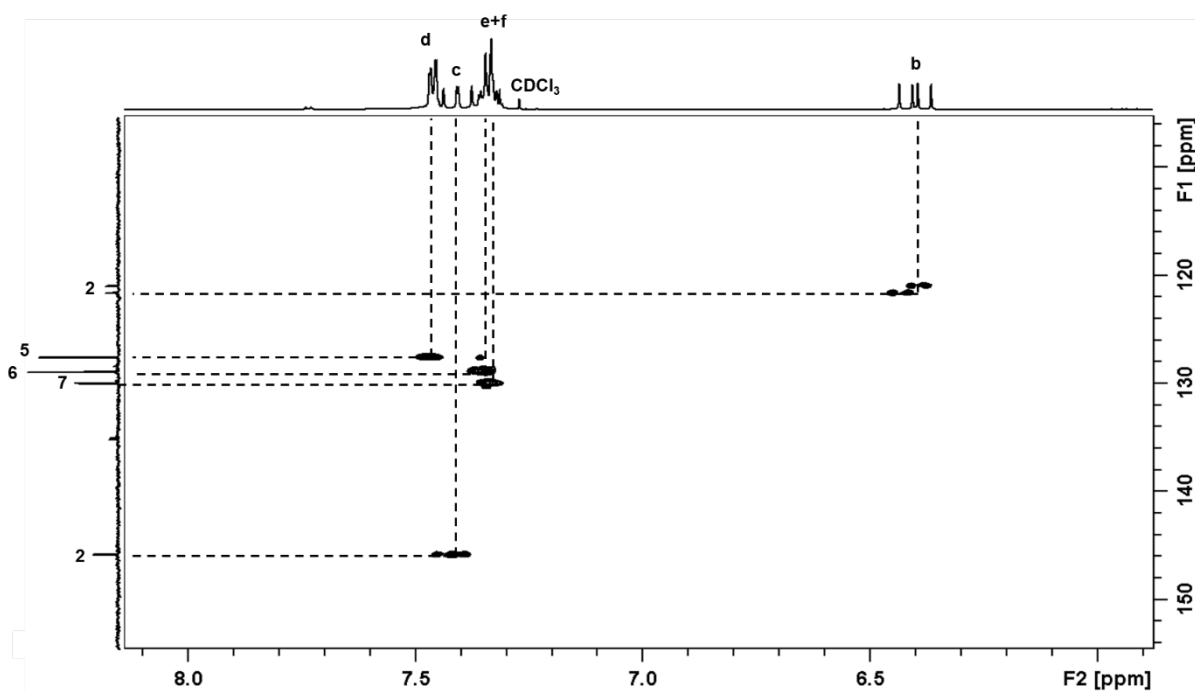


Figure S8d. Selected region of ^1H - ^{13}C { ^1H } HSQC (CDCl_3) of **(E)-dimethyl(styryl)phosphine oxide**. Note: ^1H = 600 MHz

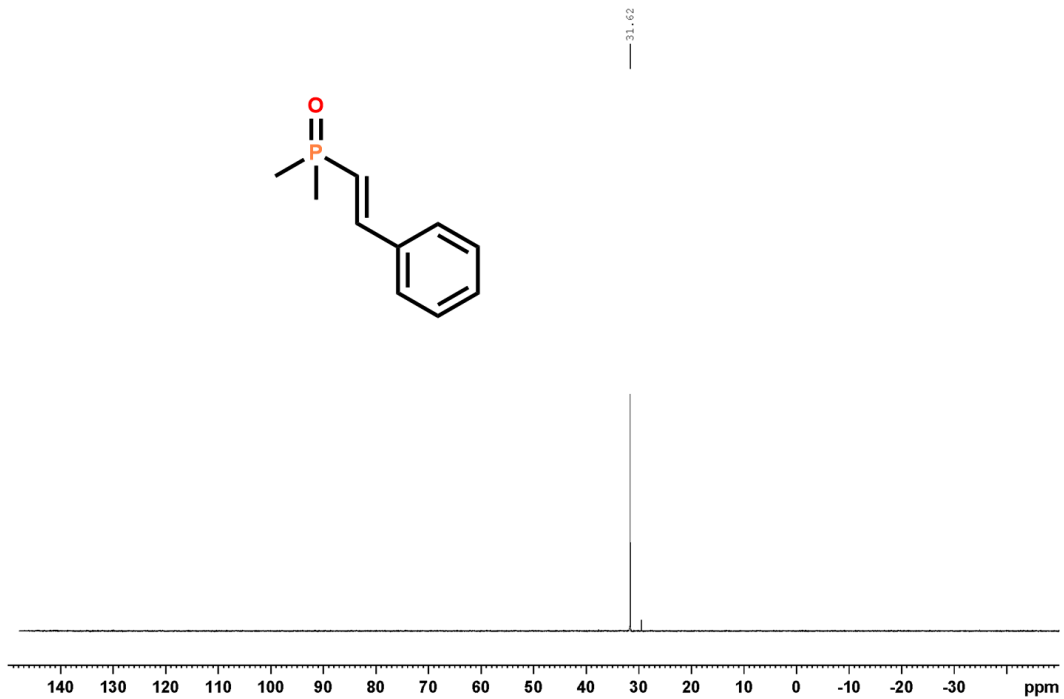


Figure S8e. ^{31}P { ^1H } -NMR (CDCl_3 , 243 MHz,) spectrum of **dimethyl(styryl)phosphine oxide** from reaction of $\text{Y}_2(\text{H}^{\text{Me}}\text{L})_6$ with benzaldehyde.

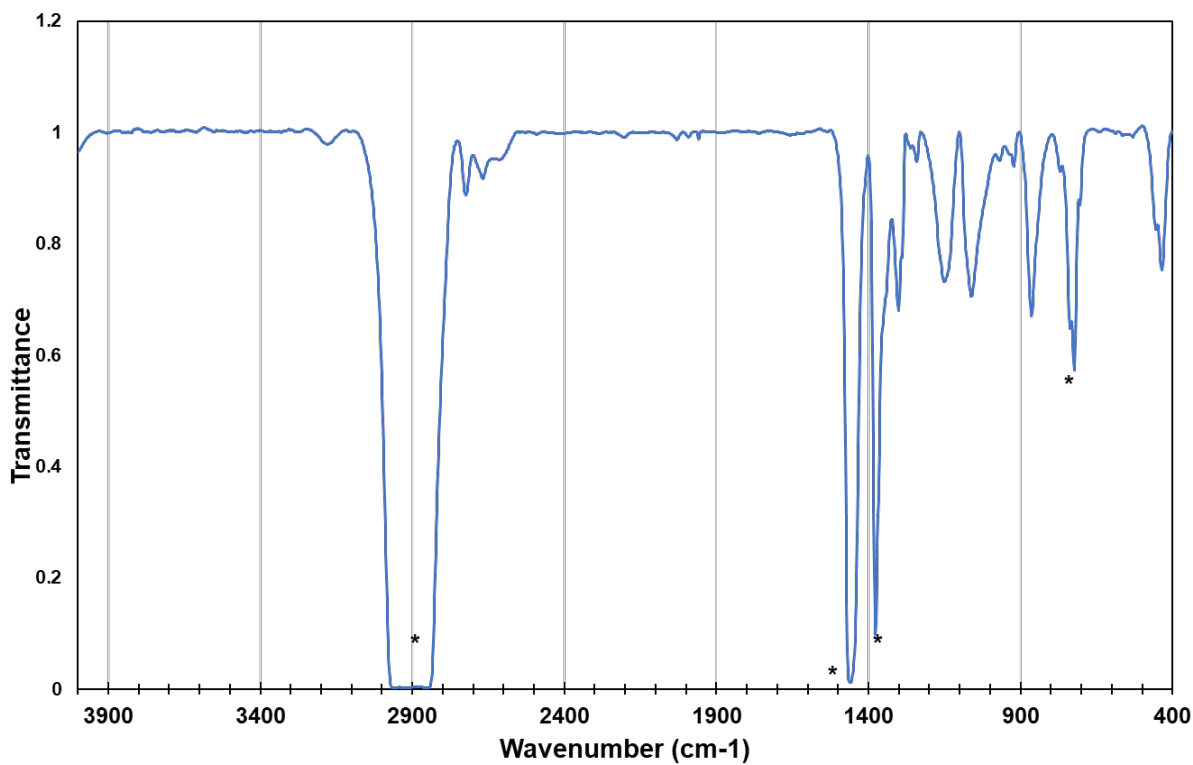


Figure S9. IR (Nujol) spectrum of $\text{Y}(\text{O}_2\text{PMe}_2)_3$. (*: Nujol)

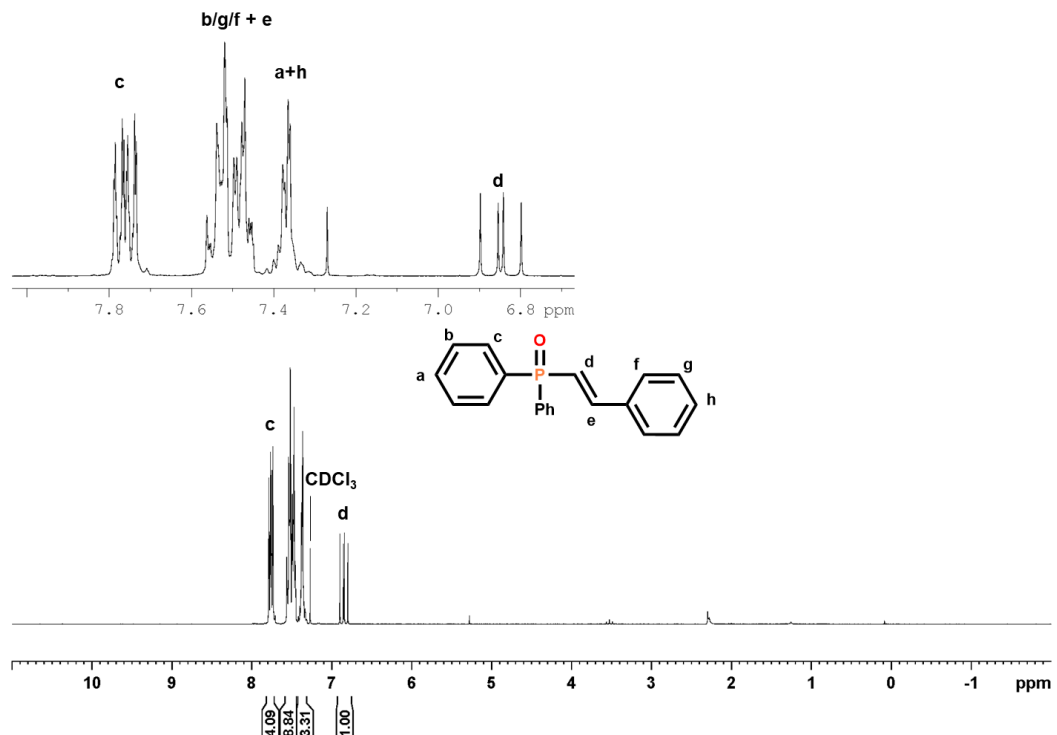


Figure S10a. ^1H -NMR (CDCl_3 , 400 MHz) spectrum of (E)-diphenyl(styryl)phosphine oxide

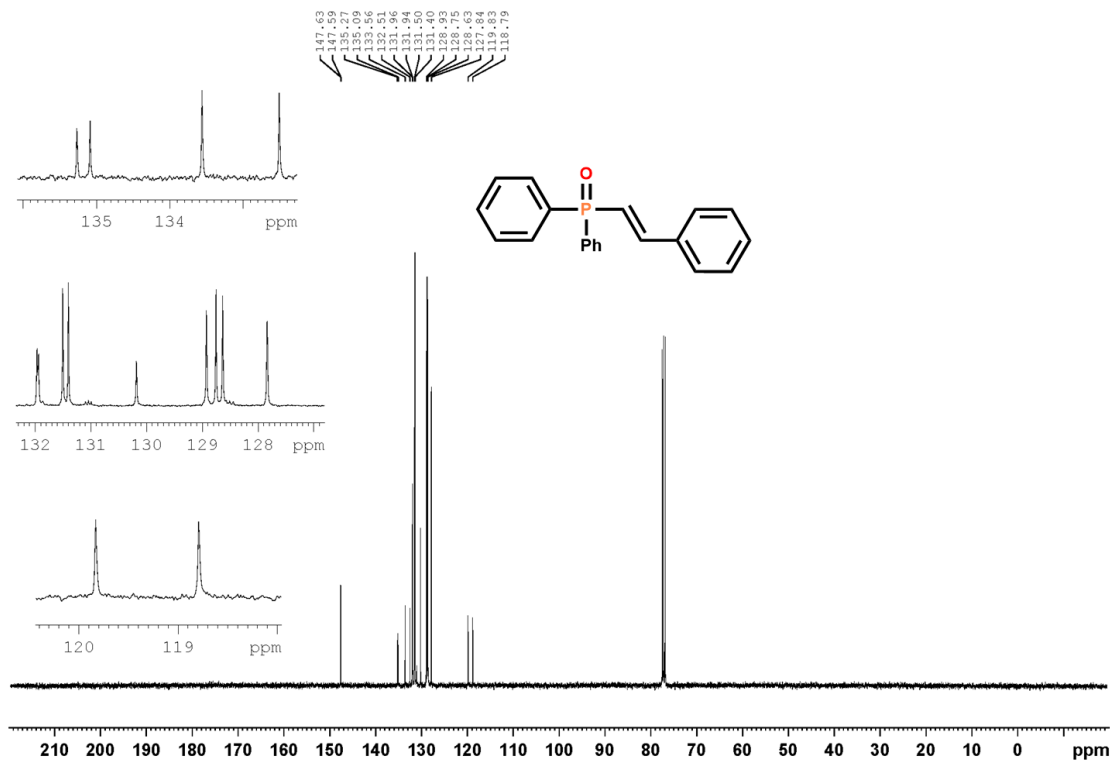


Figure S10b. $^{13}\text{C}\{^1\text{H}\}$ -NMR (CDCl_3 , 101 MHz) spectrum of **(E)-diphenyl(styryl)phosphine oxide**

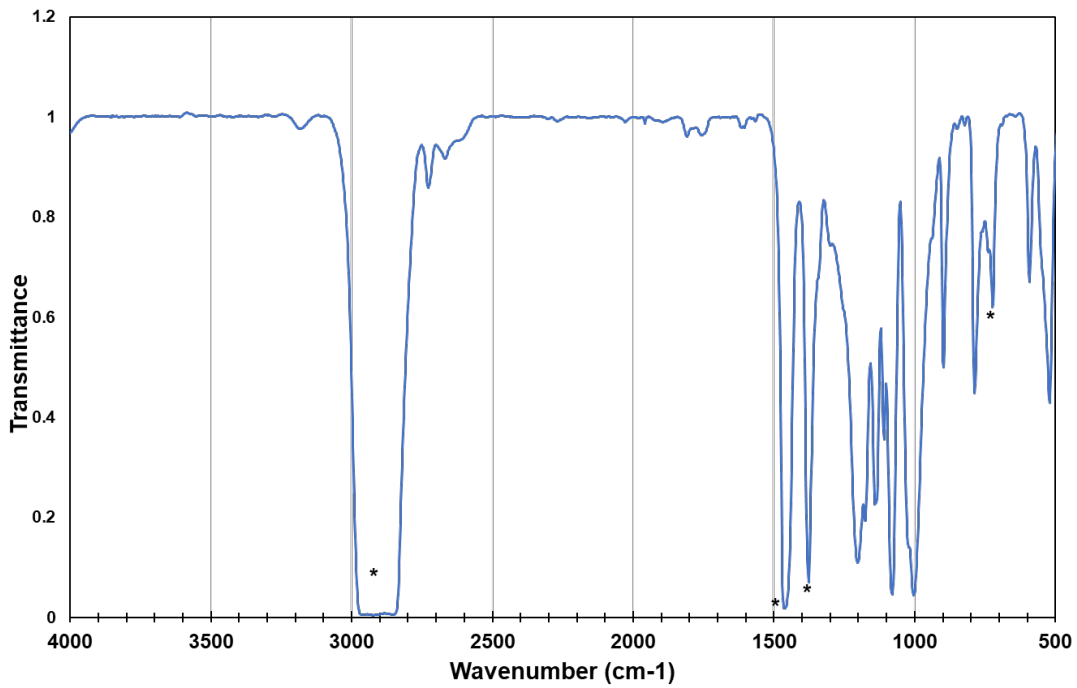


Figure S11. IR (Nujol) spectrum of $\text{Y}(\text{O}_2\text{PPh}_2)_3$. (*: Nujol)

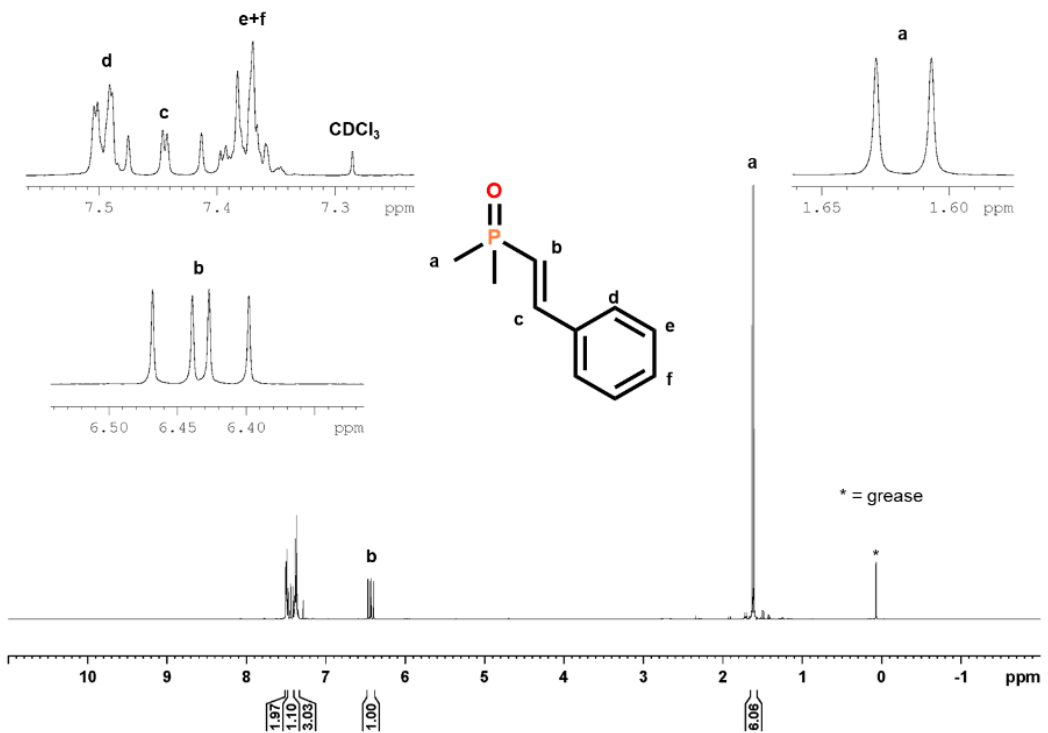


Figure S12a. ^1H -NMR (CDCl_3 , 600 MHz) spectrum of (E)-dimethyl(styryl)phosphine oxide from reaction of $\text{La}_2(\text{H}^{\text{Me}}\text{L})_6$ with benzaldehyde.

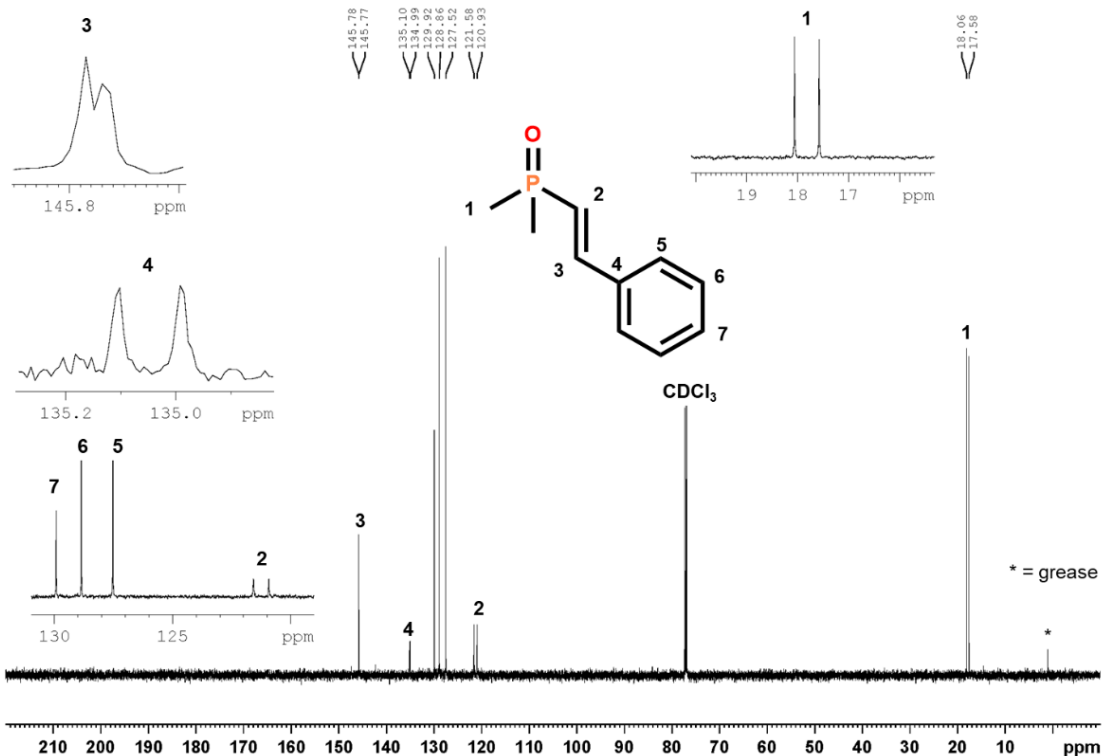


Figure S12b. ^{13}C -NMR (CDCl_3 , 152 MHz) spectrum of (E)-dimethyl(styryl)phosphine oxide from reaction of $\text{La}_2(\text{H}^{\text{Me}}\text{L})_6$ with benzaldehyde

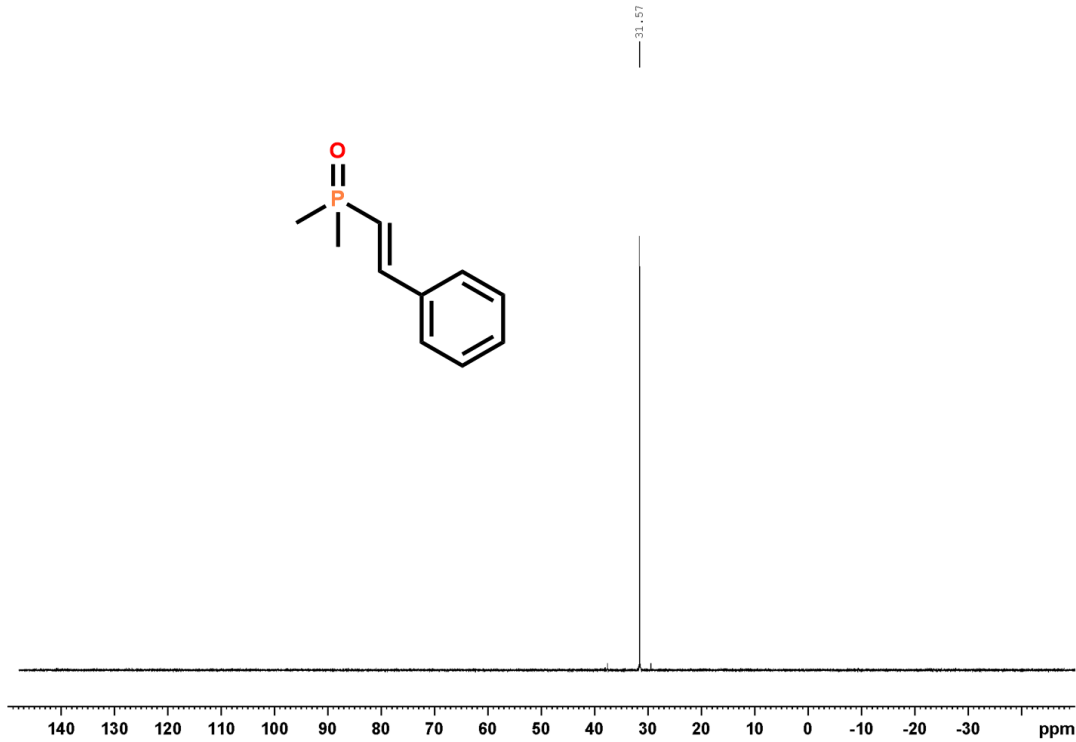


Figure S12c. $^{31}\text{P}\{\text{H}\}$ -NMR (CDCl_3 , 243 MHz) spectrum of **(E)-dimethyl(styryl)phosphine oxide** from reaction of $\text{La}_2(\text{H}^{\text{Me}}\text{L})_6$ with benzaldehyde

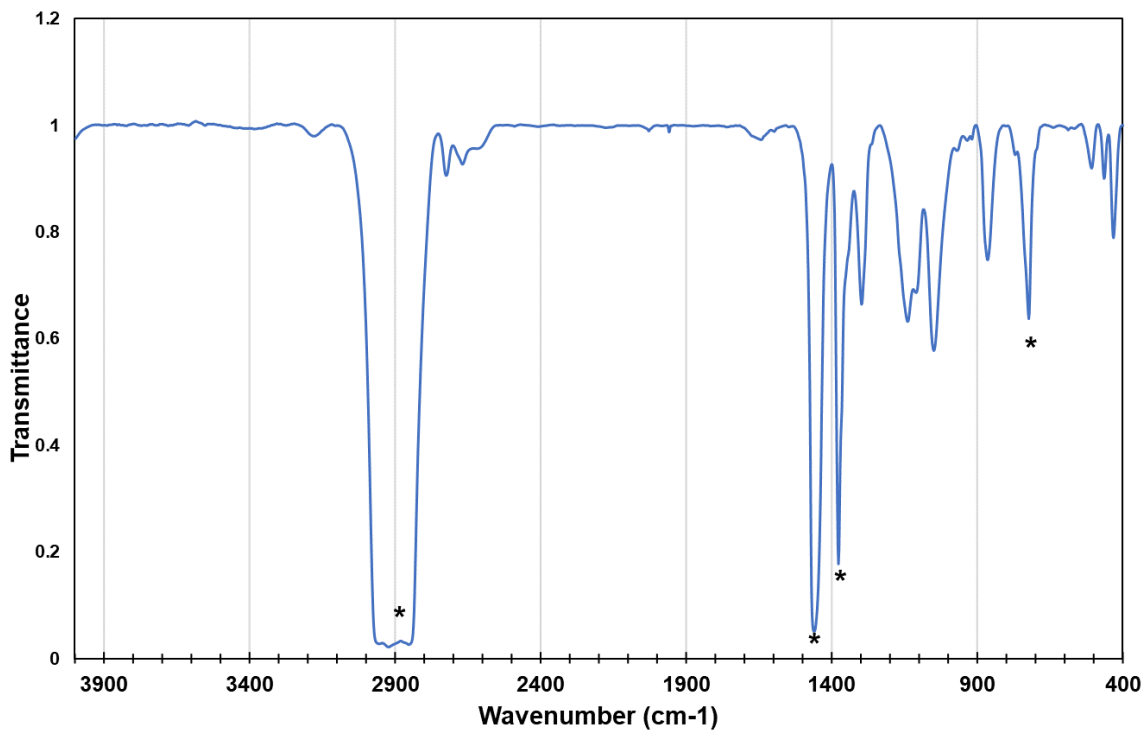


Figure S13. IR (Nujol) spectrum of $\text{La}(\text{O}_2\text{PMe}_2)_3$. (*: Nujol)

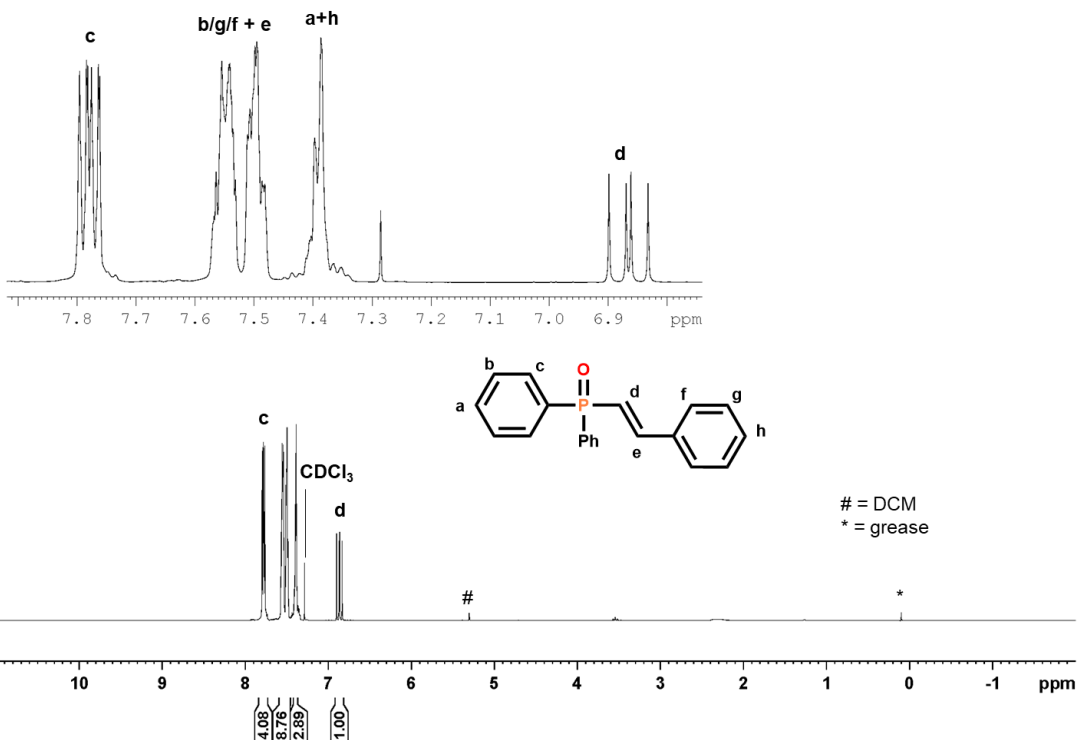


Figure S14a. ^1H -NMR (CDCl_3 , 600 MHz) spectrum of **(E)-diphenyl(styryl)phosphine oxide** obtained from reaction of **La(H^{Ph}L)₃** with benzaldehyde

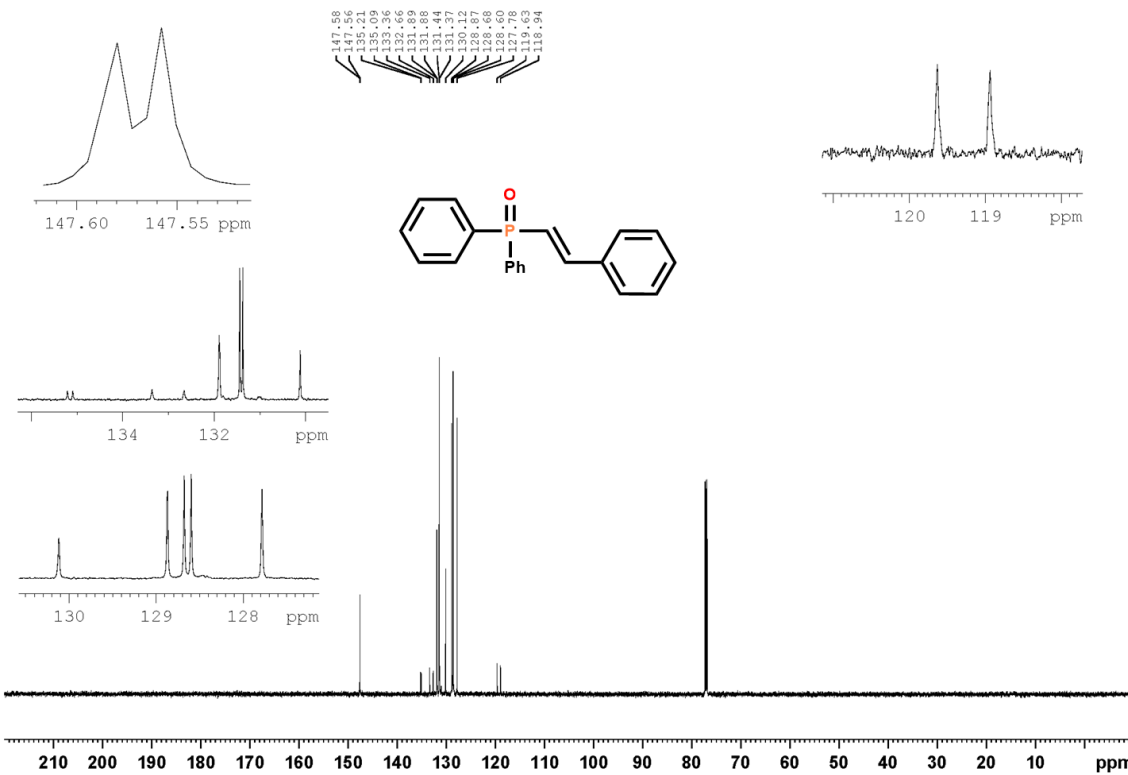


Figure S14b. ^{13}C -NMR (CDCl_3 , 152 MHz) spectrum of **(E)-diphenyl(styryl)phosphine oxide** obtained from reaction of **La(H^{Ph}L)₃** with benzaldehyde

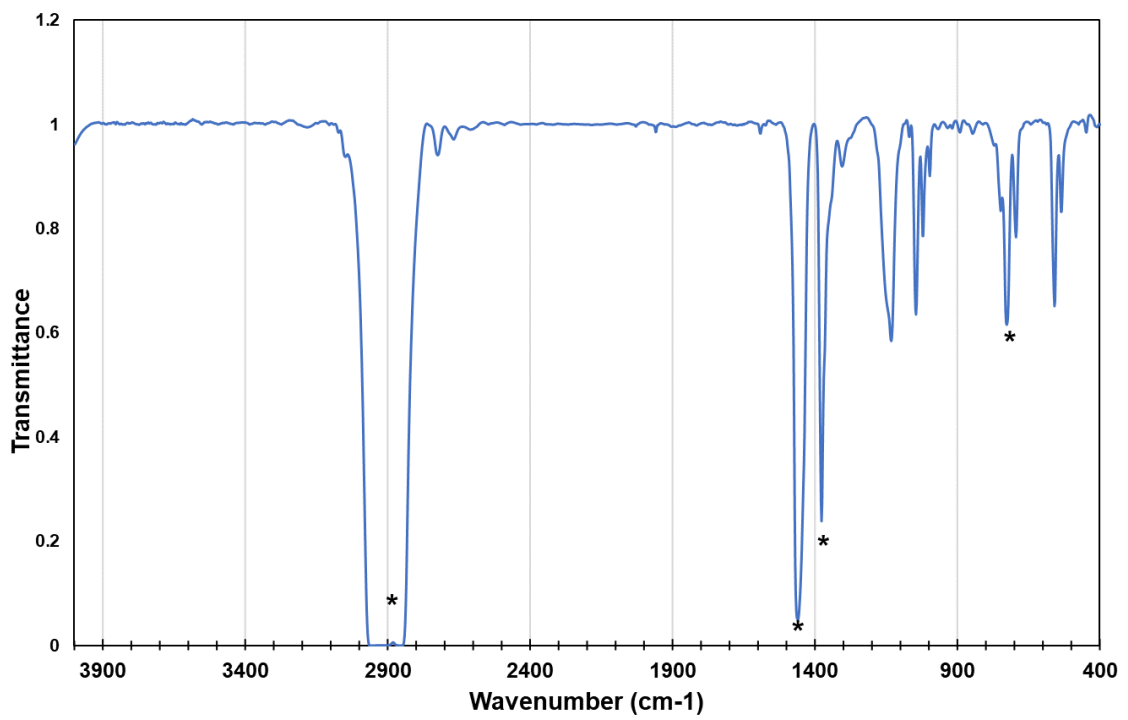


Figure S15. IR (Nujol) spectrum of $\text{La}(\text{O}_2\text{PPh}_2)_3$. (*: Nujol)

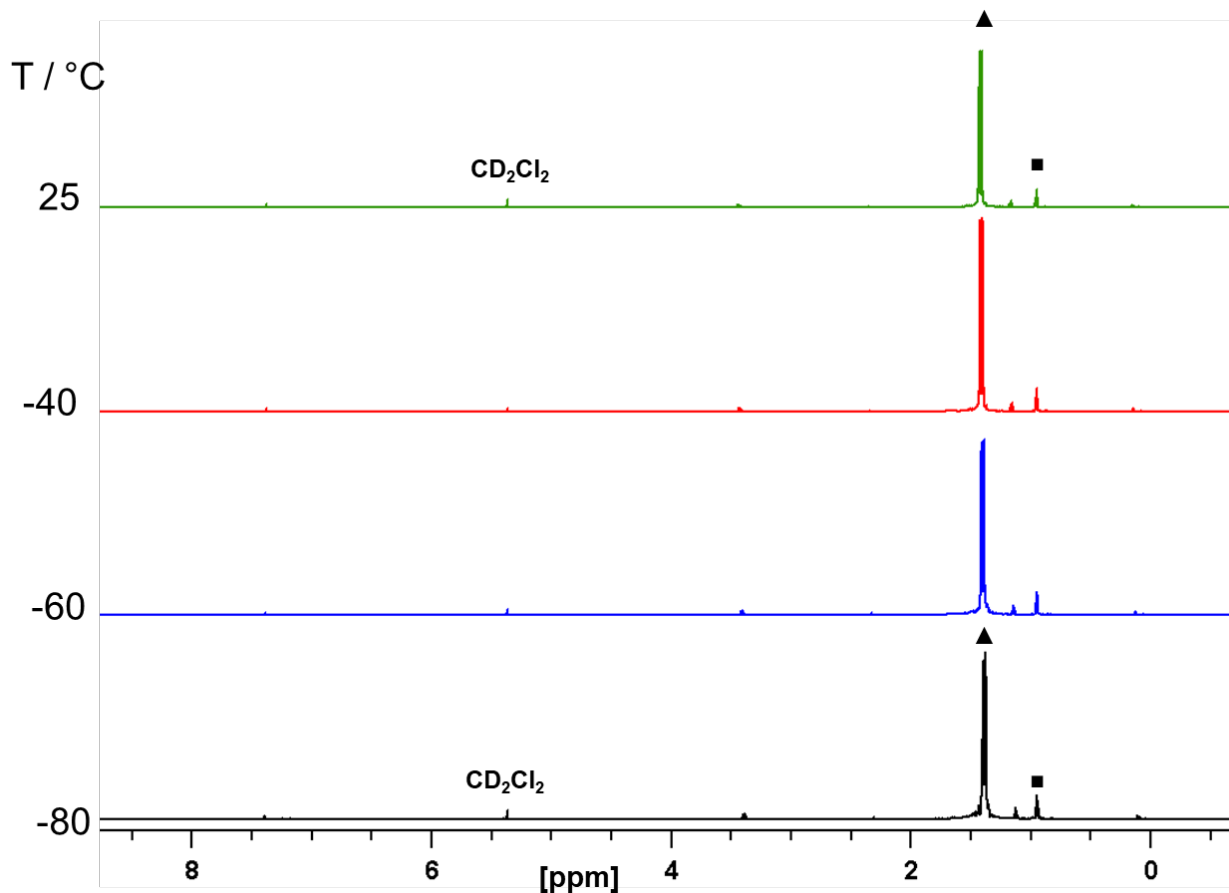


Figure S16a. Select ^1H -NMR (CD_2Cl_2 , 600 MHz) spectra of $\text{Y}_2(\text{H}^{\text{Me}}\text{L})_6$ (40 mM) collected from 25 °C to –80 °C. ▲ = CH_3 , ■ = CH

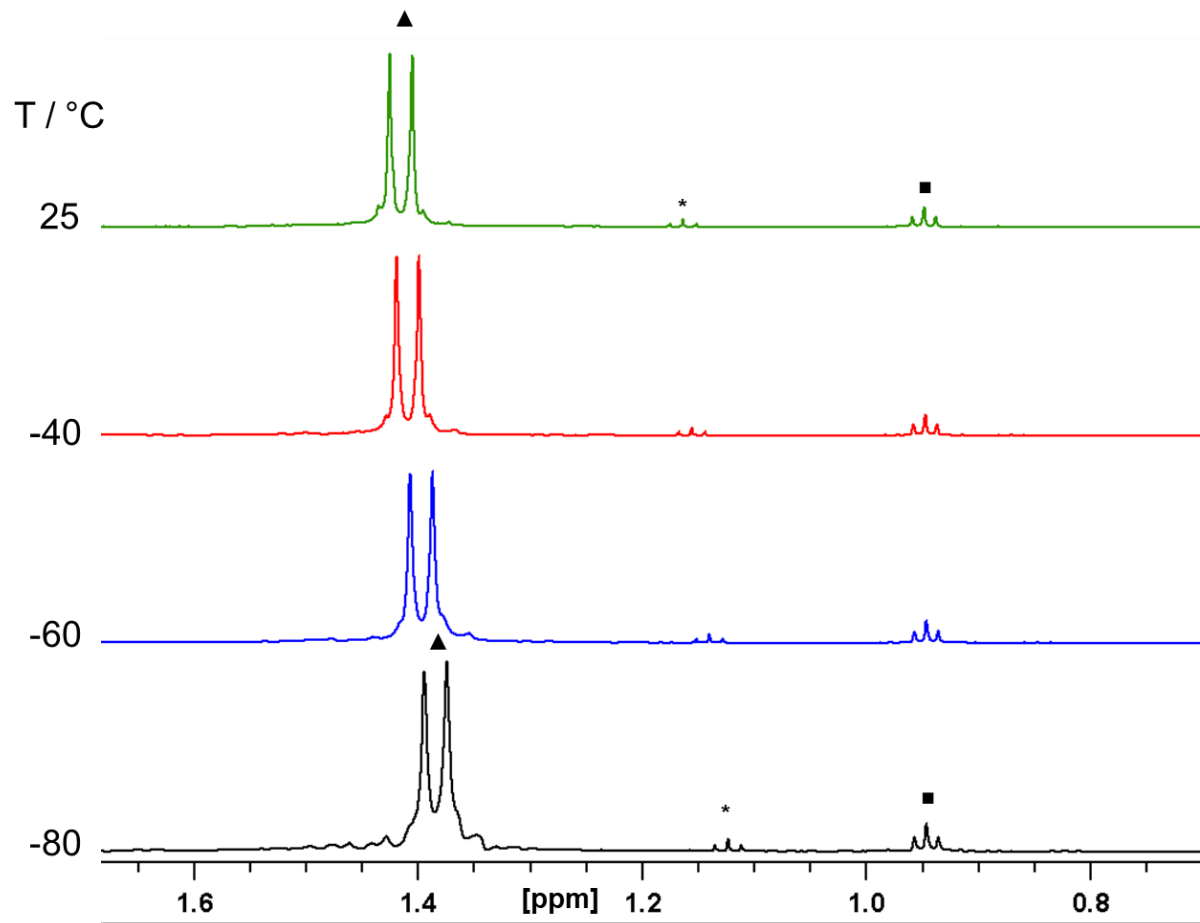


Figure S16b. Selected region of ^1H -NMR (CD_2Cl_2 , 600 MHz) spectra of $\text{Y}_2(\text{H}^{\text{Me}}\text{L})_6$ (40 mM) collected from 25 $^{\circ}\text{C}$ to -80 $^{\circ}\text{C}$. $\blacktriangle = \text{CH}_3$, $\blacksquare = \text{CH}$, * = Et_2O .

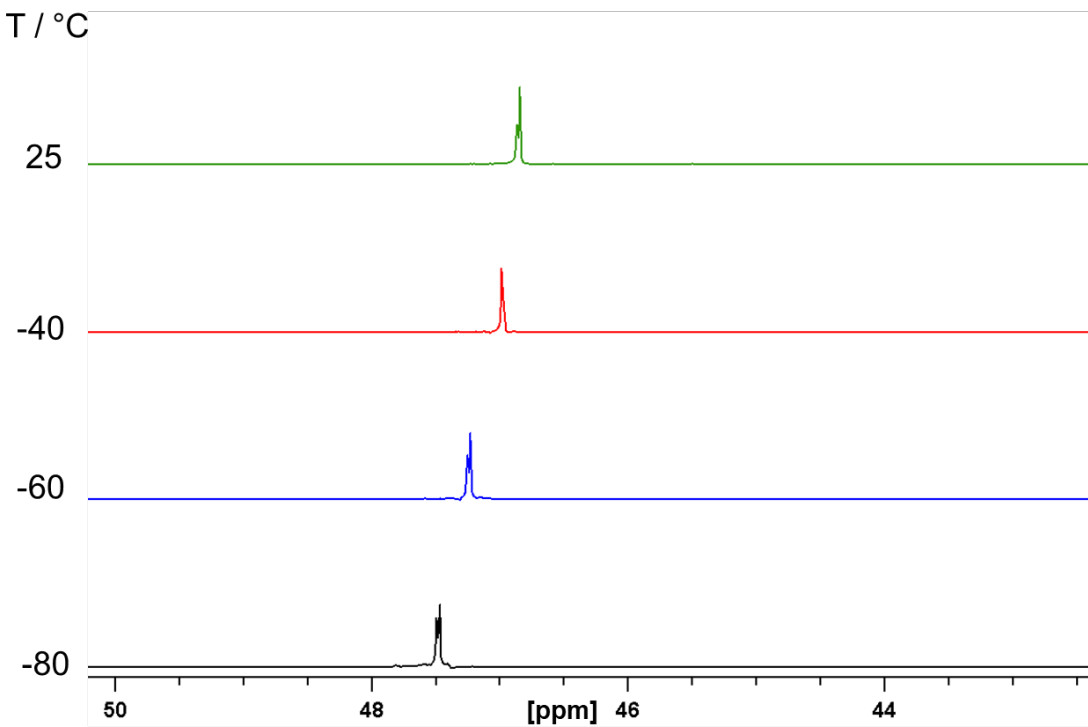


Figure S16c. Select $^{31}\text{P}\{\text{H}\}$ -NMR (CD_2Cl_2 , 243 MHz) spectra of $\text{Y}_2(\text{H}^{\text{Me}}\text{L})_6$ (40 mM) collected from 25 °C to –80 °C.

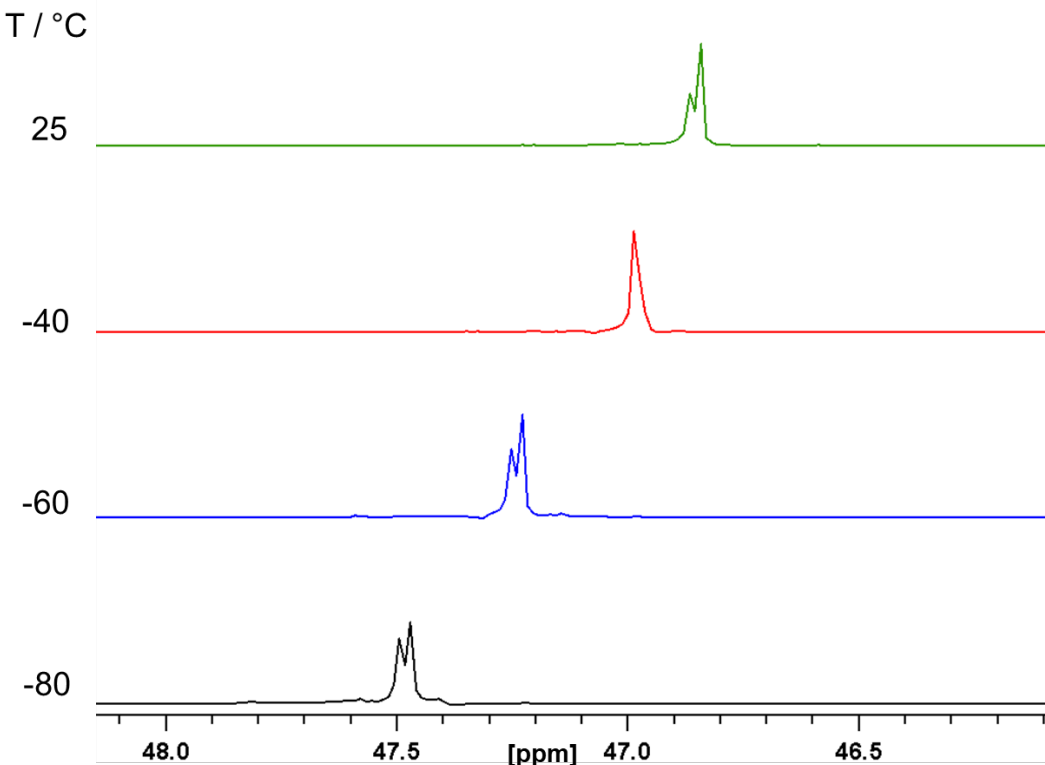


Figure S16d. Selected region of $^{31}\text{P}\{\text{H}\}$ -NMR (CD_2Cl_2 , 243 MHz) spectra of $\text{Y}_2(\text{H}^{\text{Me}}\text{L})_6$ (40 mM) collected from 25 °C to –80 °C.

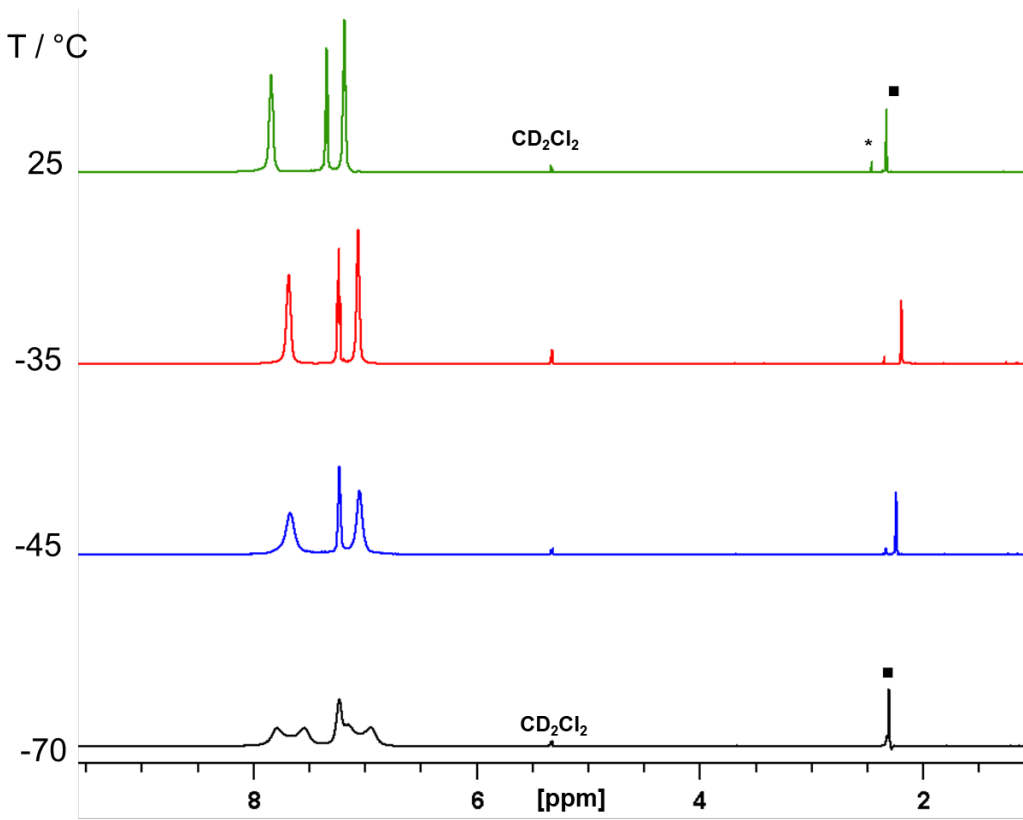


Figure S17a. Select ^1H -NMR (CD_2Cl_2 , 600 MHz) spectra of $\text{Y}(\text{HPhL})_3$ (40 mM) collected from 25 °C to –70 °C. ■ = CH , * = Toluene.

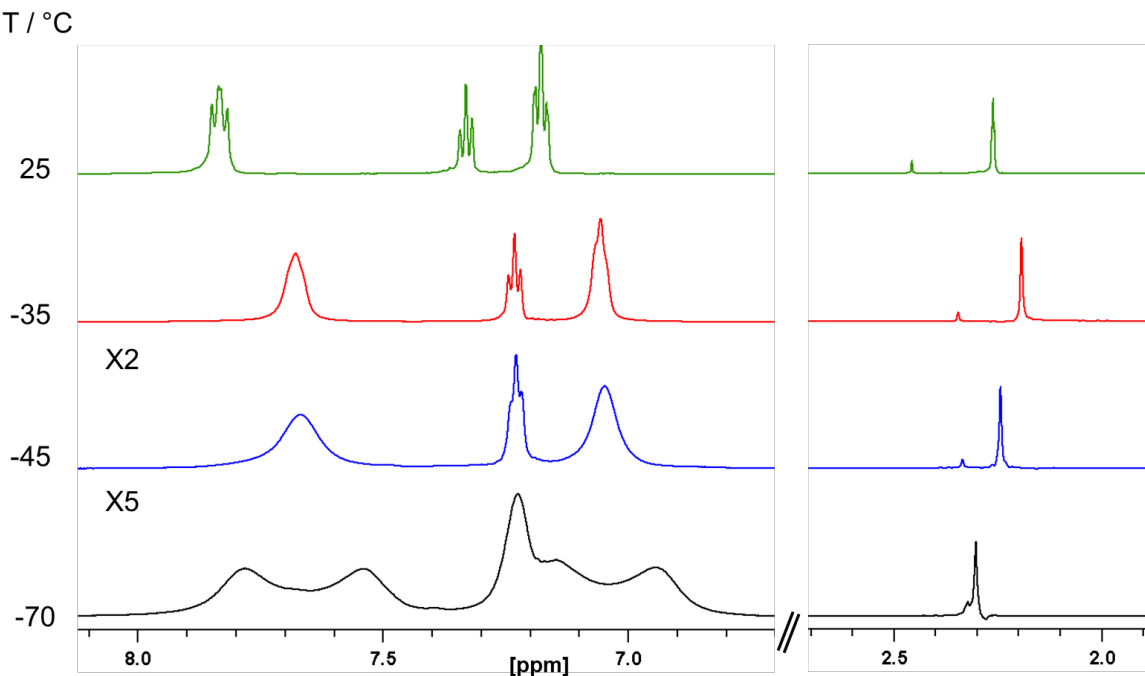


Figure S17b. Selected region of ^1H -NMR (CD_2Cl_2 , 600 MHz) spectra of $\text{Y}(\text{HPhL})_3$ (40 mM) collected from 25 °C to –70 °C.

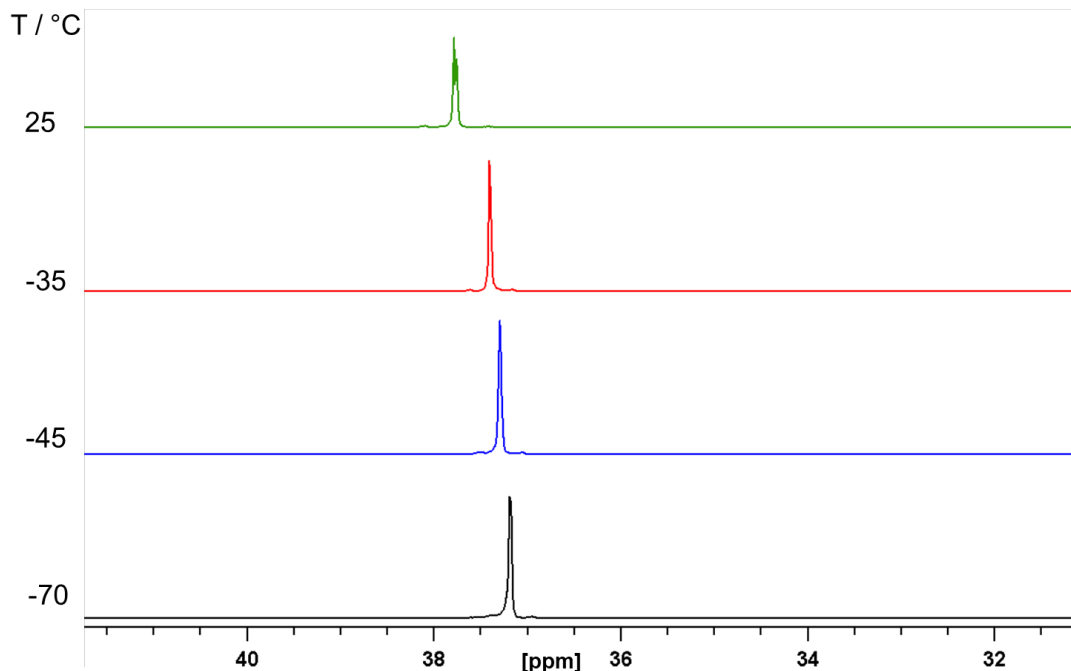


Figure S17c. Select variable temperature ^{31}P -NMR (CD_2Cl_2 , 243 MHz) spectra of $\text{Y}(\text{H}^{\text{Ph}}\text{L})_3$ (40 mM) collected from 25 °C to – 70 °C.

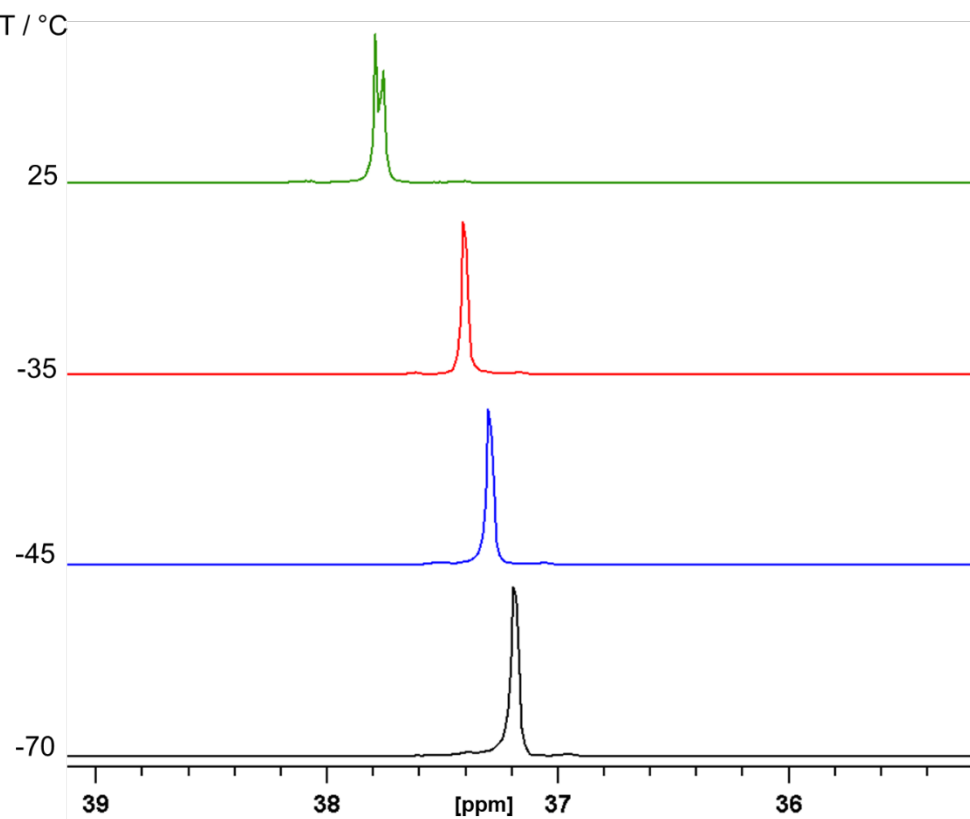


Figure S17d. Selected region of variable temperature ^{31}P -NMR (CD_2Cl_2 , 243 MHz) spectra of $\text{Y}(\text{H}^{\text{Ph}}\text{L})_3$ (40 mM) collected from 25 °C to – 70 °C.

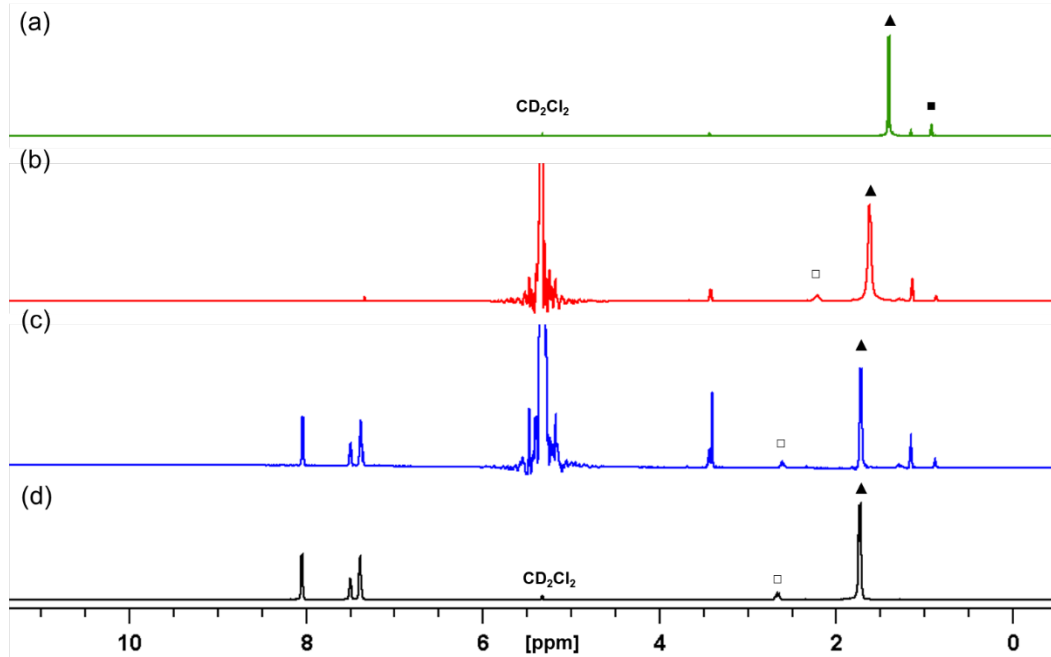


Figure S18a. Stacked ^1H -NMR spectrum of: *a* – $\text{Y}_2(\text{H}^{\text{Me}}\text{L})_6$. *b* – *a* + 3 equiv. MeOD. *c* – *b* + 3 equiv. benzoic acid. *d* – *c* after volatiles were removed. ▲ = CH_3 , ■ = CH , □ = $\text{CH}_2/\text{CHD}/\text{CD}_2$, * = diethyl ether, ● = pentane.

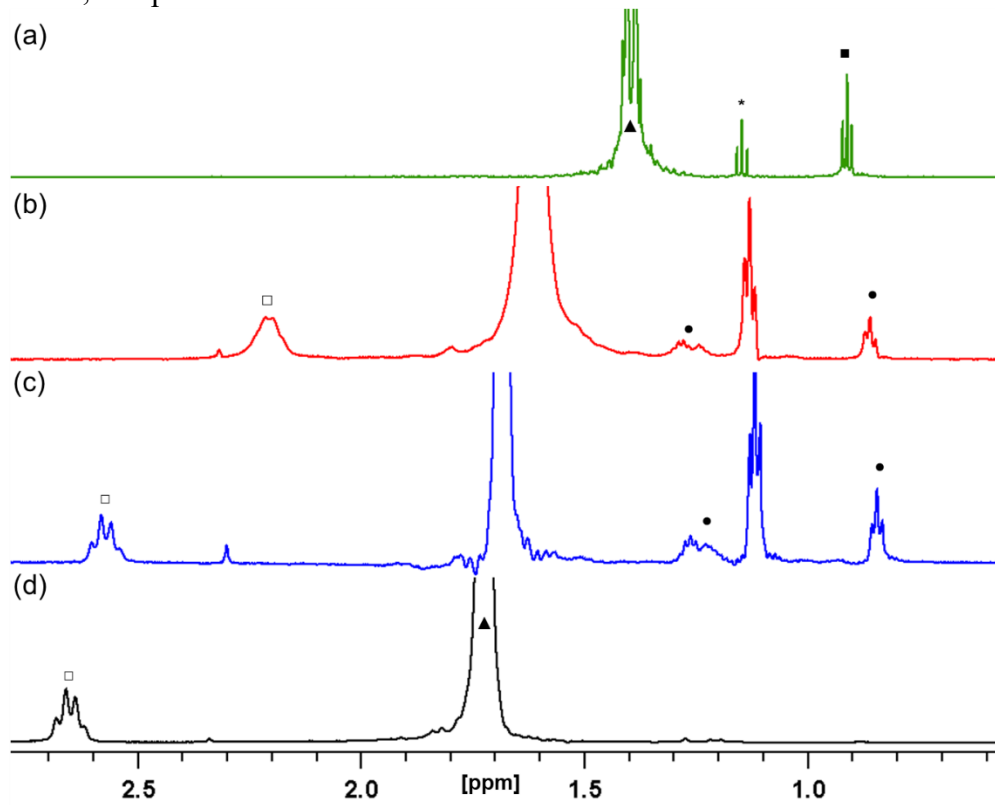


Figure S18b. Select region of stacked ^1H -NMR spectrum of: *a* – $\text{Y}_2(\text{H}^{\text{Me}}\text{L})_6$. *b* – *a* + 3 equiv. MeOD. *c* – *b* + 3 equiv. benzoic acid. *d* – *c* after volatiles were removed. ▲ = CH_3 , ■ = CH , □ = $\text{CH}_2/\text{CHD}/\text{CD}_2$, * = diethyl ether, ● = pentane.

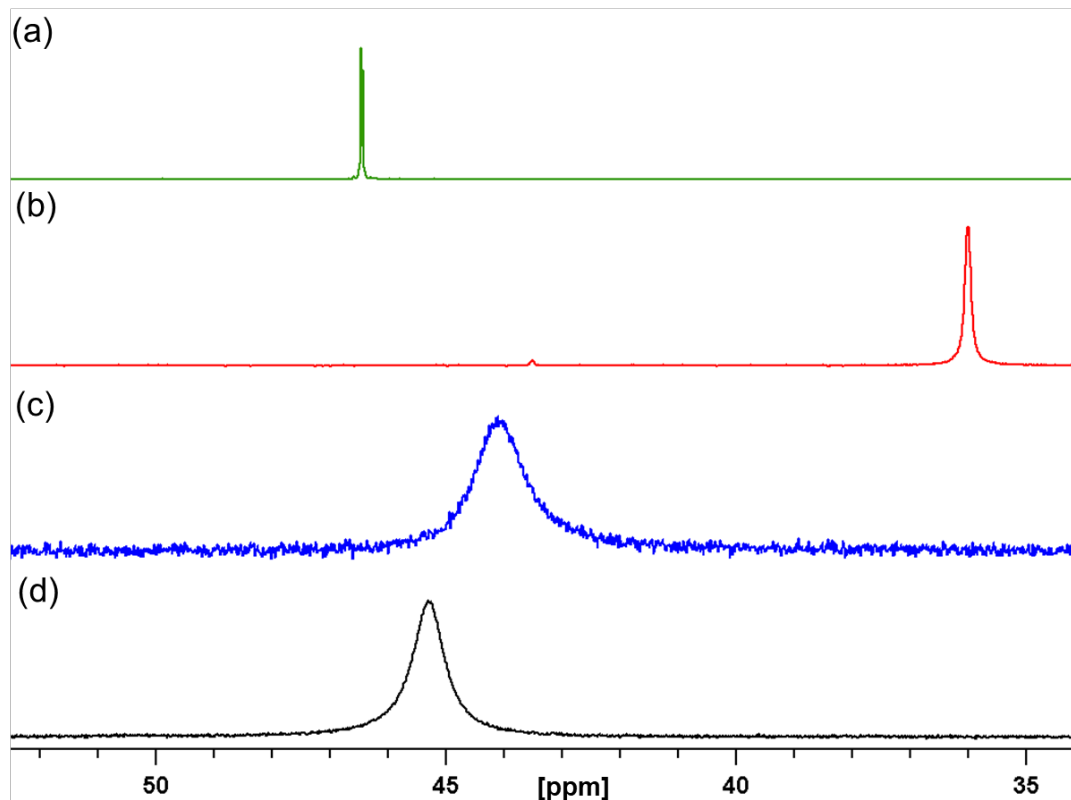


Figure S18c. Stacked $^{31}\text{P}\{\text{H}\}$ -NMR spectrum (CD_2Cl_2 , 243 MHz) of: *a* – $\text{Y}_2(\text{H}^{\text{Me}}\text{L})_6$. *b* – *a* + 3 equiv. MeOD. *c* – *b* + 3 equiv. benzoic acid. *d* – *c* after volatiles were removed.

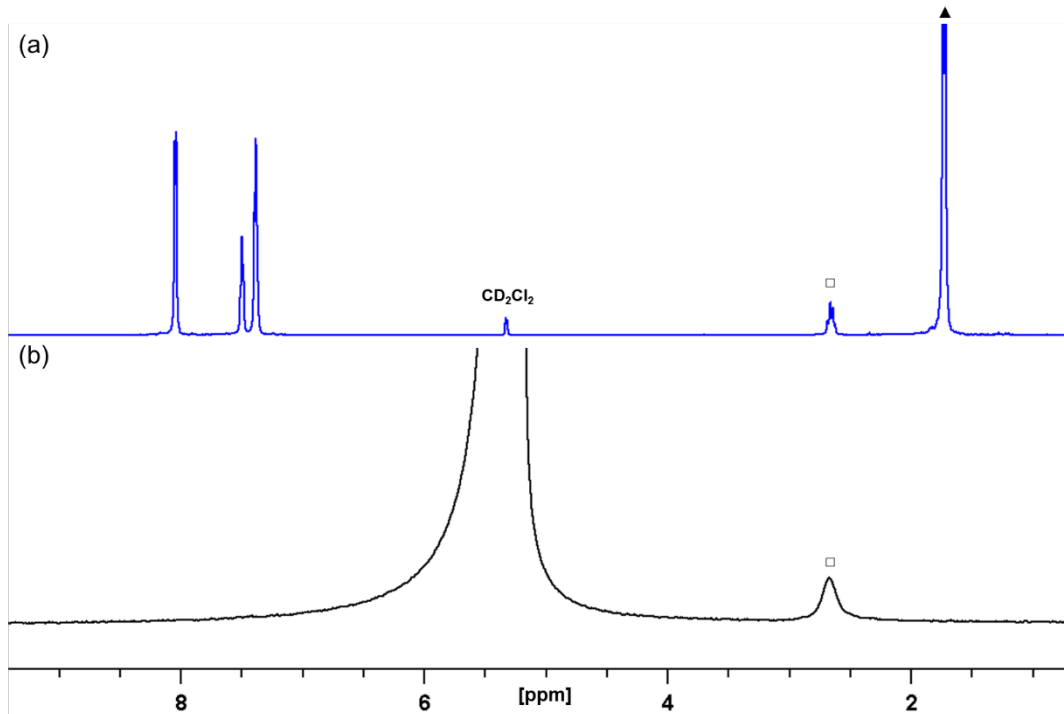


Figure S18d. Stacked *a* – ^1H NMR (CD_2Cl_2 , 600 MHz) and *b* – ^2H NMR(CD_2Cl_2 , 92 MHz) spectra of the reaction of $\text{Y}_2(\text{H}^{\text{Me}}\text{L})_6$ with MeOD after benzoic acid quench and removal of volatiles. $\blacktriangle = \text{CH}_3$, $\square = \text{CH}_2/\text{CHD}/\text{CD}_2$.

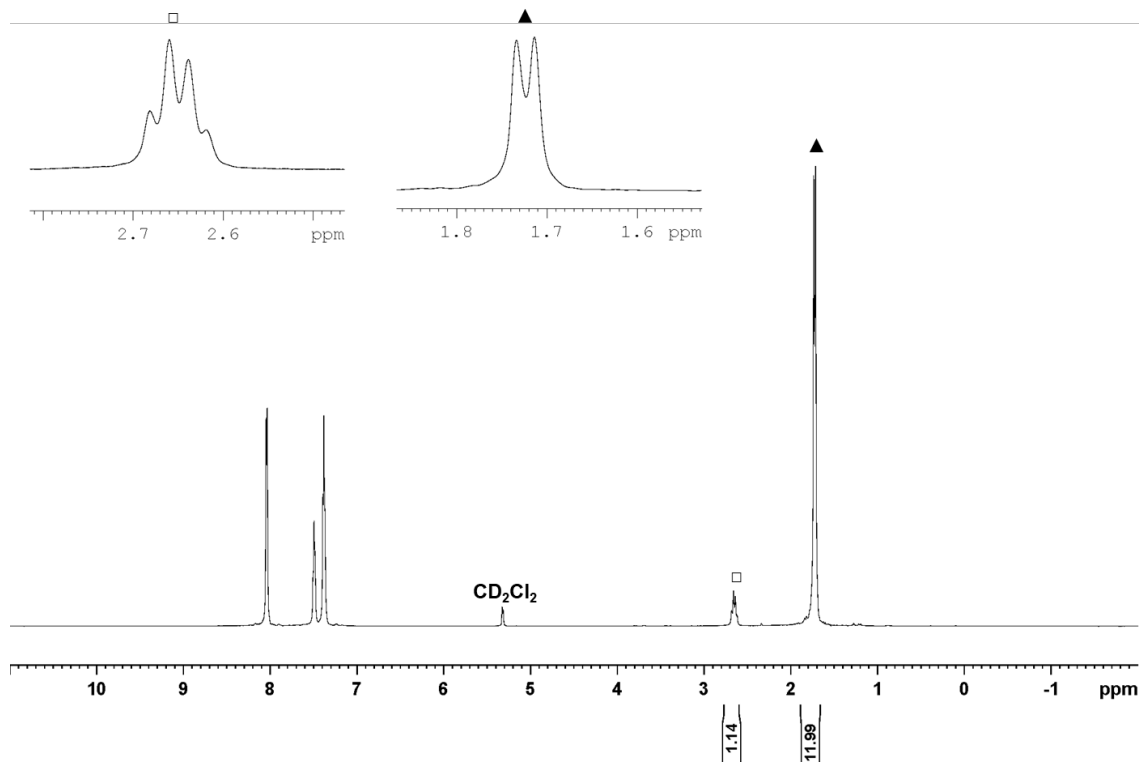


Figure S18e. ^1H -NMR (CD_2Cl_2 , 600 MHz) spectrum of reaction of $\text{Y}_2(\text{H}^{\text{Me}}\text{L})_6$ with MeOD after after benzoic acid quench and removal of volatiles. $\blacktriangle = \text{CH}_3$, $\square = \text{CH}_2/\text{CHD}/\text{CD}_2$.

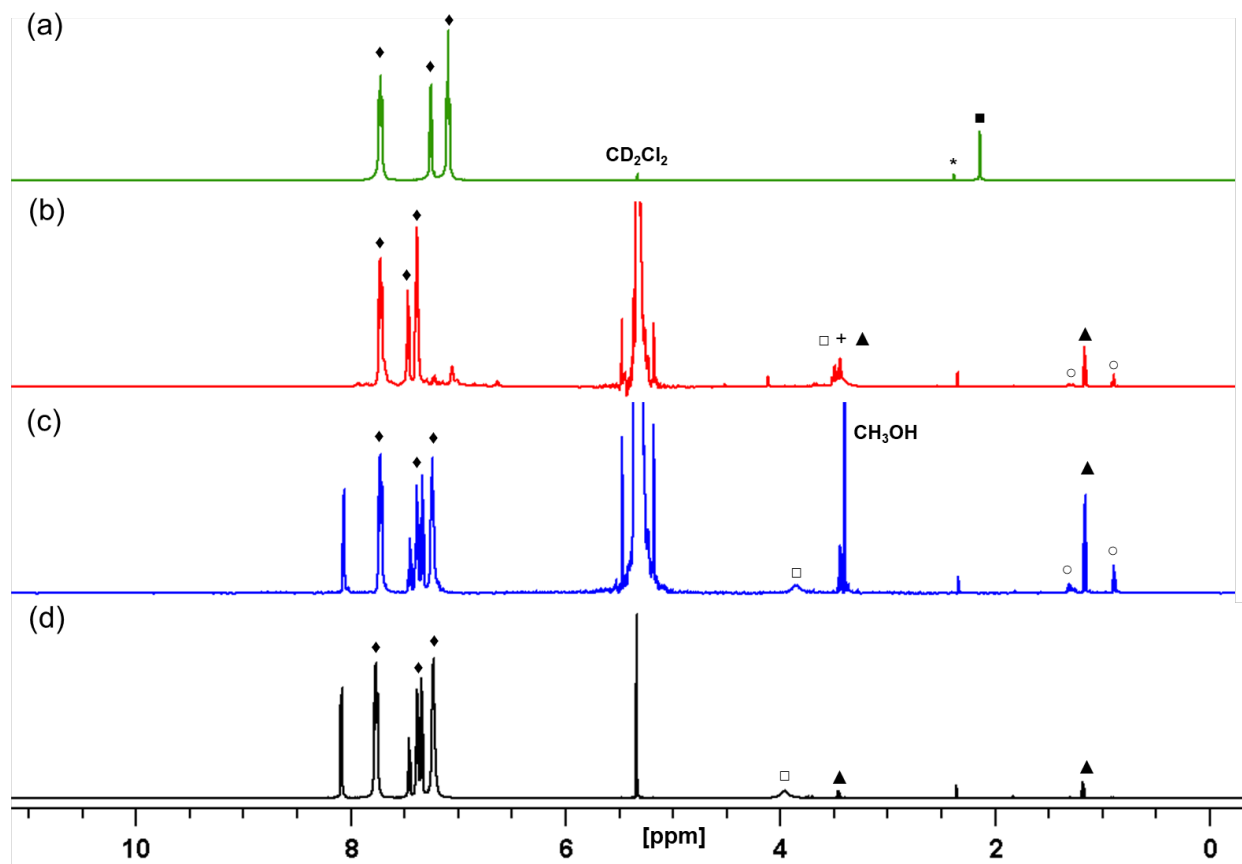


Figure S19a. Stacked ^1H -NMR spectrum (CD_2Cl_2 , 600 MHz) spectra of *a* – $\text{Y}(\text{H}^{\text{Ph}}\text{L})_3$. *b* – *a* + 3 equiv. MeOD. *c* – *b* + 3 equiv. benzoic acid. *d* – *c* after volatiles were removed. ■ = CH, □ = $\text{CH}_2/\text{CHD}/\text{CD}_2$, ♦ = CH_{Ar} ▲ = diethyl ether, ● = pentane, * = toluene.

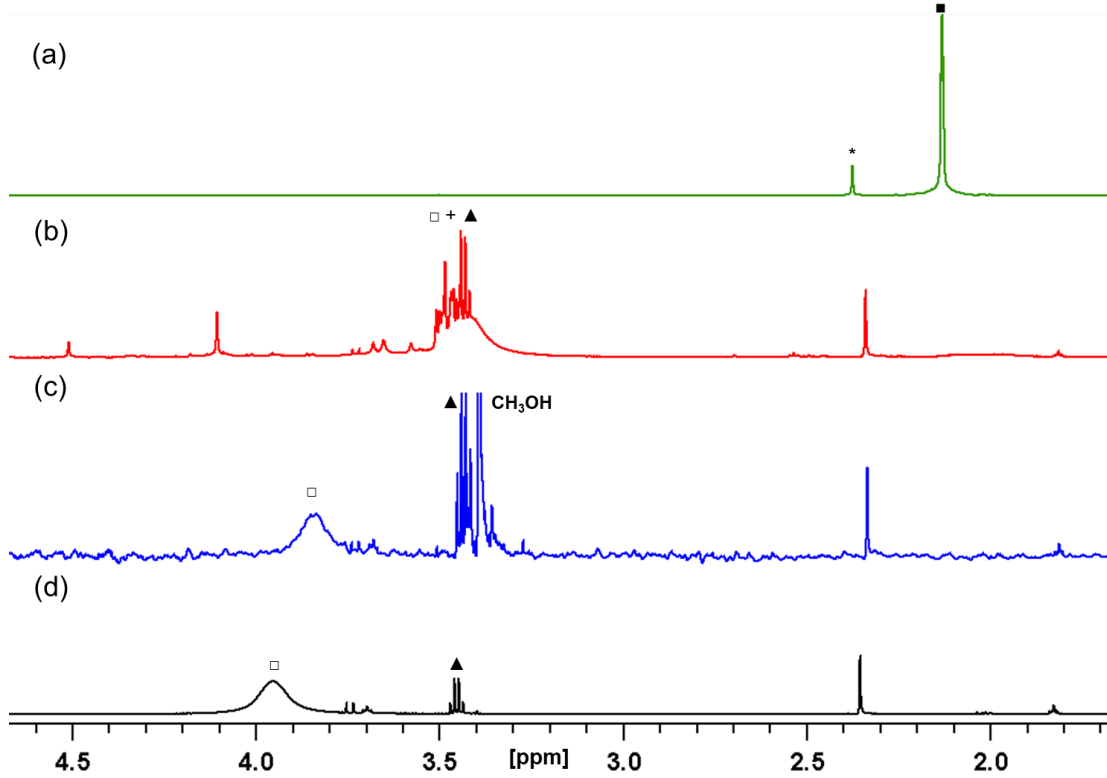


Figure S19b. Selected region of stacked ^1H -NMR spectra (CD_2Cl_2 , 600 MHz) of: *a* – $\text{Y}(\text{H}^{\text{Ph}}\text{L})_3$. *b* – *a* + 3 equiv. MeOD. *c* – *b* + 3 equiv. benzoic acid. *d* – *c* after volatiles were removed. ■ = CH_- , □ = $\text{CH}_2/\text{CHD}/\text{CD}_2$, ▲ = diethyl ether, * = toluene.

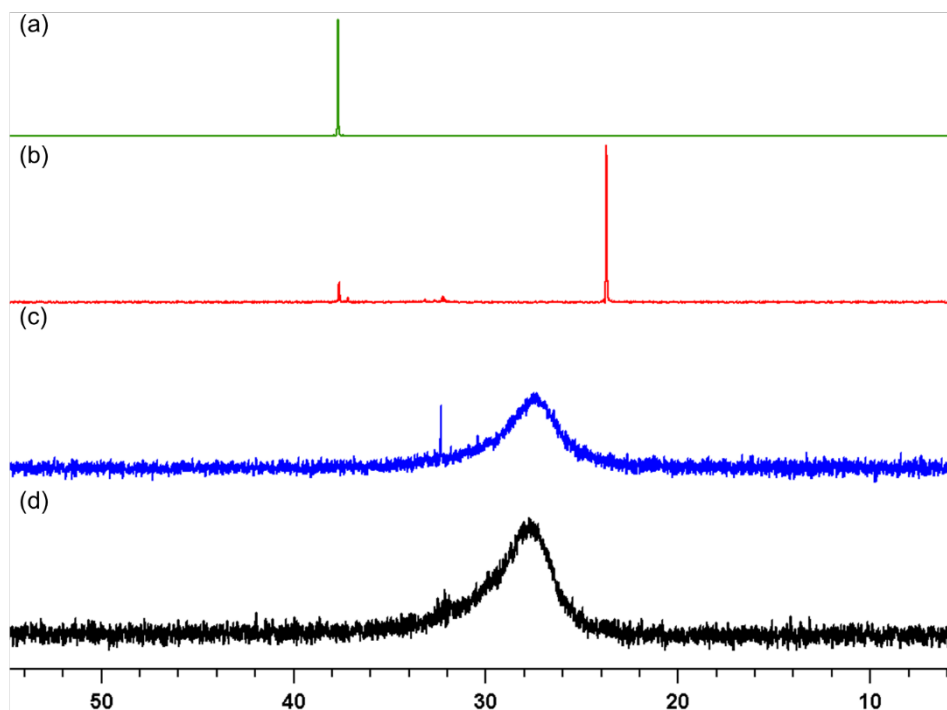


Figure S19c. Stacked $^{31}\text{P}\{\text{H}\}$ -NMR spectra (CD_2Cl_2 , 243 MHz) of: *a* – $\text{Y}(\text{H}^{\text{Ph}}\text{L})_3$. *b* – *a* + 3 equiv. MeOD. *c* – *b* + 3 equiv. benzoic acid. *d* – *c* after volatiles were removed.

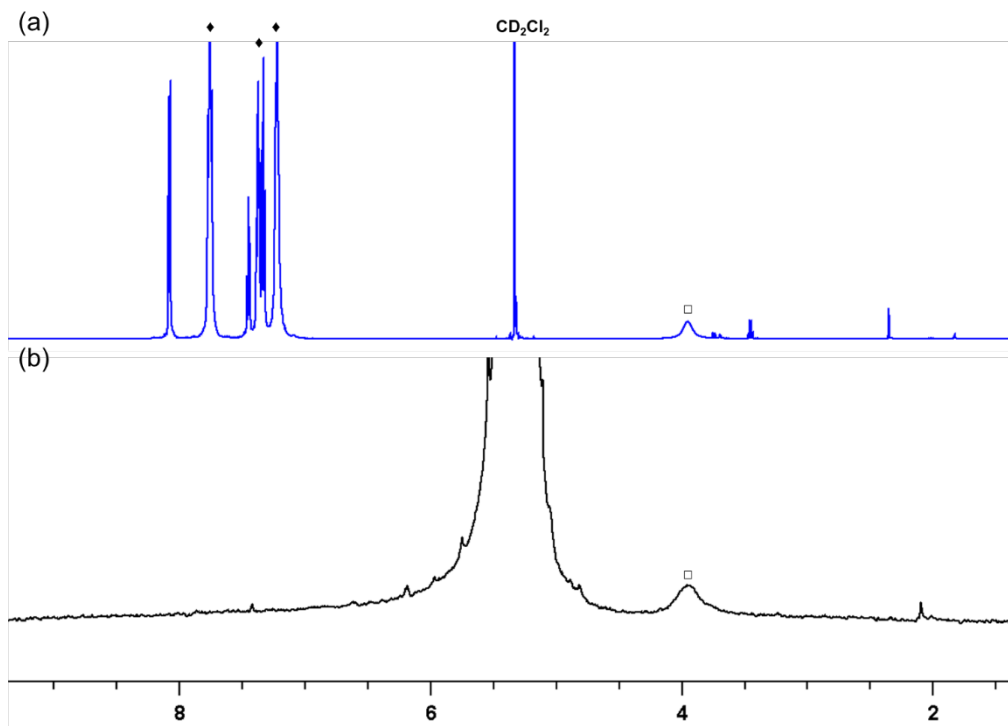


Figure S19d. Selected region of stacked (a) ^1H NMR (CD_2Cl_2 , 600 MHz), b – ^2H NMR(CD_2Cl_2 , 92 MHz) spectra of reaction of $\text{Y}(\text{H}^{\text{Ph}}\text{L})_3$ with MeOD after benzoic acid quench and removal of volatiles. □= $\text{CH}_2/\text{CHD}/\text{CD}_2$, ♦ = CH_{Ar}

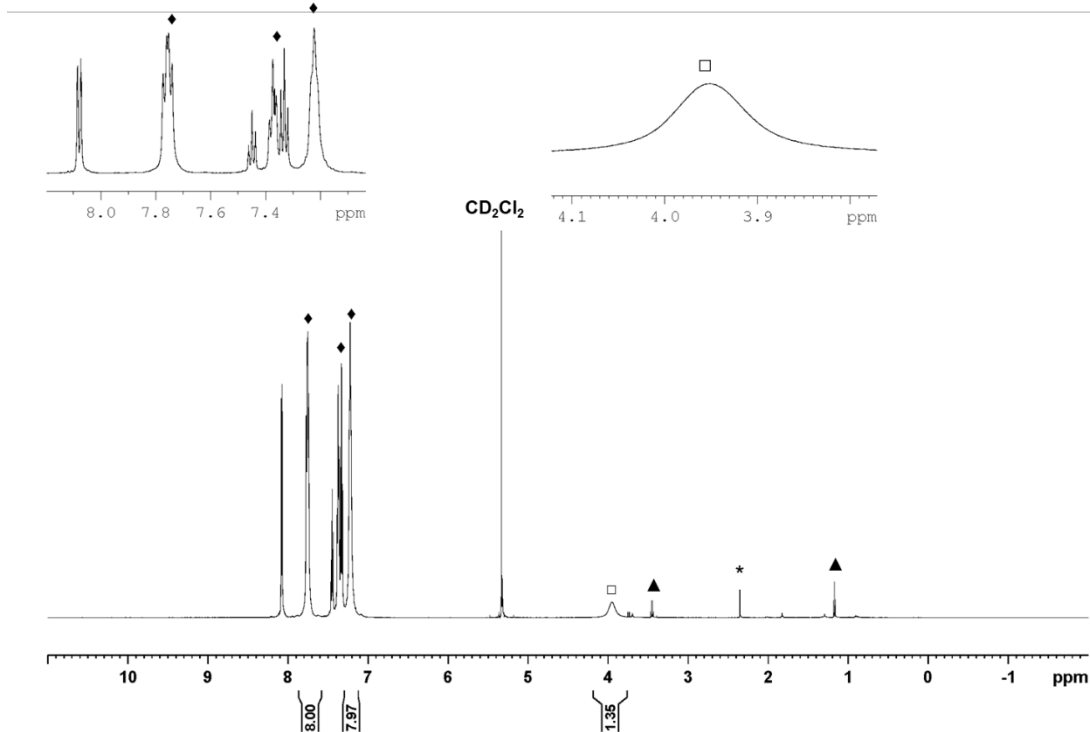


Figure S19e. ^1H -NMR (CD_2Cl_2 , 600 MHz) spectrum of reaction of $\text{Y}(\text{H}^{\text{Ph}}\text{L})_3$ with MeOD after after benzoic acid quench and removal of volatiles. ▲ = CH_3 , □= $\text{CH}_2/\text{CHD}/\text{CD}_2$.□= $\text{CH}_2/\text{CHD}/\text{CD}_2$, ▲ = diethyl ether, ♦ = CH_{Ar} *= toluene.

Table 1. DOSY measured diffusion coefficients, D , and estimated hydrodynamic radii, r_H , of $\text{RE}_2(\text{H}^{\text{Me}}\text{L})_6$, $\text{RE}(\text{H}^{\text{Ph}}\text{L})_3$.

Species	D_{Fc^*} (10^{-10} m^2/s) ^a	D (10^{-10} m^2/s)	$r_{\text{H(exp)}}^b$ (Å)	$r_{\text{H(theo-monomer)}}^c$ (Å)	$r_{\text{H(theo-dimer)}}^d$ (Å)	% Error (monomer)	% Error (dimer)	M/D ^f
Fc*	-	-	-	4.08	-	-	-	n/a
La₂(H^{Me}L)₆	9.65	5.82	6.63 ^g	5.28	6.13	20.4	7.5	D
La(H^{Ph}L)₃	12.81	6.55	7.97	8.27	-	3.6	-	M
Y₂(H^{Me}L)₆	9.91	7.1	5.57 ^g	5.17	6.05	7.2	8.6	D
Y(H^{Ph}L)₃	12.6	6.37	8.07	7.97	-	1.2	-	M

a – DOSY measured diffusion coefficient of decamethylferrocene (Fc*) in the experiment of the corresponding complex. DOSY measured diffusion coefficient of the sample. *b* – $r_H = D_{\text{Fc}}/D_{\text{sample}} \cdot r_{\text{H}}(\text{Fc}^*, \text{theo.})$. *c* – $r_{\text{H}}(\text{theo-monomer})$ determined from crystal structures and DFT optimized structures. *d* – $r_{\text{H}}(\text{theo-dimer})$ is the average of half lengths of the principal axes of the homogeneous ellipsoid with the same principal moments of inertia of the molecule, which are determined from the crystal structure. *e* – Percent error of $r_{\text{H(exp)}}$ vs $r_{\text{H(theo)}}$. *f* – Monomer (M) or Dimer (D). *g* – corrected using Equations S3, S4 and S5.

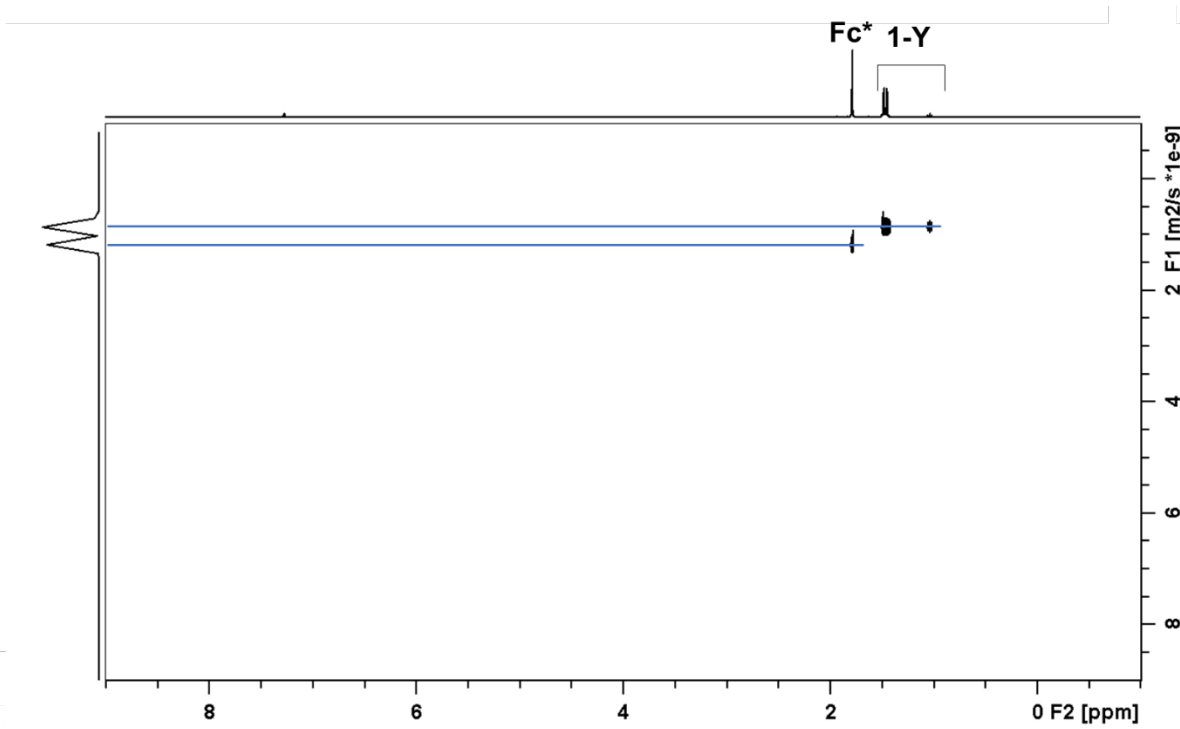


Figure S20. ¹H DOSY (400 MHz, C₆D₆) of Y(H^{Me}L)₆ (40 mM), decamethylferrocene (Fc*, 40 mM).

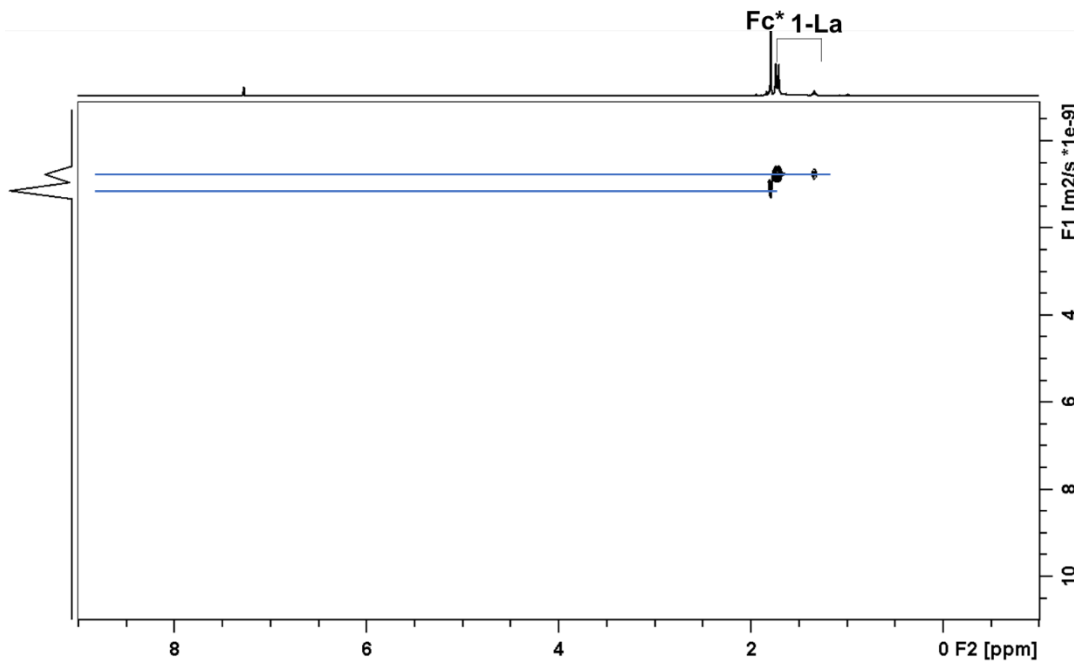


Figure S21. ¹H DOSY (400 MHz, C₆D₆) of La(H^{Me}L)₆ (40 mM), decamethylferrocene (Fc*, 40 mM).

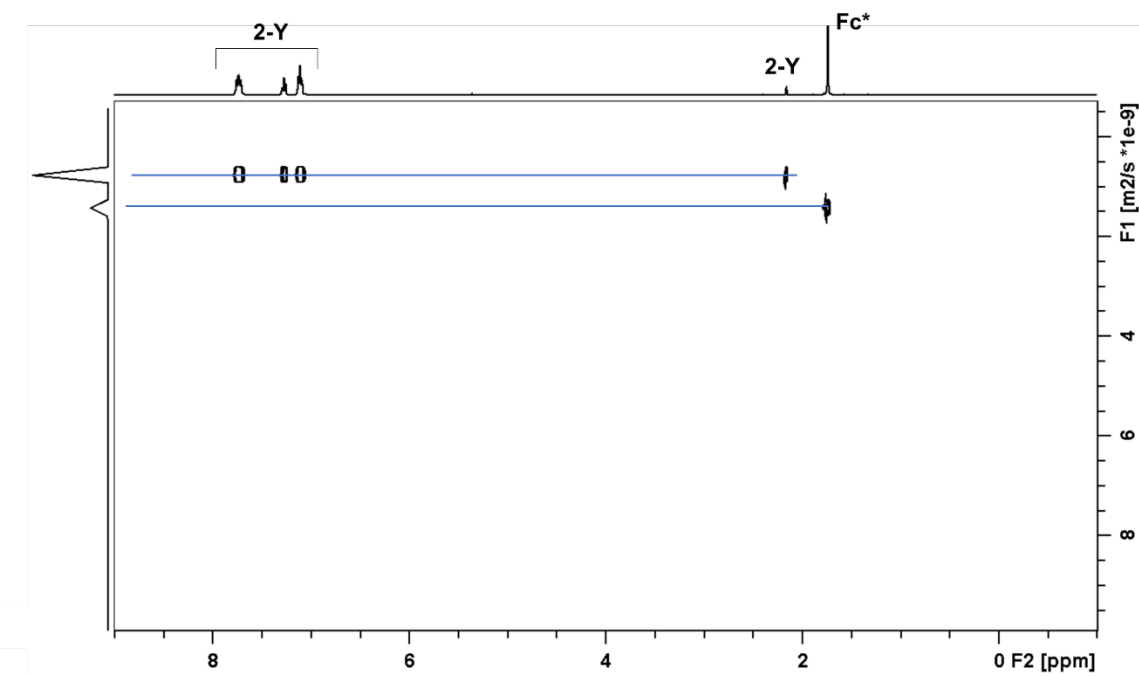


Figure S22. ^1H DOSY (400 MHz, C_6D_6) of $\text{Y}(\text{H}^{\text{Ph}}\text{L})_3$. (40 mM), decamethylferrocene (Fc^* , 40 mM).

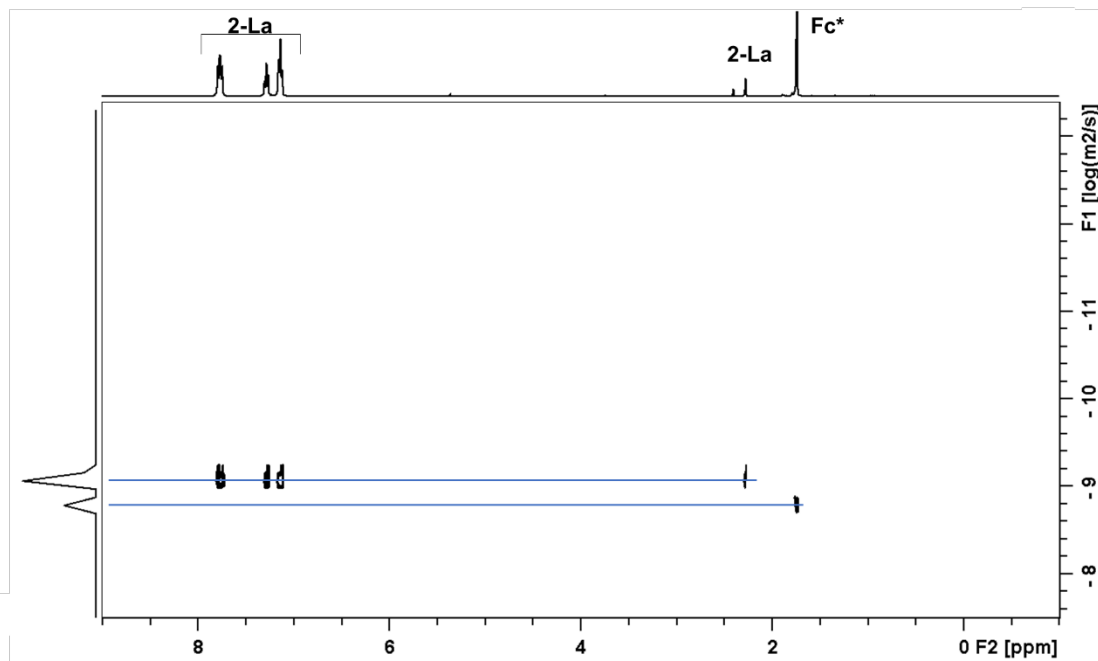


Figure S23. ^1H DOSY (400 MHz, C_6D_6) of $\text{Y}(\text{H}^{\text{Ph}}\text{L})_3$. (40 mM), decamethylferrocene (Fc^* , 40 mM).

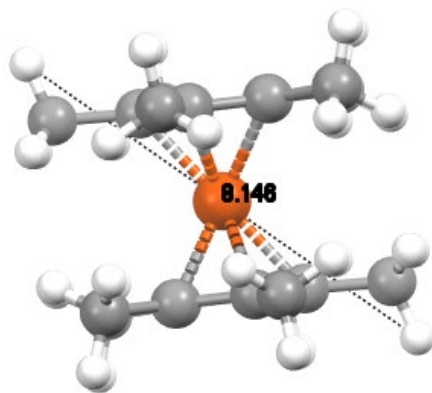


Figure S24. Points used for determination of $r_{H(\text{theo})}$ from the crystal structure of \mathbf{Fe}^* .¹⁰ CSD reference number = DMFERR04.¹³

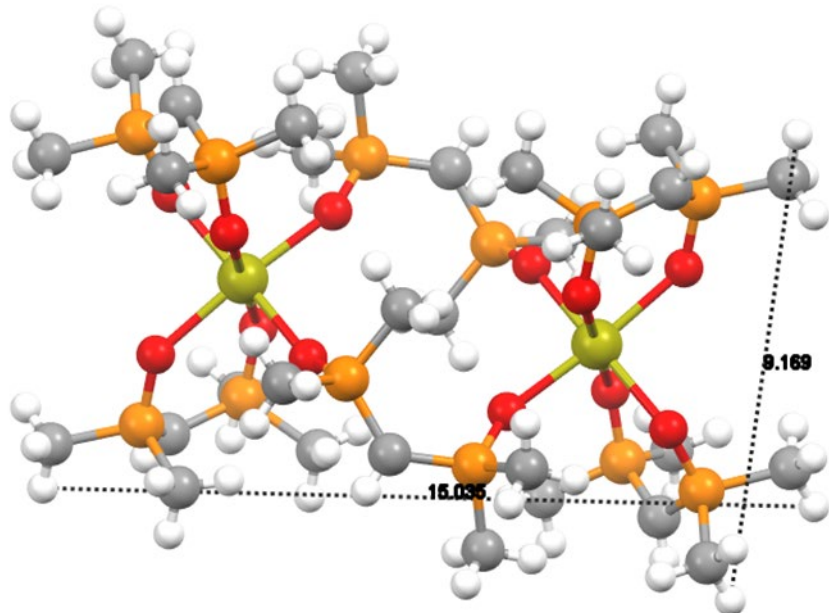


Figure S25. Points used for determination of $r_{H(\text{theo})}$ from the crystal structure of $\mathbf{Y}(\mathbf{H}^{\mathbf{M}\mathbf{e}}\mathbf{L})_6$.

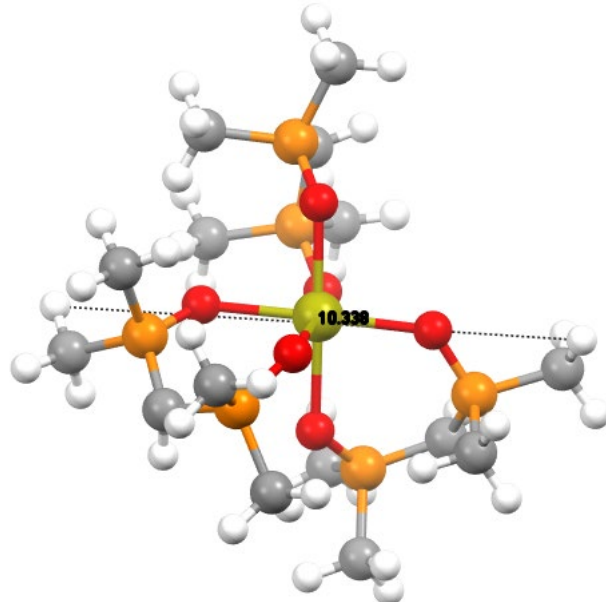


Figure S26. Points used for determination of $r_{\text{H}(\text{theo})}$ from the DFT optimized structure of $\text{Y}(\text{H}^{\text{Me}}\text{L})_6$.

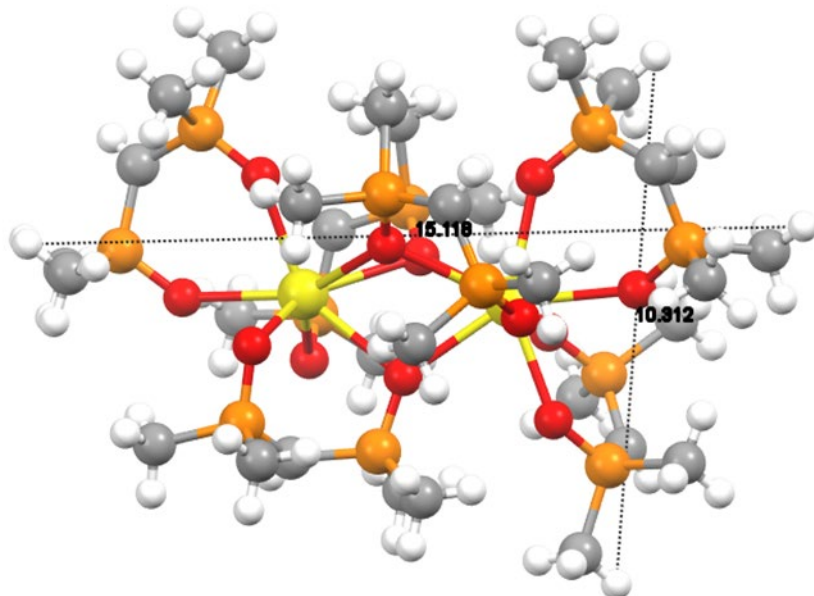


Figure S27. Points used for determination of $r_{\text{H}(\text{theo})}$ from the crystal structure of $\text{La}(\text{H}^{\text{Me}}\text{L})_6$.

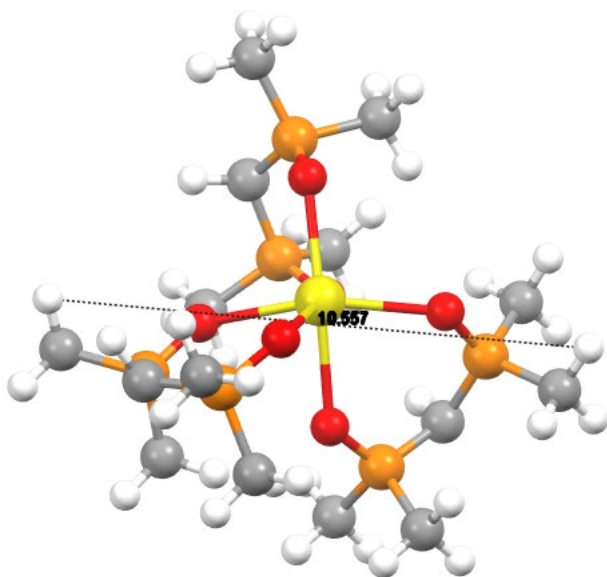


Figure S28. Points used for determination of $r_{H(\text{theo})}$ from the DFT optimized structure of $\text{La}(\text{H}^{\text{Me}}\text{L})_6$.

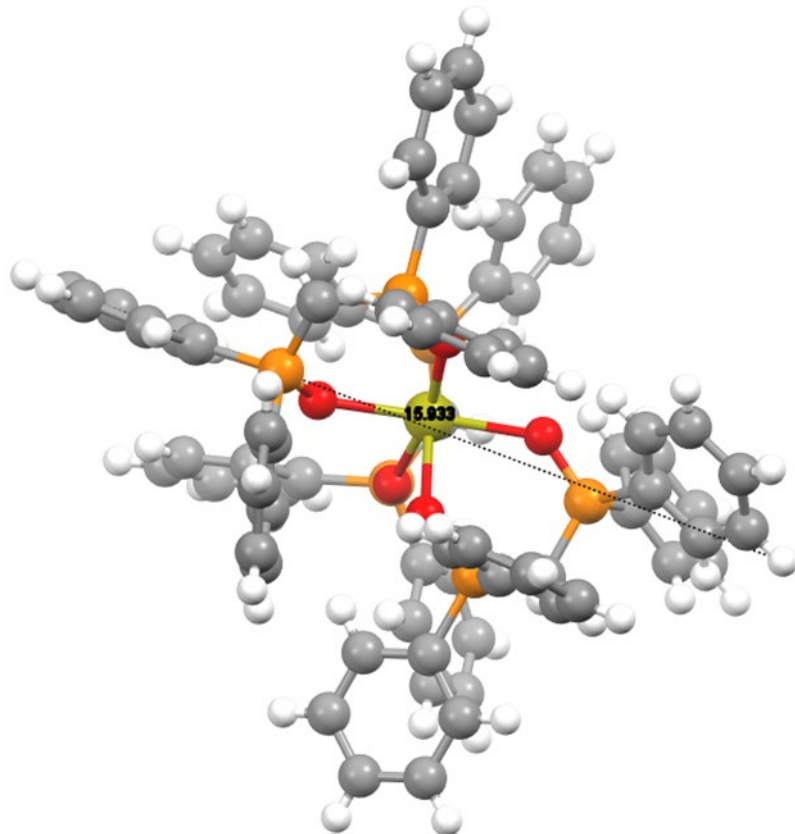


Figure S29. Points used for determination of $r_{H(\text{theo})}$ from the crystal structure of $\text{Y}(\text{H}^{\text{Ph}}\text{L})_3$.

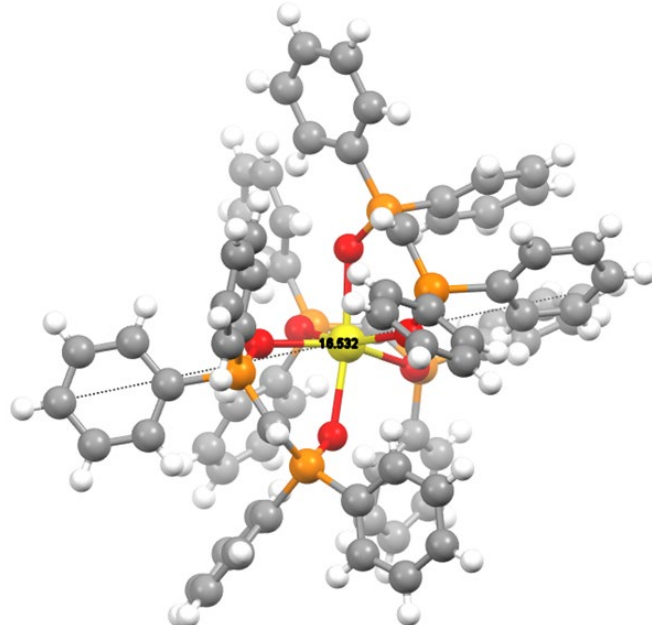


Figure S30. Points used for determination of $r_{H(\text{theo})}$ from the crystal structure of $\mathbf{La}(\mathbf{H}^{\text{Ph}}\mathbf{L})_3$.

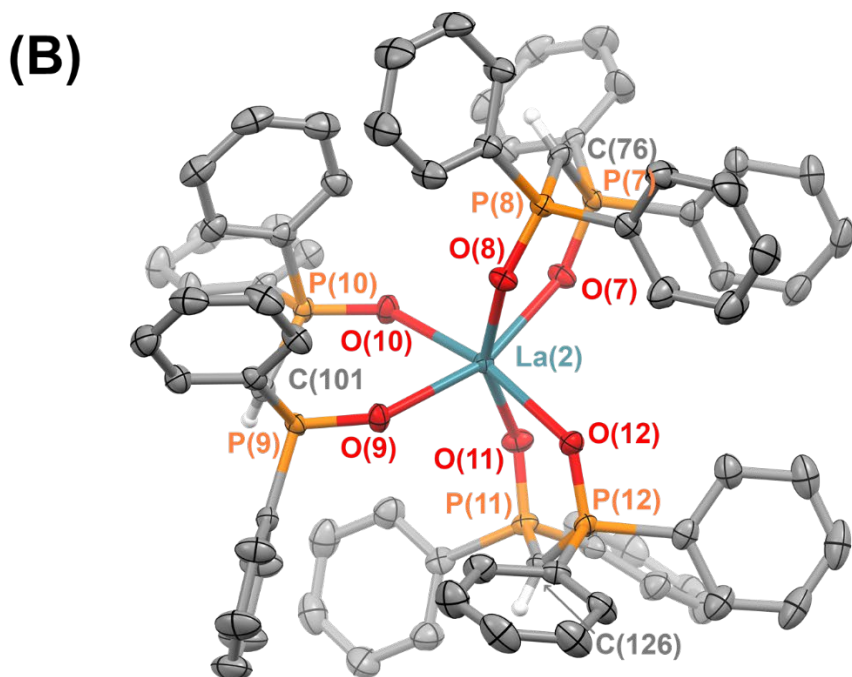
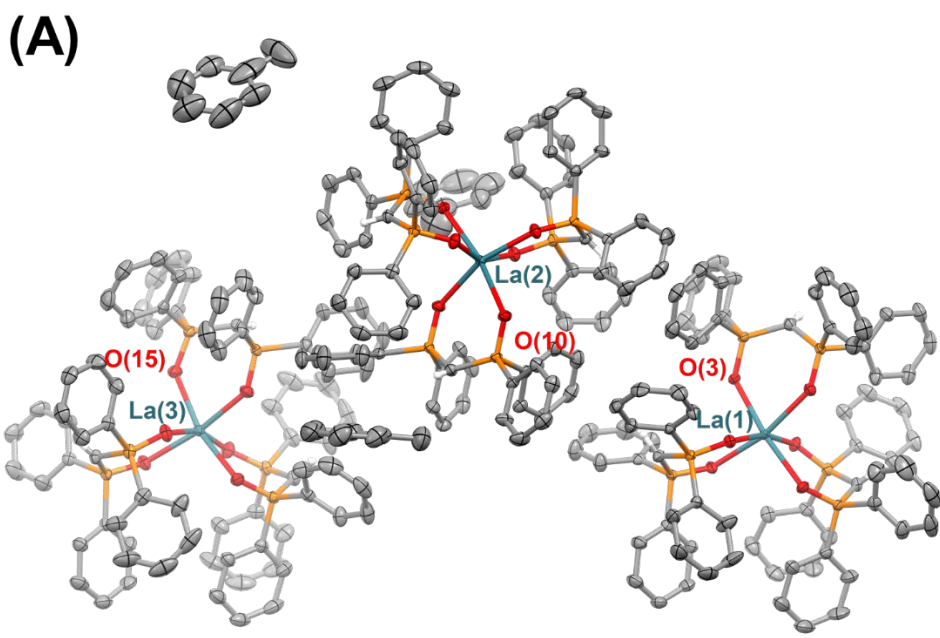


Figure S31. Thermal ellipsoid plot of $\text{La}(\text{H}^{\text{Ph}}\text{L})_3$ shown at 50% probability. Hydrogen atoms other than those attached to the methanides have been removed for clarity. (A) Full asymmetric unit. (B) La(2) only

Table S2a. Crystallographic parameters for $\text{RE}_2(\text{H}^{\text{Me}}\text{L})_6$

	$\text{Y}_2(\text{H}^{\text{Me}}\text{L})_6$	$\text{La}_2(\text{H}^{\text{Me}}\text{L})_6$
Empirical formula	$\text{C}_{15}\text{H}_{39}\text{O}_6\text{P}_6\text{Y}$	$\text{C}_{30}\text{H}_{78}\text{La}_2\text{O}_{12}\text{P}_{12}$
Formula weight	590.19	1280.38
Temperature/K	173.0	173.0
Crystal system	triclinic	monoclinic
Space group	P-1	$\text{P}2_1/\text{c}$
a/ \AA	11.1153(8)	15.9516(9)
b/ \AA	11.1205(9)	19.7431(12)
c/ \AA	14.3451(11)	18.6733(9)
$\alpha/^\circ$	105.503(3)	90
$\beta/^\circ$	95.724(3)	102.053(2)
$\gamma/^\circ$	119.484(2)	90
Volume/ \AA^3	1429.71(19)	5751.2(6)
Z	2	4
$\rho_{\text{calc}}/\text{cm}^3$	1.371	1.479
μ/mm^{-1}	2.399	1.843
F(000)	612.0	2592.0
Crystal size/ mm^3	$0.23 \times 0.13 \times 0.12$	$0.32 \times 0.23 \times 0.2$
Radiation	MoK α ($\lambda = 0.71073$)	MoK α ($\lambda = 0.71073$)
2 Θ range for data collection/ $^\circ$	4.264 to 55.074	4.126 to 55.028
Index ranges	-14 $\leq h \leq 14$, -14 $\leq k \leq 14$, -18 $\leq l \leq 18$	-20 $\leq h \leq 20$, -25 $\leq k \leq 25$, -24 $\leq l \leq 24$
Reflections collected	132469	517800
Independent reflections	6595 [$R_{\text{int}} = 0.0283$, $R_{\text{sigma}} = 0.0108$]	13221 [$R_{\text{int}} = 0.0361$, $R_{\text{sigma}} = 0.0081$]
Data/restraints/parameters	6595/0/277	13221/0/553
Goodness-of-fit on F^2	1.017	1.096
Final R indexes [$I \geq 2\sigma(I)$]	$R_1 = 0.0222$, $wR_2 = 0.0622$	$R_1 = 0.0253$, $wR_2 = 0.0546$
Final R indexes [all data]	$R_1 = 0.0246$, $wR_2 = 0.0639$	$R_1 = 0.0295$, $wR_2 = 0.0586$
Largest diff. peak/hole / e \AA^{-3}	0.81/-0.32	1.08/-1.02
CCDC Dep. #	2047855	2047852

Table S2b. Crystallographic parameters for RE(H^{Ph}L)₃

	Y(H^{Ph}L)₃	La(H^{Ph}L)₃
Empirical formula	C ₇₅ H ₆₃ O ₆ P ₆ Y	C ₈₂ H ₇₁ LaO ₆ P ₆
Formula weight	1334.98	1477.11
Temperature/K	173.2	173.22
Crystal system	triclinic	triclinic
Space group	P-1	P-1
a/Å	12.8825(11)	14.4444(10)
b/Å	14.1212(13)	25.2177(18)
c/Å	20.3872(18)	30.139(2)
$\alpha/^\circ$	93.309(4)	83.083(3)
$\beta/^\circ$	93.390(4)	88.780(3)
$\gamma/^\circ$	112.601(3)	78.946(3)
Volume/Å ³	3404.9(5)	10696.3(13)
Z	2	6
$\rho_{\text{calc}}/\text{cm}^3$	1.302	1.376
μ/mm^{-1}	1.049	0.788
F(000)	1380.0	4548.0
Crystal size/mm ³	0.3 × 0.24 × 0.2	0.3 × 0.26 × 0.22
Radiation	MoKα ($\lambda = 0.71073$)	MoKα ($\lambda = 0.71073$)
2Θ range for data collection/°	3.438 to 55.586	1.658 to 55.276
Index ranges	-16 ≤ h ≤ 16, -18 ≤ k ≤ 18, -26 ≤ l ≤ 26	-18 ≤ h ≤ 18, -32 ≤ k ≤ 32, -39 ≤ l ≤ 39
Reflections collected	233610	808224
Independent reflections	15953 [R _{int} = 0.0970, R _{sigma} = 0.0435]	49647 [R _{int} = 0.0690, R _{sigma} = 0.0269]
Data/restraints/parameters	15953/0/805	49647/0/2581
Goodness-of-fit on F ²	1.015	1.149
Final R indexes [I>=2σ (I)]	R ₁ = 0.0473, wR ₂ = 0.1160	R ₁ = 0.0481, wR ₂ = 0.1048
Final R indexes [all data]	R ₁ = 0.0678, wR ₂ = 0.1297	R ₁ = 0.0563, wR ₂ = 0.1095
Largest diff. peak/hole / e Å ⁻³	0.95/-0.63	1.81/-1.03
CCDC Dep. #	2047851	2047949

Table S3a. Distances (Å) for $\text{Y}_2(\text{H}^{\text{Me}}\text{L})_6$.

Y1 O1	2.2411(11)	P3 C6	1.7045(17)
Y1 O2	2.2566(11)	P3 C7	1.803(2)
Y1 O3	2.2597(11)	P3 C8	1.7952(18)
Y1 O4	2.2394(11)	P4 O4	1.5227(11)
Y1 O5	2.2288(11)	P4 C6	1.7028(17)
Y1 O6 ¹	2.2121(12)	P4 C9	1.793(2)
P1 O1	1.5253(11)	P4 C10	1.802(2)
P1 C1	1.7064(18)	P5 O5	1.5196(12)
P1 C2	1.7978(19)	P5 C11	1.7005(17)
P1 C3	1.7986(19)	P5 C12	1.804(2)
P2 O2	1.5184(12)	P5 C13	1.799(2)
P2 C1	1.6944(18)	P6 O6	1.5167(13)
P2 C4	1.803(2)	P6 C11	1.6980(18)
P2 C5	1.799(2)	P6 C14	1.803(2)
P3 O3	1.5249(11)	P6 C15	1.790(2)

¹1-X,1-Y,1-Z**Table S3b.** Angles (°) for $\text{Y}_2(\text{H}^{\text{Me}}\text{L})_6$

O1 Y1 O2	82.65(4)	C6 P3 C7	113.12(10)
O1 Y1 O3	92.20(4)	C6 P3 C8	108.13(9)
O2 Y1 O3	95.70(4)	C8 P3 C7	103.80(10)
O4 Y1 O1	99.51(4)	O4 P4 C6	114.41(7)
O4 Y1 O2	177.79(4)	O4 P4 C9	109.83(9)
O4 Y1 O3	83.84(4)	O4 P4 C10	106.86(8)
O5 Y1 O1	90.39(4)	C6 P4 C9	107.71(10)
O5 Y1 O2	91.89(5)	C6 P4 C10	113.33(10)
O5 Y1 O3	172.24(4)	C9 P4 C10	104.19(12)
O5 Y1 O4	88.52(4)	O5 P5 C11	115.93(8)
O6' Y1 O1	169.86(4)	O5 P5 C12	106.12(8)
O6' Y1 O2	87.47(4)	O5 P5 C13	110.91(9)
O6' Y1 O3	86.47(5)	C11 P5 C12	112.45(11)
O6' Y1 O4	90.35(4)	C11 P5 C13	106.87(10)
O6' Y1 O5	92.24(4)	C13 P5 C12	103.95(12)
O1 P1 C1	114.15(8)	O6 P6 C11	117.19(9)
O1 P1 C2	110.23(8)	O6 P6 C14	106.35(9)
O1 P1 C3	106.59(9)	O6 P6 C15	106.96(10)
C1 P1 C2	107.80(9)	C11 P6 C14	108.26(10)
C1 P1 C3	114.68(10)	C11 P6 C15	110.93(9)
C2 P1 C3	102.79(11)	C15 P6 C14	106.60(12)
O2 P2 C1	113.79(8)	P1 O1 Y1	135.93(7)
O2 P2 C4	106.83(9)	P2 O2 Y1	136.11(7)
O2 P2 C5	109.82(11)	P3 O3 Y1	134.16(6)
C1 P2 C4	113.29(13)	P4 O4 Y1	134.36(6)

C1	P2	C5	109.31(10)	P5	O5	Y1	147.62(7)
C5	P2	C4	103.25(16)	P6	O6	Y1'	145.17(8)
O3	P3	C6	114.07(7)	P2	C1	P1	123.09(10)
O3	P3	C7	106.66(9)	P4	C6	P3	121.85(10)
O3	P3	C8	110.60(8)	P6	C11	P5	126.64(11)

¹1-X,1-Y,1-Z

Table S4a. Distances (Å) for $\text{La}_2(\text{H}^{\text{MeL}})_6$.

La1	La2	4.0771(2)	P4	C10	1.816(5)
La1	O1	2.472(2)	P4	C6	1.683(5)
La1	O2	2.4483(16)	P5	O5	1.520(2)
La1	O3	2.4782(19)	P5	C11	1.700(3)
La1	O4	2.4783(18)	P5	C12	1.795(3)
La1	O5	2.4283(19)	P5	C13	1.797(3)
La1	O6	2.8625(17)	P6	O6	1.5283(17)
La1	O7	2.5404(16)	P6	C11	1.703(3)
La1	O9	2.5430(15)	P6	C14	1.809(3)
La2	P7	3.4288(6)	P6	C15	1.797(3)
La2	P8	3.3687(6)	P7	O7	1.5258(16)
La2	P9	3.4268(6)	P7	C16	1.712(2)
La2	P10	3.3494(6)	P7	C17	1.801(3)
La2	O6	2.5208(16)	P7	C18	1.788(3)
La2	O7	2.6015(16)	P8	O8	1.5159(18)
La2	O8	2.4673(17)	P8	C16	1.716(3)
La2	O9	2.5827(15)	P8	C19	1.798(3)
La2	O10	2.4676(16)	P8	C20	1.797(3)
La2	O11	2.4663(17)	P9	O9	1.5340(16)
La2	O12	2.4751(17)	P9	C21	1.710(2)
P1	O1	1.510(2)	P9	C22	1.800(2)
P1	C1	1.692(3)	P9	C23	1.794(2)
P1	C2	1.811(4)	P10	O10	1.5231(17)
P1	C3	1.793(4)	P10	C21	1.714(2)
P2	O2	1.5109(17)	P10	C24	1.810(3)
P2	C1	1.696(3)	P10	C25	1.794(2)
P2	C4	1.804(3)	P11	O11	1.5210(18)
P2	C5	1.799(3)	P11	C26	1.699(3)
P3	O3	1.505(2)	P11	C27	1.800(3)
P3	C7	1.795(5)	P11	C28	1.805(4)
P3	C8	1.769(5)	P12	O12	1.5191(18)
P3	C6	1.670(5)	P12	C26	1.706(3)
P4	O4	1.5119(19)	P12	C29	1.802(3)
P4	C9	1.764(5)	P12	C30	1.798(3)

Table S4b. Angles ($^{\circ}$) for $\text{La}_2(\text{H}^{\text{Me}}\text{L})_6$

O1	La1	La2	99.93(5)	C3	P1	C2	102.4(2)
O1	La1	O3	77.32(8)	O2	P2	C1	114.31(14)
O1	La1	O4	97.01(8)	O2	P2	C4	108.52(12)
O1	La1	O6	133.99(6)	O2	P2	C5	109.36(13)
O1	La1	O7	72.85(6)	C1	P2	C4	108.67(17)
O1	La1	O9	95.68(7)	C1	P2	C5	112.25(18)
O2	La1	La2	112.33(4)	C5	P2	C4	103.07(14)
O2	La1	O1	73.08(6)	O3	P3	C7	108.1(2)
O2	La1	O3	75.27(6)	O3	P3	C8	110.6(2)
O2	La1	O4	148.58(6)	O3	P3	C6	113.23(17)
O2	La1	O6	129.59(5)	C8	P3	C7	101.7(3)
O2	La1	O7	126.06(6)	C6	P3	C7	112.6(3)
O2	La1	O9	75.27(5)	C6	P3	C8	110.0(4)
O3	La1	La2	171.03(6)	O4	P4	C9	107.02(19)
O3	La1	O6	140.84(6)	O4	P4	C10	110.35(17)
O3	La1	O7	133.76(7)	O4	P4	C6	116.40(18)
O3	La1	O9	150.49(6)	C9	P4	C10	103.3(3)
O4	La1	La2	98.61(5)	C6	P4	C9	114.7(4)
O4	La1	O3	73.45(7)	C6	P4	C10	104.2(3)
O4	La1	O6	78.91(6)	O5	P5	C11	117.21(13)
O4	La1	O7	76.03(6)	O5	P5	C12	106.67(15)
O4	La1	O9	136.06(6)	O5	P5	C13	109.17(14)
O5	La1	La2	103.30(5)	C11	P5	C12	109.84(15)
O5	La1	O1	148.98(7)	C11	P5	C13	107.65(15)
O5	La1	O2	79.20(6)	C12	P5	C13	105.73(17)
O5	La1	O3	82.47(8)	O6	P6	C11	113.01(12)
O5	La1	O4	99.52(7)	O6	P6	C14	106.90(11)
O5	La1	O6	75.27(6)	O6	P6	C15	111.60(12)
O5	La1	O7	136.78(6)	C11	P6	C14	112.40(14)
O5	La1	O9	90.41(7)	C11	P6	C15	108.51(14)
O6	La1	La2	37.73(3)	C15	P6	C14	104.09(14)
O7	La1	La2	38.07(4)	O7	P7	La2	45.63(6)
O7	La1	O6	61.61(5)	O7	P7	C16	108.91(11)
O7	La1	O9	67.97(5)	O7	P7	C17	108.46(11)
O9	La1	La2	37.65(3)	O7	P7	C18	110.62(11)
O9	La1	O6	62.37(5)	C16	P7	La2	70.64(9)
P7	La2	La1	61.576(10)	C16	P7	C17	115.96(13)
P8	La2	La1	94.071(12)	C16	P7	C18	108.60(13)
P8	La2	P7	52.272(15)	C17	P7	La2	149.79(10)
P8	La2	P9	90.769(16)	C18	P7	La2	100.75(9)
P9	La2	La1	61.604(10)	C18	P7	C17	104.19(14)
P9	La2	P7	106.497(15)	O8	P8	La2	42.26(7)
P10	La2	La1	103.925(11)	O8	P8	C16	113.81(11)
P10	La2	P7	159.521(15)	O8	P8	C19	106.37(15)

P10	La2	P8	119.564(15)	O8	P8	C20	110.28(12)
P10	La2	P9	53.101(14)	C16	P8	La2	72.40(9)
O6	La2	La1	44.01(4)	C16	P8	C19	113.37(14)
O6	La2	P7	81.40(4)	C16	P8	C20	107.05(14)
O6	La2	P8	131.08(4)	C19	P8	La2	133.42(15)
O6	La2	P9	88.09(4)	C20	P8	La2	116.82(12)
O6	La2	P10	98.05(4)	C20	P8	C19	105.68(19)
O6	La2	O7	65.74(5)	O9	P9	La2	45.06(6)
O6	La2	O9	66.87(5)	O9	P9	C21	112.44(10)
O7	La2	La1	37.02(3)	O9	P9	C22	107.26(10)
O7	La2	P7	24.79(4)	O9	P9	C23	110.00(11)
O7	La2	P8	65.39(4)	C21	P9	La2	69.54(8)
O7	La2	P9	86.38(4)	C21	P9	C22	112.48(12)
O7	La2	P10	137.80(4)	C21	P9	C23	107.54(12)
O8	La2	La1	93.32(4)	C22	P9	La2	138.56(9)
O8	La2	P7	71.65(4)	C23	P9	La2	111.59(9)
O8	La2	P8	24.41(4)	C23	P9	C22	106.99(12)
O8	La2	P9	69.25(4)	O10	P10	La2	43.11(6)
O8	La2	P10	96.34(4)	O10	P10	C21	112.99(11)
O8	La2	O6	137.15(6)	O10	P10	C24	106.85(12)
O8	La2	O7	76.61(5)	O10	P10	C25	111.43(11)
O8	La2	O9	80.15(5)	C21	P10	La2	71.80(8)
O8	La2	O10	120.73(6)	C21	P10	C24	114.20(13)
O8	La2	O12	76.12(6)	C21	P10	C25	105.96(12)
O9	La2	La1	36.97(3)	C24	P10	La2	138.17(10)
O9	La2	P7	89.95(4)	C25	P10	La2	112.79(9)
O9	La2	P8	95.19(4)	C25	P10	C24	105.20(13)
O9	La2	P9	24.86(3)	O11	P11	C26	114.37(12)
O9	La2	P10	71.32(4)	O11	P11	C27	111.69(13)
O9	La2	O7	66.47(5)	O11	P11	C28	106.88(14)
O10	La2	La1	105.29(4)	C26	P11	C27	107.14(16)
O10	La2	P7	163.84(4)	C26	P11	C28	113.23(17)
O10	La2	P8	142.51(4)	C27	P11	C28	102.99(19)
O10	La2	P9	71.77(4)	O12	P12	C26	115.19(12)
O10	La2	P10	24.95(4)	O12	P12	C29	111.79(12)
O10	La2	O6	82.48(6)	O12	P12	C30	106.68(13)
O10	La2	O7	142.06(5)	C26	P12	C29	106.11(14)
O10	La2	O9	82.68(5)	C26	P12	C30	113.30(15)
O10	La2	O12	82.46(6)	C30	P12	C29	103.18(15)
O11	La2	La1	110.10(4)	P1	O1	La1	138.53(12)
O11	La2	P7	79.85(4)	P2	O2	La1	140.87(10)
O11	La2	P8	105.65(4)	P3	O3	La1	136.67(14)
O11	La2	P9	162.47(4)	P4	O4	La1	137.55(11)
O11	La2	P10	120.11(4)	P5	O5	La1	132.10(11)
O11	La2	O6	76.56(5)	La2	O6	La1	98.26(5)

O11	La2	O7	94.80(6)	P6	O6	La1	124.04(9)
O11	La2	O8	128.05(6)	P6	O6	La2	137.33(10)
O11	La2	O9	143.13(5)	La1	O7	La2	104.91(5)
O11	La2	O10	97.49(6)	P7	O7	La1	144.23(9)
O11	La2	O12	75.66(6)	P7	O7	La2	109.58(8)
O12	La2	La1	169.21(5)	P8	O8	La2	113.33(9)
O12	La2	P7	111.92(5)	La1	O9	La2	105.39(5)
O12	La2	P8	75.40(5)	P9	O9	La1	143.32(9)
O12	La2	P9	115.33(4)	P9	O9	La2	110.07(8)
O12	La2	P10	79.85(4)	P10	O10	La2	111.95(9)
O12	La2	O6	146.22(6)	P11	O11	La2	142.56(10)
O12	La2	O7	135.45(6)	P12	O12	La2	138.46(11)
O12	La2	O9	140.06(5)	P1	C1	P2	124.78(19)
O1	P1	C1	115.57(14)	P5	C11	P6	118.96(15)
O1	P1	C2	109.74(16)	P7	C16	P8	121.72(15)
O1	P1	C3	108.11(18)	P9	C21	P10	124.41(14)
C1	P1	C2	107.0(2)	P11	C26	P12	121.60(17)
C1	P1	C3	113.2(2)	P3	C6	P4	124.1(3)

Table S5a. Distances (Å) for $\text{Y}(\text{H}^{\text{Ph}}\text{L})_3$.

Y1	O1	2.2514(17)	C22	C23	1.372(5)
Y1	O2	2.2431(17)	C23	C24	1.379(5)
Y1	O3	2.2359(17)	C24	C25	1.392(4)
Y1	O4	2.2517(18)	C27	C28	1.394(4)
Y1	O5	2.2474(17)	C27	C32	1.389(4)
Y1	O6	2.2498(17)	C28	C29	1.384(4)
P1	O1	1.5247(18)	C29	C30	1.377(5)
P1	C1	1.706(3)	C30	C31	1.384(5)
P1	C2	1.809(3)	C31	C32	1.383(4)
P1	C8	1.805(3)	C33	C34	1.379(4)
P2	O2	1.5243(18)	C33	C38	1.373(4)
P2	C1	1.711(3)	C34	C35	1.383(5)
P2	C14	1.804(3)	C35	C36	1.364(6)
P2	C20	1.806(3)	C36	C37	1.353(6)
P3	O3	1.5204(18)	C37	C38	1.396(5)
P3	C26	1.717(3)	C39	C40	1.380(4)
P3	C27	1.810(3)	C39	C44	1.385(4)
P3	C33	1.805(3)	C40	C41	1.401(5)
P4	O4	1.5287(19)	C41	C42	1.361(6)
P4	C26	1.711(3)	C42	C43	1.363(6)
P4	C39	1.805(3)	C43	C44	1.383(4)
P4	C45	1.803(3)	C45	C46	1.401(4)
P5	O5	1.5229(18)	C45	C50	1.383(4)
P5	C51	1.702(3)	C46	C47	1.377(4)

P5	C52	1.813(3)	C47	C48	1.380(5)
P5	C58	1.802(3)	C48	C49	1.375(5)
P6	O6	1.5232(18)	C49	C50	1.382(4)
P6	C51	1.702(3)	C52	C53	1.393(4)
P6	C64	1.808(3)	C52	C57	1.384(4)
P6	C70	1.814(3)	C53	C54	1.383(4)
C2	C3	1.374(4)	C54	C55	1.373(6)
C2	C7	1.394(4)	C55	C56	1.365(6)
C3	C4	1.381(5)	C56	C57	1.387(5)
C4	C5	1.353(6)	C58	C59	1.394(4)
C5	C6	1.374(6)	C58	C63	1.380(4)
C6	C7	1.378(5)	C59	C60	1.379(4)
C8	C9	1.391(4)	C60	C61	1.381(5)
C8	C13	1.394(4)	C61	C62	1.378(5)
C9	C10	1.386(4)	C62	C63	1.391(4)
C10	C11	1.375(5)	C64	C65	1.393(4)
C11	C12	1.376(6)	C64	C69	1.387(4)
C12	C13	1.390(4)	C65	C66	1.389(4)
C14	C15	1.388(4)	C66	C67	1.372(5)
C14	C19	1.373(4)	C67	C68	1.372(5)
C15	C16	1.384(4)	C68	C69	1.385(4)
C16	C17	1.363(6)	C70	C71	1.375(5)
C17	C18	1.373(6)	C70	C75	1.400(4)
C18	C19	1.395(5)	C71	C72	1.397(5)
C20	C21	1.397(4)	C72	C73	1.378(8)
C20	C25	1.382(4)	C73	C74	1.357(7)
C21	C22	1.383(4)	C74	C75	1.383(5)

Table S5b. Angles ($^{\circ}$) for $\text{Y}(\text{H}^{\text{Ph}}\text{L})_3$

O1	Y1	O4	89.04(7)	C17	C16	C15	120.4(3)
O2	Y1	O1	83.86(6)	C16	C17	C18	119.7(3)
O2	Y1	O4	164.31(6)	C17	C18	C19	120.5(4)
O2	Y1	O5	87.93(6)	C14	C19	C18	120.0(3)
O2	Y1	O6	101.23(7)	C21	C20	P2	118.4(2)
O3	Y1	O1	102.61(7)	C25	C20	P2	122.7(2)
O3	Y1	O2	83.22(6)	C25	C20	C21	118.9(3)
O3	Y1	O4	84.71(6)	C22	C21	C20	120.1(3)
O3	Y1	O5	87.01(7)	C23	C22	C21	120.7(3)
O3	Y1	O6	168.60(7)	C22	C23	C24	119.7(3)
O5	Y1	O1	166.49(7)	C23	C24	C25	120.3(3)
O5	Y1	O4	101.42(7)	C20	C25	C24	120.3(3)
O5	Y1	O6	82.70(6)	P4	C26	P3	114.46(15)
O6	Y1	O1	88.37(6)	C28	C27	P3	120.0(2)
O6	Y1	O4	92.51(7)	C32	C27	P3	120.6(2)
O1	P1	C1	116.57(12)	C32	C27	C28	119.4(3)

O1	P1	C2	105.85(12)	C29	C28	C27	119.9(3)
O1	P1	C8	108.05(12)	C30	C29	C28	120.2(3)
C1	P1	C2	109.91(13)	C29	C30	C31	120.3(3)
C1	P1	C8	107.80(13)	C32	C31	C30	119.8(3)
C8	P1	C2	108.42(13)	C31	C32	C27	120.3(3)
O2	P2	C1	117.25(12)	C34	C33	P3	116.4(2)
O2	P2	C14	109.73(12)	C38	C33	P3	124.0(2)
O2	P2	C20	104.58(11)	C38	C33	C34	119.6(3)
C1	P2	C14	105.59(12)	C33	C34	C35	119.8(4)
C1	P2	C20	112.40(13)	C36	C35	C34	120.7(4)
C14	P2	C20	106.91(12)	C37	C36	C35	119.7(3)
O3	P3	C26	115.96(11)	C36	C37	C38	120.8(4)
O3	P3	C27	105.95(11)	C33	C38	C37	119.4(4)
O3	P3	C33	109.31(12)	C40	C39	P4	123.0(2)
C26	P3	C27	110.63(12)	C40	C39	C44	119.4(3)
C26	P3	C33	108.76(13)	C44	C39	P4	117.5(2)
C33	P3	C27	105.75(12)	C39	C40	C41	119.1(3)
O4	P4	C26	118.43(11)	C42	C41	C40	120.7(4)
O4	P4	C39	108.74(12)	C41	C42	C43	120.3(3)
O4	P4	C45	105.53(11)	C42	C43	C44	120.0(3)
C26	P4	C39	108.27(13)	C43	C44	C39	120.4(3)
C26	P4	C45	109.44(12)	C46	C45	P4	120.5(2)
C45	P4	C39	105.71(12)	C50	C45	P4	121.0(2)
O5	P5	C51	117.02(12)	C50	C45	C46	118.5(2)
O5	P5	C52	105.78(12)	C47	C46	C45	120.1(3)
O5	P5	C58	109.22(11)	C46	C47	C48	120.6(3)
C51	P5	C52	111.71(14)	C49	C48	C47	119.7(3)
C51	P5	C58	105.94(13)	C48	C49	C50	120.1(3)
C58	P5	C52	106.76(12)	C49	C50	C45	120.9(3)
O6	P6	C51	115.30(12)	P6	C51	P5	120.33(16)
O6	P6	C64	110.21(12)	C53	C52	P5	119.3(2)
O6	P6	C70	105.81(12)	C57	C52	P5	121.6(2)
C51	P6	C64	107.22(13)	C57	C52	C53	119.1(3)
C51	P6	C70	113.17(14)	C54	C53	C52	119.8(3)
C64	P6	C70	104.64(12)	C55	C54	C53	120.4(4)
P1	O1	Y1	133.34(10)	C56	C55	C54	120.3(3)
P2	O2	Y1	132.87(10)	C55	C56	C57	120.1(4)
P3	O3	Y1	137.42(10)	C52	C57	C56	120.3(3)
P4	O4	Y1	131.79(10)	C59	C58	P5	121.1(2)
P5	O5	Y1	133.84(10)	C63	C58	P5	119.1(2)
P6	O6	Y1	140.43(11)	C63	C58	C59	119.7(3)
P1	C1	P2	117.38(15)	C60	C59	C58	120.1(3)
C3	C2	P1	120.7(2)	C59	C60	C61	119.9(3)
C3	C2	C7	118.3(3)	C62	C61	C60	120.4(3)
C7	C2	P1	120.9(2)	C61	C62	C63	119.8(3)

C2	C3	C4	120.4(3)	C58	C63	C62	120.1(3)
C5	C4	C3	121.2(3)	C65	C64	P6	122.3(2)
C4	C5	C6	119.5(3)	C69	C64	P6	119.0(2)
C5	C6	C7	120.2(4)	C69	C64	C65	118.7(3)
C6	C7	C2	120.5(3)	C66	C65	C64	120.4(3)
C9	C8	P1	117.7(2)	C67	C66	C65	120.5(3)
C9	C8	C13	119.3(3)	C66	C67	C68	119.3(3)
C13	C8	P1	123.0(2)	C67	C68	C69	121.2(3)
C10	C9	C8	120.3(3)	C68	C69	C64	120.0(3)
C11	C10	C9	120.0(3)	C71	C70	P6	120.2(2)
C10	C11	C12	120.3(3)	C71	C70	C75	119.4(3)
C11	C12	C13	120.4(3)	C75	C70	P6	120.4(2)
C12	C13	C8	119.7(3)	C70	C71	C72	119.7(4)
C15	C14	P2	121.4(2)	C73	C72	C71	120.5(5)
C19	C14	P2	119.6(2)	C74	C73	C72	119.7(4)
C19	C14	C15	119.0(3)	C73	C74	C75	121.0(4)
C16	C15	C14	120.5(3)	C74	C75	C70	119.7(4)
O1	Y1	O4	89.04(7)	C17	C16	C15	120.4(3)
O2	Y1	O1	83.86(6)	C16	C17	C18	119.7(3)
O2	Y1	O4	164.31(6)	C17	C18	C19	120.5(4)
O2	Y1	O5	87.93(6)	C14	C19	C18	120.0(3)
O2	Y1	O6	101.23(7)	C21	C20	P2	118.4(2)
O3	Y1	O1	102.61(7)	C25	C20	P2	122.7(2)
O3	Y1	O2	83.22(6)	C25	C20	C21	118.9(3)
O3	Y1	O4	84.71(6)	C22	C21	C20	120.1(3)
O3	Y1	O5	87.01(7)	C23	C22	C21	120.7(3)
O3	Y1	O6	168.60(7)	C22	C23	C24	119.7(3)
O5	Y1	O1	166.49(7)	C23	C24	C25	120.3(3)
O5	Y1	O4	101.42(7)	C20	C25	C24	120.3(3)
O5	Y1	O6	82.70(6)	P4	C26	P3	114.46(15)
O6	Y1	O1	88.37(6)	C28	C27	P3	120.0(2)
O6	Y1	O4	92.51(7)	C32	C27	P3	120.6(2)
O1	P1	C1	116.57(12)	C32	C27	C28	119.4(3)
O1	P1	C2	105.85(12)	C29	C28	C27	119.9(3)
O1	P1	C8	108.05(12)	C30	C29	C28	120.2(3)
C1	P1	C2	109.91(13)	C29	C30	C31	120.3(3)
C1	P1	C8	107.80(13)	C32	C31	C30	119.8(3)
C8	P1	C2	108.42(13)	C31	C32	C27	120.3(3)
O2	P2	C1	117.25(12)	C34	C33	P3	116.4(2)
O2	P2	C14	109.73(12)	C38	C33	P3	124.0(2)
O2	P2	C20	104.58(11)	C38	C33	C34	119.6(3)
C1	P2	C14	105.59(12)	C33	C34	C35	119.8(4)
C1	P2	C20	112.40(13)	C36	C35	C34	120.7(4)
C14	P2	C20	106.91(12)	C37	C36	C35	119.7(3)
O3	P3	C26	115.96(11)	C36	C37	C38	120.8(4)

O3	P3	C27	105.95(11)	C33	C38	C37	119.4(4)
O3	P3	C33	109.31(12)	C40	C39	P4	123.0(2)
C26	P3	C27	110.63(12)	C40	C39	C44	119.4(3)
C26	P3	C33	108.76(13)	C44	C39	P4	117.5(2)
C33	P3	C27	105.75(12)	C39	C40	C41	119.1(3)
O4	P4	C26	118.43(11)	C42	C41	C40	120.7(4)
O4	P4	C39	108.74(12)	C41	C42	C43	120.3(3)
O4	P4	C45	105.53(11)	C42	C43	C44	120.0(3)
C26	P4	C39	108.27(13)	C43	C44	C39	120.4(3)
C26	P4	C45	109.44(12)	C46	C45	P4	120.5(2)
C45	P4	C39	105.71(12)	C50	C45	P4	121.0(2)
O5	P5	C51	117.02(12)	C50	C45	C46	118.5(2)
O5	P5	C52	105.78(12)	C47	C46	C45	120.1(3)
O5	P5	C58	109.22(11)	C46	C47	C48	120.6(3)
C51	P5	C52	111.71(14)	C49	C48	C47	119.7(3)
C51	P5	C58	105.94(13)	C48	C49	C50	120.1(3)
C58	P5	C52	106.76(12)	C49	C50	C45	120.9(3)
O6	P6	C51	115.30(12)	P6	C51	P5	120.33(16)
O6	P6	C64	110.21(12)	C53	C52	P5	119.3(2)
O6	P6	C70	105.81(12)	C57	C52	P5	121.6(2)
C51	P6	C64	107.22(13)	C57	C52	C53	119.1(3)
C51	P6	C70	113.17(14)	C54	C53	C52	119.8(3)
C64	P6	C70	104.64(12)	C55	C54	C53	120.4(4)
P1	O1	Y1	133.34(10)	C56	C55	C54	120.3(3)
P2	O2	Y1	132.87(10)	C55	C56	C57	120.1(4)
P3	O3	Y1	137.42(10)	C52	C57	C56	120.3(3)
P4	O4	Y1	131.79(10)	C59	C58	P5	121.1(2)
P5	O5	Y1	133.84(10)	C63	C58	P5	119.1(2)
P6	O6	Y1	140.43(11)	C63	C58	C59	119.7(3)
P1	C1	P2	117.38(15)	C60	C59	C58	120.1(3)
C3	C2	P1	120.7(2)	C59	C60	C61	119.9(3)
C3	C2	C7	118.3(3)	C62	C61	C60	120.4(3)
C7	C2	P1	120.9(2)	C61	C62	C63	119.8(3)
C2	C3	C4	120.4(3)	C58	C63	C62	120.1(3)
C5	C4	C3	121.2(3)	C65	C64	P6	122.3(2)
C4	C5	C6	119.5(3)	C69	C64	P6	119.0(2)
C5	C6	C7	120.2(4)	C69	C64	C65	118.7(3)
C6	C7	C2	120.5(3)	C66	C65	C64	120.4(3)
C9	C8	P1	117.7(2)	C67	C66	C65	120.5(3)
C9	C8	C13	119.3(3)	C66	C67	C68	119.3(3)
C13	C8	P1	123.0(2)	C67	C68	C69	121.2(3)
C10	C9	C8	120.3(3)	C68	C69	C64	120.0(3)
C11	C10	C9	120.0(3)	C71	C70	P6	120.2(2)
C10	C11	C12	120.3(3)	C71	C70	C75	119.4(3)
C11	C12	C13	120.4(3)	C75	C70	P6	120.4(2)

C12	C13	C8	119.7(3)	C70	C71	C72	119.7(4)
C15	C14	P2	121.4(2)	C73	C72	C71	120.5(5)
C19	C14	P2	119.6(2)	C74	C73	C72	119.7(4)
C19	C14	C15	119.0(3)	C73	C74	C75	121.0(4)
C16	C15	C14	120.5(3)	C74	C75	C70	119.7(4)

Table S6a. Distances (Å) for $\text{La}(\text{H}^{\text{Ph}}\text{L})_3$.

La1	O1	2.411(2)	C109	C110	1.385(5)
La1	O2	2.416(2)	C110	C111	1.369(6)
La1	O3	2.367(2)	C111	C112	1.385(6)
La1	O4	2.403(2)	C112	C113	1.387(6)
La1	O5	2.409(2)	C114	C115	1.378(5)
La1	O6	2.437(2)	C114	C119	1.386(5)
P1	O1	1.527(2)	C115	C116	1.389(5)
P1	C1	1.707(3)	C116	C117	1.369(6)
P1	C2	1.806(3)	C117	C118	1.368(5)
P1	C8	1.809(3)	C118	C119	1.386(5)
P2	O2	1.528(2)	C120	C121	1.393(5)
P2	C1	1.711(3)	C120	C125	1.394(5)
P2	C14	1.806(3)	C121	C122	1.389(5)
P2	C20	1.813(3)	C122	C123	1.375(6)
P3	O3	1.526(2)	C123	C124	1.388(6)
P3	C26	1.711(3)	C124	C125	1.385(5)
P3	C27	1.814(3)	C127	C128	1.403(5)
P3	C33	1.804(3)	C127	C132	1.385(5)
P4	O4	1.527(2)	C128	C129	1.386(5)
P4	C26	1.707(3)	C129	C130	1.373(6)
P4	C39	1.807(3)	C130	C131	1.389(6)
P4	C45	1.800(3)	C131	C132	1.384(5)
P5	O5	1.529(2)	C133	C134	1.377(5)
P5	C51	1.713(3)	C133	C138	1.387(5)
P5	C52	1.809(3)	C134	C135	1.395(6)
P5	C58	1.797(3)	C135	C136	1.376(6)
P6	O6	1.520(2)	C136	C137	1.374(6)
P6	C51	1.703(3)	C137	C138	1.390(5)
P6	C64	1.806(3)	C139	C140	1.377(5)
P6	C70	1.808(3)	C139	C144	1.401(5)
C2	C3	1.379(4)	C140	C141	1.396(5)
C2	C7	1.389(5)	C141	C142	1.359(6)
C3	C4	1.384(5)	C142	C143	1.394(6)
C4	C5	1.379(5)	C143	C144	1.385(5)
C5	C6	1.374(5)	C145	C146	1.388(5)
C6	C7	1.390(5)	C145	C150	1.394(5)
C8	C9	1.374(5)	C146	C147	1.397(5)
C8	C13	1.387(5)	C147	C148	1.371(7)

C9	C10	1.388(6)	C148	C149	1.381(7)
C10	C11	1.375(7)	C149	C150	1.385(6)
C11	C12	1.377(6)	La3	O13	2.402(2)
C12	C13	1.377(5)	La3	O14	2.409(2)
C14	C19	1.392(5)	La3	O15	2.401(2)
C14	C53	1.394(4)	La3	O16	2.390(2)
C15	C52	1.386(5)	La3	O17	2.403(2)
C15	C54	1.392(5)	La3	O18	2.401(2)
C16	C17	1.380(5)	P13	O13	1.524(2)
C16	C53	1.387(5)	P13	C151	1.706(3)
C17	C18	1.383(6)	P13	C164	1.807(3)
C18	C19	1.386(5)	P13	C170	1.810(3)
C20	C21	1.376(5)	P14	O14	1.520(2)
C20	C25	1.382(5)	P14	C151	1.706(3)
C21	C22	1.385(6)	P14	C152	1.805(3)
C22	C23	1.355(6)	P14	C158	1.825(4)
C23	C24	1.380(6)	P15	O15	1.525(2)
C24	C25	1.385(5)	P15	C176	1.719(3)
C27	C28	1.390(5)	P15	C177	1.806(4)
C27	C32	1.394(5)	P15	C183	1.809(4)
C28	C29	1.384(5)	P16	O16	1.525(2)
C29	C30	1.377(6)	P16	C176	1.716(3)
C30	C31	1.376(6)	P16	C189	1.801(3)
C31	C32	1.381(5)	P16	C195	1.805(4)
C33	C34	1.386(5)	P17	O17	1.522(2)
C33	C38	1.394(5)	P17	C201	1.711(3)
C34	C35	1.387(5)	P17	C202	1.811(3)
C35	C36	1.372(6)	P17	C208	1.807(3)
C36	C37	1.373(6)	P18	O18	1.524(2)
C37	C38	1.383(5)	P18	C201	1.710(3)
C39	C40	1.382(5)	P18	C214	1.800(4)
C39	C44	1.396(5)	P18	C220	1.803(4)
C40	C41	1.384(5)	C152	C153	1.368(5)
C41	C42	1.385(6)	C152	C157	1.389(5)
C42	C43	1.375(6)	C153	C154	1.387(6)
C43	C44	1.389(5)	C154	C155	1.375(6)
C45	C46	1.393(5)	C155	C156	1.366(6)
C45	C50	1.381(5)	C156	C157	1.393(5)
C46	C47	1.394(6)	C158	C159	1.379(6)
C47	C48	1.369(7)	C158	C163	1.377(6)
C48	C49	1.382(7)	C159	C160	1.387(6)
C49	C50	1.396(5)	C160	C161	1.349(8)
C52	C57	1.386(5)	C161	C162	1.369(9)
C54	C55	1.350(7)	C162	C163	1.403(7)
C55	C56	1.367(7)	C164	C165	1.389(5)

C56	C57	1.393(6)	C164	C169	1.382(5)
C58	C59	1.377(5)	C165	C166	1.380(5)
C58	C63	1.377(6)	C166	C167	1.371(6)
C59	C60	1.385(6)	C167	C168	1.372(6)
C60	C61	1.347(8)	C168	C169	1.390(5)
C61	C62	1.355(8)	C170	C171	1.378(5)
C62	C63	1.390(6)	C170	C175	1.374(5)
C64	C65	1.395(5)	C171	C172	1.383(6)
C64	C69	1.381(5)	C172	C173	1.372(6)
C65	C66	1.386(5)	C173	C174	1.375(6)
C66	C67	1.375(7)	C174	C175	1.381(6)
C67	C68	1.381(6)	C177	C178	1.390(5)
C68	C69	1.398(5)	C177	C182	1.384(5)
C70	C71	1.384(5)	C178	C179	1.393(6)
C70	C75	1.384(5)	C179	C180	1.367(7)
C71	C72	1.388(5)	C180	C181	1.359(6)
C72	C73	1.371(6)	C181	C182	1.386(5)
C73	C74	1.380(6)	C183	C184	1.390(6)
C74	C75	1.388(6)	C183	C188	1.387(5)
La2	O7	2.366(2)	C184	C185	1.388(6)
La2	O8	2.420(2)	C185	C186	1.362(7)
La2	O9	2.410(2)	C186	C187	1.377(8)
La2	O10	2.401(2)	C187	C188	1.392(6)
La2	O11	2.412(2)	C189	C190	1.388(5)
La2	O12	2.398(2)	C189	C194	1.376(5)
P7	O7	1.522(2)	C190	C191	1.388(6)
P7	C76	1.700(3)	C191	C192	1.374(8)
P7	C89	1.800(3)	C192	C193	1.354(7)
P7	C95	1.807(3)	C193	C194	1.392(6)
P8	O8	1.525(2)	C195	C196	1.394(5)
P8	C76	1.711(3)	C195	C200	1.389(5)
P8	C77	1.818(3)	C196	C197	1.386(6)
P8	C83	1.797(3)	C197	C198	1.375(8)
P9	O9	1.524(2)	C198	C199	1.383(7)
P9	C101	1.718(3)	C199	C200	1.370(6)
P9	C102	1.812(3)	C202	C203	1.395(5)
P9	C108	1.807(3)	C202	C207	1.386(5)
P10	O10	1.523(2)	C203	C204	1.390(5)
P10	C101	1.709(3)	C204	C205	1.366(7)
P10	C114	1.804(3)	C205	C206	1.384(7)
P10	C120	1.803(3)	C206	C207	1.387(6)
P11	O11	1.520(2)	C208	C209	1.387(5)
P11	C126	1.705(3)	C208	C213	1.378(5)
P11	C127	1.812(3)	C209	C210	1.387(5)
P11	C133	1.818(3)	C210	C211	1.369(7)

P12	O12	1.520(2)	C211	C212	1.369(7)
P12	C126	1.706(3)	C212	C213	1.395(6)
P12	C139	1.812(3)	C214	C215	1.380(6)
P12	C145	1.819(3)	C214	C219	1.398(6)
C77	C78	1.394(5)	C215	C216	1.423(7)
C77	C82	1.384(5)	C216	C217	1.372(9)
C78	C79	1.385(5)	C217	C218	1.341(9)
C79	C80	1.377(6)	C218	C219	1.382(6)
C80	C81	1.377(6)	C220	C221	1.382(5)
C81	C82	1.381(5)	C220	C225	1.392(5)
C83	C84	1.383(5)	C221	C222	1.391(6)
C83	C88	1.391(5)	C222	C223	1.363(8)
C84	C85	1.384(5)	C223	C224	1.366(8)
C85	C86	1.379(6)	C224	C225	1.381(7)
C86	C87	1.379(6)	C226	C227	1.421(9)
C87	C88	1.378(5)	C227	C228	1.3900
C89	C90	1.375(5)	C227	C232	1.3900
C89	C94	1.386(5)	C228	C229	1.3900
C90	C91	1.390(5)	C229	C230	1.3900
C91	C92	1.360(6)	C230	C231	1.3900
C92	C93	1.377(6)	C231	C232	1.3900
C93	C94	1.385(5)	C233	C234	1.446(8)
C95	C96	1.390(5)	C234	C235	1.3900
C95	C100	1.386(5)	C234	C239	1.3900
C96	C97	1.387(5)	C235	C236	1.3900
C97	C98	1.381(6)	C236	C237	1.3900
C98	C99	1.367(6)	C237	C238	1.3900
C99	C100	1.391(5)	C238	C239	1.3900
C102	C103	1.385(5)	C240	C241	1.504(7)
C102	C107	1.393(5)	C241	C242	1.360(7)
C103	C104	1.394(5)	C241	C246	1.384(7)
C104	C105	1.375(6)	C242	C243	1.376(8)
C105	C106	1.384(6)	C243	C244	1.382(8)
C106	C107	1.382(5)	C244	C245	1.362(8)
C108	C109	1.391(5)	C245	C246	1.355(7)
C108	C113	1.390(5)			

Table S6b. Angles ($^{\circ}$) for $\text{La}(\text{H}^{\text{Ph}}\text{L})_3$

O1	La1	O2	81.83(7)	P10	C101	P9	116.50(19)
O1	La1	O6	87.42(7)	C103	C102	P9	120.3(3)
O2	La1	O6	165.44(8)	C103	C102	C107	119.0(3)
O3	La1	O1	87.00(8)	C107	C102	P9	120.7(3)
O3	La1	O2	94.76(8)	C102	C103	C104	120.3(3)
O3	La1	O4	80.17(8)	C105	C104	C103	120.2(4)
O3	La1	O5	172.82(8)	C104	C105	C106	119.9(3)

O3	La1	O6	94.46(8)	C107	C106	C105	120.2(4)
O4	La1	O1	167.16(8)	C106	C107	C102	120.4(3)
O4	La1	O2	98.68(8)	C109	C108	P9	120.1(3)
O4	La1	O5	93.55(8)	C113	C108	P9	121.2(3)
O4	La1	O6	93.98(8)	C113	C108	C109	118.5(3)
O5	La1	O1	99.28(8)	C110	C109	C108	120.9(4)
O5	La1	O2	89.61(7)	C111	C110	C109	119.9(4)
O5	La1	O6	82.42(7)	C110	C111	C112	120.4(4)
O1	P1	C1	117.71(14)	C111	C112	C113	119.8(4)
O1	P1	C2	105.61(13)	C112	C113	C108	120.5(4)
O1	P1	C8	109.04(14)	C115	C114	P10	122.0(3)
C1	P1	C2	110.89(15)	C115	C114	C119	118.7(3)
C1	P1	C8	107.22(15)	C119	C114	P10	119.1(2)
C2	P1	C8	105.76(14)	C114	C115	C116	120.5(3)
O2	P2	C1	116.74(14)	C117	C116	C115	120.3(4)
O2	P2	C14	110.64(14)	C118	C117	C116	119.8(3)
O2	P2	C20	105.67(14)	C117	C118	C119	120.3(3)
C1	P2	C14	106.71(15)	C114	C119	C118	120.4(3)
C1	P2	C20	111.01(15)	C121	C120	P10	120.2(3)
C14	P2	C20	105.56(15)	C121	C120	C125	118.7(3)
O3	P3	C26	118.19(14)	C125	C120	P10	121.2(3)
O3	P3	C27	105.23(14)	C122	C121	C120	120.3(4)
O3	P3	C33	107.36(15)	C123	C122	C121	120.3(4)
C26	P3	C27	111.77(16)	C122	C123	C124	120.4(4)
C26	P3	C33	106.82(16)	C125	C124	C123	119.3(4)
C33	P3	C27	106.91(15)	C124	C125	C120	121.0(3)
O4	P4	C26	115.66(14)	P11	C126	P12	124.4(2)
O4	P4	C39	110.33(14)	C128	C127	P11	120.5(3)
O4	P4	C45	107.78(15)	C132	C127	P11	120.6(3)
C26	P4	C39	105.02(16)	C132	C127	C128	118.9(3)
C26	P4	C45	114.00(16)	C129	C128	C127	119.9(4)
C45	P4	C39	103.30(15)	C130	C129	C128	120.5(4)
O5	P5	C51	116.43(14)	C129	C130	C131	120.2(4)
O5	P5	C52	105.86(15)	C132	C131	C130	119.5(4)
O5	P5	C58	109.29(15)	C131	C132	C127	120.9(4)
C51	P5	C52	110.67(16)	C134	C133	P11	118.8(3)
C51	P5	C58	104.99(16)	C134	C133	C138	119.1(3)
C58	P5	C52	109.53(16)	C138	C133	P11	122.0(3)
O6	P6	C51	117.84(14)	C133	C134	C135	120.6(4)
O6	P6	C64	109.39(14)	C136	C135	C134	119.7(4)
O6	P6	C70	106.12(15)	C137	C136	C135	120.2(4)
C51	P6	C64	105.85(15)	C136	C137	C138	120.0(4)
C51	P6	C70	109.12(16)	C133	C138	C137	120.3(4)
C64	P6	C70	108.24(15)	C140	C139	P12	124.6(3)
P1	O1	La1	134.39(12)	C140	C139	C144	119.7(3)

P2	O2	La1	133.57(13)	C144	C139	P12	115.6(2)
P3	O3	La1	135.24(13)	C139	C140	C141	120.0(4)
P4	O4	La1	138.52(13)	C142	C141	C140	120.2(4)
P5	O5	La1	134.35(13)	C141	C142	C143	120.7(4)
P6	O6	La1	131.13(13)	C144	C143	C142	119.4(4)
P1	C1	P2	118.64(18)	C143	C144	C139	119.9(4)
C3	C2	P1	119.3(2)	C146	C145	P12	119.4(3)
C3	C2	C7	118.9(3)	C146	C145	C150	119.2(3)
C7	C2	P1	121.8(2)	C150	C145	P12	121.4(3)
C2	C3	C4	120.6(3)	C145	C146	C147	120.4(4)
C5	C4	C3	120.1(3)	C148	C147	C146	119.7(4)
C6	C5	C4	120.0(3)	C147	C148	C149	120.5(4)
C5	C6	C7	119.9(3)	C148	C149	C150	120.2(4)
C2	C7	C6	120.4(3)	C149	C150	C145	120.1(4)
C9	C8	P1	119.7(3)	O13	La3	O14	81.73(8)
C9	C8	C13	118.9(3)	O13	La3	O17	103.70(8)
C13	C8	P1	121.4(3)	O15	La3	O13	91.60(8)
C8	C9	C10	120.3(4)	O15	La3	O14	97.50(9)
C11	C10	C9	120.4(4)	O15	La3	O17	164.68(8)
C10	C11	C12	119.6(4)	O16	La3	O13	170.75(8)
C11	C12	C13	119.9(4)	O16	La3	O14	92.34(8)
C12	C13	C8	120.9(4)	O16	La3	O15	82.10(8)
C19	C14	P2	118.5(2)	O16	La3	O17	82.79(8)
C19	C14	C53	119.6(3)	O16	La3	O18	100.99(9)
C53	C14	P2	121.8(2)	O17	La3	O14	85.58(8)
C52	C15	C54	120.7(4)	O18	La3	O13	86.55(8)
C17	C16	C53	120.6(3)	O18	La3	O14	160.66(9)
C16	C17	C18	120.1(3)	O18	La3	O15	98.15(9)
C17	C18	C19	119.9(4)	O18	La3	O17	82.30(8)
C18	C19	C14	120.3(3)	O13	P13	C151	116.30(15)
C21	C20	P2	120.2(3)	O13	P13	C164	105.65(14)
C21	C20	C25	118.0(3)	O13	P13	C170	110.06(15)
C25	C20	P2	121.8(3)	C151	P13	C164	112.51(16)
C20	C21	C22	120.9(4)	C151	P13	C170	106.32(16)
C23	C22	C21	120.5(4)	C164	P13	C170	105.52(15)
C22	C23	C24	119.9(4)	O14	P14	C151	116.98(15)
C23	C24	C25	119.4(4)	O14	P14	C152	108.82(15)
C20	C25	C24	121.2(4)	O14	P14	C158	106.22(17)
P4	C26	P3	120.70(19)	C151	P14	C152	104.59(16)
C28	C27	P3	120.7(3)	C151	P14	C158	110.18(17)
C28	C27	C32	118.3(3)	C152	P14	C158	109.98(16)
C32	C27	P3	121.0(3)	O15	P15	C176	117.89(15)
C29	C28	C27	120.9(4)	O15	P15	C177	106.52(16)
C30	C29	C28	120.1(4)	O15	P15	C183	107.62(16)
C31	C30	C29	119.7(4)	C176	P15	C177	109.11(16)

C30	C31	C32	120.6(4)	C176	P15	C183	108.48(17)
C31	C32	C27	120.4(4)	C177	P15	C183	106.70(15)
C34	C33	P3	118.5(3)	O16	P16	C176	117.13(15)
C34	C33	C38	119.1(3)	O16	P16	C189	109.19(15)
C38	C33	P3	122.4(3)	O16	P16	C195	105.74(16)
C33	C34	C35	120.0(4)	C176	P16	C189	108.18(17)
C36	C35	C34	120.3(4)	C176	P16	C195	111.01(16)
C35	C36	C37	120.5(4)	C189	P16	C195	104.92(15)
C36	C37	C38	119.8(4)	O17	P17	C201	117.42(15)
C37	C38	C33	120.4(4)	O17	P17	C202	105.37(15)
C40	C39	P4	122.3(3)	O17	P17	C208	108.47(15)
C40	C39	C44	119.4(3)	C201	P17	C202	111.33(17)
C44	C39	P4	118.3(3)	C201	P17	C208	105.58(16)
C39	C40	C41	120.3(4)	C208	P17	C202	108.42(15)
C40	C41	C42	120.1(4)	O18	P18	C201	117.45(15)
C43	C42	C41	120.1(4)	O18	P18	C214	107.48(17)
C42	C43	C44	120.1(4)	O18	P18	C220	105.79(16)
C43	C44	C39	120.0(4)	C201	P18	C214	107.81(17)
C46	C45	P4	118.3(3)	C201	P18	C220	108.30(17)
C50	C45	P4	122.2(3)	C214	P18	C220	109.88(17)
C50	C45	C46	119.4(3)	P13	O13	La3	137.16(13)
C45	C46	C47	120.3(4)	P14	O14	La3	133.53(13)
C48	C47	C46	119.5(4)	P15	O15	La3	134.12(14)
C47	C48	C49	121.1(4)	P16	O16	La3	134.89(14)
C48	C49	C50	119.4(4)	P17	O17	La3	131.26(13)
C45	C50	C49	120.3(4)	P18	O18	La3	131.37(13)
P6	C51	P5	118.69(19)	P13	C151	P14	120.6(2)
C15	C52	P5	119.7(3)	C153	C152	P14	118.2(3)
C57	C52	P5	121.9(3)	C153	C152	C157	118.8(3)
C57	C52	C15	118.3(3)	C157	C152	P14	122.8(3)
C16	C53	C14	119.6(3)	C152	C153	C154	121.0(4)
C55	C54	C15	120.4(4)	C155	C154	C153	119.8(4)
C54	C55	C56	120.0(4)	C156	C155	C154	120.0(4)
C55	C56	C57	120.7(5)	C155	C156	C157	120.1(4)
C52	C57	C56	119.9(4)	C152	C157	C156	120.2(4)
C59	C58	P5	124.0(3)	C159	C158	P14	121.4(3)
C59	C58	C63	118.4(4)	C163	C158	P14	120.1(3)
C63	C58	P5	117.3(3)	C163	C158	C159	118.4(4)
C58	C59	C60	120.5(5)	C158	C159	C160	121.0(5)
C61	C60	C59	120.4(5)	C161	C160	C159	120.6(6)
C60	C61	C62	120.1(4)	C160	C161	C162	119.8(5)
C61	C62	C63	120.4(5)	C161	C162	C163	120.3(5)
C58	C63	C62	120.1(5)	C158	C163	C162	120.0(5)
C65	C64	P6	120.4(3)	C165	C164	P13	121.2(3)
C69	C64	P6	119.6(3)	C169	C164	P13	120.4(3)

C69	C64	C65	120.0(3)	C169	C164	C165	118.4(3)
C66	C65	C64	119.9(4)	C166	C165	C164	121.2(4)
C67	C66	C65	120.2(4)	C167	C166	C165	119.7(4)
C66	C67	C68	120.2(4)	C166	C167	C168	120.1(4)
C67	C68	C69	120.1(4)	C167	C168	C169	120.4(4)
C64	C69	C68	119.6(4)	C164	C169	C168	120.2(4)
C71	C70	P6	120.5(3)	C171	C170	P13	118.4(3)
C75	C70	P6	120.1(3)	C175	C170	P13	122.4(3)
C75	C70	C71	119.3(3)	C175	C170	C171	119.3(3)
C70	C71	C72	120.2(4)	C170	C171	C172	120.1(4)
C73	C72	C71	120.4(4)	C173	C172	C171	120.7(4)
C72	C73	C74	119.8(4)	C172	C173	C174	119.1(4)
C73	C74	C75	120.2(4)	C173	C174	C175	120.5(4)
C70	C75	C74	120.2(4)	C170	C175	C174	120.3(4)
O7	La2	O8	80.62(7)	P16	C176	P15	116.5(2)
O7	La2	O9	161.88(8)	C178	C177	P15	120.6(3)
O7	La2	O10	85.67(8)	C182	C177	P15	120.9(3)
O7	La2	O11	84.13(8)	C182	C177	C178	118.5(4)
O7	La2	O12	101.50(8)	C177	C178	C179	119.7(4)
O9	La2	O8	92.07(8)	C180	C179	C178	120.6(4)
O9	La2	O11	107.27(8)	C181	C180	C179	120.1(4)
O10	La2	O8	105.83(8)	C180	C181	C182	120.2(4)
O10	La2	O9	80.39(7)	C177	C182	C181	120.8(4)
O10	La2	O11	90.10(8)	C184	C183	P15	121.9(3)
O11	La2	O8	156.91(8)	C188	C183	P15	118.9(3)
O12	La2	O8	87.51(8)	C188	C183	C184	119.1(4)
O12	La2	O9	94.66(7)	C185	C184	C183	120.1(4)
O12	La2	O10	165.84(8)	C186	C185	C184	120.7(5)
O12	La2	O11	78.64(8)	C185	C186	C187	119.8(4)
O7	P7	C76	116.37(14)	C186	C187	C188	120.6(4)
O7	P7	C89	108.89(14)	C183	C188	C187	119.7(5)
O7	P7	C95	104.61(14)	C190	C189	P16	118.2(3)
C76	P7	C89	106.64(15)	C194	C189	P16	123.0(3)
C76	P7	C95	111.67(16)	C194	C189	C190	118.8(3)
C89	P7	C95	108.46(14)	C189	C190	C191	120.1(4)
O8	P8	C76	116.63(14)	C192	C191	C190	120.1(4)
O8	P8	C77	106.13(14)	C193	C192	C191	120.3(4)
O8	P8	C83	110.01(14)	C192	C193	C194	120.2(5)
C76	P8	C77	109.89(15)	C189	C194	C193	120.5(4)
C76	P8	C83	105.55(15)	C196	C195	P16	120.2(3)
C83	P8	C77	108.43(15)	C200	C195	P16	121.4(3)
O9	P9	C101	115.26(14)	C200	C195	C196	118.4(4)
O9	P9	C102	106.00(14)	C197	C196	C195	120.3(4)
O9	P9	C108	110.45(14)	C198	C197	C196	120.2(5)
C101	P9	C102	110.50(15)	C197	C198	C199	120.0(4)

C101	P9	C108	108.64(16)	C200	C199	C198	119.9(4)
C108	P9	C102	105.55(14)	C199	C200	C195	121.3(4)
O10	P10	C101	118.15(14)	P18	C201	P17	118.0(2)
O10	P10	C114	107.76(14)	C203	C202	P17	118.3(3)
O10	P10	C120	105.62(14)	C207	C202	P17	122.5(3)
C101	P10	C114	108.77(16)	C207	C202	C203	119.2(3)
C101	P10	C120	109.83(16)	C204	C203	C202	120.1(4)
C120	P10	C114	106.04(14)	C205	C204	C203	120.4(4)
O11	P11	C126	113.89(15)	C204	C205	C206	119.8(4)
O11	P11	C127	108.73(14)	C205	C206	C207	120.5(4)
O11	P11	C133	108.24(15)	C202	C207	C206	119.9(4)
C126	P11	C127	114.17(16)	C209	C208	P17	121.7(3)
C126	P11	C133	108.42(16)	C213	C208	P17	118.9(3)
C127	P11	C133	102.65(15)	C213	C208	C209	119.3(4)
O12	P12	C126	114.63(14)	C210	C209	C208	120.2(4)
O12	P12	C139	109.31(14)	C211	C210	C209	120.1(4)
O12	P12	C145	105.11(15)	C212	C211	C210	120.3(4)
C126	P12	C139	106.30(15)	C211	C212	C213	120.1(4)
C126	P12	C145	114.10(16)	C208	C213	C212	120.0(4)
C139	P12	C145	107.14(15)	C215	C214	P18	122.8(3)
P7	O7	La2	138.10(13)	C215	C214	C219	120.1(4)
P8	O8	La2	135.03(12)	C219	C214	P18	117.1(3)
P9	O9	La2	139.22(13)	C214	C215	C216	118.1(5)
P10	O10	La2	131.86(13)	C217	C216	C215	119.9(5)
P11	O11	La2	130.47(13)	C218	C217	C216	121.7(5)
P12	O12	La2	131.72(13)	C217	C218	C219	119.9(6)
P7	C76	P8	119.88(19)	C218	C219	C214	120.3(5)
C78	C77	P8	119.2(3)	C221	C220	P18	118.8(3)
C82	C77	P8	122.0(3)	C221	C220	C225	118.8(4)
C82	C77	C78	118.7(3)	C225	C220	P18	122.0(3)
C79	C78	C77	120.4(4)	C220	C221	C222	119.7(5)
C80	C79	C78	120.0(4)	C223	C222	C221	121.0(5)
C81	C80	C79	120.2(4)	C222	C223	C224	119.8(5)
C80	C81	C82	119.9(4)	C223	C224	C225	120.4(5)
C81	C82	C77	120.8(4)	C224	C225	C220	120.4(5)
C84	C83	P8	119.5(3)	C228	C227	C226	119.2(5)
C84	C83	C88	119.1(3)	C228	C227	C232	120.0
C88	C83	P8	121.1(2)	C232	C227	C226	120.8(5)
C83	C84	C85	120.3(3)	C227	C228	C229	120.0
C86	C85	C84	120.0(4)	C230	C229	C228	120.0
C85	C86	C87	120.2(4)	C231	C230	C229	120.0
C88	C87	C86	119.9(4)	C230	C231	C232	120.0
C87	C88	C83	120.5(3)	C231	C232	C227	120.0
C90	C89	P7	123.1(3)	C235	C234	C233	117.2(7)
C90	C89	C94	119.1(3)	C235	C234	C239	120.0

C94	C89	P7	117.8(2)	C239	C234	C233	122.8(7)
C89	C90	C91	119.8(4)	C236	C235	C234	120.0
C92	C91	C90	121.1(4)	C237	C236	C235	120.0
C91	C92	C93	119.4(3)	C236	C237	C238	120.0
C92	C93	C94	120.2(4)	C239	C238	C237	120.0
C93	C94	C89	120.3(4)	C238	C239	C234	120.0
C96	C95	P7	119.3(3)	C242	C241	C240	120.5(5)
C100	C95	P7	121.7(3)	C242	C241	C246	118.1(5)
C100	C95	C96	119.1(3)	C246	C241	C240	121.4(5)
C97	C96	C95	120.0(4)	C241	C242	C243	120.8(5)
C98	C97	C96	120.1(4)	C242	C243	C244	119.8(6)
C99	C98	C97	120.4(3)	C245	C244	C243	119.9(5)
C98	C99	C100	119.8(4)	C246	C245	C244	119.4(5)
C95	C100	C99	120.6(4)	C245	C246	C241	122.0(5)
O1	La1	O2	81.83(7)	P10	C101	P9	116.50(19)
O1	La1	O6	87.42(7)	C103	C102	P9	120.3(3)
O2	La1	O6	165.44(8)	C103	C102	C107	119.0(3)
O3	La1	O1	87.00(8)	C107	C102	P9	120.7(3)
O3	La1	O2	94.76(8)	C102	C103	C104	120.3(3)
O3	La1	O4	80.17(8)	C105	C104	C103	120.2(4)
O3	La1	O5	172.82(8)	C104	C105	C106	119.9(3)
O3	La1	O6	94.46(8)	C107	C106	C105	120.2(4)
O4	La1	O1	167.16(8)	C106	C107	C102	120.4(3)
O4	La1	O2	98.68(8)	C109	C108	P9	120.1(3)
O4	La1	O5	93.55(8)	C113	C108	P9	121.2(3)
O4	La1	O6	93.98(8)	C113	C108	C109	118.5(3)
O5	La1	O1	99.28(8)	C110	C109	C108	120.9(4)
O5	La1	O2	89.61(7)	C111	C110	C109	119.9(4)
O5	La1	O6	82.42(7)	C110	C111	C112	120.4(4)
O1	P1	C1	117.71(14)	C111	C112	C113	119.8(4)
O1	P1	C2	105.61(13)	C112	C113	C108	120.5(4)
O1	P1	C8	109.04(14)	C115	C114	P10	122.0(3)
C1	P1	C2	110.89(15)	C115	C114	C119	118.7(3)
C1	P1	C8	107.22(15)	C119	C114	P10	119.1(2)
C2	P1	C8	105.76(14)	C114	C115	C116	120.5(3)
O2	P2	C1	116.74(14)	C117	C116	C115	120.3(4)
O2	P2	C14	110.64(14)	C118	C117	C116	119.8(3)
O2	P2	C20	105.67(14)	C117	C118	C119	120.3(3)
C1	P2	C14	106.71(15)	C114	C119	C118	120.4(3)
C1	P2	C20	111.01(15)	C121	C120	P10	120.2(3)
C14	P2	C20	105.56(15)	C121	C120	C125	118.7(3)
O3	P3	C26	118.19(14)	C125	C120	P10	121.2(3)
O3	P3	C27	105.23(14)	C122	C121	C120	120.3(4)
O3	P3	C33	107.36(15)	C123	C122	C121	120.3(4)
C26	P3	C27	111.77(16)	C122	C123	C124	120.4(4)

C26	P3	C33	106.82(16)	C125	C124	C123	119.3(4)
C33	P3	C27	106.91(15)	C124	C125	C120	121.0(3)
O4	P4	C26	115.66(14)	P11	C126	P12	124.4(2)
O4	P4	C39	110.33(14)	C128	C127	P11	120.5(3)
O4	P4	C45	107.78(15)	C132	C127	P11	120.6(3)
C26	P4	C39	105.02(16)	C132	C127	C128	118.9(3)
C26	P4	C45	114.00(16)	C129	C128	C127	119.9(4)
C45	P4	C39	103.30(15)	C130	C129	C128	120.5(4)
O5	P5	C51	116.43(14)	C129	C130	C131	120.2(4)
O5	P5	C52	105.86(15)	C132	C131	C130	119.5(4)
O5	P5	C58	109.29(15)	C131	C132	C127	120.9(4)
C51	P5	C52	110.67(16)	C134	C133	P11	118.8(3)
C51	P5	C58	104.99(16)	C134	C133	C138	119.1(3)
C58	P5	C52	109.53(16)	C138	C133	P11	122.0(3)
O6	P6	C51	117.84(14)	C133	C134	C135	120.6(4)
O6	P6	C64	109.39(14)	C136	C135	C134	119.7(4)
O6	P6	C70	106.12(15)	C137	C136	C135	120.2(4)
C51	P6	C64	105.85(15)	C136	C137	C138	120.0(4)
C51	P6	C70	109.12(16)	C133	C138	C137	120.3(4)
C64	P6	C70	108.24(15)	C140	C139	P12	124.6(3)
P1	O1	La1	134.39(12)	C140	C139	C144	119.7(3)
P2	O2	La1	133.57(13)	C144	C139	P12	115.6(2)
P3	O3	La1	135.24(13)	C139	C140	C141	120.0(4)
P4	O4	La1	138.52(13)	C142	C141	C140	120.2(4)
P5	O5	La1	134.35(13)	C141	C142	C143	120.7(4)
P6	O6	La1	131.13(13)	C144	C143	C142	119.4(4)
P1	C1	P2	118.64(18)	C143	C144	C139	119.9(4)
C3	C2	P1	119.3(2)	C146	C145	P12	119.4(3)
C3	C2	C7	118.9(3)	C146	C145	C150	119.2(3)
C7	C2	P1	121.8(2)	C150	C145	P12	121.4(3)
C2	C3	C4	120.6(3)	C145	C146	C147	120.4(4)
C5	C4	C3	120.1(3)	C148	C147	C146	119.7(4)
C6	C5	C4	120.0(3)	C147	C148	C149	120.5(4)
C5	C6	C7	119.9(3)	C148	C149	C150	120.2(4)
C2	C7	C6	120.4(3)	C149	C150	C145	120.1(4)
C9	C8	P1	119.7(3)	O13	La3	O14	81.73(8)
C9	C8	C13	118.9(3)	O13	La3	O17	103.70(8)
C13	C8	P1	121.4(3)	O15	La3	O13	91.60(8)
C8	C9	C10	120.3(4)	O15	La3	O14	97.50(9)
C11	C10	C9	120.4(4)	O15	La3	O17	164.68(8)
C10	C11	C12	119.6(4)	O16	La3	O13	170.75(8)
C11	C12	C13	119.9(4)	O16	La3	O14	92.34(8)
C12	C13	C8	120.9(4)	O16	La3	O15	82.10(8)
C19	C14	P2	118.5(2)	O16	La3	O17	82.79(8)
C19	C14	C53	119.6(3)	O16	La3	O18	100.99(9)

C53	C14	P2	121.8(2)	O17	La3	O14	85.58(8)
C52	C15	C54	120.7(4)	O18	La3	O13	86.55(8)
C17	C16	C53	120.6(3)	O18	La3	O14	160.66(9)
C16	C17	C18	120.1(3)	O18	La3	O15	98.15(9)
C17	C18	C19	119.9(4)	O18	La3	O17	82.30(8)
C18	C19	C14	120.3(3)	O13	P13	C151	116.30(15)
C21	C20	P2	120.2(3)	O13	P13	C164	105.65(14)
C21	C20	C25	118.0(3)	O13	P13	C170	110.06(15)
C25	C20	P2	121.8(3)	C151	P13	C164	112.51(16)
C20	C21	C22	120.9(4)	C151	P13	C170	106.32(16)
C23	C22	C21	120.5(4)	C164	P13	C170	105.52(15)
C22	C23	C24	119.9(4)	O14	P14	C151	116.98(15)
C23	C24	C25	119.4(4)	O14	P14	C152	108.82(15)
C20	C25	C24	121.2(4)	O14	P14	C158	106.22(17)
P4	C26	P3	120.70(19)	C151	P14	C152	104.59(16)
C28	C27	P3	120.7(3)	C151	P14	C158	110.18(17)
C28	C27	C32	118.3(3)	C152	P14	C158	109.98(16)
C32	C27	P3	121.0(3)	O15	P15	C176	117.89(15)
C29	C28	C27	120.9(4)	O15	P15	C177	106.52(16)
C30	C29	C28	120.1(4)	O15	P15	C183	107.62(16)
C31	C30	C29	119.7(4)	C176	P15	C177	109.11(16)
C30	C31	C32	120.6(4)	C176	P15	C183	108.48(17)
C31	C32	C27	120.4(4)	C177	P15	C183	106.70(15)
C34	C33	P3	118.5(3)	O16	P16	C176	117.13(15)
C34	C33	C38	119.1(3)	O16	P16	C189	109.19(15)
C38	C33	P3	122.4(3)	O16	P16	C195	105.74(16)
C33	C34	C35	120.0(4)	C176	P16	C189	108.18(17)
C36	C35	C34	120.3(4)	C176	P16	C195	111.01(16)
C35	C36	C37	120.5(4)	C189	P16	C195	104.92(15)
C36	C37	C38	119.8(4)	O17	P17	C201	117.42(15)
C37	C38	C33	120.4(4)	O17	P17	C202	105.37(15)
C40	C39	P4	122.3(3)	O17	P17	C208	108.47(15)
C40	C39	C44	119.4(3)	C201	P17	C202	111.33(17)
C44	C39	P4	118.3(3)	C201	P17	C208	105.58(16)
C39	C40	C41	120.3(4)	C208	P17	C202	108.42(15)
C40	C41	C42	120.1(4)	O18	P18	C201	117.45(15)
C43	C42	C41	120.1(4)	O18	P18	C214	107.48(17)
C42	C43	C44	120.1(4)	O18	P18	C220	105.79(16)
C43	C44	C39	120.0(4)	C201	P18	C214	107.81(17)
C46	C45	P4	118.3(3)	C201	P18	C220	108.30(17)
C50	C45	P4	122.2(3)	C214	P18	C220	109.88(17)
C50	C45	C46	119.4(3)	P13	O13	La3	137.16(13)
C45	C46	C47	120.3(4)	P14	O14	La3	133.53(13)
C48	C47	C46	119.5(4)	P15	O15	La3	134.12(14)
C47	C48	C49	121.1(4)	P16	O16	La3	134.89(14)

C48	C49	C50	119.4(4)	P17	O17	La3	131.26(13)
C45	C50	C49	120.3(4)	P18	O18	La3	131.37(13)
P6	C51	P5	118.69(19)	P13	C151	P14	120.6(2)
C15	C52	P5	119.7(3)	C153	C152	P14	118.2(3)
C57	C52	P5	121.9(3)	C153	C152	C157	118.8(3)
C57	C52	C15	118.3(3)	C157	C152	P14	122.8(3)
C16	C53	C14	119.6(3)	C152	C153	C154	121.0(4)
C55	C54	C15	120.4(4)	C155	C154	C153	119.8(4)
C54	C55	C56	120.0(4)	C156	C155	C154	120.0(4)
C55	C56	C57	120.7(5)	C155	C156	C157	120.1(4)
C52	C57	C56	119.9(4)	C152	C157	C156	120.2(4)
C59	C58	P5	124.0(3)	C159	C158	P14	121.4(3)
C59	C58	C63	118.4(4)	C163	C158	P14	120.1(3)
C63	C58	P5	117.3(3)	C163	C158	C159	118.4(4)
C58	C59	C60	120.5(5)	C158	C159	C160	121.0(5)
C61	C60	C59	120.4(5)	C161	C160	C159	120.6(6)
C60	C61	C62	120.1(4)	C160	C161	C162	119.8(5)
C61	C62	C63	120.4(5)	C161	C162	C163	120.3(5)
C58	C63	C62	120.1(5)	C158	C163	C162	120.0(5)
C65	C64	P6	120.4(3)	C165	C164	P13	121.2(3)
C69	C64	P6	119.6(3)	C169	C164	P13	120.4(3)
C69	C64	C65	120.0(3)	C169	C164	C165	118.4(3)
C66	C65	C64	119.9(4)	C166	C165	C164	121.2(4)
C67	C66	C65	120.2(4)	C167	C166	C165	119.7(4)
C66	C67	C68	120.2(4)	C166	C167	C168	120.1(4)
C67	C68	C69	120.1(4)	C167	C168	C169	120.4(4)
C64	C69	C68	119.6(4)	C164	C169	C168	120.2(4)
C71	C70	P6	120.5(3)	C171	C170	P13	118.4(3)
C75	C70	P6	120.1(3)	C175	C170	P13	122.4(3)
C75	C70	C71	119.3(3)	C175	C170	C171	119.3(3)
C70	C71	C72	120.2(4)	C170	C171	C172	120.1(4)
C73	C72	C71	120.4(4)	C173	C172	C171	120.7(4)
C72	C73	C74	119.8(4)	C172	C173	C174	119.1(4)
C73	C74	C75	120.2(4)	C173	C174	C175	120.5(4)
C70	C75	C74	120.2(4)	C170	C175	C174	120.3(4)
O7	La2	O8	80.62(7)	P16	C176	P15	116.5(2)
O7	La2	O9	161.88(8)	C178	C177	P15	120.6(3)
O7	La2	O10	85.67(8)	C182	C177	P15	120.9(3)
O7	La2	O11	84.13(8)	C182	C177	C178	118.5(4)
O7	La2	O12	101.50(8)	C177	C178	C179	119.7(4)
O9	La2	O8	92.07(8)	C180	C179	C178	120.6(4)
O9	La2	O11	107.27(8)	C181	C180	C179	120.1(4)
O10	La2	O8	105.83(8)	C180	C181	C182	120.2(4)
O10	La2	O9	80.39(7)	C177	C182	C181	120.8(4)
O10	La2	O11	90.10(8)	C184	C183	P15	121.9(3)

O11	La2	O8	156.91(8)	C188	C183	P15	118.9(3)
O12	La2	O8	87.51(8)	C188	C183	C184	119.1(4)
O12	La2	O9	94.66(7)	C185	C184	C183	120.1(4)
O12	La2	O10	165.84(8)	C186	C185	C184	120.7(5)
O12	La2	O11	78.64(8)	C185	C186	C187	119.8(4)
O7	P7	C76	116.37(14)	C186	C187	C188	120.6(4)
O7	P7	C89	108.89(14)	C183	C188	C187	119.7(5)
O7	P7	C95	104.61(14)	C190	C189	P16	118.2(3)
C76	P7	C89	106.64(15)	C194	C189	P16	123.0(3)
C76	P7	C95	111.67(16)	C194	C189	C190	118.8(3)
C89	P7	C95	108.46(14)	C189	C190	C191	120.1(4)
O8	P8	C76	116.63(14)	C192	C191	C190	120.1(4)
O8	P8	C77	106.13(14)	C193	C192	C191	120.3(4)
O8	P8	C83	110.01(14)	C192	C193	C194	120.2(5)
C76	P8	C77	109.89(15)	C189	C194	C193	120.5(4)
C76	P8	C83	105.55(15)	C196	C195	P16	120.2(3)
C83	P8	C77	108.43(15)	C200	C195	P16	121.4(3)
O9	P9	C101	115.26(14)	C200	C195	C196	118.4(4)
O9	P9	C102	106.00(14)	C197	C196	C195	120.3(4)
O9	P9	C108	110.45(14)	C198	C197	C196	120.2(5)
C101	P9	C102	110.50(15)	C197	C198	C199	120.0(4)
C101	P9	C108	108.64(16)	C200	C199	C198	119.9(4)
C108	P9	C102	105.55(14)	C199	C200	C195	121.3(4)
O10	P10	C101	118.15(14)	P18	C201	P17	118.0(2)
O10	P10	C114	107.76(14)	C203	C202	P17	118.3(3)
O10	P10	C120	105.62(14)	C207	C202	P17	122.5(3)
C101	P10	C114	108.77(16)	C207	C202	C203	119.2(3)
C101	P10	C120	109.83(16)	C204	C203	C202	120.1(4)
C120	P10	C114	106.04(14)	C205	C204	C203	120.4(4)
O11	P11	C126	113.89(15)	C204	C205	C206	119.8(4)
O11	P11	C127	108.73(14)	C205	C206	C207	120.5(4)
O11	P11	C133	108.24(15)	C202	C207	C206	119.9(4)
C126	P11	C127	114.17(16)	C209	C208	P17	121.7(3)
C126	P11	C133	108.42(16)	C213	C208	P17	118.9(3)
C127	P11	C133	102.65(15)	C213	C208	C209	119.3(4)
O12	P12	C126	114.63(14)	C210	C209	C208	120.2(4)
O12	P12	C139	109.31(14)	C211	C210	C209	120.1(4)
O12	P12	C145	105.11(15)	C212	C211	C210	120.3(4)
C126	P12	C139	106.30(15)	C211	C212	C213	120.1(4)
C126	P12	C145	114.10(16)	C208	C213	C212	120.0(4)
C139	P12	C145	107.14(15)	C215	C214	P18	122.8(3)
P7	O7	La2	138.10(13)	C215	C214	C219	120.1(4)
P8	O8	La2	135.03(12)	C219	C214	P18	117.1(3)
P9	O9	La2	139.22(13)	C214	C215	C216	118.1(5)
P10	O10	La2	131.86(13)	C217	C216	C215	119.9(5)

P11	O11	La2	130.47(13)	C218	C217	C216	121.7(5)
P12	O12	La2	131.72(13)	C217	C218	C219	119.9(6)
P7	C76	P8	119.88(19)	C218	C219	C214	120.3(5)
C78	C77	P8	119.2(3)	C221	C220	P18	118.8(3)
C82	C77	P8	122.0(3)	C221	C220	C225	118.8(4)
C82	C77	C78	118.7(3)	C225	C220	P18	122.0(3)
C79	C78	C77	120.4(4)	C220	C221	C222	119.7(5)
C80	C79	C78	120.0(4)	C223	C222	C221	121.0(5)
C81	C80	C79	120.2(4)	C222	C223	C224	119.8(5)
C80	C81	C82	119.9(4)	C223	C224	C225	120.4(5)
C81	C82	C77	120.8(4)	C224	C225	C220	120.4(5)
C84	C83	P8	119.5(3)	C228	C227	C226	119.2(5)
C84	C83	C88	119.1(3)	C228	C227	C232	120.0
C88	C83	P8	121.1(2)	C232	C227	C226	120.8(5)
C83	C84	C85	120.3(3)	C227	C228	C229	120.0
C86	C85	C84	120.0(4)	C230	C229	C228	120.0
C85	C86	C87	120.2(4)	C231	C230	C229	120.0
C88	C87	C86	119.9(4)	C230	C231	C232	120.0
C87	C88	C83	120.5(3)	C231	C232	C227	120.0
C90	C89	P7	123.1(3)	C235	C234	C233	117.2(7)
C90	C89	C94	119.1(3)	C235	C234	C239	120.0
C94	C89	P7	117.8(2)	C239	C234	C233	122.8(7)
C89	C90	C91	119.8(4)	C236	C235	C234	120.0
C92	C91	C90	121.1(4)	C237	C236	C235	120.0
C91	C92	C93	119.4(3)	C236	C237	C238	120.0
C92	C93	C94	120.2(4)	C239	C238	C237	120.0
C93	C94	C89	120.3(4)	C238	C239	C234	120.0
C96	C95	P7	119.3(3)	C242	C241	C240	120.5(5)
C100	C95	P7	121.7(3)	C242	C241	C246	118.1(5)
C100	C95	C96	119.1(3)	C246	C241	C240	121.4(5)
C97	C96	C95	120.0(4)	C241	C242	C243	120.8(5)
C98	C97	C96	120.1(4)	C242	C243	C244	119.8(6)
C99	C98	C97	120.4(3)	C245	C244	C243	119.9(5)
C98	C99	C100	119.8(4)	C246	C245	C244	119.4(5)
C95	C100	C99	120.6(4)	C245	C246	C241	122.0(5)

Section 3. Computational Studies

Methods: All calculations were performed employing the Gaussian 09 package (revision D.01).⁶³ Geometries were optimized at the M06-L level of theory¹⁴ with Grimme's D3 dispersion correction¹⁵, using the Stuttgart [7s6p5d|5s4p3d]¹⁶ ECP46MWB^{16,17} contracted pseudopotential basis set on lanthanum, the Stuttgart [8s7p6d2f1g|6s5p3d2f1g]^{18,19} ECP28MWB¹⁸ contracted pseudopotential basis set on yttrium. The 6-31G(d',p')^{20,21} basis set was used on all other atoms. NBO²² and single point calculations were performed from optimized structures using Ahlrichs' def2-TZVP^{23,24} basis sets for yttrium and lanthanum and the 6-31G(d',p') basis set on all other atoms. Solvation effects associated with water were accounted for by using the SMD continuum solvation model.²⁵ Input geometries were generated from the crystallographic data or constructed using Avogadro.²⁶ Optimized geometries were confirmed as minima by frequency analysis (the absence of negative frequencies). $\text{RE}_2(\text{H}^{\text{Me}}\text{L})_6$ and $\text{RE}(\text{H}^{\text{Me}}\text{L})_3$ minimized without negative frequencies, while both $\text{RE}(\text{H}^{\text{Ph}}\text{L})_3$ structures minimized with a single negative frequency associated with a low barrier C–H \cdots π interaction.

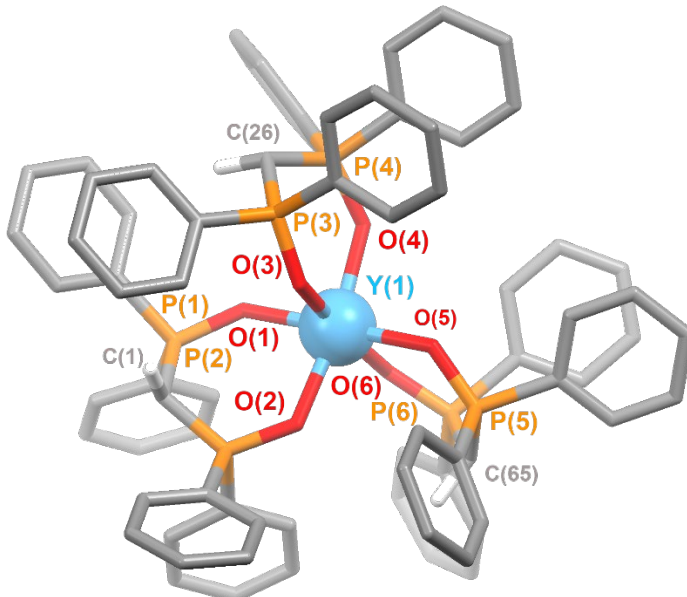


Figure S32. Labeled capped-stick image of $\text{Y}(\text{H}^{\text{Ph}}\text{L})_3$. H-atoms other than the methanide C–H were removed for clarity.

Table S7a. Comparison of select bond distances (\AA) and metrical parameters of the X-ray / DFT calculated structures of $\text{Y}(\text{H}^{\text{Ph}}\text{L})_3$. The mean unsigned error is 0.0519.

Distance (\AA)	X-ray	DFT
M(1)–O(1)	2.2514(17)	2.247
M(1)–O(2)	2.2431(17)	2.251
M(1)–O(3)	2.2359(17)	2.259
M(1)–O(4)	2.2517(18)	2.257
M(1)–O(5)	2.2474(17)	2.285

M(1)–O(6)	2.2498(17)	2.272
M(1)–C(1)	3.924(3)	3.834
M(1)–C(26)	3.841(3)	3.862
M(1)–C(65)	3.989(3)	3.804
M(1)–L plane O(1)P(1)P(2)O(2)	0.539(1)	0.533
M(1)–L plane O(3)P(3)P(4)O(4)	0.122(1)	0.316
M(1)–L plane O(5)P(5)P(6)O(6)	-0.209(1)	0.645
C(1)–L plane O(1)P(1)P(2)O(2)	0.494(1)	0.574
C(26)–L plane O(3)P(3)P(4)O(4)	0.580(1)	0.594
C(65)–L plane O(5)P(5)P(6)O(6)	0.378(1)	0.573

Table S7b. Comparison of select bond angles ($^{\circ}$) of the X-ray / DFT calculated structures of $\text{Y}(\text{H}^{\text{Ph}}\text{L})_3$.

Angle ($^{\circ}$)	X-ray	DFT
O(1)–M(1)–O(2)	83.86(6)	87.28
O(1)–M(1)–O(3)	102.61(7)	93.92
O(1)–M(1)–O(4)	89.04(7)	87.62
O(1)–M(1)–O(5)	166.49(7)	173.12
O(1)–M(1)–O(6)	88.37(6)	86.79
O(2)–M(1)–O(3)	83.22(6)	85.23
O(2)–M(1)–O(4)	164.31(6)	170.61
O(2)–M(1)–O(5)	87.93(6)	92.33
O(2)–M(1)–O(6)	101.23(7)	95.2
O(3)–M(1)–O(4)	84.71(6)	88.48
O(3)–M(1)–O(5)	87.01(7)	92.89
O(3)–M(1)–O(6)	168.60(7)	179.19
O(4)–M(1)–O(5)	101.42(7)	93.53
O(4)–M(1)–O(6)	92.51(7)	91.16
O(5)–M(1)–O(6)	82.70(6)	86.41
O(1)–P(1)–P(2)–O(2)	6.3(1)	-3.6
O(3)–P(3)–P(4)–O(4)	7.6(1)	5.93
O(5)–P(5)–P(6)–O(6)	-12.8(1)	-20.77

Table S8. Hybridization, hyperconjugation, and $E(2)$ stabilization energy for $\mathbf{Y}(\mathbf{H}^{\mathbf{Ph}}\mathbf{L})_3$.

Occupancy	Methanide Lone Pair			Interaction	$E(2)$ (kcal/mol)
	% s	% p	Label #		
1.69259	11.25	88.39	338	C14 LP - σ^* P2/O8	15.50
			338	C14 LP - σ^* P2/C38	3.62
			338	C14 LP - σ^* P3/O9	15.02
			338	C14 LP - σ^* P3/C27	3.72
1.69701	12.19	87.43	339	C60 LP - σ^* P4/O10	15.74
			339	C60 LP - σ^* P4/C62	2.67
			339	C60 LP - σ^* P4/C73	0.68
			399	C60 LP - σ^* P5/O11	14.37
			339	C60 LP - σ^* P5/C95	4.36
1.69076	10.67	88.94	340	C106 LP - σ^* P6/O12	11.19
			340	C106 LP - σ^* P6/C108	6.62
			340	C106 LP - σ^* P7/O13	16.24
			340	C106 LP - σ^* P7/C130	0.78
			340	C106 LP - σ^* P7/C141	2.83
				Average $E(2)$ / Ligand	37.78±0.086

Table S9. Cartesian coordinates of $\mathbf{Y}(\mathbf{H}^{\mathbf{Ph}}\mathbf{L})_3$.

Atom	X	Y	Z
Y	-0.048040	-0.084660	0.462759
P	0.847238	3.106958	1.265959
P	-0.397872	2.833421	-1.317441
P	3.267289	-0.250649	-0.617311
P	2.571734	-2.044057	1.538119
P	-2.175867	-2.414304	-1.066981
P	-3.067614	-1.443151	1.516489
O	0.764014	1.620578	1.712329
O	-1.053726	1.539353	-0.773191
O	1.773450	0.086025	-0.863301
O	1.082595	-1.619283	1.655529
O	-0.930454	-1.491817	-1.095951
O	-1.884352	-0.455605	1.717409
C	-0.916805	5.250033	1.696549
C	-2.116584	5.814786	2.118529
C	-3.066696	5.027679	2.770169
C	-2.806820	3.680508	3.014299
C	-1.601181	3.115095	2.600719
C	-0.649709	3.896112	1.934199
C	2.942809	3.181742	3.103569

C	4.116900	3.698878	3.646659
C	4.693593	4.846547	3.102639
C	4.099595	5.476488	2.009999
C	2.927864	4.961332	1.462439
C	2.340360	3.813713	2.008519
C	0.116223	1.217150	-3.515851
C	0.667742	0.926628	-4.762971
C	1.332815	1.916846	-5.484191
C	1.448919	3.204966	-4.959321
C	0.902670	3.499787	-3.713181
C	0.232917	2.507869	-2.985481
C	-1.469125	5.400574	-1.625111
C	-2.504822	6.321147	-1.755271
C	-3.830454	5.888171	-1.714841
C	-4.116817	4.534042	-1.546601
C	-3.080610	3.609379	-1.426241
C	-1.749449	4.038255	-1.465191
C	0.910670	3.502187	-0.411581
C	5.044815	-1.776674	-2.164791
C	5.373072	-2.626765	-3.216101
C	4.374821	-3.091602	-4.074391
C	3.050932	-2.703939	-3.879181
C	2.720305	-1.847608	-2.829931
C	3.716436	-1.380170	-1.968031
C	5.317204	1.629625	-0.088281
C	6.020378	2.800863	-0.365671
C	5.662290	3.589704	-1.457711
C	4.595229	3.211707	-2.273461
C	3.888786	2.045349	-1.996821
C	4.244863	1.247608	-0.900311
C	2.148781	-2.957896	4.119149
C	2.536710	-3.369557	5.391209
C	3.884760	-3.356891	5.748929
C	4.847101	-2.931084	4.834159
C	4.464003	-2.522973	3.558579
C	3.112453	-2.533079	3.195569
C	3.753208	-4.070511	-0.012711
C	3.717355	-5.202050	-0.822291
C	2.497343	-5.813347	-1.113881
C	1.313155	-5.290214	-0.597881
C	1.344888	-4.150534	0.202559
C	2.565750	-3.531127	0.497399
C	3.718267	-0.913030	0.913559
C	-4.216680	-3.284428	3.297729
C	-4.580611	-3.728777	4.566449

C	-4.262569	-2.967488	5.690629
C	-3.577895	-1.760900	5.548019
C	-3.209034	-1.314761	4.281789
C	-3.526696	-2.075550	3.149769
C	-4.366658	0.967452	1.063749
C	-5.418625	1.777455	0.641529
C	-6.555667	1.202928	0.075619
C	-6.646781	-0.183871	-0.055491
C	-5.602373	-0.995844	0.376859
C	-4.451471	-0.423107	0.931589
C	-3.387321	-0.250040	-2.358421
C	-4.391409	0.359012	-3.111871
C	-5.438221	-0.400075	-3.631171
C	-5.489085	-1.773965	-3.391971
C	-4.497067	-2.383577	-2.630311
C	-3.439275	-1.626980	-2.110941
C	-2.358785	-5.181523	-1.554091
C	-2.027968	-6.347774	-2.243051
C	-1.096778	-6.305057	-3.280031
C	-0.490285	-5.097339	-3.625801
C	-0.814161	-3.932188	-2.936871
C	-1.753311	-3.967115	-1.897561
C	-2.857788	-2.802232	0.473389
H	-0.188524	5.852771	1.152879
H	-2.321981	6.864767	1.917479
H	-4.011785	5.465591	3.086569
H	-3.549992	3.060150	3.514369
H	-1.402414	2.054994	2.758879
H	2.494606	2.274453	3.506189
H	4.586179	3.201667	4.493559
H	5.612865	5.246334	3.527149
H	4.555738	6.364477	1.575799
H	2.468995	5.428613	0.591349
H	-0.379439	0.438731	-2.933671
H	0.584430	-0.081682	-5.166861
H	1.765624	1.685065	-6.455521
H	1.972131	3.978224	-5.518981
H	1.012372	4.499447	-3.291441
H	-0.430314	5.732561	-1.612981
H	-2.279579	7.379546	-1.875071
H	-4.640492	6.609183	-1.809021
H	-5.150968	4.192125	-1.512131
H	-3.294133	2.550019	-1.284281
H	1.883049	3.259825	-0.848011
H	5.818496	-1.419876	-1.483401

H	6.407731	-2.929218	-3.368161
H	4.632699	-3.755553	-4.897661
H	2.273031	-3.061666	-4.552191
H	1.691125	-1.530395	-2.660481
H	5.599893	1.007494	0.759979
H	6.846018	3.100631	0.277239
H	6.213662	4.503522	-1.672051
H	4.310241	3.828448	-3.124141
H	3.042515	1.750091	-2.619291
H	1.098071	-2.947623	3.833219
H	1.785149	-3.696705	6.107239
H	4.185679	-3.676612	6.744989
H	5.898352	-2.916227	5.115099
H	5.206644	-2.184325	2.836539
H	4.700410	-3.575823	0.203049
H	4.642214	-5.601173	-1.235451
H	2.467391	-6.693867	-1.754241
H	0.357714	-5.757501	-0.835061
H	0.421519	-3.716121	0.587059
H	3.902159	-0.119321	1.647109
H	-4.458841	-3.872277	2.412619
H	-5.111903	-4.671986	4.678959
H	-4.549540	-3.315427	6.681239
H	-3.326304	-1.168801	6.425569
H	-2.662631	-0.380202	4.158159
H	-3.459836	1.406100	1.478569
H	-5.335592	2.859145	0.741029
H	-7.373195	1.835701	-0.266791
H	-7.530702	-0.632619	-0.505661
H	-5.658946	-2.078604	0.263039
H	-2.567619	0.341807	-1.946961
H	-4.351316	1.432592	-3.294931
H	-6.21722	0.078458	-4.222171
H	-6.304577	-2.369802	-3.798241
H	-4.54392	-3.455557	-2.433721
H	-3.091415	-5.203611	-0.747691
H	-2.499781	-7.290093	-1.971091
H	-0.841061	-7.215398	-3.819171
H	0.244815	-5.068911	-4.427871
H	-0.334949	-2.985259	-3.187991
H	-2.30717	-3.605683	0.974549

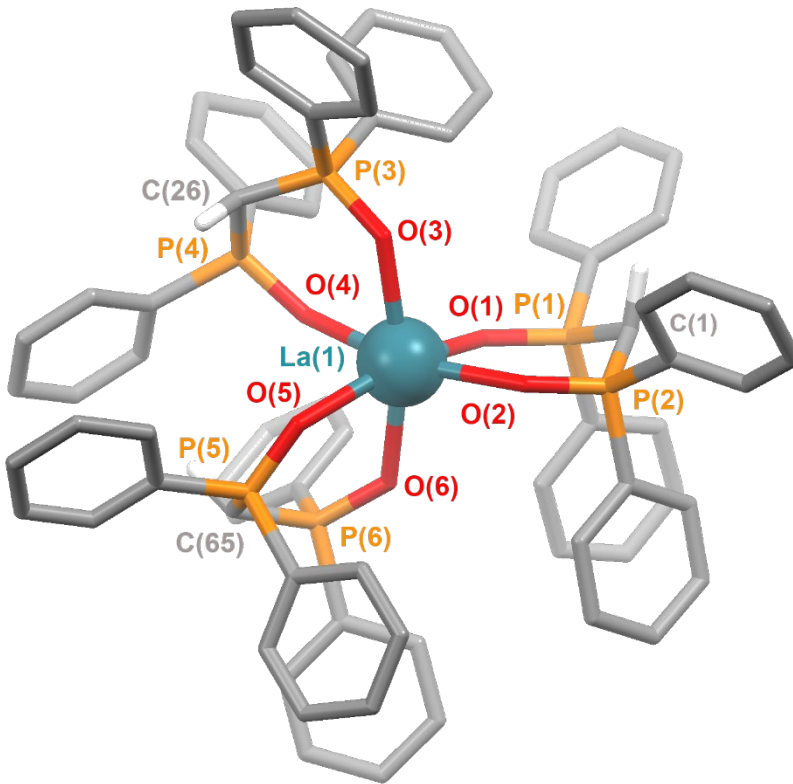


Figure S33. Labeled capped-stick image of $\text{La}(\text{HPhL})_3$. H-atoms other than the methanide C-H were removed for clarity.

Table S10a. Comparison of select bond distances (\AA) and metrical parameters of the X-ray / DFT calculated structures of $\text{La}(\text{HPhL})_3$. The mean unsigned error is 0.0519.

Distance (\AA)	X-ray	X-ray	X-ray	DFT
M(1)–O(1)	2.437	2.42	2.409	2.472
M(1)–O(2)	2.409	2.366	2.402	2.445
M(1)–O(3)	2.403	2.401	2.401	2.451
M(1)–O(4)	2.367	2.41	2.39	2.435
M(1)–O(5)	2.416	2.412	2.401	2.47
M(1)–O(6)	2.411	2.398	2.403	2.457
M(1)–C(1)	4.014(3)	4.042(3)	4.049(3)	4.149
M(1)–C(26)	4.0373(3)	4.086(3)	4.034(3)	4.083
M(1)–C(65)	3.979(3)	3.846(3)	3.910(4)	4.037
M(1)–L plane O(1)P(1)P(2)O(2)	0.330(1)	0.178(1)	0.002(1)	0.034
M(1)–L plane O(3)P(3)P(4)O(4)	0.212(1)	0.019(1)	0.539(1)	0.325
M(1)–L plane O(5)P(5)P(6)O(6)	0.276(1)	0.330(1)	0.950(1)	0.758

C(1)–L plane O(1)P(1)P(2)O(2)	0.561(1)	0.499(1)	0.494(1)	0.597
C(26)–L plane O(3)P(3)P(4)O(4)	0.409(1)	0.571(1)	0.494(1)	0.605
C(65)–L plane O(5)P(5)P(6)O(6)	0.543(1)	0.399(1)	0.580(1)	0.535

Table S10b. Comparison of select bond angles ($^{\circ}$) of the X-ray / DFT calculated structures of $\text{La}(\text{H}^{\text{Ph}}\text{L})_3$.

Angle ($^{\circ}$)	X-ray	X-ray	X-ray	DFT
O(1)–M(1)–O(2)	82.42(7)	80.62(7)	81.73(8)	81.34
O(1)–M(1)–O(3)	93.98(8)	105.83(8)	97.50(9)	103.87
O(1)–M(1)–O(4)	94.46(8)	92.07(8)	92.34(8)	81.31
O(1)–M(1)–O(5)	165.44(8)	156.91(8)	160.66(9)	155.36
O(1)–M(1)–O(6)	87.42(7)	87.51(8)	85.58(8)	78.66
O(2)–M(1)–O(3)	93.55(8)	85.67(8)	91.60(8)	95.51
O(2)–M(1)–O(4)	172.82(8)	161.88(8)	170.75(8)	160.95
O(2)–M(1)–O(5)	89.61(7)	84.13(8)	86.55(8)	111.85
O(2)–M(1)–O(6)	99.28(8)	101.50(8)	103.70(8)	99.06
O(3)–M(1)–O(4)	80.17(8)	80.39(7)	82.10(8)	81.09
O(3)–M(1)–O(5)	98.68(8)	90.10(8)	98.15(9)	95.7
O(3)–M(1)–O(6)	167.16(8)	165.84(8)	164.68(8)	165.43
O(4)–M(1)–O(5)	94.76(8)	107.27(8)	100.99(9)	87.17
O(4)–M(1)–O(6)	87.00(8)	94.66(7)	82.79(8)	85.18
O(5)–M(1)–O(6)	81.83(7)	78.64(8)	82.30(8)	78.72
O(1)–P(1)–P(2)–O(2)	8.1(1)	-4.6(1)	9.1(1)	-5.6
O(3)–P(3)–P(4)–O(4)	-12.3(1)	12.6(1)	1.0(1)	-17.37
O(5)–P(5)–P(6)–O(6)	7.7(1)	5.4(1)	-3.7(1)	23.36

Table S11. Hybridization, hyperconjugation, and $E(2)$ stabilization energy for $\text{La}(\text{H}^{\text{Ph}}\text{L})_3$.

Occupancy	Methanide Lone Pair			Interaction	$E(2)$ (kcal/mol)
	% s	% p	Label #		
1.69467	10.93	88.7	345	C14 LP - σ^* P2/O8	15.59
			345	C14 LP - σ^* P2/C38	3.82
			345	C14 LP - σ^* P3/O9	14.30
			345	C14 LP - σ^* P3/C27	4.47
1.68897	10.22	89.45	346	C60 LP - σ^* P4/O10	0.55
			346	C60 LP - σ^* P4/C62	15.93
			346	C60 LP - σ^* P4/C73	2.33
			346	C60 LP - σ^* P5/O11	1.19
			346	C60 LP - σ^* P5/C95	13.00
1.6888	9.69	89.94	347	C106 LP - σ^* P6/O12	10.70
			347	C106 LP - σ^* P6/C108	7.06
			347	C106 LP - σ^* P7/O13	16.09
			347	C106 LP - σ^* P7/C130	0.97
			347	C106 LP - σ^* P7/C141	2.93
				Average $E(2)$ / Ligand	36.31±2.35

Table S12. Cartesian coordinates of $\text{La}(\text{H}^{\text{Ph}}\text{L})_3$.

Atom	X	Y	Z
La	-0.060160	-0.147950	0.863420
P	1.306352	3.185040	1.333260
P	-0.140948	2.895430	-1.146200
P	3.247650	-0.612731	-0.723750
P	2.699629	-2.440601	1.453950
P	-2.595971	-2.074329	-1.080160
P	-3.443700	-1.394258	1.641430
O	1.119131	1.754150	1.907780
O	-0.908419	1.733721	-0.470140
O	1.748740	-0.219121	-0.764940
O	1.318110	-1.888610	1.902080
O	-1.241400	-1.333939	-0.955960
O	-2.108600	-0.721019	2.067160
C	-0.228387	5.514610	1.609870
C	-1.327836	6.248071	2.042960
C	-2.281037	5.652061	2.869010
C	-2.122017	4.327841	3.274790
C	-1.015038	3.595761	2.847750
C	-0.064848	4.180230	2.001850
C	3.468302	3.221108	3.084760

C	4.680732	3.697958	3.577370
C	5.310913	4.776458	2.957830
C	4.733063	5.373788	1.837700
C	3.523073	4.896428	1.339770
C	2.880772	3.820469	1.964700
C	0.021281	1.099250	-3.248800
C	0.417481	0.670900	-4.514990
C	1.113951	1.530430	-5.362460
C	1.414102	2.828499	-4.946350
C	1.017162	3.263650	-3.683750
C	0.317762	2.401000	-2.829380
C	-0.953047	5.535201	-1.667540
C	-1.896336	6.549291	-1.809410
C	-3.247616	6.282652	-1.582450
C	-3.651127	5.002022	-1.209110
C	-2.708038	3.984202	-1.071460
C	-1.353137	4.242741	-1.305720
C	1.299662	3.446980	-0.370080
C	4.774989	-2.136422	-2.513480
C	4.951099	-2.966502	-3.615480
C	3.847369	-3.359942	-4.374420
C	2.570889	-2.920391	-4.029670
C	2.392069	-2.082481	-2.929520
C	3.494530	-1.689852	-2.165280
C	5.280301	1.292748	-0.225560
C	5.961602	2.475337	-0.503300
C	5.620542	3.231157	-1.622920
C	4.602672	2.797208	-2.474230
C	3.919891	1.616138	-2.197970
C	4.250341	0.858658	-1.063820
C	2.687379	-3.605641	3.975230
C	3.269398	-4.198451	5.092300
C	4.652958	-4.361032	5.155450
C	5.455939	-3.928672	4.100810
C	4.877109	-3.337242	2.980330
C	3.488539	-3.171402	2.912150
C	3.391058	-4.457711	-0.372960
C	3.107288	-5.470271	-1.283860
C	1.782478	-5.826971	-1.539620
C	0.743348	-5.175620	-0.878650
C	1.026438	-4.161580	0.034270
C	2.351229	-3.790591	0.288360
C	3.833550	-1.368182	0.717740
C	-5.488401	-2.429787	3.280690
C	-5.955991	-3.135237	4.386100

C	-5.055061	-3.652867	5.316550
C	-3.685521	-3.457488	5.145360
C	-3.215041	-2.745078	4.044770
C	-4.114781	-2.232418	3.102410
C	-4.267519	1.261872	1.544190
C	-5.104288	2.309843	1.166760
C	-6.251249	2.049573	0.417200
C	-6.568249	0.739983	0.054610
C	-5.733020	-0.308197	0.430560
C	-4.573940	-0.054148	1.176450
C	-3.423439	0.368812	-2.151060
C	-4.275899	1.198272	-2.879550
C	-5.389589	0.666273	-3.525990
C	-5.659300	-0.700457	-3.438110
C	-4.815530	-1.529977	-2.705700
C	-3.689880	-1.001488	-2.060510
C	-3.092212	-4.741528	-1.854610
C	-2.859432	-5.874318	-2.633640
C	-1.901222	-5.840899	-3.645430
C	-1.172062	-4.674949	-3.877150
C	-1.393721	-3.546229	-3.093730
C	-2.356431	-3.570619	-2.076480
C	-3.398721	-2.562098	0.372200
H	0.498163	5.963650	0.932690
H	-1.452976	7.280011	1.719050
H	-3.149027	6.221662	3.195960
H	-2.863968	3.860552	3.920700
H	-0.885378	2.559011	3.156800
H	2.972522	2.371429	3.551620
H	5.136802	3.225188	4.445320
H	6.257893	5.147997	3.345050
H	5.231533	6.206068	1.343810
H	3.075033	5.336849	0.449200
H	-0.491989	0.416850	-2.569760
H	0.185820	-0.343830	-4.837290
H	1.427821	1.189189	-6.347160
H	1.962972	3.500329	-5.604260
H	1.267943	4.271930	-3.351690
H	0.108943	5.745900	-1.804290
H	-1.578176	7.552251	-2.088660
H	-3.984336	7.076602	-1.690630
H	-4.704117	4.790852	-1.025530
H	-3.011358	2.982892	-0.766490
H	2.210822	3.094299	-0.858730
H	5.631180	-1.838793	-1.906780

H	5.948459	-3.310023	-3.884430
H	3.984399	-4.013072	-5.234600
H	1.710869	-3.229811	-4.621750
H	1.402670	-1.731120	-2.634330
H	5.555121	0.701427	0.645810
H	6.757342	2.808717	0.160320
H	6.149142	4.159577	-1.833260
H	4.333872	3.382498	-3.352090
H	3.111701	1.284539	-2.852650
H	1.609269	-3.462571	3.919200
H	2.643138	-4.531111	5.917940
H	5.106768	-4.823632	6.030080
H	6.536148	-4.050883	4.151890
H	5.494529	-2.988232	2.152980
H	4.422648	-4.153622	-0.191950
H	3.919708	-5.971942	-1.806700
H	1.558797	-6.612351	-2.260390
H	-0.291272	-5.450900	-1.079980
H	0.219049	-3.641410	0.549550
H	4.217810	-0.649632	1.448960
H	-6.193051	-2.025077	2.554380
H	-7.025691	-3.280256	4.522830
H	-5.422032	-4.204427	6.180000
H	-2.981541	-3.854468	5.874230
H	-2.147751	-2.572609	3.910680
H	-3.358699	1.458822	2.111160
H	-4.848358	3.330583	1.448200
H	-6.899738	2.869684	0.1124
H	-7.457469	0.537104	-0.5395
H	-5.94724	-1.329337	0.11471
H	-2.550519	0.783151	-1.64445
H	-4.061268	2.264802	-2.94494
H	-6.048539	1.315033	-4.10058
H	-6.52752	-1.120037	-3.9434
H	-5.029881	-2.597037	-2.63356
H	-3.847092	-4.759608	-1.06994
H	-3.429413	-6.783198	-2.45049
H	-1.720573	-6.725019	-4.25395
H	-0.421912	-4.65302	-4.66535
H	-0.806481	-2.639809	-3.24677
H	-3.051891	-3.533588	0.73802

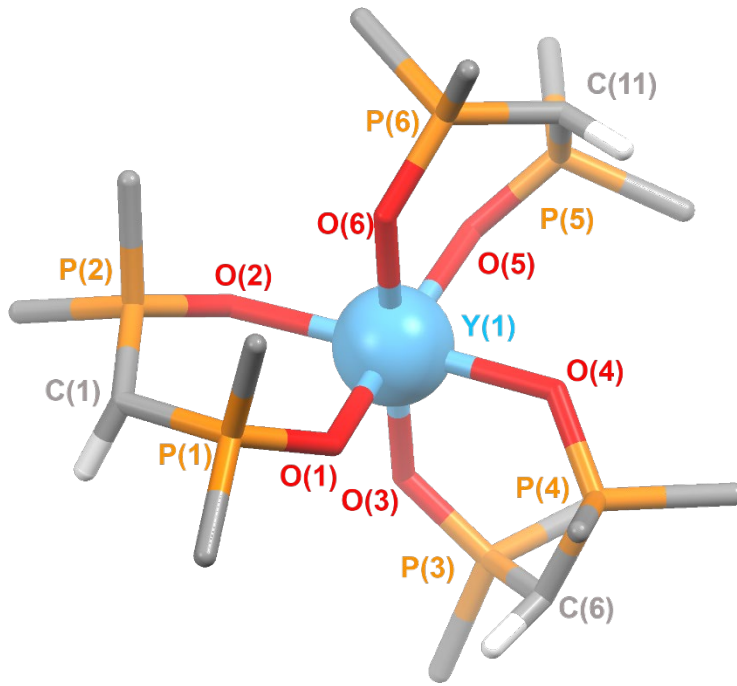


Figure S34. Labeled capped-stick image of $\text{Y}(\text{H}^{\text{Me}}\text{L})_3$. H-atoms other than the methanide C-H were removed for clarity.

Table S13a. Comparison of select bond distances (\AA) and metrical parameters of the DFT calculated structure, $\text{Y}(\text{H}^{\text{Me}}\text{L})_3$.

Distance (\AA)	$\text{Y}(1)$
$\text{M}(1)-\text{O}(1)$	2.267
$\text{M}(1)-\text{O}(2)$	2.251
$\text{M}(1)-\text{O}(3)$	2.259
$\text{M}(1)-\text{O}(4)$	2.296
$\text{M}(1)-\text{O}(5)$	2.274
$\text{M}(1)-\text{O}(6)$	2.301
$\text{M}(1)-\text{C}(1)$	3.963
$\text{M}(1)-\text{C}(6)$	3.822
$\text{M}(1)-\text{C}(11)$	3.820
$\text{M}(1)-\text{L plane}$ $\text{O}(1)\text{P}(1)\text{P}(2)\text{O}(2)$	0.54
$\text{M}(1)-\text{L plane}$ $\text{O}(3)\text{P}(3)\text{P}(4)\text{O}(4)$	0.609
$\text{M}(1)-\text{L plane}$ $\text{O}(5)\text{P}(5)\text{P}(6)\text{O}(6)$	0.643
$\text{C}(1)-\text{L plane}$ $\text{O}(1)\text{P}(1)\text{P}(2)\text{O}(2)$	0.533

C(6)–L plane	
O(3)P(3)P(4)O(4)	0.500
C(11)–L plane	
O(5)P(5)P(6)O(6)	0.507

Table S13b. Select bond angles ($^{\circ}$) of the DFT calculated structure, $\mathbf{Y}(\mathbf{H}^{\mathbf{Me}}\mathbf{L})_3$.

Angle ($^{\circ}$)	Y(1)
O(1)–M(1)–O(2)	87.81
O(1)–M(1)–O(3)	94.27
O(1)–M(1)–O(4)	88.19
O(1)–M(1)–O(5)	168.05
O(1)–M(1)–O(6)	84.46
O(2)–M(1)–O(3)	95.44
O(2)–M(1)–O(4)	175.94
O(2)–M(1)–O(5)	98.56
O(2)–M(1)–O(6)	85.94
O(3)–M(1)–O(4)	86.02
O(3)–M(1)–O(5)	95.16
O(3)–M(1)–O(6)	178.09
O(4)–M(1)–O(5)	85.17
O(4)–M(1)–O(6)	92.51
O(5)–M(1)–O(6)	85.92
O(1)–P(1)–P(2)–O(2)	-1.16
O(3)–P(3)–P(4)–O(4)	-28.40
O(5)–P(5)–P(6)–O(6)	24.21

Table S14. Hybridization, hyperconjugation, and $E(2)$ stabilization energy for $\mathbf{Y}(\mathbf{H}^{\text{Me}}\mathbf{L})_3$.

Methanide Lone Pair				Interaction	$E(2)$ (kcal/mol)
Occupancy	% s	% p	Label #		
1.69582	1.21	98.51	140	C14 LP - σ^* P2/O8	10.15
			140	C14 LP - σ^* P2/C14	3.11
			140	C14 LP - σ^* P2/C32	0.66
			140	C14 LP - σ^* P2/C64	9.59
			140	C14 LP - σ^* P3/O9	16.38
			140	C14 LP - σ^* P3/C14	3.64
			140	C14 LP - σ^* P3/C28	3.68
			140	C14 LP - σ^* P3/C60	0.97
1.69541	1.09	98.63	141	C16 LP - σ^* P4/O10	9.02
			141	C16 LP - σ^* P4/C16	2.88
			141	C16 LP - σ^* P4/C40	1.08
			141	C16 LP - σ^* P4/C44	10.31
			141	C16 LP - σ^* P5/O11	16.59
			141	C16 LP - σ^* P5/C16	3.49
			141	C16 LP - σ^* P5/C36	1.13
			141	C16 LP - σ^* P5/C48	3.48
1.70039	1.77	97.96	142	C18 LP - σ^* P6/O12	15.42
			142	C18 LP - σ^* P6/C18	3.34
			142	C18 LP - σ^* P6/C52	5.46
			142	C18 LP - σ^* P7/O13	15.59
			142	C18 LP - σ^* P7/C18	3.35
			142	C18 LP - σ^* P6/C56	5.55
				Average $E(2)$ / Ligand	48.29±0.27

Table S15. Cartesian coordinates of $\mathbf{Y}(\mathbf{H}^{\text{Me}}\mathbf{L})_3$.

Atom	X	Y	Z
Y	0.002917	-0.084884	-0.452314
P	-3.238932	-0.919876	-1.342127
P	-2.241028	-2.216232	1.110588
P	2.688774	-2.025835	-1.250695
P	2.693822	-1.057289	1.498110
P	-1.115786	2.807687	1.056499
P	1.237129	3.132114	-0.645876
O	-1.839543	-0.348419	-1.717714
O	-0.774534	-1.751651	0.872841
O	1.310434	-1.450093	-1.690283
O	1.804866	0.097481	0.958874
O	-1.299192	1.272765	0.871672

O	0.780308	1.839611	-1.380825
C	0.999988	4.483210	-1.831686
C	-1.698391	3.246248	2.711792
C	-4.201070	0.472456	-0.694056
C	-2.906123	-1.159992	2.423438
C	3.931203	-0.819756	-1.790031
C	4.275328	-0.290958	1.952842
C	2.030467	-1.706798	3.049764
C	2.999513	-3.534675	-2.195597
C	3.019807	3.099687	-0.336312
C	-2.257090	3.616076	-0.100091
C	-4.091491	-1.434283	-2.851035
C	-2.217704	-3.884258	1.811582
C	-3.307461	-2.253728	-0.248286
C	2.930791	-2.383293	0.417600
C	0.459019	3.473728	0.858371
H	1.388608	5.424444	-1.429181
H	1.500081	4.258941	-2.780605
H	-0.068642	4.615477	-2.032557
H	-1.711498	4.331503	2.852043
H	-2.705650	2.847337	2.875340
H	-1.030660	2.804869	3.458973
H	-4.215502	1.287871	-1.425915
H	-5.227037	0.172846	-0.457409
H	-3.709484	0.837878	0.214697
H	-3.940402	-1.422600	2.667014
H	-2.283150	-1.249615	3.321261
H	-2.853956	-0.116320	2.094570
H	4.952033	-1.160807	-1.591228
H	3.814004	-0.618660	-2.860495
H	3.753890	0.123679	-1.258829
H	4.120210	0.564228	2.620939
H	4.928496	-1.019494	2.444766
H	4.785695	0.059461	1.048644
H	1.995202	-0.915094	3.805590
H	2.640278	-2.534230	3.427588
H	1.010930	-2.061553	2.863011
H	2.843839	-3.348591	-3.263133
H	2.296643	-4.311720	-1.878107
H	4.019088	-3.896902	-2.032078
H	3.237617	2.259159	0.331364
H	3.567262	2.967816	-1.275652
H	3.350101	4.028899	0.139977
H	-2.019578	3.298493	-1.122659
H	-3.289957	3.316923	0.110678

H	-2.182092	4.706413	-0.038682
H	-4.109716	-0.610396	-3.571936
H	-5.117523	-1.744575	-2.629711
H	-3.559303	-2.275350	-3.306434
H	-1.819805	-4.590958	1.076335
H	-3.225463	-4.202963	2.096262
H	-1.572860	-3.910431	2.696491
H	-3.214736	-3.203223	-0.784564
H	2.418439	-3.295385	0.732874
H	1.101723	3.265031	1.717216

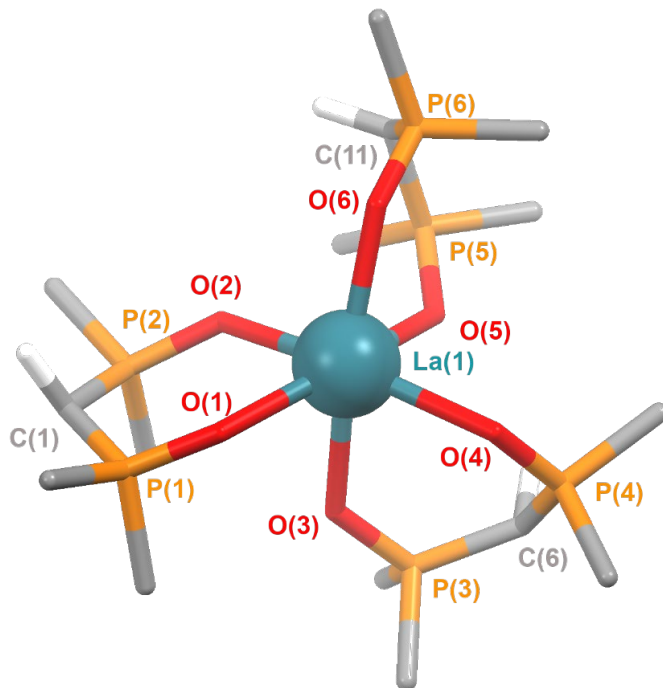


Figure S35. Labeled capped-stick image of $\text{La}(\text{H}^{\text{Me}}\text{L})_3$. H-atoms other than the methanide C-H were removed for clarity.

Table S16a. Comparison of select bond distances (\AA) and metrical parameters of the DFT calculated structure, $\text{La}(\text{H}^{\text{Me}}\text{L})_3$.

Distance (\AA)	La(1)
M(1)–O(1)	2.459
M(1)–O(2)	2.463
M(1)–O(3)	2.447
M(1)–O(4)	2.484
M(1)–O(5)	2.456
M(1)–O(6)	2.486
M(1)–C(1)	4.163
M(1)–C(6)	4.027

M(1)–C(11)	3.955
M(1)–L plane O(1)P(1)P(2)O(2)	0.643
M(1)–L plane O(3)P(3)P(4)O(4)	0.684
M(1)–L plane O(5)P(5)P(6)O(6)	0.496
C(1)–L plane O(1)P(1)P(2)O(2)	0.557
C(6)–L plane O(3)P(3)P(4)O(4)	0.623
C(11)–L plane O(5)P(5)P(6)O(6)	1.598

Table S16b. Select bond angles ($^{\circ}$) of the DFT calculated structure, **La(H^{Me}L)₃**.

Angle ($^{\circ}$)	La(1)
O(1)–M(1)–O(2)	82.03
O(1)–M(1)–O(3)	92.46
O(1)–M(1)–O(4)	79.40
O(1)–M(1)–O(5)	154.99
O(1)–M(1)–O(6)	82.25
O(2)–M(1)–O(3)	113.77
O(2)–M(1)–O(4)	157.53
O(2)–M(1)–O(5)	112.14
O(2)–M(1)–O(6)	81.14
O(3)–M(1)–O(4)	79.71
O(3)–M(1)–O(5)	99.72
O(3)–M(1)–O(6)	163.46
O(4)–M(1)–O(5)	81.38
O(4)–M(1)–O(6)	83.91
O(5)–M(1)–O(6)	79.91
O(1)–P(1)–P(2)–O(2)	-0.12
O(3)–P(3)–P(4)–O(4)	-27.94
O(5)–P(5)–P(6)–O(6)	6.26

Table S17. Hybridization, hyperconjugation, and $E(2)$ stabilization energy for $\text{La}(\text{H}^{\text{Me}}\text{L})_3$.

Occupancy	Methanide Lone Pair			Interaction	$E(2)$ (kcal/mol)
	% s	% p	Label #		
1.72394	11.37	88.28	153	C13 LP - σ^* P2/O8	14.61
			153	C13 LP - σ^* P2/C64	5.24
			153	C13 LP - σ^* P3/O9	15.65
			153	C13 LP - σ^* P3/C28	4.18
1.71624	8.04	91.63	154	C16 LP - σ^* P4/O10	9.37
			154	C16 LP - σ^* P4/C40	0.86
			154	C16 LP - σ^* P4/C44	8.45
			154	C16 LP - σ^* P5/O11	17.36
			154	C16 LP - σ^* P5/C36	0.85
			154	C16 LP - σ^* P5/C48	3.56
1.72229	10.41	89.28	155	C18 LP - σ^* P6/O12	15.27
			155	C18 LP - σ^* P6/C52	4.90
			155	C18 LP - σ^* P7/O13	15.42
			155	C18 LP - σ^* P6/C56	4.92
				Average $E(2)$ / Ligand	40.21±0.38

Table S18. Cartesian coordinates of $\text{La}(\text{H}^{\text{Me}}\text{L})_3$.

Atom	X	Y	Z
La	0.037307	0.115590	-0.898630
P	3.659024	0.619761	-1.202013
P	2.463620	1.914658	1.174766
P	-2.753614	2.419932	-1.028761
P	-2.382475	1.227664	1.617411
P	0.625830	-2.825347	1.204040
P	-1.628158	-3.106414	-0.691551
O	2.293196	0.283113	-1.871709
O	0.991147	1.699729	0.721735
O	-1.535066	1.781987	-1.761397
O	-1.697129	0.050835	0.877764
O	1.200310	-1.540738	0.544443
O	-1.118461	-1.938802	-1.586557
C	-1.298959	-4.633254	-1.612225
C	0.823967	-2.696834	2.998837
C	4.274709	-0.930221	-0.493470
C	2.800528	0.675319	2.453903
C	-4.179174	1.371477	-1.425925
C	-3.932280	0.558083	2.287541

C	-1.438401	1.730021	3.077778
C	-3.087859	4.026692	-1.788270
C	-3.429214	-3.013711	-0.542605
C	1.709351	-4.186764	0.690558
C	4.851190	1.066944	-2.487761
C	2.585575	3.514787	2.012965
C	3.703857	1.881869	-0.025036
C	-2.673460	2.645609	0.674327
C	-1.024688	-3.231071	0.920968
H	-1.706547	-5.503760	-1.088459
H	-1.731578	-4.575759	-2.616995
H	-0.218225	-4.773666	-1.721304
H	0.482686	-3.606148	3.503549
H	1.871420	-2.510104	3.259334
H	0.227675	-1.850176	3.357745
H	4.401573	-1.675526	-1.287372
H	5.225608	-0.787135	0.029673
H	3.520117	-1.318797	0.199989
H	3.804203	0.792189	2.875411
H	2.054355	0.749629	3.254656
H	2.703746	-0.318999	2.005367
H	-5.111153	1.769008	-1.011528
H	-4.279009	1.269354	-2.511859
H	-4.005367	0.368089	-1.017232
H	-3.749567	-0.371101	2.840975
H	-4.414121	1.283049	2.952561
H	-4.627776	0.341717	1.469375
H	-1.301396	0.878248	3.753248
H	-1.943672	2.536101	3.620428
H	-0.455540	2.075419	2.739916
H	-3.139765	3.925125	-2.877083
H	-2.272008	4.717010	-1.549980
H	-4.024685	4.453643	-1.417465
H	-3.684547	-2.140143	0.066968
H	-3.890280	-2.899342	-1.529155
H	-3.831359	-3.908067	-0.055718
H	1.698261	-4.268604	-0.402185
H	2.743246	-3.985130	0.993266
H	1.386230	-5.142156	1.115927
H	4.881909	0.287604	-3.255962
H	5.851957	1.196622	-2.063809
H	4.547187	2.004867	-2.963543
H	2.382073	4.321773	1.301655
H	3.584158	3.663747	2.435861
H	1.844262	3.574440	2.817226

H	3.813179	2.860350	-0.502685
H	-2.052485	3.496591	0.962648
H	-1.657474	-2.635075	1.586332

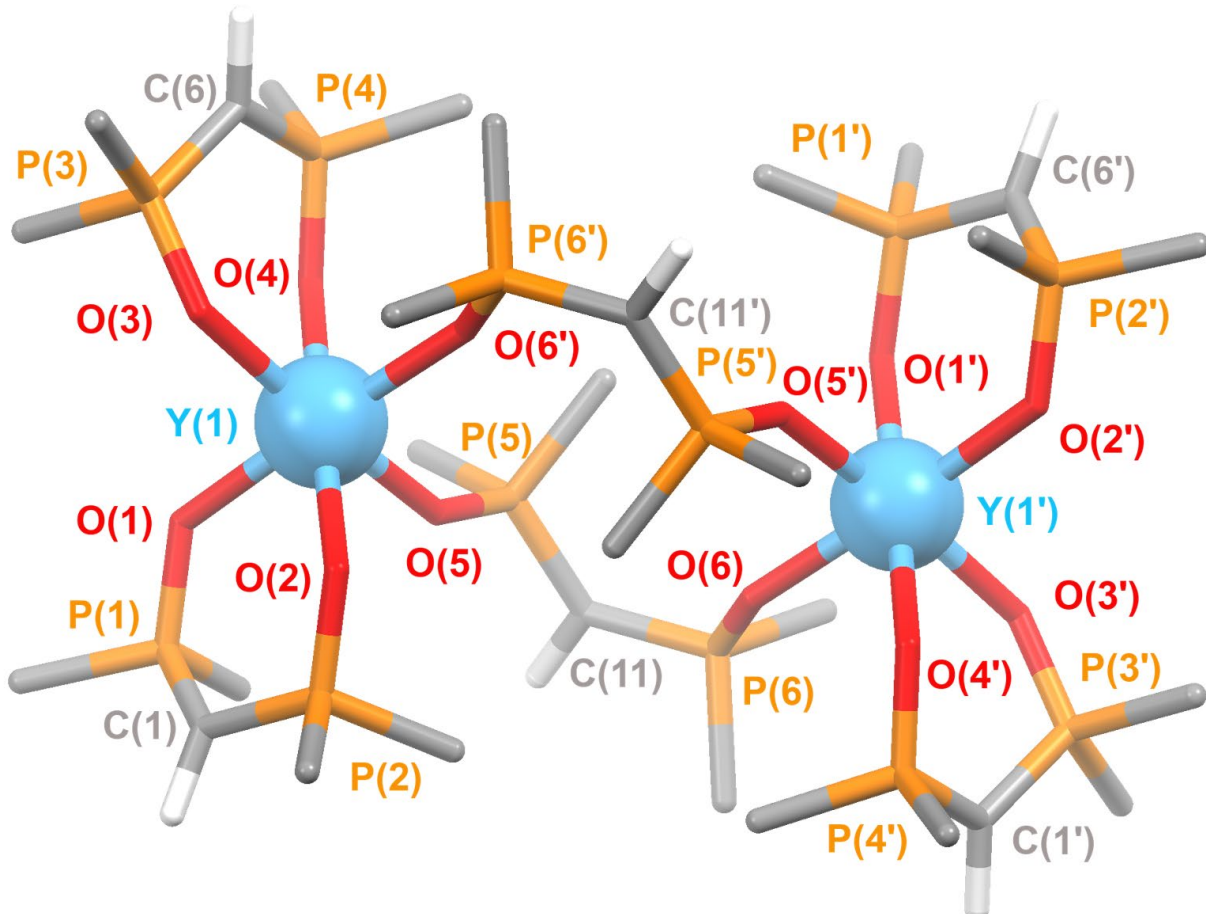


Figure S36. Labeled capped-stick image of $\text{Y}_2(\text{H}^{\text{Me}}\text{L})_6\text{-A}$. H-atoms other than the methanide $\text{C}-\text{H}$ were removed for clarity.

Table S19a. Comparison of select bond distances (\AA) and metrical parameters of the X-ray / DFT calculated structures of $\text{Y}_2(\text{H}^{\text{Me}}\text{L})_6$ / $\text{Y}_2(\text{H}^{\text{Me}}\text{L})_6\text{-A}$. The mean unsigned error is 0.0519.

Distance (\AA)	X-ray	DFT
$\text{M}(1)-\text{O}(1)$	2.2411(9)	2.264
$\text{M}(1)-\text{O}(2)$	2.257(2)	2.251
$\text{M}(1)-\text{O}(3)$	2.260(1)	2.267
$\text{M}(1)-\text{O}(4)$	2.239(9)	2.292
$\text{M}(1)-\text{O}(5)$	2.229(1)	2.222
$\text{M}(1)-\text{O}(6)$	2.2121(9)	2.261
$\text{M}(1)-\text{C}(1)$	3.880(2)	3.909
$\text{M}(1)-\text{C}(6)$	3.924(2)	3.888

M(1)–C(11)	4.865(2)	4.859
M(1)–L plane O(1)P(1)P(2)O(2)	0.362(1)	0.697
M(1)–L plane O(3)P(3)P(4)O(4)	0.541(1)	0.446
M(1)–L plane O(5)P(5)P(6)O(6)	0.044(1)	0.003
C(1)–L plane O(1)P(1)P(2)O(2)	0.464(1)	0.496
C(6)–L plane O(3)P(3)P(4)O(4)	0.253(1)	0.370
C(11)–L plane O(5)P(5)P(6)O(6)	0.495(1)	0.456

Table S19b. Comparison of select bond angles ($^{\circ}$) of the X-ray / DFT calculated structures of $\text{Y}_2(\text{H}^{\text{Me}}\text{L})_6\text{-A}$.

Angle ($^{\circ}$)	X-ray	DFT
O(1)–M(1)–O(2)	82.65(4)	95.22
O(1)–M(1)–O(3)	92.20(4)	93.03
O(1)–M(1)–O(4)	99.51(4)	92.79
O(1)–M(1)–O(5)	90.39(4)	86.39
O(1)–M(1)–O(6)	169.86(4)	177.42
O(2)–M(1)–O(3)	95.70(4)	101.17
O(2)–M(1)–O(4)	177.79(4)	175.13
O(2)–M(1)–O(5)	91.89(5)	87.05
O(2)–M(1)–O(6)	87.47(4)	92.91
O(3)–M(1)–O(4)	83.84(4)	83.35
O(3)–M(1)–O(5)	172.24(4)	171.69
O(3)–M(1)–O(6)	86.47(5)	89.07
O(4)–M(1)–O(5)	88.52(4)	88.4
O(4)–M(1)–O(6)	90.35(4)	88.94
O(5)–M(1)–O(6)	92.24(4)	91.75
O(1)–P(1)–P(2)–O(2)	-17.75(1)	1.51
O(3)–P(3)–P(4)–O(4)	-0.14(1)	33.43
O(5)–P(5)–P(6)–O(6)	-57.20(1)	56.67

Table S20. Hybridization, hyperconjugation, and $E(2)$ stabilization energy for $\mathbf{Y}_2(\mathbf{H}^{\text{Me}}\mathbf{L})_6-\mathbf{A}$.

Methanide Lone Pair				Binding Mode	Interaction	$E(2)$ (kcal/mol)
Occupancy	% s	% p	Label #			
1.69122	0.26	99.57	264	Terminal	C14 LP - σ^* P2/O8	9.25
			264		C14 LP - σ^* P2/C15	0.53
			264		C14 LP - σ^* P2/C19	13.75
			264		C14 LP - σ^* P3/O9	0.60
			264		C14 LP - σ^* P3/C23	13.64
			264		C14 LP - σ^* P3/C27	7.69
1.70455	3.59	96.23	265	Terminal	C31 LP - σ^* P4/O10	3.40
			265		C31 LP - σ^* P4/C32	16.14
			265		C31 LP - σ^* P4/C36	2.95
			265		C31 LP - σ^* P5/O11	3.80
			265		C31 LP - σ^* P5/C40	2.87
			265		C31 LP - σ^* P5/C44	16.32
1.69275	0.71	99.12	266	Bridging	C48 LP - σ^* P6/O12	4.05
			266		C48 LP - σ^* P6/C49	13.65
			266		C48 LP - σ^* P6/C53	3.99
			266		C48 LP - σ^* P7/C13	17.46
			266		C48 LP - σ^* P7/C57	3.88
			266		C48 LP - σ^* P7/C61	2.35
				Average $E(2)$ / Ligand	45.38±0.43	

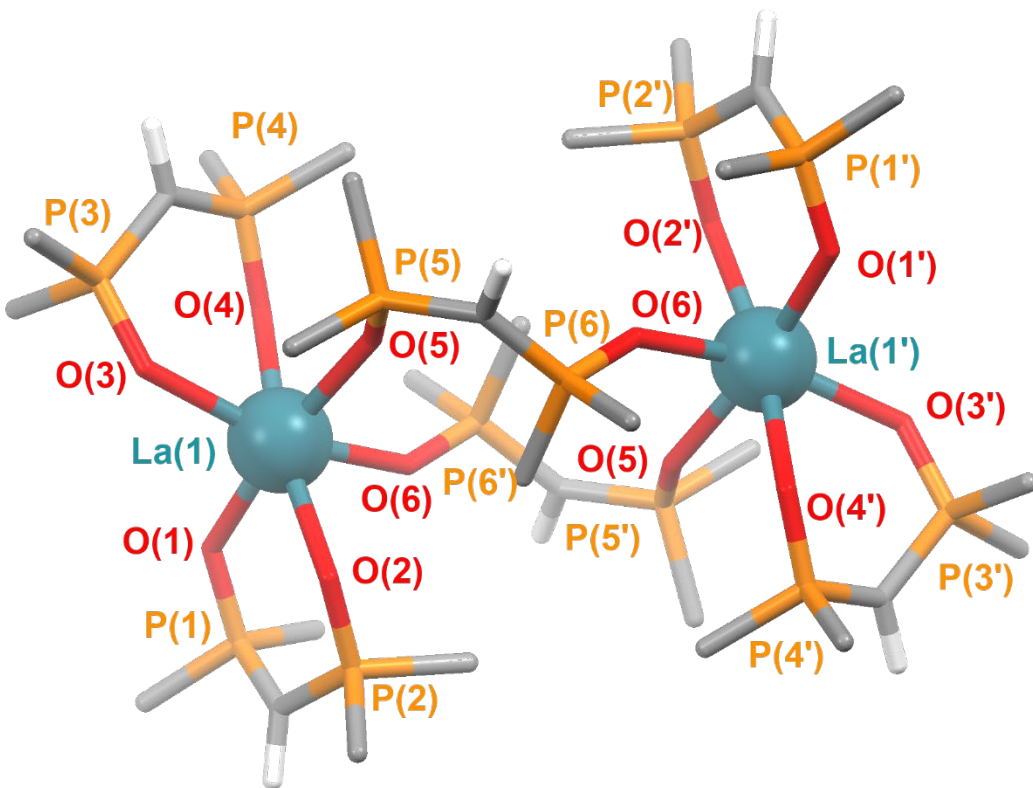
Table S21. Cartesian coordinates of $\mathbf{Y}_2(\mathbf{H}^{\text{Me}}\mathbf{L})_6-\mathbf{A}$.

Atom	X	Y	Z
Y	3.455316	0.289460	-0.175800
Y	-3.455323	-0.289492	0.175789
P	-1.014644	-0.988893	-2.361975
P	1.780955	-2.160496	-2.218711
P	2.719179	3.298199	-1.730654
P	4.624270	3.481576	0.580765
P	4.246685	-2.605568	1.648122
P	6.074771	-1.923976	-0.592574
P	1.014652	0.988746	2.361982
P	-1.780968	2.160284	2.218858
P	-2.719332	-3.298257	1.730630
P	-4.624710	-3.481479	-0.580625
P	-4.246325	2.605568	-1.648275
P	-6.074534	1.924280	0.592410
O	-1.849944	-1.196341	-1.065082
O	2.046892	-1.296599	-0.962049
O	2.882179	1.757883	-1.783497

O	4.790507	1.945232	0.597185
O	3.952661	-1.088160	1.588251
O	5.176906	-0.799814	-1.170461
O	1.849699	1.196112	1.064915
O	-2.046782	1.296444	0.962133
O	-2.882239	-1.757923	1.783449
O	-4.790792	-1.945113	-0.596993
O	-3.952482	1.088132	-1.588344
O	-5.176837	0.799993	1.170316
C	-0.269757	0.651357	-2.248252
C	-2.199273	-0.889101	-3.731387
C	2.278596	-3.883119	-1.944741
C	2.937519	-1.593072	-3.499678
C	0.154378	-2.168527	-2.760330
C	1.037247	3.635404	-1.112129
C	2.684806	3.979722	-3.409177
C	6.219793	4.289740	0.864413
C	3.664285	3.932838	2.060497
C	3.979396	4.096990	-0.884103
C	2.697710	-3.548627	1.605729
C	4.911476	-2.962825	3.301042
C	7.422413	-1.061303	0.268117
C	6.887636	-2.825418	-1.935230
C	5.282182	-3.098452	0.373544
C	0.269976	-0.651630	2.248426
C	2.199464	0.889172	3.731245
C	-2.278679	3.882903	1.944975
C	-2.937513	1.592763	3.499793
C	-0.154391	2.168308	2.760488
C	-1.037399	-3.635522	1.112136
C	-2.685004	-3.979746	3.409167
C	-6.220363	-4.289497	-0.863957
C	-3.665082	-3.932744	-2.060583
C	-3.979597	-4.096983	0.884095
C	-2.697263	3.548472	-1.605711
C	-4.910940	2.962812	-3.301264
C	-7.422309	1.061812	-0.268270
C	-6.887245	2.825905	1.935037
C	-5.281862	3.098634	-0.373790
H	-0.213414	-3.103458	-3.183380
H	4.112194	5.161379	-1.079949
H	5.485765	-4.152493	0.196443
H	-1.082338	1.376291	-2.122006
H	0.307485	0.898183	-3.145845
H	0.387053	0.717243	-1.374635

H	-2.583643	-1.887864	-3.965259
H	-1.718734	-0.490438	-4.631478
H	-3.040821	-0.248458	-3.440752
H	3.299234	-3.915990	-1.542046
H	2.241351	-4.446834	-2.884142
H	1.594706	-4.355760	-1.231231
H	2.715813	-0.547567	-3.744430
H	2.822947	-2.188804	-4.412476
H	3.972813	-1.647673	-3.141370
H	0.281595	3.289828	-1.827210
H	0.897625	4.710562	-0.944403
H	0.890679	3.100856	-0.163749
H	3.647522	3.803320	-3.897707
H	2.497137	5.059236	-3.385038
H	1.892900	3.502027	-3.996645
H	6.635884	3.978792	1.828880
H	6.110593	5.379910	0.865107
H	6.918146	4.010159	0.069976
H	2.660093	3.502934	1.963651
H	3.570850	5.022620	2.138017
H	4.133438	3.550904	2.975494
H	2.147418	-3.441822	2.548513
H	2.891665	-4.613767	1.432366
H	2.090029	-3.154673	0.782657
H	5.853607	-2.420368	3.435234
H	5.112491	-4.034436	3.415223
H	4.210177	-2.651215	4.084527
H	7.911331	-0.334280	-0.390796
H	8.166027	-1.768519	0.652097
H	6.997048	-0.511806	1.116150
H	6.141592	-3.374504	-2.519493
H	7.618207	-3.541275	-1.544000
H	7.402889	-2.122975	-2.598349
H	0.213282	3.103027	3.184099
H	-4.112655	-5.161307	1.080111
H	-5.484642	4.152738	-0.196182
H	1.082668	-1.376436	2.122148
H	-0.307172	-0.898489	3.146072
H	-0.386873	-0.717639	1.374847
H	2.583767	1.887983	3.965009
H	1.719098	0.490488	4.631418
H	3.041041	0.248606	3.440531
H	-3.299310	3.915804	1.542269
H	-2.241486	4.446518	2.884442
H	-1.594764	4.355629	1.231544

H	-2.715809	0.547220	3.744407
H	-2.822912	2.188377	4.412660
H	-3.972808	1.647422	3.141505
H	-0.281761	-3.290029	1.827276
H	-0.897835	-4.710677	0.944355
H	-0.890746	-3.100937	0.163790
H	-3.647688	-3.803194	3.897706
H	-2.497482	-5.059287	3.385054
H	-1.893023	-3.502140	3.996604
H	-6.636645	-3.978456	-1.828310
H	-6.111244	-5.379677	-0.864748
H	-6.918508	-4.009921	-0.069337
H	-2.660803	-3.503022	-1.963852
H	-3.571852	-5.022527	-2.138302
H	-4.134335	-3.550572	-2.975427
H	-2.146810	3.441547	-2.548390
H	-2.891104	4.613645	-1.432440
H	-2.089753	3.154470	-0.782523
H	-5.853133	2.420463	-3.435478
H	-5.111829	4.034442	-3.415492
H	-4.209643	2.651084	-4.084703
H	-7.911391	0.334902	0.390639
H	-8.165762	1.769187	-0.652271
H	-6.997035	0.512235	-1.116291
H	-6.141120	3.374829	2.519348
H	-7.617614	3.541926	1.543726
H	-7.402724	2.123604	2.598127



H-atoms other than the methanide

C-H were removed for clarity.

Table S22a. Comparison of select bond distances (\AA) and metrical parameters of the DFT calculated structure, $\text{La}_2(\text{H}^{\text{Me}}\text{L})_6\text{-A}$.

Distance (\AA)	La(1)	La(1')
M(1)-O(1)	2.446	2.444
M(1)-O(2)	2.457	2.450
M(1)-O(3)	2.457	2.467
M(1)-O(4)	2.494	2.494
M(1)-O(5)	2.447	2.451
M(1)-O(6)	2.408	2.404
M(1)-C(1)	4.086	4.09
M(1)-C(6)	4.057	4.009
M(1)-C(11)	5.211	5.211
M(1)-L plane O(1)P(1)P(2)O(2)	0.746	0.715
M(1)-L plane O(3)P(3)P(4)O(4)	0.611	0.662

M(1)–L plane O(5)P(5)P(6)O(6)	0.306	0.234
C(1)–L plane O(1)P(1)P(2)O(2)	0.516	0.521
C(6)–L plane O(3)P(3)P(4)O(4)	0.453	0.476
C(11)–L plane O(5)P(5)P(6)O(6)	0.333	0.352

Table S22b. Select bond angles ($^{\circ}$) of the DFT calculated structure, $\text{La}_2(\text{H}^{\text{Me}}\text{L})_6\text{-A}$.

Angle ($^{\circ}$)	La(1)	La(1')
O(1)–M(1)–O(2)	80.95	80.85
O(1)–M(1)–O(3)	99.05	97.62
O(1)–M(1)–O(4)	95.70	95.77
O(1)–M(1)–O(5)	170.14	169.96
O(1)–M(1)–O(6)	82.82	82.75
O(2)–M(1)–O(3)	117.49	116.04
O(2)–M(1)–O(4)	165.60	165.83
O(2)–M(1)–O(5)	96.66	98.92
O(2)–M(1)–O(6)	83.70	83.24
O(3)–M(1)–O(4)	76.82	77.98
O(3)–M(1)–O(5)	90.55	92.15
O(3)–M(1)–O(6)	158.80	160.6
O(4)–M(1)–O(5)	84.24	84.01
O(4)–M(1)–O(6)	158.80	82.68
O(5)–M(1)–O(6)	87.42	87.28
O(1)–P(1)–P(2)–O(2)	1.94	-1.37
O(3)–P(3)–P(4)–O(4)	29.51	-30.84
O(5)–P(5)–P(6)–O(6)	67.96	-67.34

Table S23. Hybridization, hyperconjugation, and $E(2)$ stabilization energy for $\text{La}_2(\text{H}^{\text{Me}}\text{L})_6\text{-A}$.

Methanide Lone Pair				Binding Mode	Interaction	$E(2)$ (kcal/mol)
Occupancy	% s	% p	Label #			
1.69412	2.01	97.81	271	Terminal	C14 LP - σ^* P2/O8	8.06
			271		C14 LP - σ^* P2/C15	0.56
			271		C14 LP - σ^* P2/C19	14.97
			271		C14 LP - σ^* P3/O9	0.72
			271		C14 LP - σ^* P3/C23	14.52
			271		C14 LP - σ^* P3/C27	6.18
1.70227	2.33	97.53	272	Terminal	C31 LP - σ^* P4/O10	4.87
			272		C31 LP - σ^* P4/C32	15.96

			272		C31 LP - σ^* P4/C36	2.07
			272		C31 LP - σ^* P5/O11	5.40
			272		C31 LP - σ^* P5/C40	1.87
			272		C31 LP - σ^* P5/C44	15.88
1.69028	0.51	99.3	273		C48 LP - σ^* P6/O12	1.35
			273		C48 LP - σ^* P6/C49	13.52
			273	Bridging	C48 LP - σ^* P6/C53	7.05
			273		C48 LP - σ^* P7/O13	16.85
			273		C48 LP - σ^* P7/C57	4.01
			273		C48 LP - σ^* P7/C61	2.41
1.69300	1.80	98.02	308		C81 LP - σ^* P69/O75	9.01
			308		C81 LP - σ^* P69/C86	14.11
			308	Terminal	C81 LP - σ^* P70/O76	0.92
			308		C81 LP - σ^* P70/C90	14.73
			308		C81 LP - σ^* P70/C94	5.84
1.7018	2.30	97.56	309		C98 LP - σ^* P71/O77	5.03
			309		C98 LP - σ^* P71/C99	15.83
			309	Terminal	C98 LP - σ^* P71/C103	1.98
			309		C98 LP - σ^* P72/O78	5.45
			309		C98 LP - σ^* P72/C107	1.82
			309		C98 LP - σ^* P72/C111	15.83
1.6893	0.42	99.39	310		C115 LP - σ^* P73/O79	1.69
			310		C115 LP - σ^* P73/C116	13.91
			310	Bridging	C115 LP - σ^* P73/C120	6.46
			310		C115 LP - σ^* P74/O80	16.66
			310		C115 LP - σ^* P74/C124	4.38
			310		C115 LP - σ^* P74/C128	2.11
					Average E(2) / Ligand	45.34±0.51

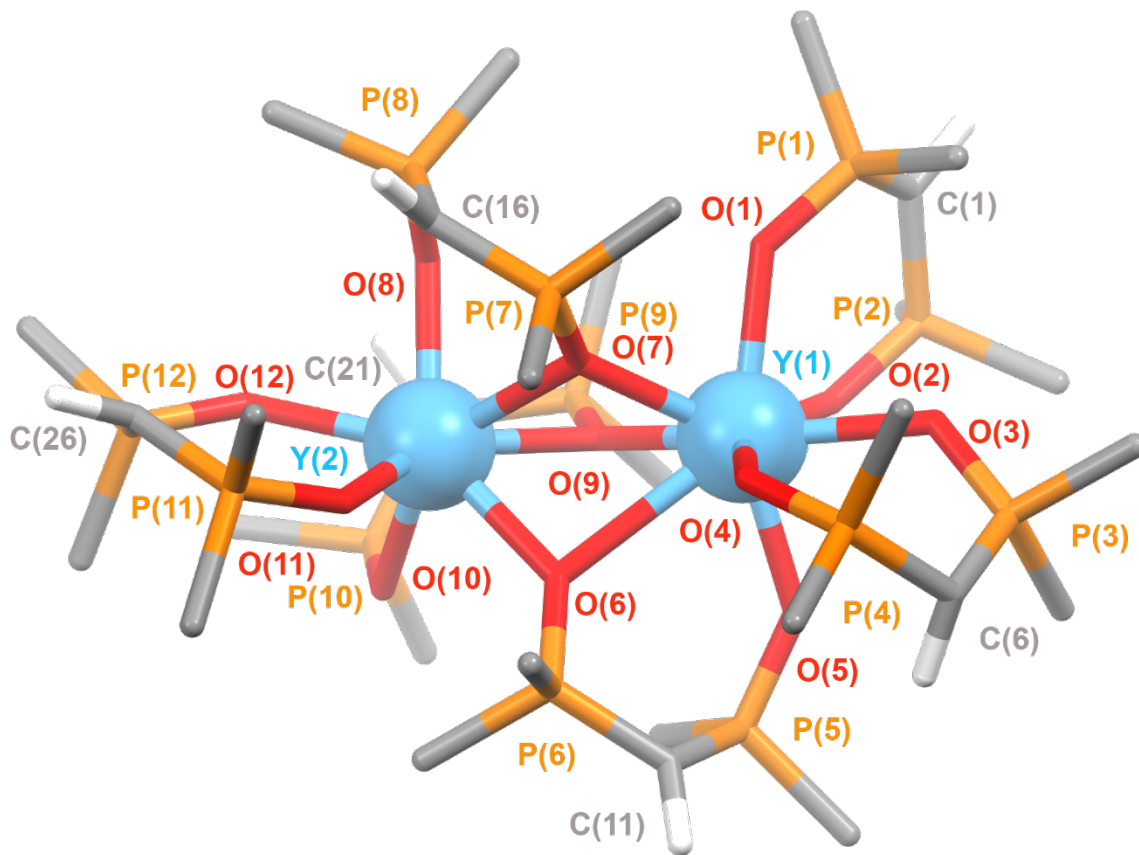
Table S24. Cartesian coordinates of $\text{La}_2(\text{H}^{\text{Me}}\text{L})_6\text{-A}$.

Atom	X	Y	Z
La	3.647845	0.392155	-0.354645
La	-3.658537	-0.400316	0.368736
P	-1.015481	-0.951032	-2.297685
P	1.731180	-2.266820	-2.237560
P	2.559007	3.657940	-1.610636
P	4.565794	3.807453	0.632531
P	4.319151	-2.667958	1.601022
P	6.280288	-2.132317	-0.564086
P	1.009398	0.910640	2.334431
P	-1.724533	2.247498	2.249595
P	-2.628158	-3.670432	1.651421
P	-4.622961	-3.801962	-0.610173

P	-4.246077	2.643238	-1.679527
P	-6.221712	2.235557	0.502518
O	-1.944201	-1.255281	-1.085511
O	2.072221	-1.358343	-1.035405
O	2.803235	2.145425	-1.843789
O	4.889132	2.296407	0.543493
O	4.114854	-1.137144	1.559094
O	5.580752	-0.896340	-1.186312
O	1.930194	1.207680	1.115131
O	-2.059924	1.318312	1.062466
O	-2.866479	-2.157888	1.890846
O	-4.930654	-2.286907	-0.526990
O	-4.061608	1.114213	-1.570683
O	-5.529212	0.999787	1.129657
C	-0.202574	0.620170	-1.935703
C	-2.109544	-0.634104	-3.708929
C	2.125291	-4.001284	-1.883944
C	2.939064	-1.860369	-3.539284
C	0.111150	-2.146805	-2.775362
C	0.914102	3.795790	-0.843263
C	2.343602	4.515951	-3.192463
C	6.072154	4.769447	0.926685
C	3.604745	4.037200	2.162022
C	3.821810	4.457313	-0.769131
C	2.725029	-3.531010	1.617216
C	5.035815	-3.081580	3.221196
C	7.626841	-1.453008	0.453925
C	7.118213	-3.099758	-1.844572
C	5.258048	-3.225146	0.274900
C	0.200751	-0.667598	1.988284
C	2.112658	0.600379	3.740057
C	-2.095243	3.976197	1.843938
C	-2.953203	1.889008	3.545419
C	-0.114685	2.108116	2.815315
C	-0.975440	-3.822496	0.900939
C	-2.436375	-4.536546	3.231863
C	-6.139131	-4.748530	-0.904972
C	-3.661996	-4.047347	-2.137043
C	-3.889011	-4.457231	0.794492
C	-2.640144	3.484052	-1.696001
C	-4.925436	3.000065	-3.328863
C	-7.628941	1.563905	-0.437248
C	-6.986090	3.264328	1.781744
C	-5.196527	3.274615	-0.396345
H	-0.287112	-2.997492	-3.329920

H	3.974306	5.516017	-0.974531
H	5.414191	-4.292912	0.129039
H	-0.990307	1.367412	-1.791834
H	0.475787	0.944262	-2.732372
H	0.362781	0.546140	-1.000242
H	-2.566016	-1.575781	-4.034387
H	-1.553761	-0.213396	-4.553865
H	-2.911091	0.049267	-3.403145
H	3.160300	-4.077771	-1.525111
H	2.009368	-4.608779	-2.789100
H	1.446356	-4.392705	-1.118818
H	2.813276	-0.811611	-3.836036
H	2.789475	-2.479046	-4.431521
H	3.965079	-1.998836	-3.172547
H	0.144386	3.409235	-1.521482
H	0.686354	4.842112	-0.604757
H	0.890678	3.197670	0.077985
H	3.268422	4.463454	-3.774430
H	2.085139	5.569051	-3.035549
H	1.538374	4.039804	-3.763100
H	6.567400	4.422334	1.839857
H	5.840781	5.834628	1.037695
H	6.757750	4.645685	0.083278
H	2.656264	3.496611	2.057165
H	3.384861	5.097920	2.331229
H	4.140676	3.640305	3.032853
H	2.193598	-3.350191	2.559931
H	2.859293	-4.612678	1.497011
H	2.126764	-3.149395	0.781682
H	6.010373	-2.591319	3.321792
H	5.187387	-4.163481	3.313472
H	4.390316	-2.746389	4.042126
H	8.293594	-0.817726	-0.140483
H	8.211152	-2.249994	0.927644
H	7.187266	-0.830371	1.242259
H	6.376419	-3.572191	-2.497020
H	7.741886	-3.883037	-1.400675
H	7.751607	-2.446172	-2.452994
H	0.284160	2.951451	3.380707
H	-4.046724	-5.516576	0.993403
H	-5.360948	4.348975	-0.325148
H	0.991304	-1.415604	1.858816
H	-0.479461	-0.980998	2.787683
H	-0.361842	-0.607129	1.050062
H	2.582496	1.540377	4.050988

H	1.562434	0.192726	4.594801
H	2.904620	-0.093882	3.433099
H	-3.120971	4.052352	1.457334
H	-1.995256	4.607310	2.734803
H	-1.396516	4.343183	1.084618
H	-2.849018	0.843486	3.861844
H	-2.801393	2.521267	4.427696
H	-3.972132	2.038998	3.164538
H	-0.208174	-3.441797	1.586149
H	-0.755892	-4.872014	0.668587
H	-0.934208	-3.229762	-0.023155
H	-3.367460	-4.479484	3.803383
H	-2.183365	-5.590831	3.074127
H	-1.634607	-4.067677	3.813192
H	-6.629241	-4.398580	-1.819852
H	-5.918471	-5.816282	-1.013221
H	-6.824839	-4.615944	-0.062983
H	-2.709988	-3.513635	-2.031691
H	-3.450348	-5.110660	-2.300265
H	-4.192857	-3.650478	-3.011019
H	-2.081913	3.250070	-2.611323
H	-2.761582	4.571905	-1.629094
H	-2.073461	3.136504	-0.825023
H	-5.906261	2.521618	-3.425939
H	-5.056439	4.079163	-3.471300
H	-4.270514	2.618298	-4.121473
H	-8.304042	0.992967	0.211024
H	-8.193277	2.360342	-0.935477
H	-7.245187	0.879571	-1.203339
H	-6.207334	3.750932	2.378270
H	-7.618131	4.039403	1.334867
H	-7.601592	2.646167	2.443093



H-atoms other than the methanide C-H were removed for clarity.

Table S25a. Select bond distances (\AA) and metrical parameters of the DFT calculated structure, $\text{Y}_2(\text{H}^{\text{Me}}\text{L})_6\text{-B}$.

Distance (\AA)	Y(1)	Y(2)
M(1)–O(1)	2.319	---
M(1)–O(2)	2.367	---
M(1)–O(3)	2.375	---
M(1)–O(4)	2.349	---
M(1)–O(5)	2.271	---
M(1)–O(6)	2.841	---
M(1)–O(7)	2.386	---
M(1)–O(9)	2.361	---
M(2)–O(6)	---	2.347
M(2)–O(7)	---	2.433
M(2)–O(8)	---	2.296

M(2)–O(9)	---	2.412
M(2)–O(10)	---	2.345
M(2)–O(11)	---	2.295
M(2)–O(12)	---	2.337
M(1)–C(1)	4.109	---
M(1)–C(6)	3.917	---
M(1)–C(11)	4.141	---
M(2)–C(16)	---	3.486
M(2)–C(21)	---	3.207
M(2)–C(26)	---	4.022
M(1)–L plane O(1)P(1)P(2)O(2)	0.795	---
M(1)–L plane O(3)P(3)P(4)O(4)	0.941	---
M(1)–L plane O(5)P(5)P(6)O(6)	0.674	---
M(2)–L plane O(7)P(7)P(8)O(8)	---	1.501
M(2)–L plane O(9)P(9)P(10)O(10)	---	1.739
M(2)–L plane O(11)P(11)P(12)O(12)	---	0.113
C(1)–L plane O(1)P(1)P(2)O(2)	0.382	
C(6)–L plane O(3)P(3)P(4)O(4)	0.496	
C(11)–L plane O(5)P(5)P(6)O(6)	0.521	
C(16)–L plane O(7)P(7)P(8)O(8)	0.569	
C(21)–L plane O(9)P(9)P(10)O(10)	0.254	
C(26)–L plane O(11)P(11)P(12)O(12)	0.498	

Table S25b. Select bond angles ($^{\circ}$) of the DFT calculated structure, $\mathbf{Y}_2(\mathbf{H}^{\mathbf{Me}}\mathbf{L})_6\text{--B}$.

Angle ($^{\circ}$)	DFT
O(1)–M(1)–O(2)	76.81
O(1)–M(1)–O(3)	79.84
O(1)–M(1)–O(4)	102.58
O(1)–M(1)–O(5)	153.78
O(1)–M(1)–O(6)	132.60

O(1)–M(1)–O(7)	73.10
O(1)–M(1)–O(9)	94.71
O(2)–M(1)–O(3)	73.58
O(2)–M(1)–O(4)	151.79
O(2)–M(1)–O(5)	81.06
O(2)–M(1)–O(6)	126.55
O(2)–M(1)–O(7)	131.65
O(2)–M(1)–O(9)	75.05
O(3)–M(1)–O(4)	78.53
O(3)–M(1)–O(5)	80.57
O(3)–M(1)–O(6)	141.69
O(3)–M(1)–O(7)	134.47
O(3)–M(1)–O(9)	148.59
O(4)–M(1)–O(5)	90.36
O(4)–M(1)–O(6)	59.60
O(4)–M(1)–O(7)	72.69
O(4)–M(1)–O(9)	132.54
O(5)–M(1)–O(6)	72.57
O(5)–M(1)–O(7)	132.98
O(5)–M(1)–O(9)	92.98
O(6)–M(1)–O(7)	60.83
O(6)–M(1)–O(9)	61.25
O(7)–M(1)–O(9)	70.76
O(6)–M(2)–O(7)	68.05
O(6)–M(2)–O(8)	136.10
O(6)–M(2)–O(9)	68.60
O(6)–M(2)–O(10)	81.56
O(6)–M(2)–O(11)	79.69
O(6)–M(2)–O(12)	146.95
O(7)–M(2)–O(8)	74.00
O(7)–M(2)–O(9)	69.11
O(7)–M(2)–O(10)	144.71
O(7)–M(2)–O(11)	90.74
O(7)–M(2)–O(12)	137.82
O(8)–M(2)–O(9)	82.00
O(8)–M(2)–O(10)	125.27
O(8)–M(2)–O(11)	118.52
O(8)–M(2)–O(12)	74.84
O(9)–M(2)–O(10)	83.68
O(9)–M(2)–O(11)	146.87
O(9)–M(2)–O(12)	132.64
O(10)–M(2)–O(11)	101.36
O(10)–M(2)–O(12)	77.31
O(11)–M(2)–O(12)	79.92
O(1)–P(1)–P(2)–O(2)	-3.84

O(3)–P(3)–P(4)–O(4)	24.54
O(5)–P(5)–P(6)–O(6)	36.32
O(7)–P(7)–P(8)–O(8)	10.86
O(9)–P(9)–P(10)–O(10)	1.54
O(11)–P(11)–P(12)–O(12)	-17.09

Table S26. Hybridization, hyperconjugation, and $E(2)$ stabilization energy for $\mathbf{Y}_2(\mathbf{H}^{\mathbf{Me}}\mathbf{L})_6\text{--B}$.

Methanide Lone Pair				Binding Mode	Interaction	$E(2)$ (kcal/mol)
Occupancy	% s	% p	Label #			
1.69715	4.00	95.7	291	Bridging	C27 LP - σ^* P3/O15	15.82
			291		C27 LP - σ^* P3/C91	5.84
			291		C27 LP - σ^* P4/C22	16.47
			291		C27 LP - σ^* P4/C87	6.20
1.6706	3.15	96.62	292	Bridging	C33 LP - σ^* P5/O16	6.77
			292		C33 LP - σ^* P5/C43	0.69
			292		C33 LP - σ^* P5/C47	14.54
			292		C33 LP - σ^* P6/O17	3.20
			292		C33 LP - σ^* P6/C35	16.19
			292		C33 LP - σ^* P6/C39	3.25
1.69625	4.03	95.75	293	Terminal	C55 LP - σ^* P7/O18	1.32
			293		C55 LP - σ^* P7/C51	4.38
			293		C55 LP - σ^* P7/C65	15.99
			293		C55 LP - σ^* P8/O19	4.73
			293		C55 LP - σ^* P8/C57	15.84
			293		C55 LP - σ^* P8/C61	1.60
1.68934	2.28	97.50	294	Bridging	C69 LP - σ^* P9/C79	14.39
			294		C69 LP - σ^* P9/C83	6.05
			294		C69 LP - σ^* P10/O21	9.60
			294		C69 LP - σ^* P10/C71	13.16
1.70042	2.98	96.82	295	Terminal	C107 LP - σ^* P11/O23	1.97
			295		C107 LP - σ^* P11/C99	4.50
			295		C107 LP - σ^* P11/C103	16.11
			295		C107 LP - σ^* P12/O24	1.22
			295		C107 LP - σ^* P12/C109	14.85
			295		C107 LP - σ^* P12/C113	5.40
1.72505	11.54	88.05	296	Terminal	C125 LP - σ^* P13/O25	16.74
			296		C125 LP - σ^* P13/C117	0.72
			296		C125 LP - σ^* P13/C121	2.87
			296		C125 LP - σ^* P14/O26	10.30
			296		C125 LP - σ^* P14/C127	6.52
				Average $E(2)$ / Ligand		42.87±2.60

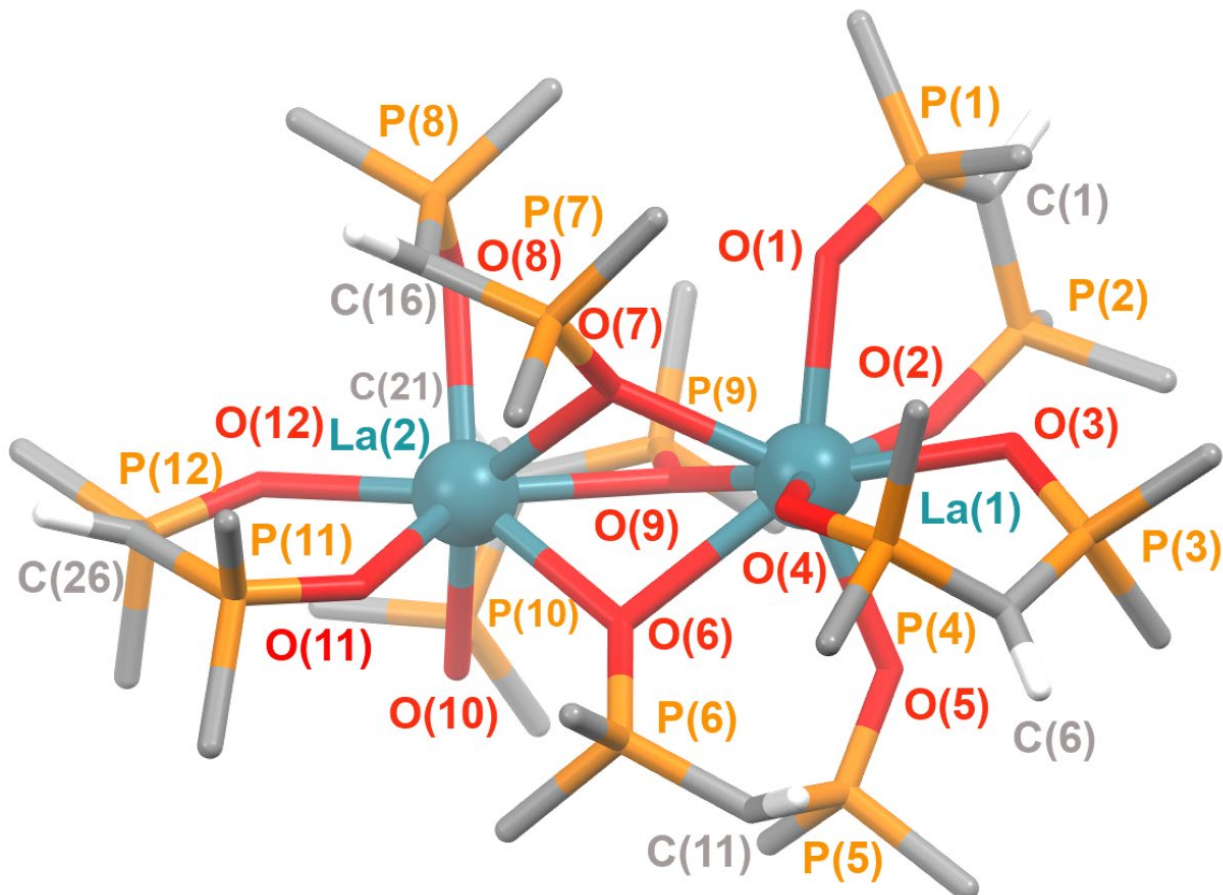
Table S27. Cartesian coordinates of $\text{Y}_2(\text{H}^{\text{Me}}\text{L})_6\text{-B}$.

Atom	X	Y	Z
Y	-2.054101	-0.220937	0.196334
Y	1.727162	0.017544	0.019198
P	4.924288	1.480719	0.101858
P	2.946402	3.080358	-1.229113
P	3.884721	-2.813444	0.797211
P	3.183441	-2.480894	-2.093205
P	1.607023	2.028679	2.942831
P	-0.683259	2.908826	1.380823
P	-5.628918	-0.336574	-0.152935
P	-4.410419	2.096263	-1.305369
P	-0.529347	0.466433	-2.837104
P	-2.153940	-1.989825	-2.654061
P	-2.781516	-1.611962	3.013291
P	-0.304091	-2.599243	1.673369
O	4.055334	0.286690	-0.364498
O	1.776835	2.062401	-1.137689
O	2.798501	-1.781418	1.123363
O	2.043893	-1.531324	-1.678281
O	-2.677735	-0.165643	2.455989
O	2.301445	1.077440	1.943872
O	-0.562048	1.437481	0.925199
O	-4.263568	-0.979297	0.136511
O	-3.100691	1.655934	-0.608396
O	-0.215001	0.098123	-1.365319
O	-2.009282	-2.101373	-1.122367
O	-0.017846	-1.186247	1.056554
C	5.509912	1.304696	1.811012
C	6.457386	1.396603	-0.875266
C	4.208017	3.048430	-0.054943
C	3.674362	2.861368	-2.880936
C	2.291471	4.769533	-1.229963
C	3.737034	-4.248327	1.909972
C	5.526128	-2.173314	1.260815
C	3.823639	-3.416953	-0.808489
C	4.415183	-1.511817	-3.024302
C	2.616188	-3.665340	-3.351489
C	0.185204	-3.878181	0.503919
C	0.716362	-2.756400	3.157183
C	-2.211710	-1.524049	4.737526
C	-0.908926	4.035448	-0.017087
C	-2.233838	3.097220	2.311789
C	2.843617	2.770381	4.042750

C	0.621596	0.936545	4.014893
C	0.713203	3.334849	2.281060
C	-4.967768	3.604546	-0.440932
C	-6.842755	-1.581738	-0.663065
C	-6.304741	0.261713	1.434902
C	-5.592403	0.861628	-1.381633
C	-4.139368	2.700212	-2.992053
C	-0.970041	-3.203595	-3.307304
C	-3.797701	-2.513594	-3.202934
C	-0.799899	2.240599	-3.051238
C	0.942571	0.183239	-3.863966
C	-1.943944	-0.397645	-3.283863
C	-4.492121	-2.178413	3.181117
C	-1.964609	-2.814239	2.081282
H	6.300094	0.549918	1.875229
H	5.912032	2.258481	2.170266
H	4.663744	1.001005	2.434461
H	6.248768	1.624606	-1.926302
H	7.182822	2.131241	-0.508492
H	6.905089	0.396325	-0.820599
H	3.839957	3.428230	0.903574
H	2.903949	2.980105	-3.652753
H	4.482955	3.575201	-3.069387
H	4.072924	1.842541	-2.963679
H	1.907154	4.997670	-0.229498
H	3.088043	5.481190	-1.469578
H	1.478510	4.884639	-1.955960
H	2.753961	-4.715456	1.788918
H	4.499213	-4.996571	1.662025
H	3.868370	-3.958027	2.959407
H	5.535827	-1.809025	2.295270
H	6.280638	-2.962816	1.157363
H	5.780166	-1.353488	0.583157
H	4.478329	-4.251230	-1.064992
H	4.824298	-0.755069	-2.347633
H	5.229372	-2.156465	-3.377190
H	3.961282	-1.015655	-3.892462
H	2.207910	-3.154428	-4.231960
H	3.457405	-4.288758	-3.677582
H	1.850879	-4.323070	-2.926932
H	1.213206	-3.695466	0.163400
H	0.099625	-4.877292	0.943975
H	-0.486341	-3.794862	-0.357725
H	0.317342	-2.099083	3.935039
H	0.685580	-3.784511	3.534760

H	1.740387	-2.450651	2.927078
H	-2.926854	-0.926730	5.315388
H	-2.127065	-2.517220	5.190309
H	-1.244947	-1.014624	4.801526
H	-1.904482	3.903085	-0.452607
H	-0.780071	5.077178	0.300790
H	-0.149851	3.782093	-0.761501
H	-2.231564	2.404625	3.159554
H	-2.334006	4.124173	2.684900
H	-3.090710	2.858955	1.670605
H	3.487069	3.451498	3.475747
H	2.361055	3.337393	4.846178
H	3.469505	1.991865	4.491873
H	1.256484	0.160526	4.460594
H	0.115211	1.495200	4.810933
H	-0.133592	0.457768	3.376689
H	0.828699	4.329246	2.708077
H	-4.194167	4.383273	-0.431286
H	-5.862940	4.011100	-0.927118
H	-5.230144	3.361844	0.594632
H	-6.910285	-2.374231	0.090210
H	-7.834629	-1.132975	-0.787650
H	-6.538147	-2.028551	-1.614693
H	-5.548460	0.878854	1.935946
H	-7.200961	0.870800	1.267738
H	-6.564710	-0.566117	2.105053
H	-6.516413	1.072176	-1.920806
H	-3.674156	1.904058	-3.581237
H	-5.109275	2.944349	-3.441294
H	-3.510752	3.597445	-3.016140
H	-1.199050	-4.222827	-2.972054
H	-0.920065	-3.186630	-4.402174
H	0.006682	-2.915725	-2.897927
H	-4.508059	-1.726455	-2.922334
H	-3.831751	-2.654923	-4.289078
H	-4.080370	-3.449909	-2.710155
H	0.150747	2.763702	-2.901424
H	-1.189565	2.454100	-4.053798
H	-1.519359	2.573157	-2.298476
H	1.123500	-0.888136	-3.983291
H	0.780747	0.634786	-4.851267
H	1.818540	0.640002	-3.388450
H	-2.490634	-0.134300	-4.188711
H	-4.913122	-2.341982	2.185382
H	-4.521608	-3.116145	3.746381

H	-5.086756	-1.425880	3.709544
H	-2.579398	-3.299418	1.322492



H-atoms other than the methanide

C-H were removed for clarity.

Table S28a. Comparison of select bond distances (\AA) and metrical parameters of the X-ray / DFT calculated structures of $\text{La}_2(\text{H}^{\text{Me}}\text{L})_6$ / $\text{La}_2(\text{H}^{\text{Me}}\text{L})_6\text{-B}$. The mean unsigned error is 0.0519.

Distance (\AA)	<u>X-ray</u>		<u>DFT</u>	
	La(1)	La(2)	La(1)	La(2)
M(1)-O(1)	2.472(2)	---	2.514	---
M(1)-O(2)	2.448(2)	---	2.525	---
M(1)-O(3)	2.478(2)	---	2.559	---
M(1)-O(4)	2.478(2)	---	2.545	---
M(1)-O(5)	2.428(2)	---	2.491	---
M(1)-O(6)	2.862(1)	---	2.744	---
M(1)-O(7)	2.540(1)	---	2.552	---
M(1)-O(9)	2.543(2)	---	2.523	---
M(2)-O(6)	---	2.521(2)	---	2.614

M(2)–O(7)	---	2.602(2)	---	2.614
M(2)–O(8)	---	2.467(2)	---	2.508
M(2)–O(9)	---	2.583(2)	---	2.598
M(2)–O(10)	---	2.468(2)	---	2.564
M(2)–O(11)	---	2.466(2)	---	2.489
M(2)–O(12)	---	2.475(2)	---	2.486
M(1)–C(1)	4.210(3)	---	4.273	---
M(1)–C(6)	4.088(9)	---	3.964	---
M(1)–C(11)	4.014(3)	---	4.037	---
M(2)–C(16)	---	3.286(2)	---	3.392
M(2)–C(21)	---	4.181(3)	---	4.148
M(2)–C(26)	---	3.251(2)	---	3.12
M(1)–L plane O(1)P(1)P(2)O(2)	0.718(1)	---	0.737	---
M(1)–L plane O(3)P(3)P(4)O(4)	0.686(1)	---	1.045	---
M(1)–L plane O(5)P(5)P(6)O(6)	0.925(1)	1.437 (1)	1.008	---
M(2)–L plane O(7)P(7)P(8)O(8)	1.158(1)	1.708 (1)	---	1.662
M(2)–L plane O(9)P(9)P(10)O(10)	0.691(1)	1.559 (1)	---	1.737
M(2)–L plane O(11)P(11)P(12)O(12)	---	0.026(1)	---	0.143
C(1)–L plane O(1)P(1)P(2)O(2)	0.230(1)		0.476	
C(6)–L plane O(3)P(3)P(4)O(4)	0.452(1)		0.518	
C(11)–L plane O(5)P(5)P(6)O(6)	0.557(1)		0.553	
C(16)–L plane O(7)P(7)P(8)O(8)	0.607(1)		0.697	
C(21)–L plane O(9)P(9)P(10)O(10)	0.613(1)		0.678	
C(26)–L plane O(11)P(11)P(12)O(12)	0.454(1)		0.492	

Table S28b. Comparison of select bond angles ($^{\circ}$) of the X-ray / DFT calculated structures of $\text{La}_2(\text{H}^{\text{Me}}\text{L})_6$ / $\text{La}_2(\text{H}^{\text{Me}}\text{L})_6\text{--B}$.

Angle ($^{\circ}$)	X-ray	DFT
O(1)–M(1)–O(2)	73.08(6)	74.26
O(1)–M(1)–O(3)	77.32(8)	76.62
O(1)–M(1)–O(4)	97.01(8)	97.49
O(1)–M(1)–O(5)	148.98(7)	148.95

O(1)–M(1)–O(6)	133.99(6)	133.22
O(1)–M(1)–O(7)	72.85(6)	71.25
O(1)–M(1)–O(9)	95.68(7)	81.07
O(2)–M(1)–O(3)	75.27(6)	76.62
O(2)–M(1)–O(4)	148.58(6)	149.71
O(2)–M(1)–O(5)	79.20(6)	78.44
O(2)–M(1)–O(6)	129.59(5)	133.22
O(2)–M(1)–O(7)	126.06(6)	126.78
O(2)–M(1)–O(9)	75.27(5)	74.4
O(3)–M(1)–O(4)	73.45(7)	74.79
O(3)–M(1)–O(5)	82.47(8)	82.29
O(3)–M(1)–O(6)	140.84(6)	141.69
O(3)–M(1)–O(7)	133.76(7)	131.64
O(3)–M(1)–O(9)	150.49(6)	149.34
O(4)–M(1)–O(5)	99.52(7)	98.66
O(4)–M(1)–O(6)	78.91(6)	77.39
O(4)–M(1)–O(7)	76.03(6)	74.69
O(4)–M(1)–O(9)	136.06(6)	135.87
O(5)–M(1)–O(6)	75.27(6)	76.42
O(5)–M(1)–O(7)	136.78(6)	138.89
O(5)–M(1)–O(9)	90.41(7)	91.28
O(6)–M(1)–O(7)	61.61(5)	62.49
O(6)–M(1)–O(9)	62.37(5)	63.35
O(7)–M(1)–O(9)	66.47(5)	69.94
O(6)–M(2)–O(7)	65.74(5)	63.95
O(6)–M(2)–O(8)	137.15(6)	134.58
O(6)–M(2)–O(9)	66.87(5)	64.69
O(6)–M(2)–O(10)	82.48(6)	81.07
O(6)–M(2)–O(11)	76.56(5)	76.29
O(6)–M(2)–O(12)	146.22(6)	144.63
O(7)–M(2)–O(8)	76.61(5)	74.79
O(7)–M(2)–O(9)	66.47(5)	67.84
O(7)–M(2)–O(10)	142.06(5)	140.09
O(7)–M(2)–O(11)	94.80(6)	93.45
O(7)–M(2)–O(12)	135.45(6)	141.34
O(8)–M(2)–O(9)	80.15(5)	83.27
O(8)–M(2)–O(10)	120.73(6)	126.29
O(8)–M(2)–O(11)	128.05(6)	126.16
O(8)–M(2)–O(12)	76.12(6)	80.52
O(9)–M(2)–O(10)	82.68(5)	80.57
O(9)–M(2)–O(11)	143.13(5)	140.89
O(9)–M(2)–O(12)	140.06(5)	138.09
O(10)–M(2)–O(11)	97.49(6)	96.52
O(10)–M(2)–O(12)	82.46(6)	78.56
O(11)–M(2)–O(12)	75.66(6)	77.61

O(1)–P(1)–P(2)–O(2)	-1.09(1)	-1.07
O(3)–P(3)–P(4)–O(4)	17.56(1)	-0.07
O(5)–P(5)–P(6)–O(6)	28.88(1)	0.93
O(7)–P(7)–P(8)–O(8)	13.46(1)	1.93
O(9)–P(9)–P(10)–O(10)	1.94(1)	2.93
O(11)–P(11)–P(12)–O(12)	-10.53(1)	3.93

Table S29. Hybridization, hyperconjugation, and $E(2)$ stabilization energy for $\text{La}_2(\text{H}^{\text{Me}}\text{L})_6\text{-B}$.

Methanide Lone Pair				Interaction	$E(2)$ (kcal/mol)
Occupancy	% s	% p	Label #		
1.68983	2.40	97.43	305	C27 LP - σ^* P3/O15	9.72
			305		12.45
			305		10.13
			305		13.46
1.7800	4.50	95.27	306	C33 LP - σ^* P5/O16	9.68
			306	C33 LP - σ^* P5/C47	11.50
			306	C33 LP - σ^* P6/O17	4.36
			306	C33 LP - σ^* P6/C35	16.92
			306	C33 LP - σ^* P6/C39	2.11
			307	C55 LP - σ^* P7/O18	2.30
1.69388	2.04	97.80	307		4.16
			307		16.14
			307		6.90
			307		14.86
			307		0.76
			308		12.00
1.71423	8.71	90.97	308	C69 LP - σ^* P9/O20	7.37
			308	C69 LP - σ^* P9/C79	16.88
			308	C69 LP - σ^* P10/O21	2.37
			308	C69 LP - σ^* P10/C71	1.46
			308	C107 LP - σ^* P11/O23	2.60
			309		3.27
1.70666	4.35	95.46	309		16.46
			309		2.32
			309		15.84
			309		3.56
			310	C125 LP - σ^* P13/O25	9.46
			310	C125 LP - σ^* P13/C121	13.42
1.68163	1.18	98.63	310	C125 LP - σ^* P14/O26	1.86
			310	C125 LP - σ^* P14/C127	15.44
			310	C125 LP - σ^* P14/C131	4.27
				Average $E(2)$ / Ligand	44.01±1.94

Table S30. Cartesian coordinates of **La₂(H^{Me}L)₆-B**.

Atom	X	Y	Z
La	-2.249553	-0.354203	0.098061
La	1.786295	0.056662	0.102518
P	5.126826	1.633924	0.072275
P	3.134512	3.071870	-1.558057
P	4.008237	-2.883032	1.036625
P	3.438176	-2.694991	-1.900421
P	1.698713	2.378425	2.937841
P	-0.531519	2.941720	1.126485
P	-5.953455	-0.077006	-0.176328
P	-4.571999	2.306474	-1.323871
P	-0.588348	0.168771	-2.965332
P	-2.101401	-2.356685	-2.716930
P	-2.960143	-1.508487	3.159318
P	-0.419591	-2.606786	1.896638
O	4.286255	0.403280	-0.317131
O	1.933805	2.111322	-1.391732
O	2.925251	-1.834929	1.328219
O	2.324607	-1.663361	-1.649213
O	-2.856501	-0.082105	2.574095
O	2.344244	1.135364	2.277713
O	-0.500190	1.431627	0.745542
O	-4.675135	-0.900785	0.073686
O	-3.271416	1.780074	-0.675019
O	-0.191985	-0.130864	-1.498394
O	-2.175272	-2.507917	-1.183673
O	-0.071055	-1.273332	1.174132
C	5.602764	1.623832	1.821329
C	6.734431	1.468140	-0.776471
C	4.302075	3.092839	-0.300259
C	3.838362	2.672797	-3.193255
C	2.577149	4.788954	-1.746771
C	3.929988	-4.238436	2.246471
C	5.631712	-2.135770	1.391041
C	3.896215	-3.606635	-0.518401
C	4.799713	-1.811073	-2.731796
C	2.939268	-3.909509	-3.158114
C	0.037595	-4.017005	0.873508
C	0.626523	-2.681274	3.371460
C	-2.432986	-1.411729	4.897765
C	-0.759277	3.983972	-0.333579
C	-2.044215	3.193592	2.095281
C	2.987769	3.294700	3.822059

C	0.547245	1.752561	4.192597
C	0.861189	3.521305	1.958412
C	-4.994024	3.841849	-0.433644
C	-7.327429	-1.143725	-0.683654
C	-6.477958	0.550131	1.454277
C	-5.827298	1.146329	-1.373160
C	-4.293535	2.884681	-3.019757
C	-0.670573	-3.351227	-3.228258
C	-3.554067	-3.088992	-3.508482
C	-0.880360	1.929773	-3.228200
C	0.843757	-0.174555	-4.026528
C	-2.037633	-0.710828	-3.267542
C	-4.667007	-2.101476	3.265048
C	-2.121715	-2.667813	2.186787
H	6.374503	0.869503	2.012469
H	5.993104	2.602306	2.125543
H	4.709395	1.384834	2.409060
H	6.585732	1.478231	-1.862257
H	7.397212	2.302790	-0.517409
H	7.235571	0.530443	-0.503238
H	4.643825	4.052542	0.082931
H	3.087308	2.777447	-3.986836
H	4.694783	3.314742	-3.429344
H	4.177167	1.629290	-3.185232
H	2.157526	5.156599	-0.804309
H	3.413372	5.438257	-2.028821
H	1.806690	4.856750	-2.522996
H	2.956348	-4.737511	2.185871
H	4.707630	-4.983761	2.042695
H	4.074350	-3.858806	3.264634
H	5.673474	-1.740074	2.413247
H	6.439377	-2.865623	1.256454
H	5.773955	-1.310498	0.685102
H	4.499011	-4.499904	-0.693060
H	5.145659	-1.013728	-2.064082
H	5.635874	-2.485081	-2.954692
H	4.451350	-1.356331	-3.669078
H	2.633833	-3.412897	-4.086769
H	3.772107	-4.583920	-3.389579
H	2.106636	-4.511243	-2.779766
H	1.078644	-3.897496	0.539762
H	-0.069212	-4.964704	1.413020
H	-0.614700	-4.015789	-0.007004
H	0.389945	-1.837121	4.027648
H	0.470678	-3.614143	3.925559

H	1.672842	-2.579956	3.061809
H	-3.118951	-0.771957	5.465372
H	-2.405067	-2.404175	5.361564
H	-1.435132	-0.966224	4.965352
H	-1.720951	3.737822	-0.795124
H	-0.734592	5.046179	-0.066349
H	0.047230	3.754973	-1.036390
H	-1.974480	2.673183	3.054955
H	-2.204367	4.261302	2.285000
H	-2.899173	2.785504	1.544388
H	3.657836	3.751307	3.084126
H	2.549706	4.091774	4.431244
H	3.576648	2.628259	4.461674
H	1.070719	1.072013	4.873463
H	0.079987	2.557549	4.769074
H	-0.234010	1.179963	3.675484
H	1.543507	4.087915	1.318250
H	-4.162858	4.559133	-0.438534
H	-5.873042	4.322034	-0.880007
H	-5.236070	3.601458	0.607720
H	-7.453161	-1.960490	0.035256
H	-8.264420	-0.578350	-0.739336
H	-7.117398	-1.573586	-1.667881
H	-5.647540	1.108560	1.903653
H	-7.340509	1.220215	1.361158
H	-6.737653	-0.268910	2.135886
H	-6.693095	1.334412	-2.006027
H	-3.921323	2.049098	-3.621383
H	-5.236432	3.232787	-3.457207
H	-3.571449	3.708905	-3.052836
H	-0.791181	-4.395366	-2.915385
H	-0.501067	-3.318578	-4.310933
H	0.206388	-2.939251	-2.709668
H	-4.436771	-2.502720	-3.229655
H	-3.459270	-3.091246	-4.599686
H	-3.694829	-4.116592	-3.158353
H	0.054567	2.465315	-3.028156
H	-1.216001	2.133302	-4.251752
H	-1.645592	2.257684	-2.517961
H	1.147362	-1.220239	-3.929733
H	0.601096	0.044478	-5.073394
H	1.687569	0.449866	-3.709474
H	-2.661914	-0.448409	-4.121649
H	-5.068391	-2.208317	2.251437
H	-4.712707	-3.068051	3.779253

H	-5.274102	-1.379134	3.821135
H	-2.634501	-3.601074	1.958670

4.0 References

1. C.-H. Wang and S.-D. Yang, Rh(III)-Catalyzed Phosphine Oxide Migration Reactions: Selective Synthesis of 3-Phosphinoylindoles, *Chemistry – An Asian Journal*, 2018, **13**, 2401-2404.
2. D. C. Bradley, J. S. Ghotra and F. A. Hart, Low co-ordination numbers in lanthanide and actinide compounds. Part I. The preparation and characterization of tris{bis(trimethylsilyl)-amido}lanthanides, *Journal of the Chemical Society, Dalton Transactions*, 1973.
3. A. R. Smith and T. Livinghouse, Rapid and Efficient Procedure for the Synthesis of Group 3 Metal Tris[bis(dimethylsilyl)amide] THF Complexes, *Organometallics*, 2013, **32**, 1528-1530.
4. B. SAINT, v8.37a; Bruker AXS Inc.: Madison, Wisconsin, 2012.
5. G. M. Sheldrick, SHELXT – Integrated space-group and crystal-structure determination, *Acta Crystallographica Section A: Foundations and Advances*, 2015, **71**, 3-8.
6. B. SADABS, v2014/5; Bruker AXS Inc.: Madison, Wisconsin, 2001. .
7. P. Müller, R. Herbst-Irmer, A. L. Spek, T. R. Schneider and M. R. Sawaya, *Crystal Structure Refinement: A Crystallographer's Guide to SHELXL*, Oxford University Press, 2006.
8. D. Li, G. Kagan, R. Hopson and P. G. Williard, Formula Weight Prediction by Internal Reference Diffusion-Ordered NMR Spectroscopy (DOSY), *Journal of the American Chemical Society*, 2009, **131**, 5627-5634.
9. E. J. Cabrita and S. Berger, DOSY studies of hydrogen bond association: tetramethylsilane as a reference compound for diffusion studies, *Magnetic Resonance in Chemistry*, 2001, **39**, S142-S148.
10. A. Macchioni, G. Ciancaleoni, C. Zuccaccia and D. Zuccaccia, Determining accurate molecular sizes in solution through NMR diffusion spectroscopy, *Chemical Society Reviews*, 2008, **37**, 479-489.
11. F. Perrin, Mouvement Brownien d'un ellipsoïde (II). Rotation libre et dépolarisatîon des fluorescences. Translation et diffusion de molécules ellipsoidales, *Journal de Physique et le Radium*, 1936, **7**, 1-11.
12. H. H. Karsch, Z. Naturforsch. Teil B, 1979, **34**, 31.
13. A. M. Makal, D. Plażuk, J. Zakrzewski, B. Misterkiewicz and K. Woźniak, Experimental Charge Density Analysis of Symmetrically Substituted Ferrocene Derivatives, *Inorganic Chemistry*, 2010, **49**, 4046-4059.
14. Y. Zhao and D. G. Truhlar, A new local density functional for main-group thermochemistry, transition metal bonding, thermochemical kinetics, and noncovalent interactions, *The Journal of Chemical Physics*, 2006, **125**, 194101.
15. S. Grimme, J. Antony, S. Ehrlich and H. Krieg, A consistent and accurate ab initio parametrization of density functional dispersion correction (DFT-D) for the 94 elements H-Pu, *The Journal of Chemical Physics*, 2010, **132**, 154104.
16. M. Dolg, H. Stoll, A. Savin and H. Preuss, Energy-adjusted pseudopotentials for the rare earth elements, *Theoretica chimica acta*, 1989, **75**, 173-194.
17. M. Dolg, H. Stoll and H. Preuss, A combination of quasirelativistic pseudopotential and ligand field calculations for lanthanoid compounds, *Theoretica chimica acta*, 1993, **85**, 441-450.
18. D. Andrae, U. Häußermann, M. Dolg, H. Stoll and H. Preuß, Energy-adjusted ab initio pseudopotentials for the second and third row transition elements, *Theoretica chimica acta*, 1990, **77**, 123-141.
19. J. M. L. Martin and A. Sundermann, Correlation consistent valence basis sets for use with the Stuttgart–Dresden–Bonn relativistic effective core potentials: The atoms Ga–Kr and In–Xe, *The Journal of Chemical Physics*, 2001, **114**, 3408-3420.

20. G. A. Petersson and M. A. Al-Laham, A complete basis set model chemistry. II. Open-shell systems and the total energies of the first-row atoms, *The Journal of Chemical Physics*, 1991, **94**, 6081-6090.
21. G. A. Petersson, A. Bennett, T. G. Tensfeldt, M. A. Al-Laham, W. A. Shirley and J. Mantzaris, A complete basis set model chemistry. I. The total energies of closed-shell atoms and hydrides of the first-row elements, *The Journal of Chemical Physics*, 1988, **89**, 2193-2218.
22. A. E. R. E.D. Glendening, J.E. Carpenter, F. Weinhold, , NBO Version 3.1, *TCI ,University of Wisconsin, Madison*, , 1998.
23. F. Weigend and R. Ahlrichs, Balanced basis sets of split valence, triple zeta valence and quadruple zeta valence quality for H to Rn: Design and assessment of accuracy, *Physical Chemistry Chemical Physics*, 2005, **7**, 3297-3305.
24. F. Weigend, Accurate Coulomb-fitting basis sets for H to Rn, *Physical Chemistry Chemical Physics*, 2006, **8**, 1057-1065.
25. A. V. Marenich, C. J. Cramer and D. G. Truhlar, Universal Solvation Model Based on Solute Electron Density and on a Continuum Model of the Solvent Defined by the Bulk Dielectric Constant and Atomic Surface Tensions, *The Journal of Physical Chemistry B*, 2009, **113**, 6378-6396.
26. M. D. Hanwell, D. E. Curtis, D. C. Lonie, T. Vandermeersch, E. Zurek and G. R. Hutchison, Avogadro: an advanced semantic chemical editor, visualization, and analysis platform, *Journal of Cheminformatics*, 2012, **4**, 17.